PROCEEDINGS OF THE 10TH SYMPOSIUM ON THE JOINT SIBERIAN PERMAFROST STUDIES BETWEEN JAPAN AND RUSSIA IN 2001

Masami FUKUDA

Hideyuki SAITO

editors

Proceedings of the 10th Symposium on the Joint Siberian Permafrost Studies between Japan and Russia in 2001

held at

Climate Change Research Hall

National Institute for Environmental Studies

Tsukuba, Japan

22 - 23 March 2002

edited by

Masami FUKUDA

Hideyuki SAITO

Cover Photo taken at Yakutsk by

Professor H. Hayasaka

Graduate School of Engineering, Hokkaido University

Mr. T. Onoe,

Graduate school of Agriculture, Hokkaidou University

Editors

Masami FUKUDA

Research Center for North Eurasia and North Pacific Regions,

Hokkaido University

W8 N9, Kita-ku, Sapporo, 060-0809 JAPAN

Hideyuki SAITO

Graduate School of Agriculture, Hokkaido University

W9 N9, Kita-ku, Sapporo, 060-0806 JAPAN

Printed at Kohsoku Printing Center,

Akebono 2-5, Teine-ku, Sapporo, 006-0832 JAPAN

Published in March 2003

Sapporo, JAPAN

Preface

It already elapsed ten years after Japan and Russia Joint Research Program on Siberian Permafrost was established. These ten years were not easy periods for joint research in Siberia due to transition from Soviet to Russia, which caused many confusions and troubles in Russian society. However a lot of efforts both from Japanese and Russian scientists made it possible to obtain new knowledge on physical and biological environments. The tenth Joint Research Symposium was held at Tsukuba in the end of March 2002 at Tsukuba Japan. More than 60 scientists attended the symposium including scientists from Russia. If one attempts to compare the contents and topics of first and tenth symposium, he may easily notice the change of topics. At the beginning of the joint research program, which was initiated in 1992, it was first chance to Japanese scientists to conduct their own field survey jointly with Russian scientists. The topics ranged in very widely different research fields. But accumulation of field experiences made it to be narrowly focused in recent years. Especially topics on global changes in physical and biological aspects over Siberia are enhanced based on larger research program than initial periods.

The interactions between terrestrial and atmospheric fields are major focal points of recent research. For examples, boreal forest fire is now well documented according to long term monitoring results. There exists a demand from society to minimize the total emission of carbon dioxide from fuel burning output. Kyoto Protocol was established based on the international consensus in 1997. The function of Siberian Taiga is highly evaluated such as the lung of the earth. In the report of IPCC 1995, Siberian Taiga was assumed as major sink of Carbon Dioxide in global scale. However the report of IPCC 2001, it is not clearly mentioned that Taiga is either sink or source.

In this proceedings the evaluation of Siberian Taiga as sink or source of Carbon Dioxide is most widely discussed and hopefully we will get rather definite conclusion on this argument in near future. We already published ten volumes of the proceedings of the symposiums and hopefully we will add the selected papers in separate volume of the proceedings soon.

Finally we appreciate the financial support to this publication from Japan Science and Technology Corporation.

Masami FUKUDA

Professor

Institute of Low Temperature Science,

Hokkaido University

Director

Research Center for North Eurasia and North Pacific Regions, Hokkaido University

Contents

Author index

Seasonal variation of ecosystem carbon dioxide exchange over intact, burnt and cut larch forests in east Siberia

T. Machimura[1)2)], Y. Kobayashi[2)3)], G. Iwahana[3)], K. Goto[1)], M. Fukuda[3)2)] and A. N. Fedorov[4)]

[1] Graduate School of Engineering, Osaka University, Osaka 565-0871, Japan.
Phone: +81-6-6879-7391, Fax: +81-6-6879-7391, e-mail: mach@ga.eng.osaka-u.ac.jp
[2] Japan Science and Technology Inc.
[3] Institute of Low Temperature Science, Hokkaido University, Sapporo 060-0818, Japan.
[4] Permafrost Institute, Siberian Branch, RAS, Yakutsk 677018, Russia.

1. Introduction

Siberian taiga forest is one of the most important ecosystems for the global carbon cycle because its soil retains much organic matter undecomposed. In this region, forest fire and deforestation are the most common and risky disturbance of the natural forests. Forest fire destroys not only ecosystem biomass but also soil organics, and may lead irreversible change of the surface feature into grassland or wetland. Deforestation also has similar effects on the forest landscape except for combustion of living biomass and soil organics. They result change of the surface carbon dioxide (CO_2) exchange characteristic through change of the vegetation and soil condition.

In order to evaluate effects of fire and deforestation on the ecosystem CO_2 exchange, flux observation was conducted in an intact, a burnt and a cut forest in east Siberian taiga region.

2. Methods

In 2000 and 2001, long term ecosystem CO_2 flux and environmental conditions during summer growing season from May to September were observed in three tower sites in a typical taiga vegetation region near Yakutsk, Russian Federation (62° 19' N and 129° 31' E, see Fig. 1). A 21 m and a 6 m towers were constructed in an intact forest and a burnt forest in 2000, respectively. In the intact forest site, the dominant specie was larch (*Larix gmelinii*), mean tree height was 10 m, and stem density was 1600 ha^{-1}. The burnt forest site located in about 1 km northwest of the intact forest site. The burnt forest caught a fire about ten years ago, and the present surface vegetation was grassland with sparse young birch trees. In November of 2000, all standing trees in a rectangular area of 70 m x 140 m around the intact forest tower were clear-cut. In 2001 season, two towers were constructed in the clear-cut site and a new intact larch forest site located at 150 m north of the clear-cut tower, which was once the intact forest tower in the previous season. Surface vegetation in the new intact forest site was

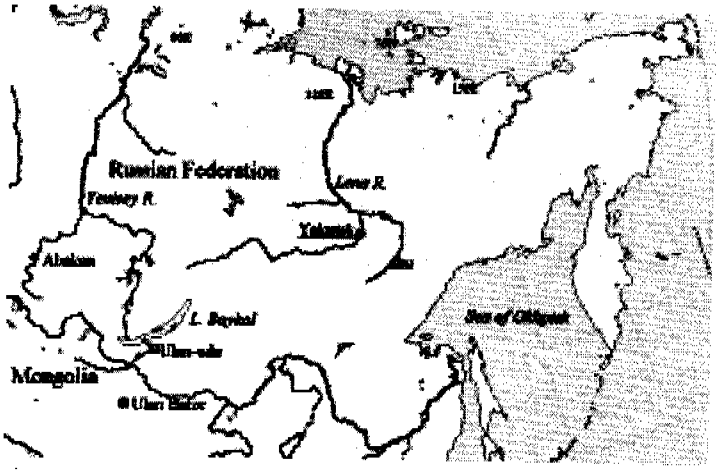

Fig. 1. Map of east Siberia.

similar to that in 2000.

CO_2 flux above the vegetation was observed using the "Edisol" eddy correlation system including a Gill model 1210R3 sonic anemometer and a Li-cor model 6262 gas analyzer. Wind vector and CO_2 concentration were measured at a sampling rate of 20 Hz and were recorded every 30 min. on PCs. The instrument height was 21m in the intact forest, however, was only 2m in the burnt and cut forests because the effective fetch was only 100m in main wind direction. Time lag between wind and gas concentration signals was removed for the maximum covariance. The linear trend removal was applied to the gas concentration signal. The band pass covariance operation to correct the gas concentration spectrum loss in the sampling tube was performed in the flux calculation for the intact forest because of very long sampling tube length (25 m). The WPL density correction was not applied because temperature of the closed path gas analyzer cells were enough stable by using 1.5 long temperature stabilizing tubes made of cupper at the gas analyzer inlets. Air temperature and wind speed above the vegetation (at 21 m high over the intact and 3 m high in the burnt and cut forests), and soil temperature at 5cm deep were measured using a Vaisala model HMP-45A in a ventilated tube, a R. M. Young model 03101 cup anemometer and a thermistor, respectively. They were recorded in a Campbell model CR10X data logger. In order to evaluate the CO_2 storage change in the forest canopy layer, CO_2 concentration at six heights below the flux instruments was measured using a Li-cor model 6262 gas analyzer. These measurements were averaged over daytime, nighttime and a day for the analysis, where the daytime and the nighttime were divided by using solar irradiance measurement.

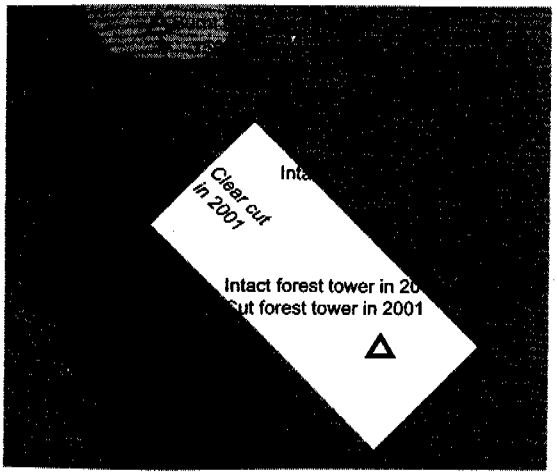

Fig. 2 Location of the tower eites.

3. Results and Discussion

3-1 CO_2 storage change in the intact forest canopy layer

CO_2 storage change in the forest canopy layer is necessary to evaluate instantaneous and daytime/nighttime mean fluxes, however, CO_2 concentration profile below the flux instruments was not measured in 2000 and in several short periods in 2001 in the intact forest. Ecosystem total CO_2 flux is sum of the eddy transfer and storage change fluxes, as below.

$$F_c = F_e + F_s \quad (1),$$

where, F_c and F_e are total and eddy CO_2 fluxes, respectively, and F_s is storage change in the canopy layer. The CO_2 storage flux in the intact forest was 30 % and 56 % of total flux in average during daytime and nighttime, respectively. In order to evaluate daytime and nighttime mean F_c during periods without CO_2 concentration profile measurement, daytime and nighttime mean F_s were estimated. Fig. 3 shows relationship between friction velocity u^* as an indicator of turbulent mixing above the canopy and fractional CO_2 storage defined as F_s/F_c during night. The fraction F_s/F_c was almost constant when friction velocity u^* was large, and increased when u^* decreased. The fraction F_s/F_c was approximated using the next bi-linear equation shown as a solid line in Fig. 3.

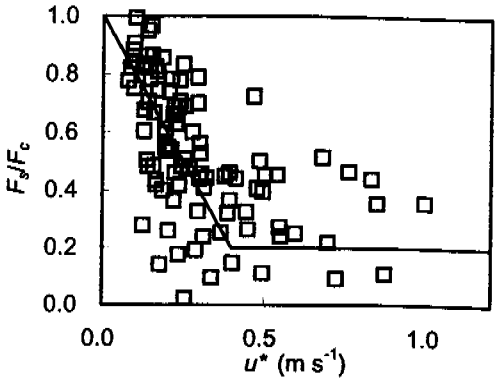

Fig. 3. Relationship between nighttime mean friction velocity u* and fraction of canopy layer CO_2 storage and total flux F_s/F_c in the intact larch forest in 2001. The solid line represents bi-linear approximation defined by equation (2).

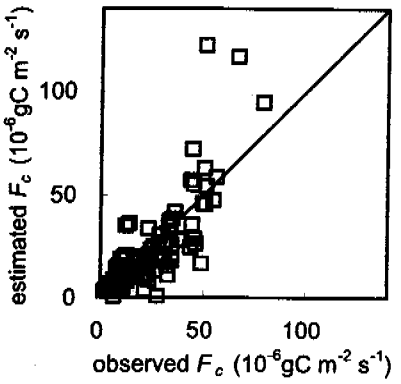

Fig. 4. Comparison between observed and estimated nighttime total CO_2 flux F_c in the intact forest in 2001 using equation (2).

$$F_s/F_c = 0.2 \quad (u^* \geq 0.4 \text{ m s}^{-1}),$$
$$= 1 - 2u^* \quad (u^* < 0.4 \text{ m s}^{-1}) \quad (2).$$

É

Observed and estimated nighttime F_c in the intact forest by using equations (1) and (2) is shown in Fig. 4. Nighttime mean total ecosystem CO_2 flux within the periods in which canopy layer CO_2 storage was not measured was estimated using the equations.

Daytime canopy layer CO_2 storage was compared with the eddy flux, total flux and turbulent strength, however no significant relationship were found. Diurnal cycle of CO_2 storage in the canopy layer increasing during night and decreasing during daytime suggested that the daytime amount of CO_2 storage change was closely related to that in the previous night. Fig. 5 shows relationship between cumulative CO_2 storage change fluxes F_s in daytime and in the previous night. Daytime and nighttime F_s were almost balanced, and daytime mean F_s can be estimated from estimated nighttime F_s during the periods without measurement.

3-2 Seasonal Variation of Ecosystem CO_2 Exchange in Intact, Burnt and Cut Forests

Monthly ecosystem CO_2 exchange in the intact, burnt and cut forests observed in 2000 and 2001 were shown in Fig. 6 together with monthly mean daytime and nighttime fluxes. The monthly total amount is also summarized in Table 1. In the intact larch forest, three months from June to August are the growing season of larch trees, and the ecosystem exchange showed negative value. Monthly exchanges of the intact forest in the two years were similar, and the five-month total exchange was –110 and –111 gC m^{-2} in 2000 and 2001, respectively. However, both mean daytime absorption and mean nighttime emission of CO_2 was larger in 2000 than 2001. In

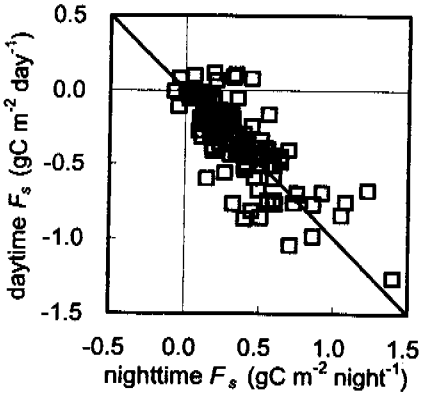

Fig. 5 Relationship between cumulative canopy layer CO_2 storages in daytime and the previous nighttime in the intact larch forest in 2001.

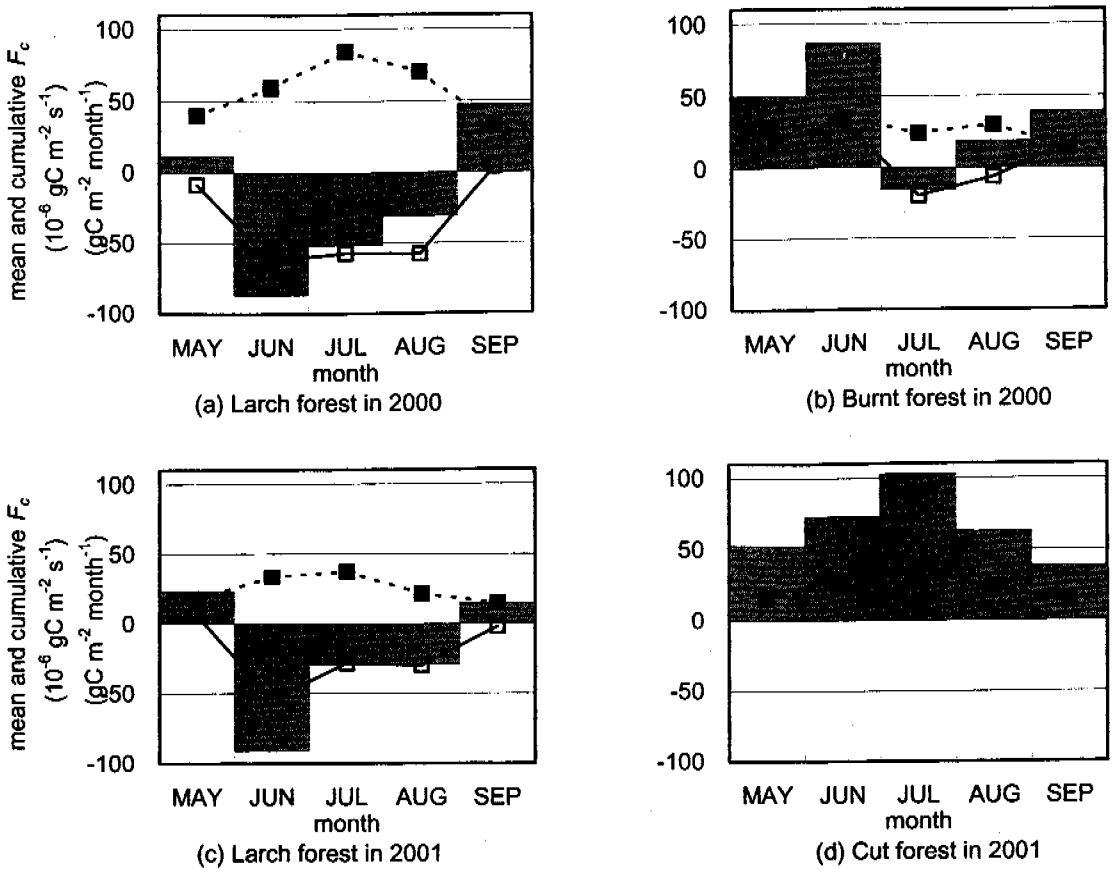

Fig. 5. Monthly ecosystem CO_2 exchange (bar) and monthly mean daytime (solid line) and nighttime (broken line) exchanges in the intact, burnt and cut forests in 2000 and 2001.

summer of 2000, rainfall was relatively large (119 mm in the five months) and more soil water was available, in contrast, in 2001, total rainfall was only 89 mm in the five months. Both photosynthesis and respiration of the trees and soil microorganisms were suppressed in 2001 because of the high water deficit during summer.

Ecosystem CO_2 exchange in the burnt forest was positive in all month in 2000 except for July, and five-month total exchange was +179 gC m^{-2}. This indicates that soil respiration exceeds net photosynthesis of regenerating vegetation at 10 years after the fire, and that the burnt forest ecosystem is losing the sequestrated carbon for many years. The cut forest emitted extremely much CO_2 during whole summer season of 2001. Daytime and nighttime mean CO_2 flux were positive and similar in all months, which indicates that photosynthesis of the ground vegetation were small and negligible for the ecosystem carbon budget at the point of 1 year after clear-cut. Five-month total ecosystem CO_2 exchange in the cut forest was +331 gC m^{-2}, which is larger than CO_2 absorption of the intact forest by factor of three.

Table 1. Monthly ecosystem CO_2 exchange in the intact, burnt and cut forests (gC m^{-2} month^{-1}).

month	intact larch forest		burnt forest	cut forest
	2000	2001	2000	2001
MAY	+12	+23	+50	+53
JUN	-87	-91	+87	+74
JUL	-51	-29	-16	+103
AUG	-31	-29	+19	+63
SEP	+47	-15	+39	+39
total	-110	-111	+179	+331

4. Conclusions

CO_2 flux was measured during growing season in 2000 and 2001 in an intact larch

forest, a forest burnt 10 years ago and a forest clear-cut in the previous autumn near Yakutsk in east Siberia using closed path eddy covariance systems. Total CO_2 exchange during summer five months was absorption of CO_2 by about 110 gC m^{-2} in the intact larch forest, whereas, was emission by 179 and 331 gC m^{-2} in the burnt forest and in the cut forest, respectively. Forest disturbance in east Siberian Taiga region such as deforestation and fire affects on the ecosystem CO_2 budgets very much, and the effect remains for at least ten years.

REFERENCES

Iwahana, G., Machimura, T., Kobayashi, Y., Fukuda, M. and Fedorov, A. N. (2000): Fire effects on fluxes and active layer dynamics in Taiga forests over east Siberia permafrost region. 2. Thermal characteristics changes of active layers induced by forest fire. *Proceedings of the Eighth Symposium on the Joint Siberian Permafrost Studies between Japan and Russia in 2000*, 162-169

Kobayashi, Y., Machimura, T., Iwahana, G., Fukuda, M. and Fedorov, A. N. (2001): Fire effects on fluxes and active layer dynamics in Taiga forests over east Siberia permafrost region. 1. Energy and water budgets in burnt and unburned larch forests. *Proceedings of the Eighth Symposium on the Joint Siberian Permafrost Studies between Japan and Russia in 2000*, 156-161.

Machimura, T., Iwahana, G., Fukuda, M., Chambers S. D. and Fedorov, A. N. (2000): Energy and CO_2 budgets over burnt and unburned larch forests in east Siberia. *Proceedings of the Eighth Symposium on the Joint Siberian Permafrost Studies between Japan and Russia in 1999*, 165-170.

Sawamoto, T., Hatano, R., Shibuya, M., Takahashi, K., Isaev, A. P. and Maximov, T. C. (2000): Effect of forest fire on carbon cycling in Taiga soil-plant system, near Yakutsk. *Proceedings of the Eighth Symposium on the Joint Siberian Permafrost Studies between Japan and Russia in 1999*, 230-236.

Yajima, T., Takahashi, K., Sasaoka, E., Hatano, R., Sawamoto, T., Ivanov, B. I., Isaev, A. P. and Maximov, T. C. (1998): Stand structure and biomass of Larix cajanderi forest in the Siberian taiga. *Proceedings of the Sixth Symposium on the Joint Siberian Permafrost Studies between Japan and Russia in 1997*, 72-80.

Spatial variations of light intensity and photosynthetic properties within a *Larix gmelinii* tree crown in eastern Siberia

H. Saito[1*], K. Yamamuro[1], Y. Tsuno[1], H. Iijima[1], M. Shibuya[1], K. Takahashi[1], and T.C. Maximov[2]

[1] Graduate School of Agriculture, Hokkaido University. Forest Dynamics Group, CREST
[2] Institute of Biological Problems of Cryolithozone, Russian Academy of Science
* Phone: +81-11-706-2523, Fax: +81-11-706-4176, e-mail: saitoo@for.agr.hokudai.ac.jp

1. Introduction

Larix gmelinii stand, largely distributes in eastern Siberia, plays a prominent role as carbon storage in the global carbon cycle. According to Sawamoto *et al.* (2001) and Schulze *et al.* (1999), the net ecosystem production in *Larix gmelinii* stand is strongly smaller than temperate forest, due to smaller net primary production (Shibuya *et al.*, 2001) compared with Japanese *Larix* stands (Kira and Shidei, 1967). However the environmental regulation of the net primary production is less understood in the *L. gmelinii* stands (Vygodskaya *et al.*, 1997).

An eco-physiological process based model for carbon budget is useful for quantitative analysis of the environmental limitation of net primary production (e.g. Kakubari, 1987, Ito & Oikawa, 2002). An understanding of the incident photosynthetic photon flux density (*PPFD*) intercepted within the stand canopy is one of the prerequisite for development of the model of productive structure and the function. In many pioneering models of photosynthesis in plant canopy, the divisions of some horizontal leaf layers from top to bottom within the canopy was designed (e.g. Monshi and Saeki, 1953, Kurachi *et al.*, 1986). The light attenuation was mathematically fitted to Lambert-Beer's low. In the *L. gmelinii* stands, it seems to be complex the light extension due to the loosely closed canopy and the thin shape of the tree crown, although *L. gmelinii* forms pure forest. For example, many direct sun spots frequently fall down in the shade leaf layer within the tree crown in sunny day. Thus applying the pioneer model to *L. gmelinii* stand canopy is questionable. It is necessary to understand quantitatively the *in situ PPFD* distribution within the *L. gmelinii* stand canopy.

Our objective is to understand the spatial and temporal variations of incident *PPFD* within a *L. gmelinii* tree crown. To evaluate the potential of *PPFD* to drive CO_2 assimilation in leaves, light response curve of CO_2 assimilation rate was determined, and the *PPFD* within the tree crown was classified into the photosynthetic properties. We examined whether the pioneer model constructing using Lambert-Beer's low was suitable for the *L. gmelinii* stand.

2. Material and methods

The study site was located in a natural *L. gmelinii* stand at Neleger (62°18'N, 129°30'E) near Yakutsk in the Republic of Sakha, Russia. The stand age was estimated to be over 200 years old.

The stand density was approximately 2100 trees/ha. The maximum tree height of the stand was approximately 21m. The leaf area index was estimated to be approximately 3 m^2 m^{-2} (H. Saito, unpublished data). The height and DBH of the sample tree was 21m and 27.1 cm, respectively. In the stand floor, the dominant vegetation is *Vaccinium vitis-idaea* (Saito *et al.*, 2001), which is a typical type of mature *L. gmelinii* stand around Yakutsk (Schulze *et al.*, 1995).

The measurements of *PPFD* and CO_2 assimilation rate were carried out in the middle of July, 2001. The *PPFD* was taken by using the *PPFD* sensor (IKS-27, Koito Ltd., Yokohama, Japan) and data-logger (MesUL120, Koito Ltd., Yokohama, Japan). The *PPFD* was measured above the tree crown (25m), on the four lowest branches at approximately 12m height above the ground level, and above the understoried vegetation. For measuring the *PPFD* above the tree crown, the *PPFD* sensor was mounted on the 25m flux-tower near the sample tree. For measuring the *PPFD* at the lowest branches, the 12 *PPFD* sensors were mounted on the four branches, northern, eastern, southern, and western direction. For measuring the *PPFD* above the understoried vegetation, the 12 *PPFD* sensors were mounted at 15-20 cm height above the ground level. On the each branch, the *PPFD* sensor was mounted at the outside, near the stem and the intermediate of the leaves distribution (Fig. 2). The interval of the data logging was 30 seconds.

For the measurement of CO_2 assimilation rate, twig with short-shoot leaves were collected at the top and the lowest leaf layer within the tree crown. The height of the top and the lower tree crown is 20.5 and 12m above the ground level, respectively. The collection was carried out before sunrise in the early morning. The CO_2 assimilation rate was measured by using a portable photosynthesis system with conifer chamber (LI6400, Li-cor, Lincoln, USA). The cut-end of collected twig was frequently cut under water. The measurements were finished within 2 days after the collection. The *PPFD* was changed by shading mesh clothes under natural solar radiation. The leaf temperature, leaf to air vapor pressure deficit, and CO_2 concentration in gas-exchange chamber were 19.2 to 26.7 °C, 0.6 to 1.5 kPa, and 359 to 361 ppm during the measurement.

The non-linear regression of light dependency of net CO_2 assimilation rate was determined to the following formula (Küpper and Schulze, 1985);

$$A_{net}=a*[1-\exp^{-k(PPFD-b)}]$$

The a was light saturated CO_2 assimilation rate (A_{max}), and the b was light compensation point of net CO_2 assimilation rate. The light saturation point was defined as *PPFD* at 95% of A_{max} from the formula.

3. Results and Discussion

3 - 1 Diurnal fluctuation of PPFD

The weather condition of the measuring day was approximately blue sky in the daytime (Fig. 1). The maximum of incident *PPFD* on the top of the tree crown was approximately 1600 μmol m^{-2} s^{-1}.

In the midday, the base-level of *PPFD* without sun spot was between 100 and 300 μmol m^{-2} s^{-1} approximately. The total time of *PPFD* over 500 μmol m^{-1} s^{-1} at the top and the lowest leaf layer was 661 min. and 162-371 min., respectively. The portion of the *PPFD* over 500 μmol m^{-1} s^{-1} was 24.5-56.1% in the lowest leaf layer compared with the top.

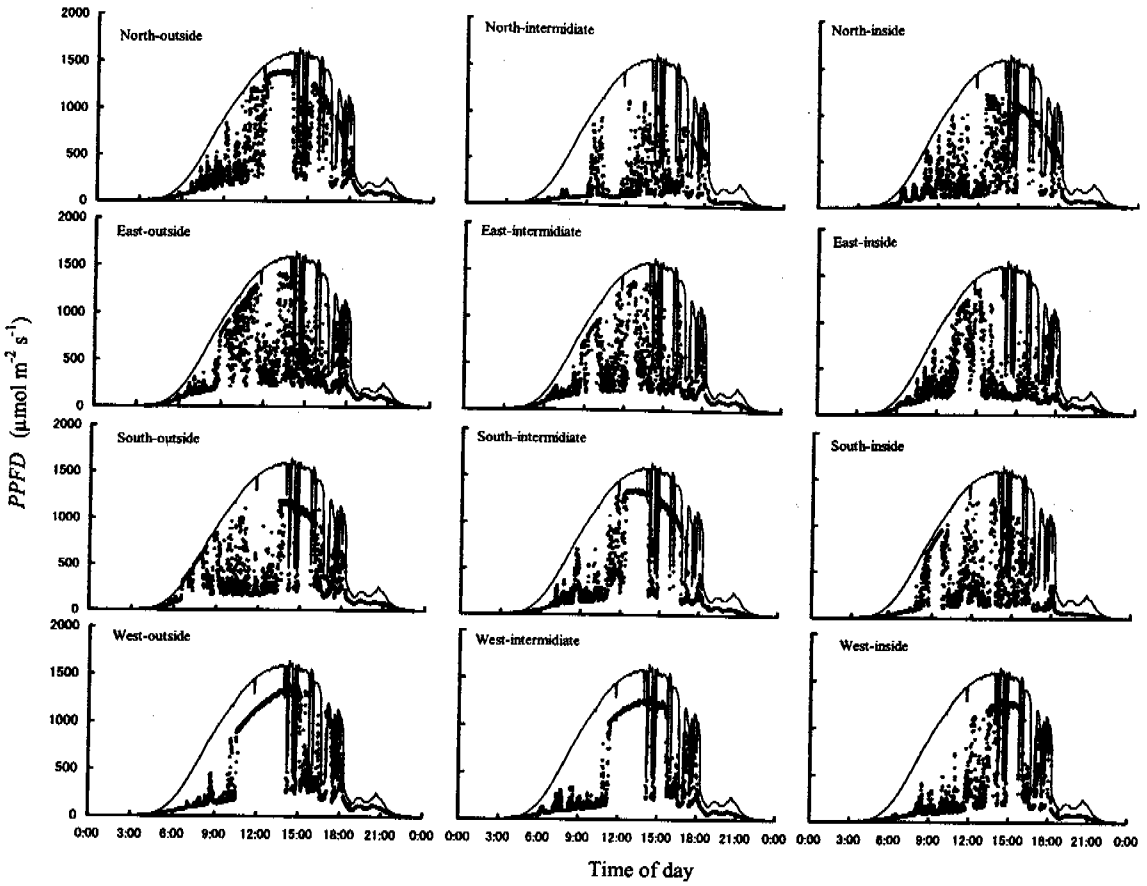

Fig 1 Diurnal fluctuation of photosynthetic photon flux density (*PPFD*) within a *Larix gmelinii* tree crown. Solid line and dots denotes *PPFD* at above stand canopy and the lowest leaf layer within the tree crown, respectively.

The daily sum of *PPFD* ($PPFD_{day}$) at top and the lowest leaf layer was 49.9 and 12.3-28.0 mol m^{-2} day^{-1}, respectively. The relative $PPFD_{day}$ at the lowest leaf layer was 24.7 to 56.2% to the top. It appears that the light attenuation within the lowest leaf layer was smaller in the *L. gmelinii* tree crown compared with a Japanese larch (*Larix leptolepis*) plantation (Kurachi *et al.*, 1986), a mature *Abies sachalinensis* stand (Saito, unpublished data), and a mature beech (*Fagus crenata*) tree crown (Saito and Kakubari, 1999).

The attenuation was dependent on the direction and the distance from the stem within the lowest tree crown. Within the lowest tree crown, the $PPFD_{day}$ decreased with nearing to the stem. Compared with the four directions, the $PPFD_{day}$ was the highest in the southern part of the lowest tree crown, and was the lowest in the northern part of the lowest tree crown. The variation of light attenuation is widely within the *L. gmelinii* compared with the *L. leptolepis* stand the *A.*

sachalinensis stand.

Incident *PPFD* above the understoried vegetation, which intercepted throughout the stand canopy, strongly fluctuated by frequent sun spot (Fig. 2). In the midday, the base-level of *PPFD* without sun spot was between approximately 100 μmol m^{-2} s^{-1}. The $PPFD_{day}$ in understory was 18.2 to 23.2% to the top. It appears that the *PPFD* extinction throughout the canopy is lower than the *L. leptolepis* stand canopy, in which the relative radiation at 1.3m above the ground level was 6% (Kurachi *et al.*, 1986), and a mature *F. crenata* forest (Naramoto *et al.*, 2002).

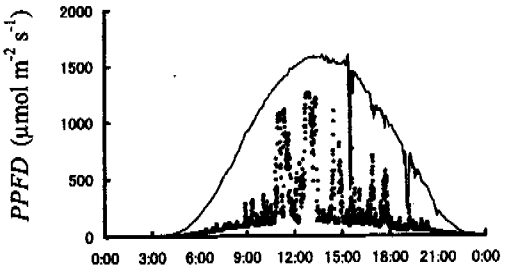

Fig 2 Diurnal fluctuation of photosynthetic photon flux density (*PPFD*) above an understoried vegetation in a *Larix gmelinii* stand. Solid line and dots denotes *PPFD* at above stand canopy and above the understoried *Vaccinium vitis-idaea*, respectively.

3 - 2 Light dependency of net CO_2 assimilation rate

The photosynthetic properties of light saturated net CO_2 assimilation rate (A_{max}), light compensation point and light saturation point were shown in Table 1. The A_{max} at top crown and lowest leaf layer was 13.6±1.3 (mean ± standard deviation) and 9.6±0.5 μmolCO_2 m^{-2} s^{-1}, respectively. The A_{max} was significantly lower in the lowest leaf layer than in the top (*t*-test, $p < 0.01$). The A_{max} at top crown was similar to field-growing *L. gmelinii* (Koike *et al.*, 1998; Koike *et al.*, 1999; Koike *et al.*, 2001), was slightly higher than *L. gmelinii* forest canopy (Vygodskaya *et al.*, 1997), and was approximately 2-fold higher than laboratory-grown *L. gmelinii* seedlings (Koike *et al.*, 2000). The light compensation point of CO_2 assimilation rate at the top crown and the lowest leaf layer was 29±6 and 18±4 μmol m^{-2} s^{-1}, respectively (Table 1). The light compensation point was significantly higher in the lowest leaf layer than the top (*t*-test, $p < 0.05$). The light saturation point of CO_2 assimilation rate at top crown and lowest leaf layer was 785±166 and 387±47 μmol m^{-2} s^{-1}, respectively (Table 1). The light compensation point was significantly higher in the lowest leaf layer than the top (*t*-test, $p < 0.01$). The light saturation point was slightly higher compared with the *L. gmelinii* forest canopy (Vygodskaya *et al.*, 1997).

These results suggest that the photosynthetic properties acclimate to the light gradients within the *L. gmelinii* tree crown (Boardman, 1977). According to Larcher (1995), the light compensation point of sun and shade shoot in coniferous tree was 30-40 and 2-10 μmol m^{-2} s^{-1}, and the light

saturation point of sun and shade shoot was 800-1100 and 150-200 μmol m^{-2} s^{-1}, respectively. Thus, our results indicate that the variation of the photosynthetic acclimation between the sunlit and the shade conditions was relatively small in term of the light compensation and saturation points. It may be that the small acclimation is caused by the small gradient of the light attenuation within the *L. gmelinii* tree crown (Fig. 1).

Table 1 Photosynthetic parameters

	Top tree crown	Lowest leaf layer
Light saturated CO_2 assimilation rate (μmol CO_2 m^{-2} s^{-1})	13.6±1.3	9.6±0.5**
Light saturation point (μmol m^{-2} s^{-1})	29±6	18±4*
Light compensation point (μmol m^{-2} s^{-1})	785±166	387±47**

Asterisk denotes statistically significant differences between the top and the lowest leaf layer within the tree crown (*t*-test, *: $p<0.05$, **: $p<0.01$).

3 - 3 Frequency distribution of PPFD classified by photosynthetic parameters

The frequency distribution of *PPFD* classified by photosynthetic properties of light saturation point and light compensation point is shown in Table 2. The portion of *PPFD* over light saturation point was 44.1% in top crown, and was 16.3–33.9% in lowest leaf layer. The portion of *PPFD* over light compensation point was 89.6% in top crown, and was 83.1 – 87.8% in lowest leaf layer.

According to Saito (2000), the portion of *PPFD* over light saturation point in a sunny day was below 10% within a mature *F. crenata* tree crown. Compared with the *F. crenata* tree crown, the *PPFD* is significantly higher within the *L. gmelinii* tree crown. These results indicate *PPFD* attenuation is not a major factor to limit CO_2 assimilation of leaves within the *L. gmelinii* tree crown.

Above the understory, the *PPFD* over light saturation point of lowest leaf layer was 11.9 %, and the *PPFD* over light compensation point was 86.7% in the daytime. Naramoto *et al.* (2001) reported the *PPFD* over light saturation point was approximately below 10% in understory of a mature *F. crenata* forest. Our results also indicate that the efficiency of *PPFD* extinction within the mature *L. gmelinii* stand canopy is strongly low.

4. Conclusion

The stand canopy of *L. gmelinii* largely penetrates the solar radiation, although the stand height reaches over 20m and the stand density is similar compared with the temperate *Larix* stand. Leaves in lowest leaf layer within the tree canopy frequently absorb high *PPFD* which can drive high CO_2 assimilation rate. The vertically low attenuation and horizontally large variation of *PPFD* is a remarkable characteristic of the matured *L. gmelinii* stand. Especially, the large variation of *PPFD* ranged between the light compensation and light saturation point of CO_2

assimilation rate may occurs the large error in estimation of CO_2 assimilation rate in the model. Therefore our results suggest that the modeling of the light distribution by using the Lambert-Beer's low is not suitable for the *L. gmelinii* stand.

Table 2 Frequency distribution of *PPFD* classified by photosynthetic parameters.

Leaf layer	Direction and position	<LCP* (%)	LCP - LSP* (%)	LSP>* (%)
Top tree crown		10.4	45.5	44.1
Lowest leaf layer	North			
	Outside	12.5	58.7	28.8
	Intermidiate	16.2	56.9	26.9
	Inside	16.9	66.7	16.3
	Average	15.2	60.8	24.0
	East			
	Outside	13.2	56.2	30.6
	Intermidiate	13.7	60.3	26.0
	Inside	15.7	63.3	21.0
	Average	14.2	59.9	25.9
	South			
	Outside	12.9	53.2	33.9
	Intermidiate	15.6	56.7	27.7
	Inside	17.3	60.4	22.2
	Average	15.3	56.8	27.9
	West			
	Outside	12.2	58.2	29.6
	Intermidiate	12.4	61.3	26.3
	Inside	13.1	66.5	20.4
	Average	12.6	62.0	25.4
Above understory**		17.3	70.8	11.9

* Abbreviation of *LCP* and *LSP* denotes light compensation point and light saturation point of CO_2 assimilation rate, respectively. Photosynthetic parameters of *LCP* and *LSP* at top and lowest leaf layer was shown in Table 2.

** *PPFD* above understory was classified by the photosynthetic parameters of the lowest leaf layer.

REFERENCES

Boardman, N. K., (1977) Comparative photosynthesis of sun and shade plants. Ann. Rev. Plant Physiol. 28: 355-377.

Ito, A. and Oikawa, T. (2002) A simulation model of the carbon cycle in land ecosystems (Sim-CYCLE): A description based on dry-matter production theory and plot-scale validation. Ecological Modelling 151: 143-176.

Kakubari, Y. (1987) Modeling the productive structure and function of natural forests of *Fagus crenata* at different altitudes in Naeba mountains. An analysis of dry matter production with an eco-physiological computer simulation model based on an individual tree. Bull. Tokyo Univ. Forests 76: 107-162.

Kira, T. and Shidei, T. (1967) Primary production and turnover of organic matter in different forest ecosystems of the western Pacific. Jpn. J. Ecol. 17: 70-87.

Koike, T., Mori, S., Matsuura, Y., Prokushkin, S. G., Zyranova, O. A., Kajimoto, T., Abaimov, A. P. (1998) Photosynthesis and foliar nutrient dynamics in larch and spruce grown on contrasting north- and south-facing slopes in the Tura experiment forest in central Siberia. In Proc. 6th Symposium on the Joint Siberian Permafrost Studies between Japan and Russia in 1997 (Eds. Mori, S., Kanazawa, Y., Matsuura, Y. and Inoue, G.), 3-10, Sapporo, Japan.

Koike, T., Mori, S., Matsuura, Y., Prokushkin, S. G., Zyranova, O. A., Kajimoto, T., Sasa, K., Abaimov, A. P. (1999) Shoot growth and photosynthetic characteristics in larch and spruce affected by temperature of the contrasting north and south facing slopes in eastern Siberia. In Proc. 7th Symposium on the Joint Siberian Permafrost Studies between Japan and Russia in 1998 (Eds. Shibuya, M., Takahashi K. and Inoue, G.), 3-12, Sapporo, Japan.

Koike, T., Yazaki, K., Funada, R., Kitao, M., Maruyama, Y., Takahashi, K., Maximov, T. C., Ivanov, B. I. (2000) Photosynthetic characteristics of dahurian larch, scotch pine and white birch seedlings native to eastern Siberia raised under elevated CO_2. Eurasian J. For. Res. 1: 31-37.

Koike, T., Wang, W. J., Kitaoka, S., Mori, S., Matsuura, Y., Prokushkin, A. S., Zyryanova, O. A., Prokushkin, S.G., Abainov, A. P. (2001) : Photosynthetic light curves of trees and shrubs grown under contrasting north- and South-facing slopes in central Siberia. In Proc. 9th Symposium on the Joint Siberian Permafrost Studies between Japan and Russia in 2000 (Eds. Fukuda, M. and Kobayashi, Y.), 35-41, Sapporo, Japan.

Küppers, M. and Schulze, E. D. (1985) : An empirical model of net photosynthesis and leaf conductance for the simulation of diurnal course of CO_2 and H_2O exchange. Aust. J. Plant Physiol. 12: 513-526.

Kurachi, N., Hagihara, A., Hozumi, K. (1986) : Evaluation of the light interception by non-photosynthetic organs in a *Larix leptolepis* plantation. Ecol. Res. 1: 173-183.

Kurachi, N., Hagihara, A., Hozumi, K. (1992) : Canopy photosynthetic production in a Japanese larch forest. I. Seasonal and vertical changes of leaf characteristics along the light gradient in a canopy. Ecol. Res. 7: 255-265.

Larcher (1995) : Physiological Plant Ecology. Ecophysiology and stress physiology of functional groups. Third edition. Springer-Verlag Berlin Heidelberg. pp506.

Monshi, M., Saeki, T. (1953) : Über den Lichtfaktor in den Pflanzengesellschften und seine

Bedeutung fur die Stoffproduktion. Jpn. J. Bot. 14: 22-52.

Naramoto, M., Han, Q., Kakubari, Y. (2001) : The influence of previous irradiance on photosynthetic induction in three species grown in the gap and understory of a *Fagus crenata* forest. Photosynthetica 39: 545-552.

Saito, H. and Kakubari, Y. (1999) : Spatial and seasonal variations in photosynthetic properties within a beech (*Fagus crenata*) crown. J. For. Res. 4: 27-34.

Saito, H. (2000) : Vertical variations of photosynthetic properties and the expression of the genes in relation to photosynthesis within a *Fagus crenata* crown. Bull. Shizuoka Univ. Forests 24, 1-54. (in Japanese with English summary)

Saito, H., Takahashi, K., Shibuya, M., Tsuno, Y., Isaev, A. P., Maximov, T. C. (2001) : Distribution of 1-years-old larch seedlings and vegetation on a matured larch forest floor in eastern Siberia In Proc. 9th Symposium on the Joint Siberian Permafrost Studies between Japan and Russia in 2000 (Eds. Fukuda, M. and Kobayashi, Y.), 75-82, Sapporo, Japan.

Sawamoto, T., Hatano, R., Shibuya, M., Saito, H., Tsuno, Y., Takahashi, K., Isaev, A. P., Desyatkin, R. V., Maximov, T. C. (2001) : Effect of forest fire on NEP in taiga soil ecosystems, near Yakutsk, Russia. In Proc. 9th Symposium on the Joint Siberian Permafrost Studies between Japan and Russia in 2000 (Eds. Fukuda, M. and Kobayashi, Y.), 120-127, Sapporo, Japan.

Schulze, E. D., Schulze, W., Kelliher, F. M., Vygodskaya, N. N., Zieger, W., Kobak, K. I., Koch, H., Kusnetsova, W.A., Sogatchev, A., Issajev, A., Bauer, G., and Hollinger, D. Y. (1995) : Aboveground biomass and nitrogen nutrition in a chronosequence of pristine Dahurian *Larix* stands in eastern Siberia. Can. J. For. Res. **25**, 943-960.

Schulze, E. D., Lloyd, J., Kelliher, F. M., Wirth, C., Rebmann, C., Lühker, B., Mund, M., Knohl, A., Milyukova, I. M., Schulze, W., Zieger, W., Varlagin, A. B., Sogachev, A. F., Valentini, R., Dore, S., Grigoriev, S., Kolle, O., Panfyorov, M. I., Tchebakova, N., Vygodskaya, N. N. (1999) Productivity of forests in the Eurosiberian boreal region and their potential to act as a acarbon sink- a synthesis. Global Change Biology: **5**, 703-722.

Shibuya, M., Tsuno, Y., Saito, H., Takahashi, K., Sawamoto, T., Hatano, R., Isaev, A. P., Maximov, T. C. (2001) : Chronosequential analysis of aboveground biomass and the carbon and nitrogen contents in natural *Larix* stands in eastern Siberia. Bull. Res. Cent. North Eurasia and North Pacific Regions, Hokkaido Univ. 1, 57-66.

Vygodskaya, N. N., Mikyukova, I., Varlagin, A., Tatarinov, F., Sogachev, A., Kobak, K. I., Desyatkin, R., Bauer, G., Hollinger, D. Y., Kelliher, F. M., and Shulze, E. D. (1997) : Leaf conductance and CO_2 assimilation of *Larix gmelinii* growing in an eastern Siberian boreal forest. Tree Physiol. 17: 607-615.

Photosynthetic and stomatal responses to air vapor pressure deficit within a larch canopy in east-Siberia

M. Suzuki[1], H. Saito[1*], H. Iijima[1], T. Onoe[1], K. Takahashi[1] and T. C. Maximov[2]

[1] Graduate School of Agriculture, Hokkaido University. Forest Dynamics Group, CREST
[2] Institute of Biological Problems of Cryolithozone, Russian Academy of Science
* Phone: +81-11-706-2523, Fax: +81-11-706-4176, e-mail: saitoo@for.agr.hokudai.ac.jp

1. Introduction

In Siberia, it is very dry and cool climate, so plants must grow in a greatly strict environment there. *Larix gmelinii* is a dominant tree species that widely distributed in eastern Siberia of Eurasian Continent (Gower *et al*, 1990), which is considered to adapt to this strict climate condition. Vgodyskaya *et al.* (1997) studied about the diurnal change of photosynthesis within a *L. gmelinii* stand canopy and reported that its carbon assimilation was strongly limited in the midday. They implied this midday depression was caused by external conditions of high temperature and low humidity in the midday. However they could not evaluate the each and multiple effects in the field conditions, because the evaluation of their study was based on the analysis of the apparent relationship between the net photosynthesis rate and each environmental factors of light intensity, leaf temperature, leaf to air water vapor pressure deficit from the results of the diurnal changes. The understanding about how much each environmental factor affects to the metabolism of *L. gmelinii* has been lacking yet.

Leaf to air water vapor pressure deficit (*Vpd*L) is a factor to limit CO_2 assimilation rate in general (Schulze, 1986). The increasing of *Vpd*L decreases the CO_2 assimilation rate accompanied with closing of stomata in many plant. However the quantity of the decrease is dependent on the species and their growing habitat (e.g. Schulze, 1986; Guehl & Aussenac, 1987). In eastern Siberia, the air water vapor pressure is strongly low due to small precipitation in the growing season (Sugimoto *et al.*, 2002). The air water vapor pressure deficit within the *L. gmelinii* stand canopy frequently reaches to over 3 kPa (e.g. Vgodyskaya *et al.*, 1997). Thus the *Vpd*L can predict to be a major factor to limit the CO_2 assimilation rate within the *L. gmelinii* stand canopy.

It is well known that stomatal behavior plays an important role for CO_2 and H_2O gas-exchange of leaf. The depression of photosynthesis can be divided to two processes of stomatal limitation and non-stomatal limitation (Jones, 1985). If the non-stomatal limitation is constant, the increase of stomatal limitation is accompanied by intercellular CO_2 concentration. In contrast, the increase of non-stomatal limitation is believed to be accompanied by the decrease of demand function like content and/or activity of photosynthetic enzymes. In order to understand the effect of *Vpd*L on CO_2 assimilation rate, it is necessary to understand the role of stomata behavior.

Our aims are (1) to understand the effect of *Vpd*L on CO_2 assimilation rate, stomatal conductance

and transpiration rate, and (2) to understand the contribution of stomatal limitation in the depression of the CO_2 assimilation rate of leaves within the *L. gmelinii* stand canopy.

2. Study site and methods

Study site was located in Neleger (62°18'N, 129°30'E), approximately 30 km from Yakutsk in the Republic of Sakha, Russia. The stand age was estimated to be over 200 years old. The stand density was approximately 2100 trees/ha. The maximum tree height of the stand was approximately 21m. The annual precipitation was 200-300mm. The mean annual temperature was approximately -10°C. The leaf mass of this stand was estimated to approximately 2 ton ha^{-1} (Shibuya *et al.*, 2001).

The measurement of *A*net was conducted in 18-27 July 2002. The sample twig was collected before 4:00AM from the sunlit upper layer of the tree crown of 3 *L. gmelinii* dominant trees. The cut ends of twigs were immediately soaked in water, and then the measurement was carried out within a day. The A_{net} of only short shoot was measured by using a portable photosynthesis measurement system with conifer chamber (LI6400, Li-cor, Lincoln, USA). The light source was a halogen lamp using a fiber illuminator (KL2500, Walz, Germany). The photosynthetic photon flux density in the gas-exchange chamber was measured by using of portable sensor (IKS-27, Koito Ltd., Yokohama, Japan).

In the measurement of A_{net}, the *PPFD* and CO_2 concentration was controlled at 1500 μmol m^{-2} s^{-1} and at 330ppm, respectively. The air temperature inside the chamber was controlled at 10°C, 20°C, and 30°C. Leaf temperature was controlled at 12.8-14.1°C, 21.4-22.4°C and 29.5-29.9°C. We changed *Vpd*L at different temperatures, the range of *Vpd*L at that time were 0.5-1.4kPa (10°C), 1.0-2.4kPa (20°C), and 1.5–3.8kPa (30°C) respectively.

To examine a contribution of stomatal and non-stomatal limitation in the change of photosynthetic rate, the demand function and supply function were analyzed. By considering simultaneous CO_2 and H_2O fluxes through the stomatal pore, CO_2 diffusion is described by equation 1 (Caemmerer and Farquhar, 1981).

$$A = g_s(C_a - C_i) - E(C_a - C_i)/2 \qquad \text{(Eq.1)}$$

where A is net CO_2 assimilation rate, g_s is stomatal conductance, C_a and C_i is air in the gas-exchange chamber and intercellular CO_2 partial pressure, respectively, E is transpiration rate. This equation 1 is possible to be arranged as follow;

$$C_a - C_i = (A + E * C_a) / (g_s + E/2) \qquad \text{(Eq.2)}$$

From equation 2, the supply function (constant g_s and E) is defined by a line with an x-axis interceptual to $C_a(1-E(g_s + E/2))$ and a negative slope equal to $-(g_s + E/2)$ on a photosynthetic rate versus intercellular CO_2 concentration graph. The demand function is described as a typical A versus C_i curve. If photosynthesis rate increases due to only stomatal limitation, i.e. no contribution of non-stomatal limitation, the photosynthesis rate increases along the demand function

accompanied with increasing of C_i. In contrast, if photosynthesis rate increases due to only non-stomatal limitation, the photosynthesis increases along supply function.

3. Results and discussion

The responses of net CO_2 assimilation rate (A_{net}), stomatal conductance (g_s), transpiration rate (E) and water use efficiency (WUE; A_{net}/E) to VpdL are shown in Fig.1. No significant difference of A_{net} and g_s was detected under low VpdL at 10 and 20°C (below 1.5 kPa), respectively. The A_{net} and g_s decreased linearly with increasing of VpdL from 1.5 to 3.5 kPa, respectively. So the responses of A_{net} and g_s with increasing of VpdL were different in dry and humid conditions. The percentage of the reduction in A_{net} and g_s with increasing VpdL (from 1.5 kPa to 3.5 kPa) at 30°C reached 38% and 64%, respectively. Thus it can be considered that high VpdL is one of the important factors to limit the carbon assimilation of within the *L.gmelinii* stand canopy.

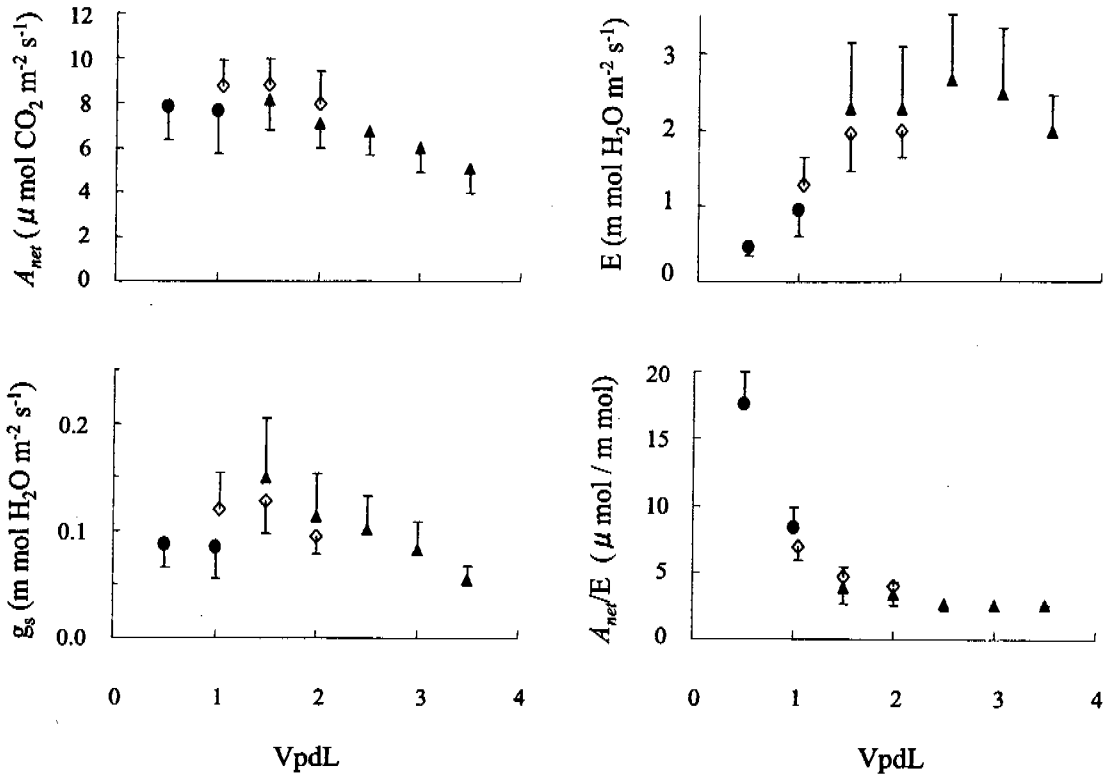

Fig.1. Responses of net CO_2 assimilation rate (A_{net}), stomatal conductance (g_s), transpiration rate (E), water use efficiency (A_{net}/E), to increasing of leaf to air water vapor pressure deficit (VpdL). Solid circle, open diamond, and solid triangle indicates 10°C, 20 °C, and 30 °C as air temperature in the measuring chamber, respectively. Values represent means with standard deviation (n=3-6).

The decrease of A_{net} was represented in A_{net} versus C_i graph in Fig 2. The A_{net} decreased along the demand function, and no significant depression of the demand function was detected with increasing of VpdL. This result indicates the decrease of A_{net} with increasing of VpdL was contributed by stomatal limitation. Thus the response of stomata to change in VpdL plays the

important role in regulation of the photosynthesis.

The E exhibited a peak rate around 2.5 kPa of *Vpd*L (Fig. 1). At 30°C, the E at 3.5 kPa was 86% compared with that at 1.5 kPa. The non-linear increase of the E was accompanied by decreasing of the g_s. Thus the sensitivity of stomata to change in *Vpd*L also plays the important role in avoidance of water loss in the leaves under dry air condition.

The water use efficiency of photosynthesis (A_{net}/E) decreased with increasing between 0.5 and 2.5 kPa of *Vpd*L. The decrease of A_{net}/E was accompanied by both the decrease of A_{net} and the increase of E. In contrast, the A_{net}/E kept approximate constant between 2.5 and 3.5 kPa of *Vpd*L. The minimum of A_{net}/E was 2.5 μ mol / m mol. The constant A_{net}/E was due to the slight decrease of E accompanied by decreasing of g_s despite of the decrease of A_{net}.

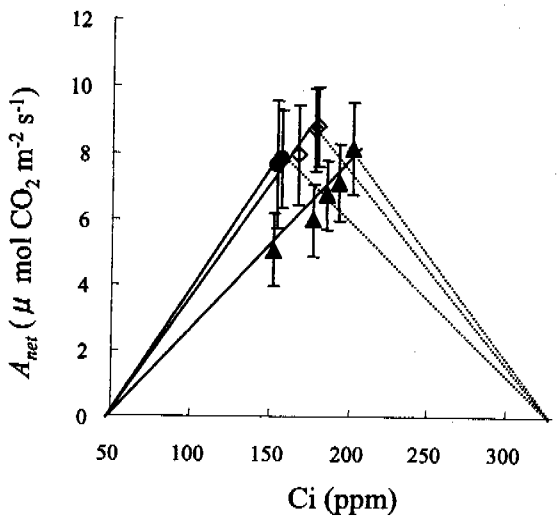

Fig.2. Relationship between net CO_2 assimilation rate (A_{net}) and intercellular CO_2 concentration (C_i) with increasing VpdL. Lines are located between CO_2 compensation points and the maximum of A_{net} (solid line; demand function) and between ambient CO_2 concentration points and the maximum of A_{net}(dotted line; supply function). Values are means with standard deviations (n=3-6). Symbols are as Fig.1.

Sandford *et al.* (1986) reported that *Larix*×*eurolepis* could not close stomata sufficiently to decrease transpiration with increasing *Vpd*L. Matyssek *et al.* (1987) reported similarly about *L.decidua*, *L. leptolepis*, and their hybrid. In contrast, Benecke *et al.* (1981) reported *L.decidua* showed the decrease of transpiration under high *Vpd*L condition. The similar manner was observed in shaded needles of *L.decidua*×*leptolepis*, but not at sun needles within the same *Vpd*L range (Matyssek *et al.* 1988). The previous study suggested that the responses of photosynthesis and stomata of *Larix* in world is not regulated by the similar manner to high *Vpd*L. In the eastern Siberia, it is very dry climate, so this response was considered to have a particularly importance to living strategy of water balance in the *L. gmelinii* individuals. Also this physiological characteristic might be a kind of adaptation to the very strict climate condition in Siberia.

REFERENCES

Benecke, U., Schulze, E.-D., Matyssek, R. Havranek, W.H. (1981) Environmental control of CO_2-assimilation and leaf conductance in *Larix decidua* Mill. I .A comparison of contrasting natural environments. Oecologia **50**: 54-61

Caemmerer S. & Farquhar G. D. (1981) Some relationships between the biochemistry of photosynthesis and the gas exchange of leaves. *Planta* **153**: 376-387.

Guehl, J. M., & Aussenac, G. (1987) Photosynthesis decrease and stomatal control of gas exchange in *Abies alba* Mill. in response to vapor pressure difference. Plant Physiol., **83**: 316-322.

Matyssek, R. & Schulze, E.-D. (1987) Heterosis in hybrid larch (*Larix decidua* × *leptolipis*) I .The role of leaf characteristics. Trees **1**: 219-224.

Matyssek, R. & Schulze, E.-D. (1988) Carbon assimilation and respiration in above-ground parts of a *Larix decidua* × *leptolipis* tree. Trees **2**: 233-241.

Sandford, A.P. & Jarvis, P.G. (1986) Stomatal responses to humidity in selected conifers. Tree Physiol. **2**: 89-103.

Schulze, E.-D. (1986) Carbon dioxide and water vapor exchange in response to drought in the atmosphere and in the soil. Ann. Rev. Plant Physiol., 37: 247-274.

Shibuya, M., Tsuno, Y., Saito, H., Takahashi, K., Sawamoto, T., Hatano, R., Isaev, A. P., Maximov, T. C. (2001) Chronosequential analysis of aboveground biomass and the carbon and nitrogen contents in natural *Larix* stands in eastern Siberia. Bull. Res. Cent. North Eurasia and North Pacific Regions, Hokkaido Univ. **1**: 57-66.

Sugimoto, A., Yanagisawa, N., Naito, D., Fujita, N., Maximov, T. C. (2002) Importance of permafrost as a source of water for plants in east Siberia Taiga. Ecol. Res., 17 493-503.

Vygodskaya, N. N., Mikyukova, I., Varlagin, A., Tatarinov, F., Sogachev, A., Kobak, K. I., Desyatkin, R., Bauer, G., Hollinger, D. Y., Kelliher, F. M., Shulze, E. D. (1997) Leaf conductance and CO_2 assimilation of *Larix gmelinii* growing in an eastern Siberian boreal forest. Tree Physiol. 17: 607-615.

Characteristics of Evapotranspiration at Cutover, Burnt and Intact Larch forest in Eastern Siberia

Y. Kobayashi[(1) (2)], T. Machimura[(3)], G. Iwahana[(4)], M. Fukuda[(4)], and A. N. Fedorov [(5)]

[(1)] Japan Science and Technology Corporation
[(2)] Research Center for North Eurasia and North Pacific Regions, Hokkaido University, Sapporo, 060-0809, Japan
[(3)] Global Architecture, Graduate School of Engineering, Osaka University, Suita, 565-0871, Japan
[(4)] Institute of Low Temperature Science, Hokkaido University, Sapporo, 060-0809, Japan
[(5)] Permafrost Instituter, Siberian Branch, Ras, Yakutsk, 677018, Russia

1. Introduction

Precise evaluations of hydrological and thermal environments and carbon dynamics over various types of surface vegetation are essential issues to predict and control the change of global environment. Especially, characteristics of heat, water and mass exchanges over Siberian taiga has become of major interest lately. The precipitation in Siberian taiga spreading in permafrost region is at the almost same level of that in steppe (semiarid) climatic zone (Japan Resources Association, 2002). The root systems of Siberian taiga are in upper part of active layer which repeats freezing-melting processes, so the Siberian taiga uses extremely limited water in the active layer. Because of severe water condition surrounding Siberian taiga, it can be considered that Siberian taiga region shows particular characteristics of evapotranspiration compared to other forest zones belonging to temperate or tropical zones. To grasp the characteristics of evapotranspiration in Siberian taiga region will contribute greatly to deeper understanding of hydrological and thermal environment of Siberian taiga.

We conducted continuous measurements of water, heat and CO_2 fluxes at intact larch forest which is typical vegetation type of Siberian taiga during growing season in 2000 and 2001. Same measurements were also conducted at burnt and cutover forest in 2000 and 2001, respectively. This paper gives brief summaries of characteristics of Evapotranspiration at the observation sites.

2. Study Site

The observation area, Neleger, is located at about 25 km northwest of the city of Yakutsk, Russia (in 62°19'N and 129°31'E). Two flux stations were constructed in an intact larch (*Larix cajanderi*) forest (*2000 Forest site*) and in a burnt forest (*2000 Burnt Site*) in 2000. The tree heights of typical larch trees are 16 ~ 18 m, and stand density was 2100 trees/ha (Yajima, et al., 1998). The forest floor is covered with a kind of moss in patches. The *2000 Burnt Site*, located at about 2 km north of 2000 Forest site, suffered a forest fire in 1989. Juvenile birches and herbaceous plants, which grew up to about 50 cm in mid summer, were scattered in *2000 Burnt Site*. The observation period in 2000 was from 16 May to 4 October.

All the larch stands, which grew up in a plot of 100×170 m surrounding the flux station of *2000 Forest site*, were cut down just after the observation period in 2000. The clear-cutting was used as a new flux station, called as *2001 cutover site*, in the observation period in 2001. Considering the dominant wind direction and the location of *2001 cutover sit*, a flux station in the larch forest (*2001 Forest site*) was relocated at about 150 m northwest from *2001 cutover site* in 2001.The flux observation in 2001 was performed from 25 April to 10 October. It is assumed that there is no significant difference of surrounding aspects such as canopy and soil moisture conditions between *2000- and 2001 Forest Site* in the present study.

3. Methods and data analyses

3. 1 Observation metod

Sensible heat (*H*), latent heat (*lE*) and CO_2 fluxes were measured by "Edisol" eddy correlation system, which consisted of an ultrasonic anemometer (Gill solnet, model R3), and a closed path infrared CO_2/H_2O gas analyzer (IRGA; LICOR Inc., model 6262). The eddy correlation measurements were conducted at 21 m in *2000- and 2001 Forest site*, and at 2 m in *2000 Burnt site* and *2001 cutover site*. Correction for inclination of the ultrasonic anemometer and "band pass-covariance method" considering the response characteristics of the IRGA, were applied in flux calculations.

Net radiation (*Rn*) was evaluated from four radiation components which were measured by a net radiometer (Kipp & Zonen, model CNR1) . Ground heat flux (*G*) was obtained by the average of outputs from three heat flux plates (REBS, model HFP-01). Soil temperature and soil moisture content were monitored with thermistor sensors (Campbell, model 107) and TDR probes (Campbell, model CS615), respectively. At the same time, vertical profile of air temperature and relative humidity were measured with humicap sensors (Vaisala, model HMP45A). The arrangements of these instruments at the each flux stations are summarized in Table 1.

Table 1. List of arrangements of the field observation instruments.

	2000 & 2001 F Site	*2000 B Site*	*20001 Cutover Site*
Wind speed	21 m, 18m	2, 0.5 m	2, 0.5 m
	* 3-cups anemometer (R. M. Young, 31002)		
Wind direction	21 m	3 m	3 m
	* Wind vane (R. M. Young, 31012)		
Sensible heat flux Latent heat flux	21 m	2 m	2 m
	*Ultrasonic anemometer (Gill Solnet, R3) and closed path infrared CO2/H2O gas analyzer (Licor-inc., 6262)		
Four radiation components	21 m	10 m	10 m
	* Radiometer (Kipp & Zonen, CNR1)		
Soil heat flux	-0.05 m	-0.05 m	-0.05 m
	* Evaluated by the average of outputs of 3 heat flux plates (REBS, HFP-01)		
Temperature & humidity	0.5, 2, 8, 14, 18, 21 m	0.5, 2 m	0.5, 2 m
	* Humicap sensor (Vaisala, HMP45A)		
Soil moisture	<2000 F Site> -0.05, -0.2, -0.45, 0.8 m <2001 F Site> -0.05, -0.15, -0.25, -0.4, -0.6, -0.92 m	-0.05, -0.2, -0.45, -0.8 m	-0.05, -0.15, -0.25, -0.4, -0.7, -1.1 m
	* TDR probe (Campbell, CS615)		
Soil temperature	Monitoring depths were same as soil moisture. * Thermistor (Campbell, 107)		

3. 2 Data analyses

3.2.1 Determination of H and lE

In general, heat, vapor and mass transports are almost took place by turbulent diffusion in a boundary layer under a certain level of wind, and the transports by molecular diffusion are approximately negligible small. However, the Neleger area is characterized by low wind, especially in night. This means that consideration of molecular diffusion is required on the occasion of determination of *H* and *lE*. For this reason, we determined *H* and *lE* by using following equation (e.g., Arita *et al.*, 2000);

$$F_C = \overline{u'C'} - \nu \frac{\partial \overline{C}}{\partial z} \quad \cdots\cdots\cdots\cdots (1)$$

where F_C is flux of a material, u' is turbulent part of u (mean wind speed), C is average concentration of a material and C' is turbulent part of C, z and ν are height and molecular diffusion coefficient, respectively. The molecular diffusion coefficient for heat (ν_{heat}) and vapor (ν_{vapor}) are given by next equation;

$$\left.\begin{aligned} \nu_{heat} &= 1.87\times10^{-5}\times\left(\frac{273.15+T_a}{273.15}\right)^{1.78}\times\frac{101.3}{P} \\ \nu_{vapor} &= 2.23\times10^{-5}\times\left(\frac{273.15+T_a}{273.15}\right)^{1.81}\times\frac{101.3}{P} \end{aligned}\right\} \quad \cdots\cdots\cdots\cdots (2)$$

where T_a and P is air temperature and pressure.

The second term in the right side of equation (1) is corresponding to the transports by molecular diffusion. The first term in the right side of equation (1), $u'C'$, is described as follows;

$$\overline{u'C'} = -K\frac{\partial \overline{C}}{\partial z} \qquad \left(K = \frac{\kappa \cdot u_* \cdot (z-d)}{\Phi}\right) \quad \cdots\cdots\cdots\cdots (3)$$

where K is turbulent diffusion coefficient, κ is Karman constant (=0.41), u_* is friction velocity, d is zero plane displacement, Φ is non-dimensional gradient profile function which is correction factor for K by considering atmospheric stability condition. Because all terms in equation (3) except for $\frac{\partial \overline{C}}{\partial z}$ are given from eddy correlation and micrometeorological data, $\frac{\partial \overline{C}}{\partial z}$ can be obtained by solving the equation (3).

3.2.2 Determination of aerodynamic and canopy resistances

Analysis of aerodynamic and canopy resistance are performed to make clear the characteristics of evapotranspiration from the larch forest. Aerodynamic resistance is evaluated by following equation (Monteith and Unsworth, 1990);

$$r_a = \frac{ln[(z-d)/z_0]}{\kappa^2 \cdot U(z)} \quad \cdots\cdots\cdots\cdots (4)$$

where r_a is aerodynamic resistance, z_0 is roughness length and $U(z)$ is wind speed at the height of z. Canopy resistance is obtained by solving the following Penman-Monteith equation (e.g. Hattori, 1985);

$$r_c = \frac{\rho \cdot c_p \cdot (e_s(T_a) - e_a)}{lE \cdot \gamma} + r_a\left\{\frac{\Delta}{\gamma}\left(\frac{Rn-G}{lE} - 1\right) - 1\right\} \quad \cdots\cdots\cdots\cdots (5)$$

where r_c is canopy resistance, ρ is air density, c_p is specific heat of air, $e_s(T_a)$ is saturated water vapor pressure at T_a, e_a is water vapor pressure, γ is psycrometric constant. The calculation for r_c are conducted under neutral condition except for rainy days and nighttime.

4.Results

Figure 1 shows the seasonal variations of energy fluxes (*Rn*, *H*, *lE* and *G*), evapotranspiration (*E*), rain (through fall for *2001 Forest Sites*) and soil water content observed at four flux stations. Evapotranspiration, *E*, increased with progress of foliation and reached its maximum level in July at *2000 Burnt* and *Forest Site*. The representative daily *E* for the larch forest during its peak was about 2 mm/day for the larch forest. The total *E* during summer season (from June to August) at *2000 Burnt* and *Forest Site* were 120 and 134 mm, respectively. The deviation of *E* between the both sites was, against expectations, about 10% at the most.

There was a significant difference of soil water condition between 2000 and 2001. Submerged soil surfaces were observed at both *2000 Burnt* and *Forest Sites* at the beginning of the observation periods (mid May), and the soil water content observed in 2000 shifted in higher range compared to that in 2001. Whereas any submerged soil surface was not found at both *2001 Cutover* and *Forest Sites* even during snow melting period. Variations in melting depths determined from the profiles of soil temperatures are also shown in Fig. 2. There was about two weeks lag of progress in the melting depth in 2001 compared to that in 2000. Due to relatively small amount of snow cover, the soil layer was subjected to severe cooling during the winter from end of 2000 (Konstantinov, personal communication). This agreed with the observation results of the non-appearance of

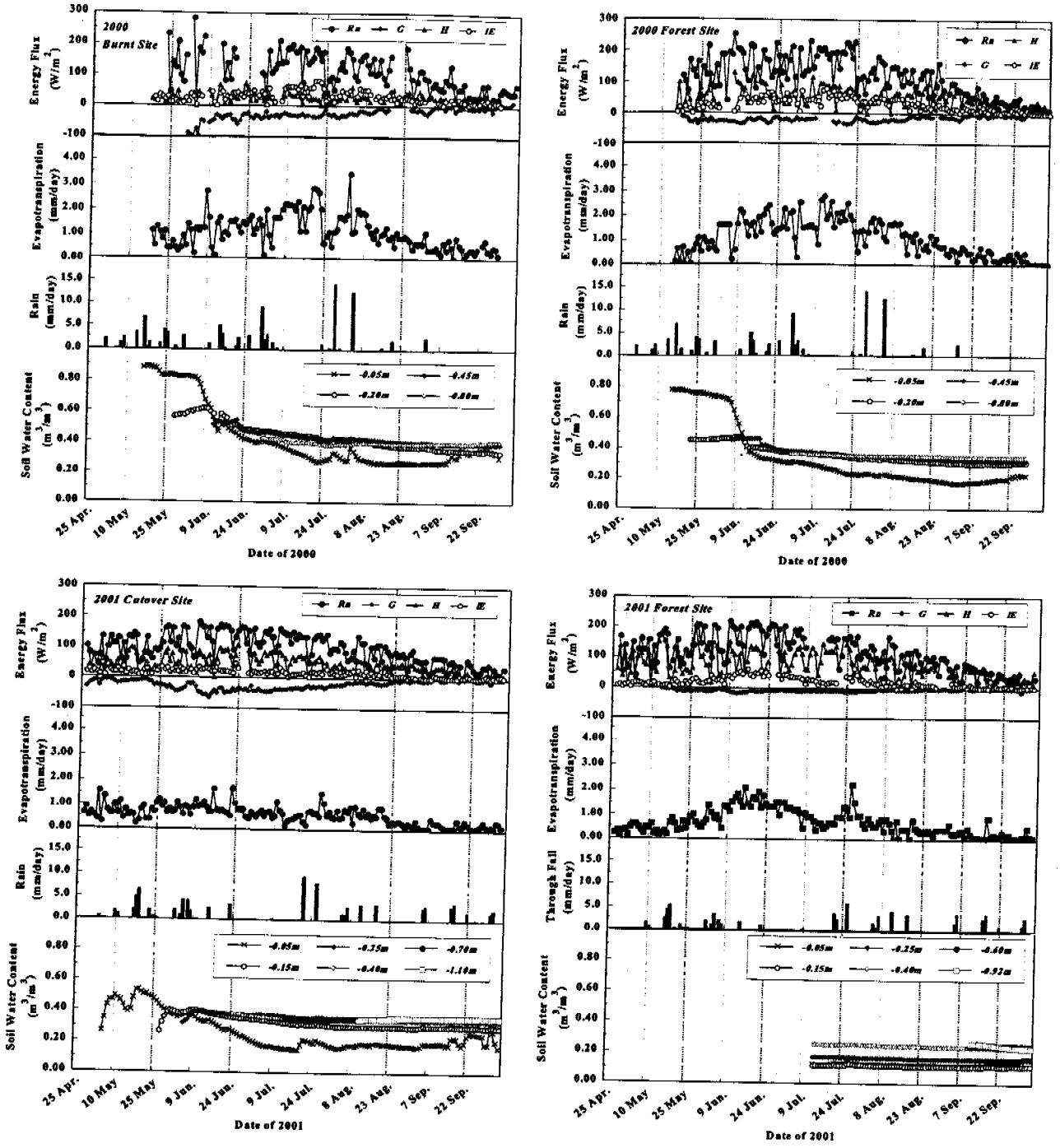

Fig. 1 Seasonal variations of field observation items

submerged soil surfaces in early spring and dry soil condition in 2001.

Although there were almost the same of no-rainfall periods in the summer of 2000 and 2001, clear decrease in E was observed only in *2001 Forest Site*. It can be considered that E measured at *2001 Forest Site* was highly controlled due to the lower soil water condition, especially after beginning of July. The total amount of E during summer season at *2001 Forest Site* was only about 70% of that at *2000 Forest Site* in the equivalent period.

A clear effect of cutover on the evapotranspiration was observed at *2001 Cutover Site*. Variations in E depended on the water content of surface soil and rainfall events (Fig. 1). The discrepancy of soil water content between *2001 Cutover* and *Forest Site* showed the effect of water uptake by the root system of the larch stands, and little supply of precipitation on forest floor due to the interception at the forest (Fig. 1). When the soil water content at the depth of 5 cm (SWC_5) was

more than 0.2, daily amount of E showed almost constant value of 1.0 mm/day. Remarkable decrease in E was actualized when SWC_5 was less than 0.2. This result suggested that the water movement in the surface layer of soil was took place in not liquid phase but vapor phase under the condition of $SWC_5 < 0.2$.

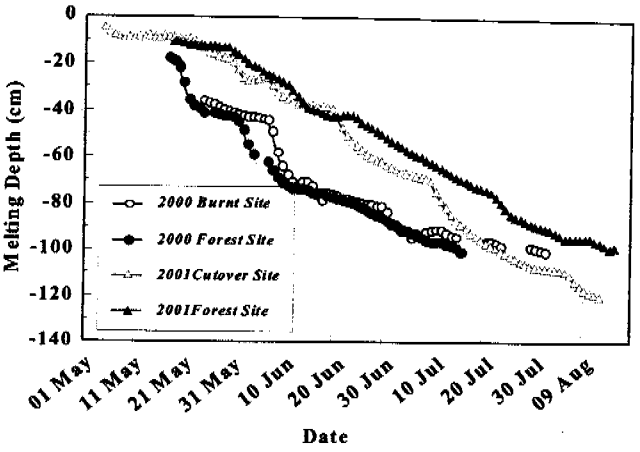

Fig. 2 Progress of melting depth in active layer.

5. Discussions

As mentioned above, the difference of seasonal variations in E observed at *2000* and *2001 Forest Sites* were mainly caused by the difference of soil water condition. The observation results may show that it is the soil water condition at the beginning of growing season that significant influences the evapotranspiration during growing season. Appearances of submerged soil surfaces found in 2000 suggested that the snowfall in winter following the autumn in 1999 was more than that in 2000. As the result, the sever cooling of soil layer was relatively relieved in winter, then the progress of the melting depth was accelerated in melting and growing seasons in 2000 (Fig. 2). It can be said that the progress of the melting depth means the increase in the capacity of soil layer against the melting water infiltrating from the soil surface (Figs. 1 and 2). Evapotranspiration, E, at *2001 Forest Sites* in summer season, including for about three weeks of rain free period, was maintained under the relatively high soil water condition caused by larger amounts of snowfall and moderate cooling of soil layer.

Comparisons of diurnal variations in observation items with vapor pressure deficit (VPD), r_c

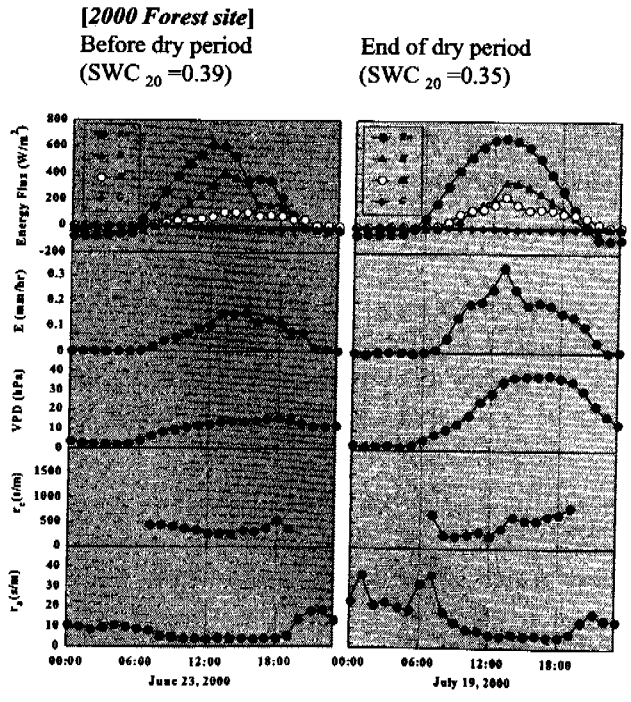

Fig. 3a Comparison of diurnal variations in energy fluxes, E, VPD, r_a and r_c observed in before and end of dry period in *2000 Forest Site.*

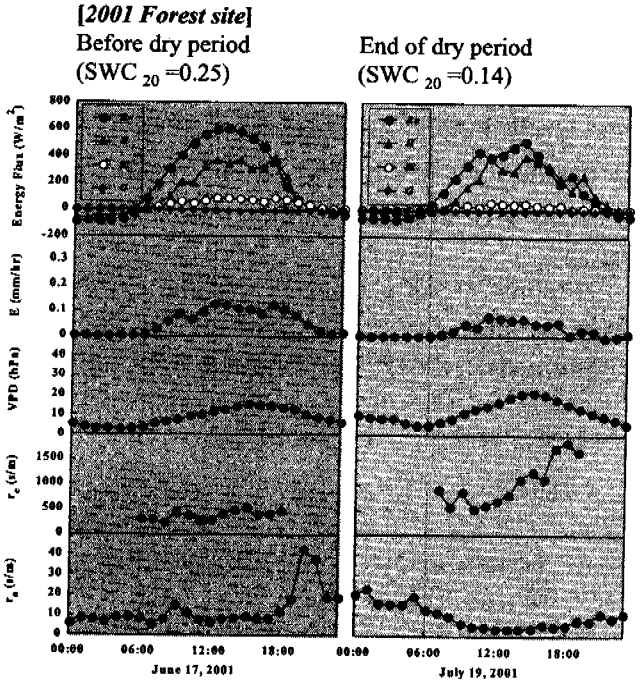

Fig. 3b Same as Fig. 3a, but for *2001 Forest Site.*

and r_a at mid June (before dry period) and mid July (end of dry period) in *2000* and *2001 Forest Sites* are shown in Figs. 3a and 3b, respectively. Corresponding average soil water contents at near root zone (20 cm in depth, SWC_{20}) of larch stands are also listed. On the whole except for the end of dry period in 2001, the patterns of change in E were similar to those in VPD, and r_c changes in the same range of under 500 s/m. Decrease in E and increase in r_c were clearly observed at the end of dry period at *2001 Forest Site*. The variation in E, being highly inhibited, did not keep pace with that in *VPD* at the period. Furthermore corresponding SWC_{20} was less than 0.2, and judging from the relationship between daily E and SWC_5 at *2001 Cutover Site* (Fig. 1), the soil water condition of $SWC_{20} < 0.2$ meant that the larch stands were under extremely sever water stress. The interrelationship among E, *VPD* and SWC_{20} at the larch forest is shown in Fig. 4. This figure suggests that *VPD* is main control factor of E under relatively wet soil condition, *i.e.* $SWC_{20} > 0.25$. It can be concluded that *VPD* in the range of 15 ~ 20 (hPa) was the most suitable condition for active transpiration of the larch stands under the condition of enough supply of soil water. On the other hand, *VPD* lost its function as a control factor of the transpiration from the larch stands when SWC_{20} decreased to less than 0.2. Various r_c are also plotted against *VPD*, SWC_{20} and E in Fig. 5. Relatively high E (*i.e.* E > 0.25 mm/hr) appears in the range of 100 ~ 400 s/m of r_c. Canopy resistance, r_c, in the range of 100 ~ 400 s/m concentrate in the ranges of $10 < VPD < 20$ and $0.25 < SWC_{20} < 0.4$. This also supports the conclusion about the controlling factors of E and their effective ranges.

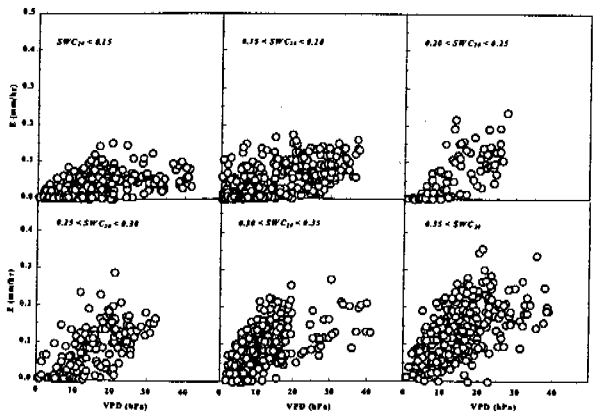

Fig. 4 Relationship between VPD and E at the larch forest.

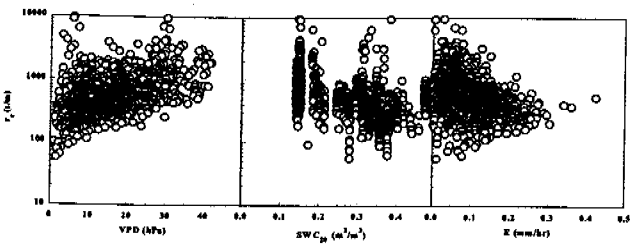

Fig. 5 Canopy resistance (r_c) as a function of *VPD*, SWC_{20} and E at the larch forest.

Figures 4 and 5 indicate that the environmental conditions during the growing season in 2000 were suitable for transpiration of the larch forest compared to that in 2001. However, the total amount of E at *2000 Forest Site* was only about 10 % higher than that at *2000 Burnt Site* (see Result). The fact may require a reassessment of general view about the role of Siberian taiga in local and/or regional hydrological cycle.

REFERENCES

Arita, M and T., Nakai (2000): "*Science of atmosphere*"(Arita, M. Editor), TokyoDenki University Press, Tokyo.

Hattori, S. (1985): Explanation on deviation process of equations to estimate Evapotranspiration and problems on the application to forest stand. *Bull. For. and For. Prod. Res. Inst.*, **232**, 139-165.

Japan Resources Association (2002): Environmental and resources problems in subarctic regions. In *Research report of surveillance study on maintenance of global environment and earth resources by earth satellites*, pp.104-112. (in Japanese)

Monteith, J. L. and Unsworth, M. H. (1990) "*Principles of environmental physics*", 2nd edn. Edward Arnold, London.

Yajima, T., Takahashi, K., Sasaoka, E., Hatano, R., Sawamoto, T., Ivanov, B. I., Isaev, A. P. and Maximov, T. C. (1988): Stand structure and biomass of *Larix Cajyandrei* forest in Siberian taiga. *Proceedings of the 6th Symposium on the Joint Siberian Permafrost Studies between Japan and Russia in 1997*, 72-80.

Comparison of the Surface Energy Balance Conditions in Different Stages after Forest Disturbance in Yakutsk Region, Eastern Siberia

G. Iwahana[1], T. Machimura[2], Y. Kobayashi[3], M. Fukuda[1] and A. N. Fedrov[4]

1. Institute of Low Temperature Science, Hokkaido University, e-mail: go@pop.lowtem.hokudai.ac.jp 2. Graduate School of Engineering, Osaka University 3. Japan Science and Technology Corporation 4. Permafrost Institute, Russian Academy of Science

1. Introduction

It has been recognized that forest disturbance is one of the triggers in the formation of Alas with Thermokarst Lake, which is developing in the continuous permafrost region, Central Yakutia, Eastern Siberia, Russia. The disturbance of surface vegetation and the organic layer changes the energy balance on the surface significantly. Depending on the degree of surface disturbance, forest recovery seems to be the usual result, rather than the formation of Alas under present climatic conditions. The permafrost, which impedes downward water drainage, is very thick in this region (400m, Fig.1). It has been considered that decreased evapotranspiration and excess water from thawed layers would be found in disturbed forest areas, and that soil water content would tend to increase. Within a few years after a fire, thick aspens or weeds will cover the burnt forest surface, if the ground surface is not completely submerged. This regenerated surface vegetation reduces the solar radiation to the ground. The objectives of this study are to compare the difference of the radiant environment in a larch forest and at the disturbed sites and to compare the surface energy balance components in a larch forest and at the disturbed sites.

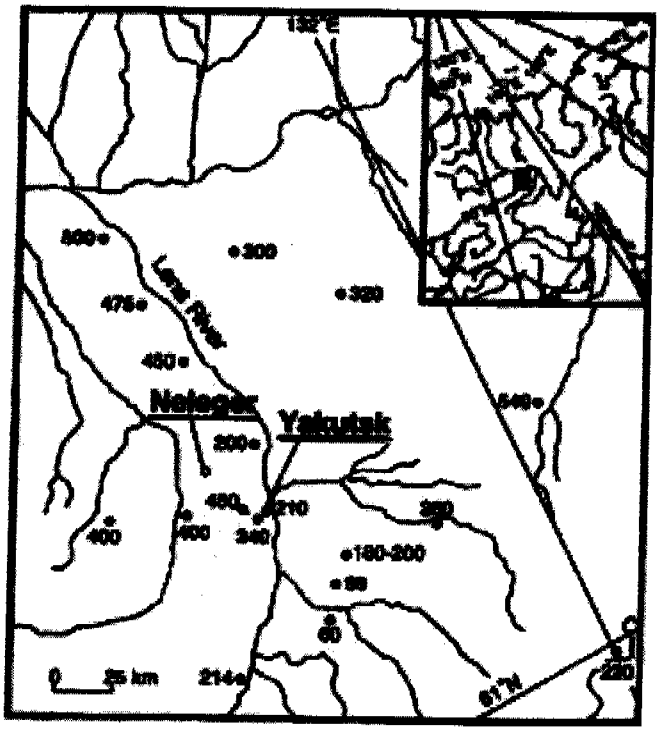

Figure 1. Location of research area Neleger near Yakutsk. The numbers in closed circles are the permafrost thickness in meters (after Wada et al. 2000).

2. Site description

The research area Neleger was about 35km northwest of Yakutsk (62°19'N, 129°31'E), Russia (Fig. 1), 24km from the Lena River course and 14km from the slope edge of the Lena valley. The mean annual temperature at Yakutsk was approximately −10.2°C and annual precipitation about 234mm. The study sites were located on the highest terrace of the left bank of the Lena River. The geological basement of this area was covered with a thin layer (6-8m) of Quaternary deposits consisting of alluvial deposits with ice complex of the Lena River or recent temporary streams and creeks. The landscape on this terrace was almost flat and consisted of pure and mixed stands of larch, birch, pine, swamp and thermocarsts called as Alas. The research area was 215-221m above mean sea level. The measurement points were chosen for their possible stages after forest destruction and designated as shown in Table1.

Site A was a mature larch stand (*Larix gmelinii*; over 200 years old) with a mean tree height of 8m and a density of 2100 trees/ha

Table 1. Designation and instruments configuration of research sites.

Instruments	Site						
	A	B	C	D	E	F	G
	Larch forest	1-yr cutover	5-yr cutover	12-yr burnt	19-yr burnt birch forest	Swamp	Alas
Net radiometer (m)	21	9	2.5	2.5	5	2.5	2.5
Soil temperature probe (cm)	0,10,20,30, 40,60,80, 100,120,140 , 160	0,5,10,20, 40,70,110, 160	0,3,13,23, 33,53,73, 93,113,128, 153,173,193	0,5,10,20, 40,70,110, 160	0,5,10,20, 30,40,60, 80,100,120, 140,160	0,5,10,20, 30,49,68, 88,108,128, 148,168,188	0,5,10,20, 30,40,60, 80,100,120, 140,160,180 , 200,220
Heat flux plate (cm)	10	10	1	1	1	1	1
TDR probe (cm)	5,15,25, 40,60,92	5,15,25, 40,70,110	-	-	-	-	-

(Yajima *et al.*, 1998). The mean canopy height was approximately 20m. The distance from the measurement point to the nearest Alas is about 100-150m. The underlying vegetation comprises lichen, some mosses and some shrubs.

Site B was a cutover site, which was deforested in the November 2000. The deforested area was a rectangle of 100m×170m about 100m from Site A. The surface vegetation was disturbed during logging; however, the moss and organic layers remained as they were.

Site C was a 5 yr old cutover site with a diameter of 200m. The site was covered with shrubs or grasses and small ponds.

Site D was about 1km from site A and had experienced a wild fire in 1989. The vegetation of site D consists of short grass averaging 15cm in height and ground lichen with sparse birch saplings. The diameter of site D was about 150m.

Site E was a predominantly covered by birch stand with a diameter of about 100m, which had experienced a wild fire 19 years ago. The mean canopy height was approximately 3m. This birch stand was surrounded by a mixed stand of larch and birch developing toward larch forests or Alasses.

Site F was a swamp filled with mounds with a mean diameter of 40cm and a mean height of 40cm. The mounds were about 30cm apart from each other. Each mound was covered by grass to a height of 15-25cm and the soil surface was almost invisible. Occasionally, there were some spaces with no mounds forming small ponds.

Site G was an Alas with the dimensions of 300m×900m. There was a thermokarst lake with two pingos in the center of this Alas. The measurement point was 200m south of the lake margin and covered with tall grass to a height of 0.3m.

Table 2. Observation period at each site

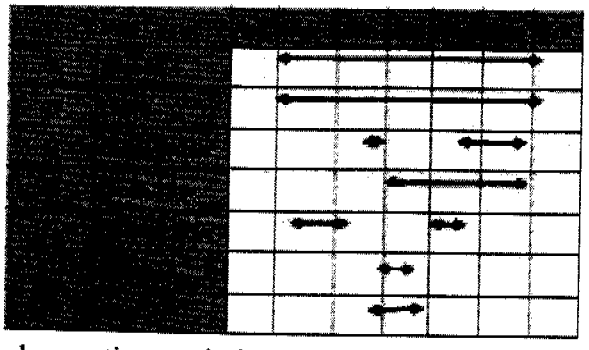

3. Instruments and Methods

A 21 m tower and 9 m tower with micrometeorological measuring instruments were installed at sites A and B, respectively. The instrument towers at sites A and B were set throughout the field season. At other sites, simple 3-5 m pines were used to mount the measuring instruments and 2 measuring sets were used to cover wide range of the observation period. The observation period at each site is shown in table2. The instruments of all sites-treated in this paper are shown in table1. All measurements in the towers were made every 10 seconds and data were recorded as 10 minute averages on dataloggers (CR10X, Campbell Scientific, Inc.) All components

of net radiation were measured separately by net radiometer (CNR1, Kipp &Zonen) at each site. Calibrations were made after observation and found to differ from each other by less than 1%.

Net radiation, Rn, is defined as

$$Rn = Si - So + Li - Lo$$

and albedo α as

$$\alpha = So / Si$$

where and Si, So, Li and Lo are solar radiation, reflected solar radiation, longwave radiation emitted from the surface and atmospheric longwave radiation, respectively.

Soil temperatures were measured by calibrated 107 temperature probes (Campbell Scientific, Inc.) at sites B and D. Calibrated temperature probes with thermistors (104ET, Isizuka denshi) were used at other sites. The overall probe accuracy for the temperature range of -10° to 40°C was calculated as less than ±0.1°C. The measurement depths of soil temperatures are shown in table1. During non-tower observations at sites C, D, E, F and G, soil temperatures were measured manually at 4-10 day intervals.

Volumetric soil water contents at sites A and B were measured with TDR probes (CS615 Campbell Scientific, Inc.) at the depths shown in table1. At all sites, soil samples were taken from layers every 10 cm at 4-10 day intervals and used for calibration of TDR probes.

Soil heat fluxes at sites A and B were measured by placing 3 heat flux plates (HFP-01, REBS) and averaged. At other sites, soil heat fluxes were evaluated by averaging 2-3 plates (HFP01SC, Hukseflux)

Ground heat flux was estimated as the sum of heat flux at sensor position Gs and heat storage change above the plates according to

$$G = Gs + C(dT/dt)dz$$

where C is the volumetric heat capacity, dT is the temporal change of average temperature over the depth interval dz and time interval dt. The heat capacities of the upper layer over plates were determined based on the density and volumetric water content and specific heats of the constituents (De Vries, 1963).

Air temperatures at each site were measured at 1.5 m above the ground surface in ventilated shelters using (HMP45A, Vaisala) at sites A and B, and 107 temperature probes (Campbell Scientific, Inc.) at other sites. Precipitation was measured using a tipping bucket rain gauge at site B.

Sensible and latent heat fluxes were measured using the University of Edinburgh Edisol system (Moncrieff *et al.*, 1997). Three-dimensional sonic anemometer (Solent, Gill Instruments Ltd., Lymington, England) was mounted 21 m and 1.5 m above the ground at site A and site B, respectively. Water vapor pressure was measured by a closed pass method using an infrared gas analyzer (LI-6262, LI-COR Inc.).

4. Results and discussion

4 - 1 Comparison of radiant environments over all observation sites

Snow melting was completed in the beginning of May at all sites this year. The foliation in the forest was completed in the beginning of June. Seasonal net radiation was greatest during June and continuously decreased to the season of leaf falling at the end of August. In table 3, albedo, the ratio of net radiation to solar radiation and the ratio of net radiation to net radiation at site A during the growing season (14 June to 14 August) are shown.

Net radiation at the sites after forest disturbance was 81 to 92% of the value at the control site (site A) and increased as the vegetation recovered. Less net radiation at disturbed sites is mainly due to the higher albedo. The exception is site C, where small ponds covered a few parts of the site area. The albedo at site C increased significantly as the small ponds dried up. Seasonal change of albedo was associated with vegetation change at each site. The peak values in spring and fall represent snowfall.

Table 3. Albedo, the ratio of net radiation to solar radiation and the ratio of net radiation to net radiation at site A.

14jun-14jly	site						
	A	B	C	D	E	F	G
albedo	0.10	0.16	0.13	0.19	0.16	0.19	0.21
Rn / Si	0.64	0.53	0.64	0.53	0.59	0.52	0.50
Rn / Rn(siteA)	1	0.83	1.03	0.81	0.92	0.84	0.83

4 - 2 Comparison of energy balance components between site A (forest) and site B (cutover)

The daily sum of rainfall and the seasonal change of the fluxes of sensible, latent and ground heat at site A and site B together with the ratio of the value at site B to that at site A were compared. Latent heat flux at site B was 80% of that at site A, indicating less evapotranspiration at site B and the possibility of geographical change into swamp. The ratio of latent heat flux at site B to that at site A changed seasonally and showed a U shape over the observation period, with the value 0.5 in the mid summer and 3 at the beginning and the end of observation period. At site B, the sensible heat flux was 32% less than at site A while ground heat flux was about 3.6 times greater. Consequently, the maximum thaw depth at site B was about 20 cm deeper than at site A. Seasonal variations of soil temperature at sites A and B are shown in figure 13. Daily amounts of energy balance components from 14 June to 14 August and the ratio of the value at site B to site A are shown in table 4. The percentages of each value to net radiation are shown in the lower part of the table.

4-3 Change of active layer condition after forest disturbance

Seasonal variation of soil temperature at site A and B is shown in Figure 2. Thawing of frozen ground commenced at the beginning of May and maximum thaw depth were measured at the beginning of September at each site. Maximum thaw depth at site B (126cm) was 20cm deeper than that at site A (106cm). Freeze back from top down and from permafrost was observed from in the middle of September.

The trends of the changes in radiation environment after forest disturbance found in this study were similar to those found in the study of (Rouse W. R., 1976). In this study, sites C, F and G were far from the most likely trend. This suggests that the excess water from permafrost has an important role in irreversible topographic changes such as Alas forming, a swamp forming. Other trends of radiant environment change should be found in future research.

Sharratt B.S., 1998 concluded that clearing forest land will enhance soil drying in the subarctic. However, in this study, deforestation reduces the evapotranspiration of the site resulting in higher soil water content in early stage of vegetation recovery. Since small ponds forming at the disturbed site could

Table 4. Daily amounts of energy balance components from 14 June to 14 August and the ratio of the value at site B to site A. The percentages of each value with respect to net radiation are shown below.

	Rn	H	lE	G	
site A	1211	671	222	61	
site B	1034	457	177	216	(MJ/m^2)
A/B	0.85	0.68	0.80	3.55	
ratio to Rn	Rn	H	lE	G	
site A	100%	55%	18%	5%	
site B	100%	44%	17%	21%	

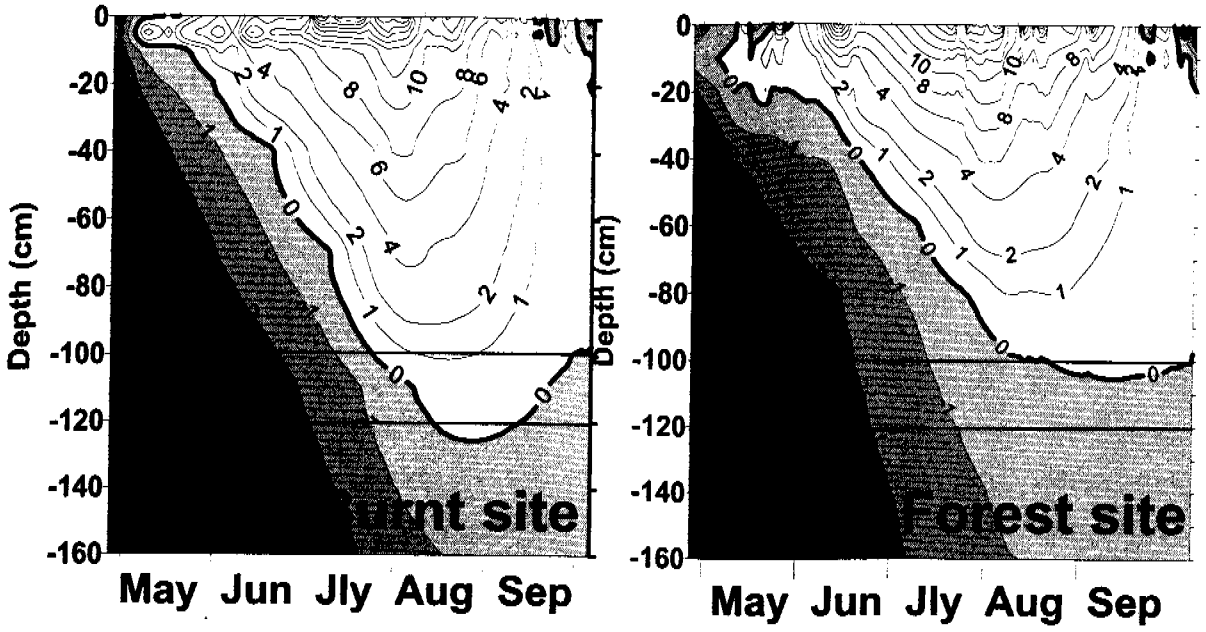

Fig. 2 Seasonal variation of soil temperature at site A and B. The numbers on isothermal lines are in degree Celsius.

receive more net radiation, maximum active layer deepening should occur in the early stage of vegetation recovery.

5. Conclusions

Net radiation at the sites after forest disturbance was 81 to 92% of the value at the control site (site A) and increased as the vegetation recovered. Less net radiation at disturbed sites is mainly due to the higher albedo. The exception is site C, where small ponds covered a few parts of the site area. The albedo at site C increased significantly as the small ponds dried up.

Comparison of the energy balance components shows that latent heat flux at site B was 80% of that at site A, indicating lower evapotranspiration at site B and the possibility of geographical change into swamp. At site B, the sensible heat flux was 32% less than at site A while ground heat flux was about 3.6 times greater. Consequently, the maximum thaw depth at site B was about 20 cm deeper than at site A.

REFERENCES

De Vries, D.A. (1963) : Thermal properties of soils. In Van Wijk, W.R. (ed.), *Physics of the Plant Environment*. Amsterdam: 210-235.

Isaev, A.P. (2000) : Post-fire dynamic of larch forests in north-east Siberia (Yakutia). *Proceedings of the 9th Symposium on the Joint Siberian Permafrost Studies between Japan and Russia in 2000*: 3-9.

Moncrieff, J.B., J. M. Massheder, A. Verhoef, J. Elbers, B.H. Heutsunkveld, S. Scott, H. de Bruin, P. Kabat, H. Soegaard, and P. G. Jarvis. (1997) : *A system to measure surface fluxes of energy, momentum and carbon dioxide, J. Hydrol.*, 188-189, 589-611.

Rouse, W.R. 1976. Microclimate changes accompanying burning in subarctic lichen woodland. *Arctic and Alpine Research* 8(4): 357-376.

Sharratt, B.S. (1998) : Radiative exchange, near-surface temperature and soil water of forest and cropland in interior Alaska. *Agricultural and Forest Meteorology* 89: 269-280.

Wada, K., Harada, K. & Fukuda, M. (2000) : Deep resistively structure of permafrost area in Siberia by transient electromagnetic method. *Proceedings of the 8th Symposium on the Joint Siberian Permafrost Studies between Japan and Russia in 1999*: 264-272.

Yajima, T., Takahashi, K., Sasaoka, E., Hatano, T., Sawamoto, T., Ivanov, B. I., Isaev, A. P. &

Maximov, T. C. (1998) : Stand structure and biomass of *Larix cajanderi* forest in the Siberian taiga. *Proceedings of the 6th Symposium on the Joint Siberian Permafrost Studies between Japan and Russia in 1997*: 72-80.

Drought limitation of CO_2 assimilation rate in *Larix gmelinii* saplings growing on understory of the mature stand

H. Saito[1*], K. Yamamuro[1], Y. Tsuno[1], H. Iijima[1], K. Takahashi[1], T.C. Maximov[2]

[1] Graduate School of Agriculture, Hokkaido University. Forest Dynamics Group, CREST
[2] Institute of Biological Problems of Cryolithozone, Russian Academy of Science* Phone: +81-11-706-2523, Fax: +81-11-706-4176, e-mail: saitoo@for.agr.hokudai.ac.jp

1. Introduction

In mature *Larix gmelinii* stands, widely distributed in boreal coniferous forest of Eastern Siberia, regeneration of the *L. gmelinii* seedlings occurs on the stand floor (Saito *et al.*, 2000), although *L. gmelinii* is classified as the most shade-intolerance as well as the other *Larix* species (Nikolov & Helmisaari, 1992). In general, light conditions are the most important factor to limit the growth of regenerated seedlings and saplings in mature stands. However, *L. gmelinii* stand floor is frequent sunlit by sunspot due to loosely closed stand canopy (Tsuno *et al.*, 2000; Saito *et al.*, 2003). While, the soil moisture condition is strongly dry due to a little precipitation, which is approximately 200 to 300 mm of mean annual precipitation (Archibold, 1995; Sugimoto *et al.*, 2002), because this region belongs continental climatic zone. Therefore we focused on the drought condition as a limiting factor of the regenerated *L. gmelinii* seedlings and saplings in the matured stands. To examine the drought limitation, in this study, an irrigation trial was carried out in the understory conditions. The diurnal change in net CO_2 assimilation rate (A_{net}) was compared between before and after the irrigation.

2. Methods

Study site was located in Neleger (62°18'N, 129°30'E), approximately 30 to 40 km from Yakutsk in the Republic of Sakha, Russia. The maximum height of the *L gmelinii* stand was 21 m. The tree density was 1275 per hector. Their details were described by Saito *et al.* (2001) and Shibuya *et al.* (2001). The texture of the underlying soil horizons was silt loam.

The samples for experiment were naturally regenerated saplings of *L. gmelinii*. The height of sample tree was approximately 1.5 to 2.5 m. The diurnal change in A_{net} was measured under a natural condition on clear blue sky day from 13 July and 17 July, 2001. The photosynthetic photon flux density (*PPFD*) above the stand canopy was measured by *PPFD* sensor (L190SA, Li-cor, Lincoln, USA). The air temperature and air humidity was measured by air temperature and humidity sensors with data-logger (RS11, Espec Mic Co., Tokyo, Japan). The air water vapor pressure deficit was calculated from the air temperature and relative humidity. The soil moisture of the volumetric water content at approximately 20 cm depth was measured by TDR sensor (Trime-como, Tohoku electronic industry, Sendai, Japan). The A_{net} was measured by using a portable photosynthesis system with conifer chamber (LI6400, Li-cor, Lincoln, USA). The light

conditions, air temperature and air vapor pressure deficit in the gas-exchange chamber depend on the ambient conditions. The CO_2 concentration in the gas-exchange chamber was controlled at 490 ppm until 1000h and 375 ppm after 1100h, the CO_2 concentration was similar to the actual CO_2 concentration. The irrigation was treated at 2100h – 2200h from 13 to 16 July. The amount of the water in the irrigation was 5 little per saplings. The volumetric soil moisture content before the treatment of irrigation was 7 to 10%, and in the measuring day of CO_2 assimilation rate after the treatment of irrigation, the volumetric soil moisture content was 25 to 30%.

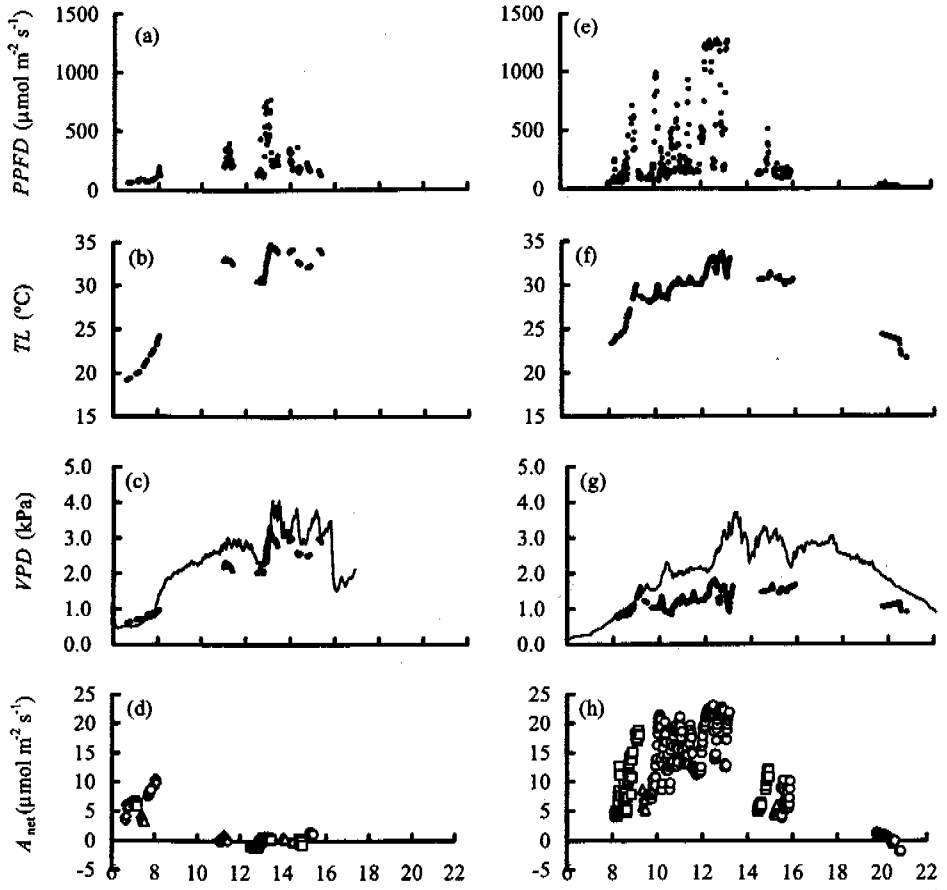

Fig. 1 Diurnal change in photosynthetic photon flux density (*PPFD*; a, e), estimated leaf temperature (*LT*; b, f), air water vapor pressure deficit and the estimated leaf to air water vapor pressure deficit (*VPD;* c, g), and net CO_2 assimilation rate (A_{net};d, h) in *Larix gmelinii* saplings growing on understory. Panel a to d and panel e to h denote before and after treatment of irrigation, respectively. The line and dot in panel c and g denotes air water vapor pressure deficit and leaf to air water vapor pressure deficit, respectively. The four different symbols in panel d and h denote the different saplings for the replication.

3. Results and Discussions

In the morning before the treatment of irrigation, the A_{net} increased with increasing of *PPFD*, air temperature, and leaf to air vapor pressure deficit (Fig. 1a-d). Thereafter, the A_{net} deceased to near 0 μmol CO_2 g^{-1} s^{-1} before noon time. At the time, *PPFD* was over 200 μmol m^{-1} s^{-1}, air temperature was over 30°C, and leaf to air vapor pressure deficit was over 2.0 kPa. In the afternoon, the low A_{net} was kept, although the *PPFD* increased to over 600 μmol m^{-1} s^{-1}. These results suggest that the *PPFD* is not a major factor to limit A_{net} in the midday.

In the morning after 4 days treatment of irrigation, the A_{net} increased with increasing of *PPFD*, air temperature, and leaf to air vapor pressure deficit (Fig. 1e-h). Thereafter, no strong midday depression of A_{net} like the before the treatment of irrigation was detected. The A_{net} changed as following the fluctuation of the *PPFD*. When the *PPFD* was over 500 μmol m^{-1} s^{-1}, the A_{net} increased to approximately 20 μmol CO_2 g^{-1} s^{-1}.

The apparent relationships among *PPFD*, leaf temperature, leaf to air water vapor pressure deficit, and A_{net} represented from the diurnal changes were shown in Fig. 2-4, respectively. The tendency after the treatment of the irrigation represented a typical light response curve of A_{net} (Fig. 2). It appeared that the light saturation point of A_{net} was between 400 to 500 μmol m^{-1} s^{-1}. Fig. 3 shows the apparent relationship between leaf temperature and A_{net} over 500 μmol m^{-1} s^{-1} of *PPFD* as the light saturation point in the irrigated saplings. No significant depression of A_{net} was represented with increasing of leaf temperature, but the hysteresis roop was described passing to afternoon. Fig. 4 shows the apparent relationship between leaf to air water vapor pressure deficit and A_{net} over 500 μmol m^{-1} s^{-1} of *PPFD* as the light saturation point in the irrigated saplings. No significant depression of A_{net} was represented with increasing of the leaf to air water vapor pressure deficit. These results indicate that the high leaf temperature and the leaf to air water vapor pressure deficit are not a major factor to limit the A_{net} in the midday.

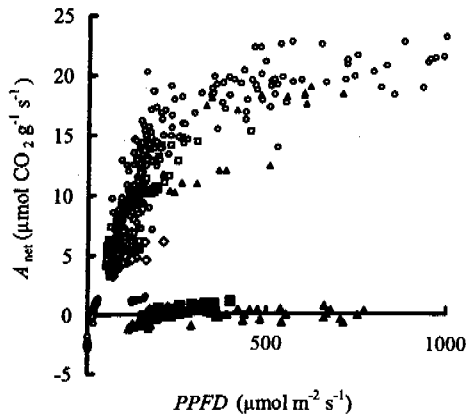

Fig. 2 Light dependency of CO_2 assimilation rate in understoried *Larix gmelinii* saplings comparing between bofore and after irrigation.. Closed and open symbol denotes result before and after treatment of irrigation, respectively. The four different symbols denote the different samples.

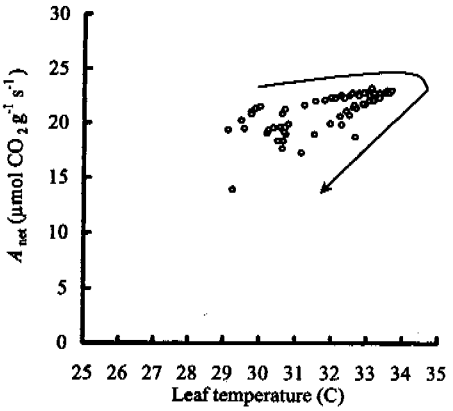

Fig. 3 Temperaure dependency of net CO_2 assimilation rate in understoried *Larix gmelinii* saplings after the treatment of irrigation. Arrow denotes progress in the diurnal change.

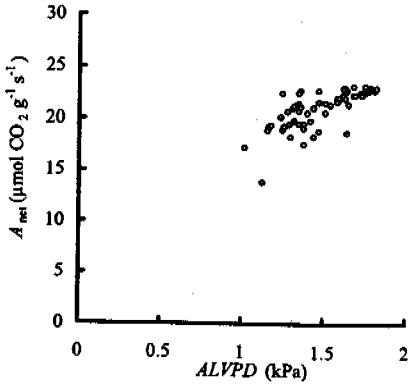

Fig. 4 Leaf to air water vapor pressure deficit (*ALVPD*) dependency of net CO_2 assimilation rate in understoried *Larix gmelinii* saplings after irrigation.

In contrast, the A_{net} before the treatment of irrigation was significantly lower compared with the

after the treatment of the irrigation in the apparent relationship between *PPFD* and A_{net} (Fig. 2). Compared between the environmental conditions before and after the treatment of the irrigation, the range of the leaf temperature was similar. The air water vapor pressure deficit in the measuring day before the treatment of the irrigation was also similar to that after the treatment of the irrigation. Nevertheless the higher leaf to air vapor pressure deficit before the treatment of irrigation was due to lower transpiration rate (data not shown). Therefore the increasing of the soil moisture condition causes the increasing of the diurnal change in A_{net} after the treatment of the irrigation. Our results indicate that the drought condition in the *L. gmelinii* stand floor is a major factor to limit the A_{net} in the understoried *L. gmelinii* saplings in the summer.

REFERENCES

Archiboldo, W. (1995) : Coniferous forests. In: Ecology of world vegetation pp.238-279. Chapman & Hall, London.

Nikolov, N., Helmisaari, H. (1992) : Silvics of the cirvumpolar boreal forest tree. In A systems analysis of the grobal boreal forest (Eds., Shugart, H. H., Leemans, R., Bonan, G. B.) pp. 565, 13-84, Cambridge University press, New York.

Saito, H., Takahashi, K., Shibuya, M., Tsuno, Y., Isaev, A. P., Maximov, T. C. (2001) : Distribution of 1-years-old larch seedlings and vegetation on a matured larch forest floor in eastern Siberia In Proc. 9th Symposium on the Joint Siberian Permafrost Studies between Japan and Russia in 2000 (Eds. Fukuda, M. and Kobayashi, Y.), 75-82, Sapporo, Japan.

Saito, H., Yamamuro, K., Tsuno, Y., Iijima, H., Shibuya, M., Takahashi, K., Maximov, T.C. (2003) : Spatial variations of light intensity and photosynthetic properties within a *Larix gmelinii* tree crown in eastern Siberia. In Proc. 10th Symposium on the Joint Siberian Permafrost Studies between Japan and Russia in 2001 (Eds. Fukuda, M. and Saito, H.), Sapporo, Japan (in press).

Shibuya, M., Tsuno, Y., Saito, H., Takahashi, K., Sawamoto, T., Hatano, R., Isaev, A. P., Maximov, T. C. (2001) : Chronosequential analysis of aboveground biomass and the carbon and nitrogen contents in natural *Larix* stands in eastern Siberia. Bull. Res. Center North Eurasia North Pacific Regions Hokkaido Univ., 1, 57-66.

Sugimoto, A., Yanagisawa, N., Naito, D., Fujita, N., Maximov, T. C. (2002) : Importance of permafrost as a source of water for plants in east Siberia Taiga. Ecol. Res., 17 493-503.

CH_4 flux from a forest-Alas ecosystem near Yakutsk, Eastern Siberia, Russia

T. Morishita[1], R. Hatano[2] and R. V. Desyatkin[3]

[1]Graduate School of Agriculture, Hokkaido University, Sapporo, 060-8589, Japan,

Phone: +81-11-706-2503, Fax: +81-11-706-4960, e-mail: morimori@chem.agr.hokudai.ac.jp

[2]Field Science Center for Northern Biosphere, Sapporo, 060-8589, Japan

[3]Institute of Biological Problems of Cryolithzone, Russian Academy of Sciences,

Yakutsk 677891, Republic of Sakha, Russia

1. Introduction

CH_4 is an important greenhouse gas that contributes about 20% to the radiative forcing of the global climate (IPCC, 1995). Major sources of atmospheric CH_4 are the production and use of energy, biomass burning, rice fields, natural wetland systems, landfills, and enteric fermentation in animals and termites. Estimates of total CH_4 emission range from 400 to 600 Tg y^{-1} (IPCC, 1995). The major sinks are thought to be atmosphere and soils: 470 Tg y^{-1} is estimated to be consumed by the reaction of CH_4 with hydroxyl radicals in the atmosphere, while forest soils consume 30 Tg CH_4 y^{-1} (IPCC, 1995). CH_4 flux from soils is affected by soil temperature and moisture (Castro et al., 1994; Whalen and Reeburgh, 1996; Prime and Christensen, 1997; Boden et al., 1998), because microbiological processes regulate the production and consumption of CH_4 in soil (Mer and Roger, 2001). As land-cover change often changes the thermo-hydrological conditions of the soil, forest disturbance is generally considered to decrease the CH_4 consumption activity of soil (Dobbie et al., 1996).

Taiga forests in Eastern Siberia cover 2.8×10^6 km^2, corresponding to 8% of the total forested area of the world (Alexeyev et al., 2000). However, the Taiga forests are disappearing due to forest fires (Goldammer and Furyaev, 1996). The area of burnt forest in Eastern Siberia amounts to 1.27×10^4 km^2 y^{-1} (Sheingauz, 1996); 70%–80% of the fires were caused by human activity with the remainder caused by natural events such as lightning (Goldammer and Stocks, 2000). After severe forest fires in Siberia, the permafrost melts and grasslands called Alases are formed (Desyatkin, 1993). Because Alases are thermokarsts, water supplied from the thawing permafrost flows laterally into the Alas forming ponds with diameters from several 10s of meters to 100 m. Some Alases have a Pingo which is a small hill (10–20 m in diameter, 10–20 m in height) formed by the refreezing of water in the pond (Fitzpatrick, 1983).

The disappearance of forest may decrease CH_4 uptake in the Taiga ecosystem, and the appearance of ponds may increase CH_4 emission. Furthermore, changing pond area associated with climate change is expected to change the CH_4 dynamics in Alases. Almost all estimates for northern region CH_4 flux have been based on

data from North America and Eurasian Arctic between 67° and 77°N (Christensen et al., 1995; Tsuyuzaki et al., 2001). Furthermore, these flux measurements were carried out only wetland and tundra. Not only the influence of forest fires on CH_4 dynamics but also no CH_4 flux data have so far been available from Taiga region, though that region covers vast area and meet serious forest fire described above. The purpose of this study is to assess the change in CH_4 dynamics caused by land-cover change in the forest-Alas ecosystem.

2. Materials and Methods

2-1 Site description

This study was conducted in an Alas and adjacent forest in Neleger, located 30 km north-northwest from the city of Yakutsk (lat 62° 05'N, long 129° 45'E), Russia (Fig. 1).

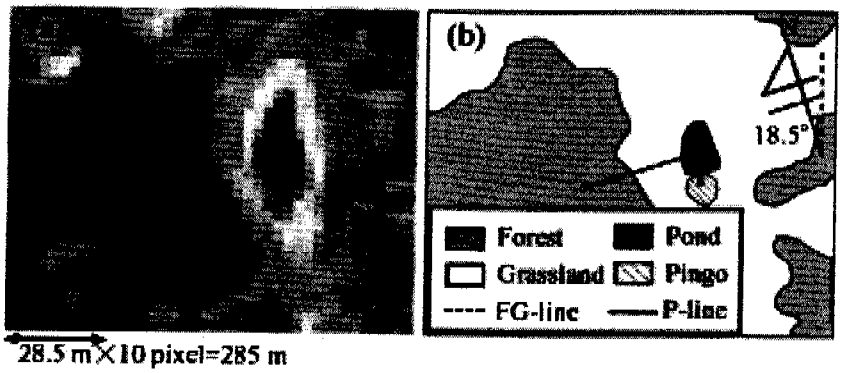

Fig. 1. Study area in Neleger. (a) Satellite image (LANDSAT 7, ETM+; Date: 27 Aug., 1999; Path/Row: 122/016; RGB = Band 5,4,3). (b) Outline of the satellite image and location of line transects.

The Alas is about 500 m × 1000 m, with a pond 100 m in diameter and 1 m deep. All measurements were carried out in July 2000, and June and July 2001. The average annual precipitation for the past 100 years in Yakutsk is 209 mm and the average annual temperature is –10.4 °C; the minimum and maximum temperatures are –42.5 °C (January) and 19 °C (July), respectively (Robert, 1997).

The forest is dominantly Larch (*Larix cajanderi*) of more than 200 years old, with *Vaccinium vitis-idaea* dominant on the forest floor. The grassland of the Alas is dominantly *Elytriga repens* near the forest and *Carex resucata* near the pond. *Potentilla anserina* is dominant on the Pingo.

2-2 Measurements

Establishment of line transects

The locations and topographies of the 2 line transects are shown in Figures 1, 2, and 4. One transect of 300 m was established from the forest to the pond through grassland (the FG-line), and the other transect of 26 m was established from the top of the Pingo to the pond (the P-line). The grassland was 2 m lower than the forest and there was a steep slope at the edge of the forest (Fig. 2). One of the measuring points was established in the forest (A), the other points were established through the grassland every 10 to 20 m from the edge of the forest to the pond (B–E in 2000, B–F in 2001) (Figs. 1 and 2). The water depth at E in 2000 or F in 2001 was 10 cm. In 2001, E was in grassland because the area of the pond in 2001 had decreased compared to the area in 2000. On the P-line, 14 measurement points were established every 2 m from the top of the Pingo to the edge of the pond (P_0, P_2, P_4,..., P_{22}, P_{24}, P_{26}; numbers are the distance in meters from the top of the Pingo). The top of the

Pingo was 5 m above the pond surface (Fig. 4).

Soil environment

Examination of the soil profile and soil sampling were conducted in the forest (near A), in the grassland (between B and C, and near D), and on the top of the Pingo (Fig. 1). Intact 100-mL cores (5 cm diameter, 3 replications) and bulk samples (PVC bag: about 500 mL) were collected from each horizon of each soil profile. Using the intact cores, bulk density was determined gravimetrically by drying to a constant weight at 105 °C overnight. Bulk samples were air-dried for more than 3 weeks in the laboratory, and then sieved through a 2-mm-mesh sieve to use for chemical analysis.

Soil pH was determined by glass electrode pH meter in a supernatant suspension of 1:2.5 (O horizon, 1:20) soil:deionized water mixture. EC was determined by EC meter in a 1:5 soil:deionized water mixture. The EC value was modified by multiplying by 5 to approximate the EC value for a water-saturated soil paste. After the soil samples were air-dried and ground, total carbon and nitrogen contents were determined by using a C/N analyzer (Vario-EL, ELEMENTER). Carbonate-carbon content was analyzed by measuring the amount of CO_2 produced from 0.3 to 0.8 g of soil samples to which 15 mL of 2M HCl solution was added in an Erlenmeyer flask. Organic carbon content was calculated by subtracting the carbonate-carbon content from the total carbon content (Loeppert and Suarez, 1996; Sawamoto et al., 2000).

Soil temperature and moisture

Soil temperature and soil moisture was measured at each point on the line transects (A–F, P_0–P_{26}). Soil temperatures were measured with a digital thermometer at a depth of 4 cm. Soil moistures were measured as volumetric water content with an FDR (ML2 Theta Probe, Delta-T Devices, Co.) at a depth of 0 to 7 cm. All measurements were taken with 5 replications.

CH_4 flux

CH_4 flux measurements were carried out by a closed chamber technique. To more easily transport the chambers into the field, they were constructed in way that allowed 6 chambers of slightly differing sizes to fit into the largest of them in the manner of a Russian matryoshka doll. That is, the 6 chambers each had the same height (25 cm), but were of different diameters (18.5, 19, 19.5, 20, 21.5, and 22 cm). CH_4 fluxes were measured at A–F on the FG-line (3 to 6 replications) and at P_0–P_{26} on the P-line (no replication). CH_4 fluxes on the P-line were measured only in June 2001. The day before the measurement, chambers were installed 3 cm deep into the soil. At 0, 10, 20 and 40 min after setting up the chamber, a 20-mL gas sample was taken into a 10-mL glass bottle vacuum-sealed with a butyl rubber stopper and a plastic cap.

Table. 1 soil properties of forests and grasslands in Nelegei

layer	depth cm	soil texture	Bulk density Mg m^{-3}	pH	EC dS m^{-1}	Org-C %	T-C %	T-N %	C/N
Forest (A)									
L	-10	SiCL		4.3	1.7	50.3	50.3	0.58	86
FH	-7	SiCL		4.5	0.7	52.0	52.0	1.43	36
E1	2	SiCL	1.12	4.8	0.1	1.8	1.8	0.04	47
E2	25	SiCL	1.51	6.3	0.1	0.6	0.6	0.03	22
$B2_h$	56	SiCL	1.51	8.7	0.9	0.5	0.5	0.03	17
B3	73	SiCL	1.50	9.2	1.0	0.4	0.9	0.03	35
C	108+	SiCL	1.52	9.1	1.1	0.5	1.0	0.03	40
Grassland (near B)									
A1	12	SiC	0.72	6.7	0.7	10.4	10.4	0.98	11
A2	19	SiC	1.52	8.7	1.2	1.2	2.0	0.06	35
$B2_{ir}$	31.5	SiC	1.55	9.0	1.8	0.9	1.8	0.04	52
$B2_h$	49	SiC	1.60	8.7	2.9	0.2	0.9	0.03	32
$B3_g$	78	SiC	1.53	8.5	3.1	0.2	0.8	0.03	31
C_g	120+	SiC	1.50	8.3	2.6	0.9	1.1	0.05	23
Grassland (Between C and D)									
A	20	SiC	1.08	7.1	3.6	13.3	13.7	1.06	13
AB	28	SiC	1.36	8.8	2.1	1.7	1.98	0.13	15
B1g	50	SiC	1.63	8.8	3.6	0.7	0.74	0.05	15
B2g	130+	SiC	1.60	8.4	4.2	0.5	1.12	0.04	28
Pingo									
A	7	SiC	0.95	5.8	1.2	4.4	4.41	0.33	13
B1	36	SiC	0.84	4.5	14.1	5.1	5.07	0.41	12
B2	130+	SiC	1.14	8.2	1.9	1.2	1.66	0.05	33

CH_4 concentration in the soil

To collect gases in the soil, 9-mm-diameter stainless steel pipes were installed at depths of 5, 10, 15, 20, 30, and 50 cm (3 pipes at each depth). After setting up the pipes, 50 mL of air was exhausted from each pipe. The pipes were then sealed by using a 3-way cock and kept overnight to allow gas concentrations in the pipes to equilibrate with the soil air. From each of the pipes installed at each depth, air samples (50 mL) were taken into a Tedlar bag. At the same time, air at the soil surface was taken into a Tedlar bag as a sample of soil air at a depth of 0 cm. Within the same day, 20-mL air samples from each of the Tedlar bags were transferred to 10-mL glass bottles.

Sometimes we could get only water from the pipes. In that case, dissolved CH_4 concentrations were measured according to the method proposed by McAullife (1971) and Sawamoto et al. (2002). A 30-mL water sample was taken from the pipe with a 60-mL syringe, and 30 mL of air was immediately drawn into the syringe. Then the syringe was vigorously shaken for 3 min and a 20-mL air sample from the headspace was taken into a 10-mL glass bottle.

Gas analysis and calculation of CH_4 flux

CH_4 concentrations were analyzed with a Shimadzu GC-8A gas chromatograph (GC) after the gas samples in the 10-mL glass bottles were brought back to the laboratory of Hokkaido University in Sapporo, Japan. Analysis was done within 3 weeks of sampling.

The GC was equipped with a flame ionization detector and a 2-m activated carbon column. Samples of 1 mL were injected into the GC. The injection/detection and column oven temperatures were 130 °C and 70 °C, respectively. Ultrapure nitrogen gas was used as the carrier gas at a flow rate of 60 mL min^{-1}. Standard CH_4 gas (1.95 μL L^{-1}) was used for calibration. Gas fluxes were calculated on the basis of the changes in chamber CH_4 concentration with time by using a linear regression law (Christensen et al., 1995). The minimum detectable CH_4 concentration was 0.02 μL L^{-1} and the minimum detectable flux was $-8 < F$ (μg C m^{-2} h^{-1}) <

+8. Non-detectable CH_4 fluxes were removed from the calculation of the average.

3. Results

3-1 Soil properties

Soil properties are listed in Table 1. At all sites, soil pH increased with increasing soil depth. Soil pH in the topsoil was higher in the grassland and on the Pingo (5.8–7.1) than in the forest (4.3). EC was also higher in the grassland and on the Pingo (0.7–14 dS m^{-1}) than in the forest (0.1–1.7 dS m^{-1}). In particular, the EC at the subsurface B_1 horizon of the Pingo was 14 dS m^{-1}, which was 10 times higher than in the forest. Only salt-tolerant vegetation is able to grow in soils with an EC value so high (Keren, 1999). With the exception of the L and FH horizons, the organic carbon contents of the soils were higher in the grassland and on the Pingo than in the forest. The C/N ratio was the highest in the L and FH horizons of the forest; the C/N ratios were in the following order: forest > grassland > Pingo.

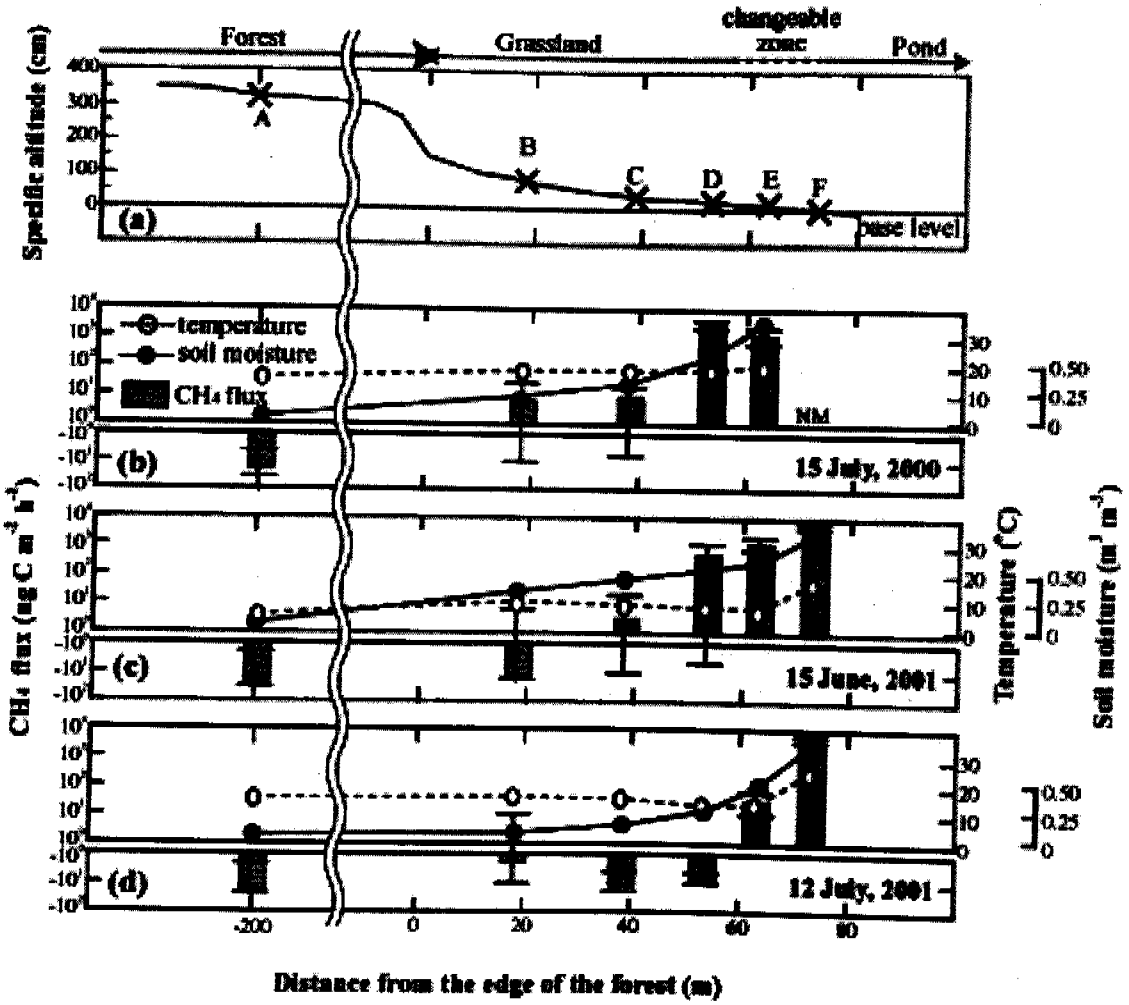

Fig. 2. Topography and CH_4 fluxes along FG-line. (a) Topography. Base level of specific altitude is at the surface of the pond. (b), (c) and (d) CH_4 fluxes with soil temperature and moisture in July, 2000; June, 2001 and July, 2001, respectively. CH_4 fluxes are shown in log scale and vertical bars indicate maximum and minimum values of CH_4 flux. NM, not measured".

3-2 CH_4 flux and concentration in the soil along the forest–pond transect (FG-line)

The CH_4 flux along the FG-line transect is shown in Figure 2. The water temperature in the pond was always higher than the soil temperatures at the other points. The soil temperatures were also higher in the grassland than in the forest. Soil moisture increased as the distance to the pond decreased. CH_4 uptake was observed in forest soils; the CH_4 flux ranged from –13 to –17 μg C m^{-2} h^{-1}. CH_4 emission in the grassland increased with the approach to pond—from –8 μg C m^{-2} h^{-1} at B to 3.8 mg C m^{-2} h^{-1} at E. Large CH_4 emissions of 0.6 to 7.0 mg C m^{-2} h^{-1} were observed at E and F. No seasonal or annual changes in CH_4 uptake were shown in the forest. On the other hand, CH_4 emission in the grassland significantly changed; that is, the CH_4 flux was higher in July 2000 than in July 2001. Notably, CH_4 uptake was observed at B, C, and D in July 2001.

CH_4 concentrations in the forest soil decreased with increasing soil depth (Fig. 3). The CH_4 concentration in grassland soil (B and C), where very small CH_4 flux was observed, increased slightly with increasing soil depth. However, the distribution of CH_4 concentration in the soil at C and D in July 2000 was similar to D and E in June and July 2001. The CH_4 concentration in the soil at E was 100 times higher than that in the atmosphere (about 2 μL L^{-1}). The area of soil with the highest concentration of soil CH_4 (> 10 μL L^{-1})—i.e., the area within the range of 10 m surrounding the pond—decreased with the 10-m decrease in pond radius from 2000 to 2001. It is also true that CH_4 emission decreased as the area of the pond decreased (Fig. 2).

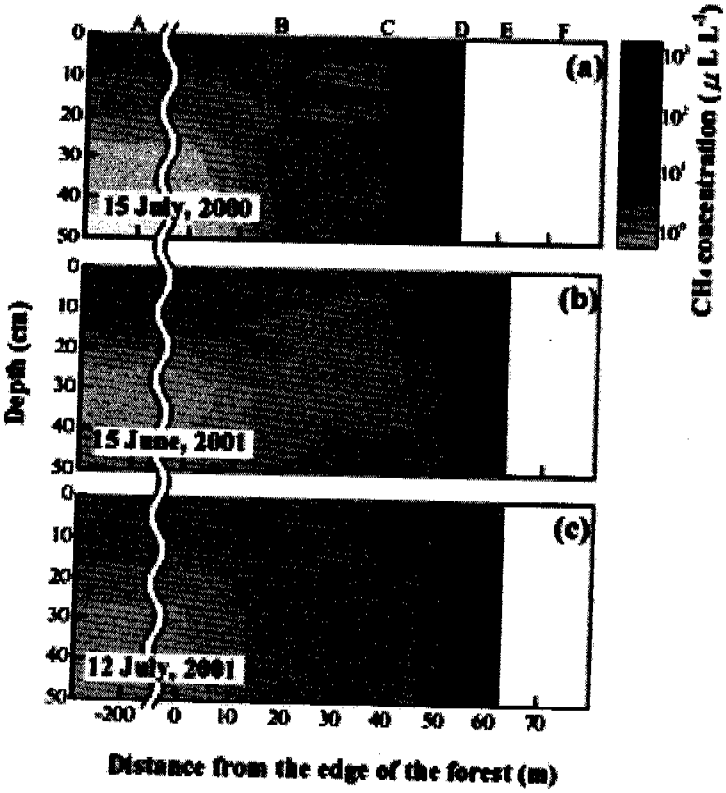

Fig. 3. CH_4 concentration (μL L^{-1}) in the soil or water along the FG-line in July, 2000 (a), June, 2001 (b) and July, 2001 (c), respectively.

3-3 CH_4 flux and concentration in the soil along the Pingo–pond line transect (P-line)

The CH_4 flux and concentration in the soil on the P-line in June 2001 are shown in Figure 4. Soil temperature decreased from the top of the Pingo (P_0) to P_6, but it increased from P_8 to P_{12} and decreased again toward the pond. The water temperature was 5 to 10 °C higher than the soil temperature. Soil moisture decreased with increasing soil temperature. Because the P-line was drawn from south to north (Fig. 1), the top of the Pingo and sites P_8–P_{12} were well exposed to sunshine. Therefore, soil temperature and moisture changed depending on the topography. At sites P_0 to P_{16}, CH_4 fluxes were below the detection limit [–8 < F (μg C m^{-2} h^{-1}) < +8] (no detectable emission

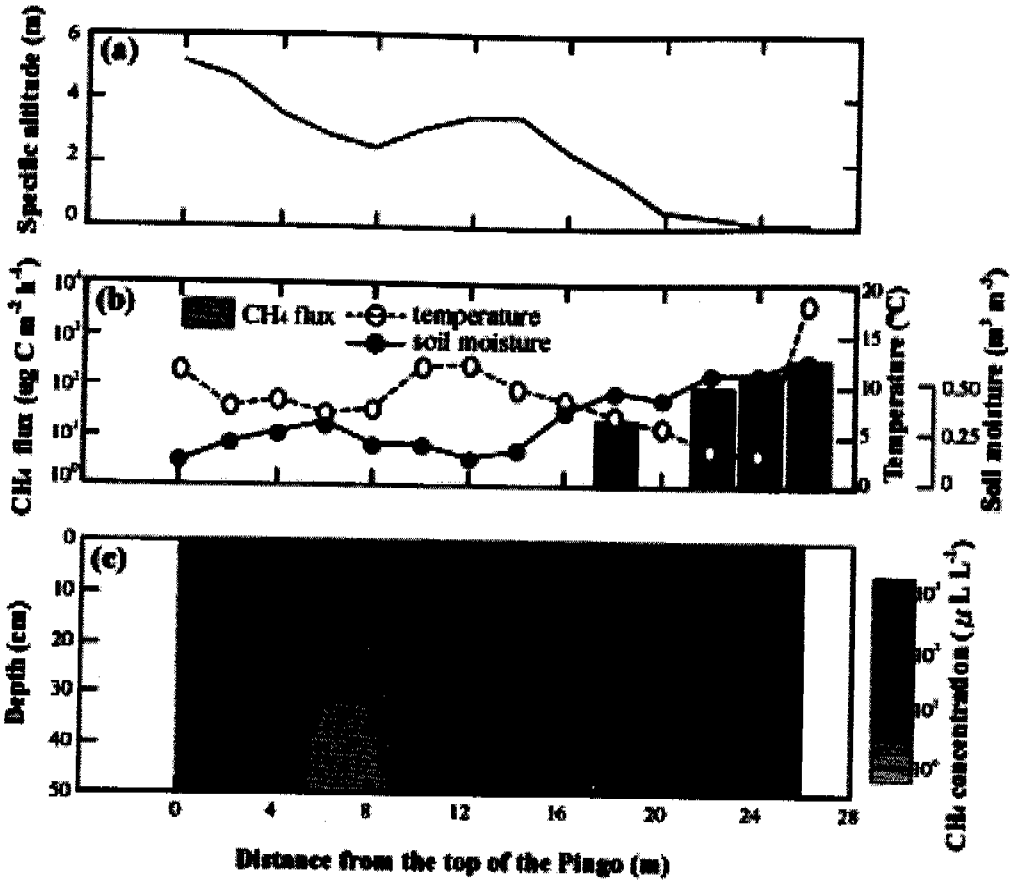

Fig. 4. Topography, CH_4 flux and soil CH_4 concentration along the P-line. (a) Topography. Base level of specific altitude is at the surface of the pond. (b) CH_4 fluxes with soil temperature and moisture in June-2001. CH_4 fluxes are shown in log scale. (c) CH_4 concentration ($\mu L\ L^{-1}$) in the soil in June-2001. P_0-P_{16}: trace ($-8<F<8$ ug C m^{-2} h^{-1}).

or uptake), while from P_{18} to the pond, large CH_4 emissions of 21 to 189 μg C m^{-2} h^{-1} were observed, similar to those at D and E on the FG-line. CH_4 concentrations in the soil closely reflected CH_4 fluxes; that is, there was no difference between CH_4 concentration in the soil and atmosphere at P_0–P_{16}, where CH_4 fluxes were below the detection limit, whereas from P_{14} to the pond, CH_4 concentrations in the soil were higher than that in atmosphere.

3-4 The relationship between CH_4 flux and soil temperature or moisture

The relationships between CH_4 flux and soil temperature or soil moisture are shown in Figure 5. The CH_4 fluxes outside the detection limit [$-8 < F$ (μg C m^{-2} h^{-1}) $< +8$] are shown in the 'trace zone'; there were many such fluxes in this study. There was no relationship between CH_4 flux and soil temperature (Fig. 5a). On the other hand, there was a remarkable relationship between the CH_4 flux and soil moisture (Fig. 5b). CH_4 uptake occurred in the forest where soil moisture content was low, and CH_4 emissions occurred in the

pond and the edge of the pond where soil moisture content was high; both uptake and emission of CH_4 occurred in the grassland where the soil moisture conditions were changeable. The CH_4 flux on the Pingo showed a similar tendency to that in the grassland. However, at low soil moisture, CH_4 uptake was observed in the grassland, but not on the Pingo. Soil moisture contents at A, B, and C in July 2000 were lower than in June 2001 and higher than in July 2001, but there was no clear difference in CH_4 flux among them (Fig. 6a). On the other hand, CH_4 emissions at D and E decreased (Fig. 6b) with decreasing soil moisture from July 2000 to July 2001. At D in particular, CH_4 emission was observed (maximum emission: 4.8 mg C m^{-2} h^{-1}) in July 2000, but in 2001 this site showed CH_4 uptake (maximum uptake: –8 μg C m^{-2} h^{-1}).

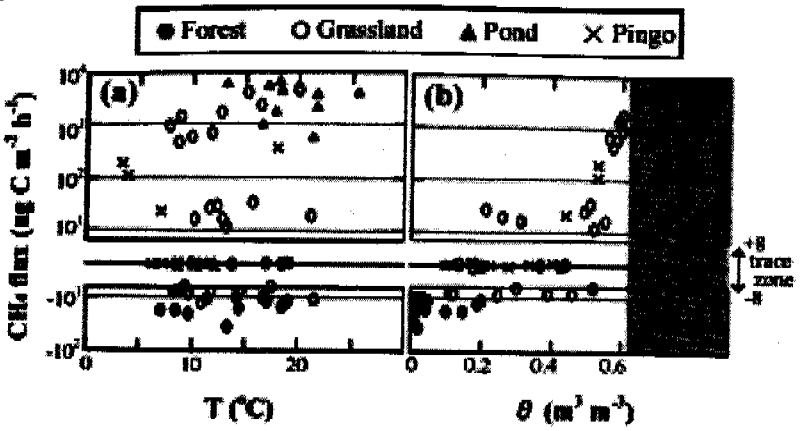

Fig. 5. Relationship between CH_4 flux and (a) soil temperature (T, °C) and (b) soil moisture (θ, m^3 m^{-3}). CH_4 fluxes are shown in log scale and CH_4 fluxes beyond the detection limit [–8 < F (mg C m^{-2} h^{-1}) < +8] are shown in the 'trace zone'. 'saturated' (gray zone)) indicates beyond the detection limit [θ (m^3 m^{-3}) > 0.60] of an FDR.

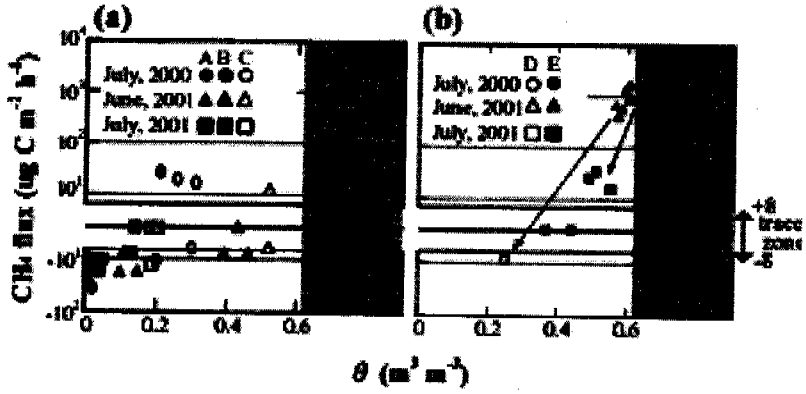

Fig. 6. Relationship between CH_4 flux and soil moisture (θ, m^3 m^{-3}) obtained in the FG-line. (a) Relatively drier plots (A, B and C). (b) Relatively wetter plots (D and E). CH_4 fluxes are shown in log scale and CH_4 fluxes beyond the detection limit [-8 < F (mg C m^{-2} h^{-1}) < +8] are shown in the 'trace zone'. "saturated"(gray zone) indicates beyond the detection limit [θ (m^3 m^{-3}) > 0.60] of an FDR. Arrows in (b) stand for outline of seasonal change in methane flux at D (dotted line) and E (solid line).

4. Discussion

4-1 The effect of changes in soil characteristics caused by forest fires on CH_4 flux

This study showed that soil moisture, pH, EC, and organic carbon content were higher in the grassland than in the forest (Table 1, Figs. 2 and 5). Thermokarsts in Siberia develop due to subsidence associated with melting permafrost after severe forest fires (Desyatkin, 1993). In the initial stage of Alas formation, a pond forms in the Alas; the pond then gradually dries up due to the small amount of precipitation. As the pond dries up, a heavy accumulation of salts forms in the Alas soil (Desyatkin, 1993). We ascribe the increase in soil moisture in the Alas grassland to the thermokarst geomorphology. The increase in EC occurred due to the salt accumulation and low precipitation; the increase of pH and organic carbon content occurred from the forest fires supplying

ash and organic matter to the soil (Sawamoto et al., 2000).

The CH_4 dynamics in the Alas as determined in this study showed that, although no detectable CH_4 flux occurred on the salt-accumulated Pingo (Fig. 4), overall the Alas acted as a source of CH_4 emission (Fig. 2). In particular, CH_4 was strongly emitted at the edge of the pond. Similar results were presented in a previous work conducted in grassy marshlands near the Kolyma River, northeastern Siberia (Tsuyuzaki et al., 2001).

CH_4 flux from the soil occurs as a net CH_4 production and consumption in the soil, because an aerobic zone develops at the surface of the soil aggregates and an anaerobic zone develops inside the aggregates (Conrad, 1995). Microbiological processes regulate CH_4 production and consumption in soil (Mer and Roger, 2001), and they are strongly affected by soil temperature and moisture. Dunfield et al. (1993) reported that increasing soil temperature promoted both CH_4 production and consumption in soil. An increase in soil moisture increases CH_4 production due to the development of anaerobic conditions (Jean, 2001); an increase in soil moisture also decreases CH_4 consumption due to depression of soil gas diffusivity (Castro et al., 1995; MacDonald et al., 1997; Hu et al., 2001). Our study showed no relationship between CH_4 flux and soil temperature (Fig. 5). This was probably caused by the positive temperature dependency of both CH_4 production and consumption in the soil. The low-soil-moisture forest soil showed steady CH_4 uptake, while large CH_4 emission was observed near and in the pond (Figs. 2 and 5). These facts clearly indicate that CH_4 production and consumption strongly depended on the soil moisture. However, soils at the top of the Pingo showed no detectable CH_4 fluxes, regardless of the fact that they had a low soil moisture content similar to that of the forest soil (Figs. 2 and 4). This may be caused by the higher EC values in the Pingo soils than in the forest soil (Table 1). Nesbit and Breitenbeck (1992) reported that KCl of 3.5 $cmol_c\ kg^{-1}$ inhibited CH_4 oxidation in soil. In addition, MacDonald et al. (1997) showed that sodium inhibited CH_4 oxidation in soil. In this study, the EC was very high
(14 $dS\ m^{-1}$) at 30 cm depth in the Pingo soil. EC is an indicator of total cation concentration, and an EC of 14 $dS\ m^{-1}$ corresponds to a total cation concentration of 14 $cmol_c\ kg^{-1}$ (Kamewada, 1991). Furthermore, salt-tolerant vegetation, such as *Puccinellia tenuiflora* and *Artemisa commutata*, were dominant at the top of the Pingo. However, although the soil pH at the surface of the Pingo soil was about 6—good conditions for the growth of methanotrophs (Hutsch et al., 1994)—CH_4 uptake was not observed. Therefore, salinity rather than pH may influence CH_4 flux. Christensen et al. (1995) showed that CH_4 production increased with increasing organic carbon content, and Dunfield et al. (1993) showed that both CH_4 production and consumption were highest at the top of mineral soils. Therefore, more CH_4 production might occur in the grassland than in the forest.

These results suggest that in Alases formed by strong forest fires, CH_4 production increases and CH_4 consumption decreases due to the accumulated salts and the increased soil moisture and organic carbon content in the Alas soil.

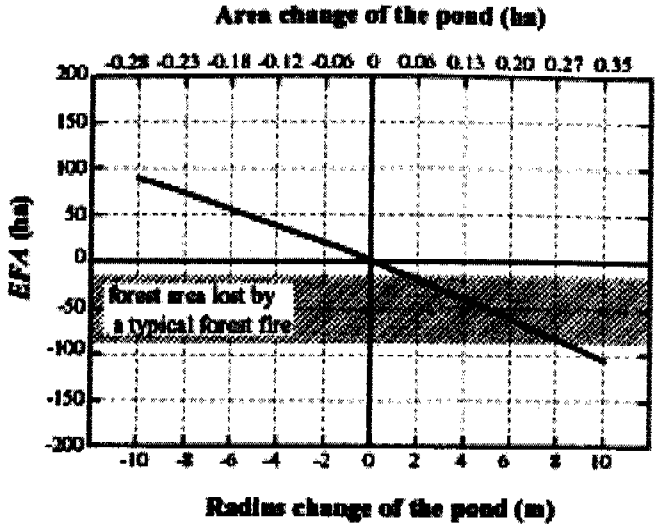

Fig. 7. Equivalent forest area (EFA) for CH_4 emission change with changing the size of pond (initial radius=50 m).

4-2 The effect of change in pond area on CH_4 emissions from Alas ecosystems

The average precipitation in Yakutsk over the past 100 years has been 209 mm y^{-1} (Robert, 1997). However, the precipitation is predicted to increase by 20% over the next 100 years; furthermore, 'intense precipitation' is predicted to increase (IPCC, 2001). This increased precipitation may increase the area of ponds in Alases, which will in turn increase the amount of CH_4 emitted from Alases. In the present study, however, the radius of the pond decreased by 10 m from 2000 to 2001. Because considerably higher CH_4 emissions occurred at the edge of the pond and inside the pond (Figs. 2 and 3), the decrease in the area of the pond area decreased the amount of CH_4 emitted from the Alas.

The change in the amount of CH_4 emitted as the pond area changes can be estimated as a product of the rate of CH_4 emission from the pond and the area by which the pond changes. The left hand side of the following equation (Eq. 1) indicates the change in CH_4 emission associated with a change in pond area. The change in CH_4 emission can be converted to the amount of CH_4 taken up by an area of forest. The right hand side of the equation indicates the CH_4 uptake in the forest. Using this conversion, the impact of changing pond area can be evaluated as a change in forest area.

$$[r^2 - (r+a)^2]\ \pi \times F_p = EFA \times F_f \qquad (1)$$

$$EFA = F_p/F_f \times (-2ar - a^2)\ \pi \qquad (2)$$

where r is the radius of the pond (m), a is the radius change of the pond (m), F_p is the rate of CH_4 emission from the pond (μg C m^{-2} h^{-1}), *EFA* is the equivalent forest area for CH_4 emission change (m^2), and F_f is the rate of CH_4 uptake in the forest (μg C m^{-2} h^{-1}). Substituting $r = 50$ (m), $F_p = 4641$ (max., 6247; min., 2677) (μg C m^{-2} h^{-1}) and $F_f = 15$ (max., 17; min., 13) (μg C m^{-2} h^{-1}) into Eq. 2, *EFA* as a function of a [−10 (m) $\leqq a \leqq$ 10 (m)] was estimated (Fig. 7). A positive *EFA* indicates that the effect of pond area change corresponds to an increase in forest area, while a negative *EFA* indicates a decrease in forest area. A 10-m increase in pond radius corresponds to a decrease in forest area of 107 ha (54–166 ha), and a 10-m decrease in pond radius corresponds to an increase in forest area of 87 ha (45–136 ha), which is larger than the area of 20 to 80 ha lost by a typical forest fire in Russia (Korovin, 1996). There are about 16 000 Alases in Yakutia (Desyatkin, 1993). Assuming that each Alas has a pond of the same area as the one in this study, the increase of CH_4 emissions associated with a 10-m increase in the radius of each pond may be from 16 to 40 times larger than the decrease in CH_4 uptake associated with annual forest fires, from 400 to 1000 cases in Yakutia (Valencik, 1996).

5. Conclusion

Although the Taiga forest soil in Yakutia showed CH_4 uptake, CH_4 emissions occurred in the Alas due to high soil moisture caused by the pond formed in the Alas. The amount of CH_4 emitted from the Alas was shown to change as pond area changed. The increase in CH_4 emission associated with increased pond area, which may occur with an increase of precipitation due to climate change, may be from 16 to 40 times larger than the decrease of CH_4 uptake in forests induced annually by forest fires in Yakutia. These results indicate that formation of Alases after severe forest fires and the change in the area of the pond associated with climate change can severely influence the CH_4 dynamics in Yakutia.

Acknowledgements

The authors thank Prof. M. Fukuda of Hokkaido University, the leader of the CREST program of the Japan Science and Technology Corporation (JST), for his supporting this study and his valuable comments. The authors thank Prof. K. Takahashi, Dr. M. Shibuya, Dr. H. Saito, Dr. K. Kushida, Dr. Y. Kobayashi, and Dr. G. Iwahana of Hokkaido University; Dr. T. C. Maximov, Dr. A.P. Isaev, and the staff of the Institute of Biological Problems of Cryolithzone, Russian Academy of Sciences; and Dr. A. N. Fedrov and the staff of the Permafrost Institute, Siberian Branch, Russian Academy of Science for their kind support with the fieldwork in Yakutsk. We are also grateful to Dr. G. Takao of the Forestry and Forest Products Research Institute, Hokkaido Research Center for his supplying the satellite image, and Mr. K. Sakai of Hokkaido University for his assistance with the fieldwork and the laboratory work. This study was supported by the CREST program of the Japan Science Technology Corporation (JST).

References

Alexeyev, V.A., R.A. Birdsey, V.D. Stakanov and I.A. Korotkov. 2000: Carbon storage in the Asian boreal forests of Russia, *In* Fire, Climate Change, and Carbon Cycling in the Boreal Forest, Ecological Studies 138, Eds. Kasischke, E.S. and B.J. Stocks, pp. 239–257, Springer-Verlag, New York

Bowden, R.D., K.M. Newkirk and G.M. Rullo. 1998: Carbon dioxide and CH_4 fluxes by a forest soil under laboratory-controlled moisture and temperature conditions, *Soil Biol. Biochem.*, **30**, 1591–1597

Castro, M.S., J.M. Melillo, P.A. Steudler and J.W. Chapman. 1994: Soil moisture as a predictor of CH_4 uptake by temperate forest soils, *Can. J. For. Res.*, **24**, pp. 1805–1810

Castro, M.S., P.A. Steudler and J.M. Melillo. 1995: Factors controlling atmosphere CH_4 consumption by temperate forest soils, *Global Biogeochemical Cycles*, **9**, pp. 1–10

Christensen, T.R., S. Jonasson, T.V. Callaghan and M. Hvstrom. 1995: Spatial variation in high-latitude CH_4 flux along a transect across Siberian and European tundra environments, *J. Geophysical Research*, **100** (D10), pp. 21035–21045.

Conrad, R. 1995: Soil microbial processes involved in production and consumption of atmospheric trace gases, *Advances in Microbial Ecol.*, **14**, pp. 207–250

Desyatkin, R.V. 1993: Syngenetic soil salinization during themokarst Alas formation, *Eurasian Soil Sci.*, **25** (4), pp. 38–46

Dobbie, K.E., K.A. Smith, A. Prime, S. Christensen, A. Degorska and P. Orlanski. 1996: Effect of land use on the rate of CH_4 uptake by surface soils in northern Europe. *Atmospheric Environment*, **30** (7), pp. 1005–1011

Dunfield, P., R. Knowles, R. Dunmont and T.R. Moore. 1993: CH_4 production and consumption in temperate and subarctic peat soils: response to temperature and pH, *Soil Biol. Biochem.*, **25**, pp. 321–326

Fitzpatrick, E.A. 1983: *In* Soils, pp. 222. Longman, London

Goldammer, J.G. and V.V. Furyaev. 1996: Fire in ecosystems of boreal Eurasia. Ecological impacts and links to the global system, *In* Fire in Ecosystems of Boreal Eurasia, Ed. J.G. Goldammer and V.V. Furyaev, pp. 1–20, Kluwer Academic Publishers, The Netherlands

Goldammer, J.G. and B.J. Stocks. 2000: Eurasian perspective of fire: Dimension, management and policies, and scientific requirements, *In* Fire, Climate Change, and Carbon Cycling in the Boreal Forest, Ecological Studies 138, Eds. Kasischke, E.S. and B.J. Stocks, pp. 49–65, Springer-Verlag, New York

Hu, R., K. Kusa and R. Hatano. 2001: Soil respiration and CH_4 flux in adjacent forest, grassland, and cornfield soils in Hokkaido, Japan. *Soil Sci. Plant Nut.*, **47** (3), pp. 621–628

Hutsch, B.W., C.P. Webstar and D.S. Powlson. 1994: CH_4 oxidation in soil as affected by land use, soil pH and N fertilization, *Soil Biol. Biochem.*, **26** (12), pp. 1613–1622

IPCC. 1995: Contribution of working group 1 to the Second Assessment Report of the Intergovernmental panel on climate change, http://www.ipcc.ch/pub/reports.htm

IPCC. 2001: Summary for policy makers: a report of working group 1 of the Intergovernmental panel on climate change, http://www.ipcc.ch/, pp. 71–72

Kamewada, K. 1991: Estimation of EC of soil solution from ion composition and influences of differences of anion composition on EC and hydrostatic pressure, *Jpn. J. Soil Sci. Plant Nut.*, **62**, pp. 634-640 (in Japanese)

Keren, R. 1999: Salinity, *In* Handbook of Soil Science, Ed. M. E. Sumner, CRC Press, G4–G25

Korovin, G.N. 1996: Analysis of the distribution of forest fires in Russia, *In* Fire in Ecosystems of Boreal Eurasia, Eds. J.G. Goldammer and V.V. Furyaev, pp. 112–128, Kluwer Academic Publishers, The Netherlands

Loeppert, R.H. and D.L. Suarez. 1996: Carbonate and Gypsum, *In* Method of Soil Analysis Part 3-Chemical Methods, Ed. D.L. Sparks, SSSA Book Series: **5**, pp. 437–474

MacDonald, J.A., U. Skiba, L.J. Sheppard, B. Ball, J.D. Roberts, K.A. Smith and D. Fowler. 1997: The effect of nitrogen deposition and seasonal variability on CH_4 oxidation and nitrous oxide emission rates in an upland spruce plantation and moorland, *Atmospheric Environment*, **31**, pp. 3693–3706

McAullife, C. 1971: GC determination of solutes by multiple phase equilibration, *Chem. Technol.*, JAN, pp. 46–51

Mer, J.L. and P. Roger. 2001: Production, oxidation, emission and consumption of CH_4 by soils: a review, *Eur. J. Soil Biol.*, **37**, pp. 25–50

Nesbit, S.P, and G.A. Breitenbeck. 1992: A laboratory study of factors influencing CH_4 uptake by soils,

Agriculture, Ecosystems and Environment, **41**, pp. 39–54

Prime, A., and S. Christensen. 1997: Seasonal and spatial variation of CH_4 oxidation in a Danish spruce forest, *Soil Biol. Biochem.*, **29**, pp. 1165–1172

Robert, H. 1997: Climate com. (http://www.worldclimate.com/climate/)

Sawamoto, T., R. Hatano, T. Yajima, K. Takahashi and A.P. Isaev. 2000: Soil respiration in Siberian Taiga ecosystems with different histories of forest fire, *Soil Sci. Plant Nut.*, **46** (1), pp. 31–42

Sawamoto, T., K. Kusa, R. Hu and R. Hatano. 2002: Dissolved nitrous oxide, CH_4 and carbon dioxide in pipe drainage, seepage, and stream water in a livestock farm in Hokkaido, Japan, *Soil Sci. Plant Nut.*, **48** (3), pp. 433–439

Sheingauz, A.S. 1996: The role of fire in forest cover, structure, and dynamics in the Russian Far East, *In* Fire in Ecosystems of Boreal Eurasia, Eds. J.G. Goldammer and V.V. Furyaev, pp. 186-190, Kluwer Academic Publishers, The Netherlands

Tsuyuzaki, S., T. Nakano, S. Kuniyoshi and M. Fukuda. 2001: CH_4 flux in grassy marshlands near Kolyma river, north-eastern Siberia, *Soil Biol. Biochem.*, **33**, pp. 1419–1423

Valencik, E.N. 1996: Temporal and spatial distribution of forest fires in Siberia, *In* Fire in Ecosystems of Boreal Eurasia, Eds. J.G. Goldammer and V.V. Furyaev, pp. 129–138, Kluwer Academic Publishers, The Netherlands

Whalen, S.C., and W.S. Reeburgh. 1996: Moisture and temperature sensitivity of CH_4 oxidation in boreal soils, *Soil Biol. Biochem.*, **28**, pp. 1271–1281

Initial change in carbon and nitrogen storages in organic layer following clear-cutting of larch stand in eastern Siberia

H. Saito[1*], M. Suzuki[1], H. Iijima[1], M. Shibuya[1], K. Takahashi[1], T. Onoe[1], A. P. Isaev[2] and T. C. Maximov[2]

[1] Graduate School of Agriculture, Hokkaido University. Forest Dynamics Group, CREST
[2] Institute of Biological Problems of Cryolithozone, Russian Academy of Science
* Phone: +81-11-706-2523, Fax: +81-11-706-4176, e-mail: saitoo@for.agr.hokudai.ac.jp

1. Introduction

Siberian taiga is the most serious ecosystem declining the function of carbon sink in terrestrials. Schulze *et al.* (1999) estimated the net biome production (NBP), which is net ecosystem production (NEP) minus carbon loss through disturbances like fire and logging, was only approximately 13-16 mmol m^{-2} y^{-1} for Siberia, compared with approximately 67 mmol m^{-2} y^{-1} for Northern America and approximately 140-400 mmol m^{-2} y^{-1} for Scandinavia. The lower NBP in Siberia was due to the carbon loss of the disturbances. Although it is important to evaluate NBP for analysis of the carbon sink in regional scale, the understanding of carbon dynamics following the disturbances was less.

Larix gmelinii stand, widely distributed in eastern Siberia, is one of the major ecosystems in boreal forest. Primarily, the large accumulation and the slow decomposition of organic matter in the stand floor contribute the function of the carbon storage in the boreal region (Shibuya *et al.*, 2001). Recently, the stands are frequently disturbed by intensive logging (Rosencranz and Scott, 1992). The organic matter in the stand floor must be very sensitive to the environmental change caused by the disturbance. The ecosystem of *L. gmelinii* stand is very particular one that establishes on continuous permafrost, so previous manner reported from the other forest ecosystem may not be able to apply to this permafrost region. Little was understood about how the influences occur in Siberian taiga. Therefore, it is necessary to clear the influence of clear-cutting on the carbon dynamics in the *L. gmelinii* stand floor for evaluating the NBP.

Nitrogen dynamics is also an important factor for carbon dynamics in this *L. gmelinii* stand. Schulze *et al* (1995) and Shibuya *et al.* (2001) suggested the nitrogen is a limiting factor of carbon uptake within the canopy with aging of the stand after the wild fire disturbance. Thus it is also important to clear the nitrogen dynamics to understand the nitrogen limitation in the carbon uptake of this larch forest.

Our objective in this study is to understand how much the carbon and nitrogen storages decrease in the initial stage following clear-cutting, and to understand the influence on the decomposition rate of organic matter. The change of carbon and nitrogen storage in the organic layer before and at 2 years following a clear-cutting was investigated in a matured *L. gmelinii* stand

on permafrost.

2. Study site and methods

Study site was located in Neleger (62°18'N, 129°30'E), approximately 30 km from Yakutsk in the Republic of Sakha, Russia. The annual precipitation was 200-300mm. The annual mean of temperature was approximately -10°C. The texture of the underlying soil horizons was silt loam (Kamide *et al.*, 2001). This site was very flat, almost no slope was recognized. The stand density was approximately 2100 trees ha^{-1}. The maximum height of the stand was 21m above ground level. The dominant species was *L. gmelinii* and ratio of it in basal area was nearly 100%. The leaf mass of this stand was estimated to approximately 2 ton ha^{-1} (Shibuya *et al.*, 2001).

The 50m by 100m clear-cutting was conducted in winter 2000 to 2001, when the leaf-litter fall had been finished. The operation type was whole-tree harvesting. Since transportation of stems was carried out by sliding on snow, the effect to stand floor by transportation of stems was considered to be little.

The sample collection of organic layer was carried out in July 2000, before the clear-cutting, and July 2002, following the clear-cutting. The accumulation in the organic layer were collected from 0.5 by 0.5m sub-plot (n=8), dividing into leaf litter layer (L layer) and humus layer (F+H layer). Branch litter was excluded from the samples. Their dry weight was measured after dry up for more 2 days at 70°C. The total carbon and nitrogen contents were measured by using NC analyzer (NC1000, Shimazu, Kyoto, Japan).

3. Results and Discussion

Significant decreases of dry matter, carbon and nitrogen storages in leaf litter were found out for 2 years following the clear-cutting (Fig.1). The dry matter of leaf litter decreased from 15.3 ± 3.9 (S.D.) ton ha^{-1} to 8.9 ± 2.0 ton ha^{-1}, so the difference of the means was 6.4 ton ha^{-1}. Although the carbon and nitrogen contents in leaf litter and humus was not significantly different between before and following the clear-cutting (Table 1), the significant decrease of carbon and nitrogen storage in leaf litter was found out following the clear-cutting due to decrease of dry matter (Fig. 1). Therefore these results indicate evidence that the clear-cutting causes a significant carbon and nitrogen loss for two years in leaf litter layer of the mature *L. gmelinii* stand.

In humus layer, no significant change in dry mass, carbon content, and carbon storage was found. No significant difference was also found in total organic matter in the forest floor (leaf litter + humus), but the decrease between means in the dry mass, carbon storage, and nitrogen storage was 20.6 ton ha^{-1}, 5.2 ton C ha^{-1}, and 0.1 ton N ha^{-1}, respectively.

Convinton (1981) and Federer (1984) reported that northern hardwood forest stands showed a rapid substantial decrease in stand floor organic matter following clear-cutting by a chronosequence approach. Convington (1981) estimated the initial decrease rate in the stand floor was 10.8 ton

ha^{-1} of dry matter at 3 years following a clear-cutting in New Hampshire. In the *L. gmelinii* stand in eastern Siberia, therefore, it is considered that the decrease rate in the stand floor following clear-cutting is be relatively fast, though this region is in the cool and cold climate.

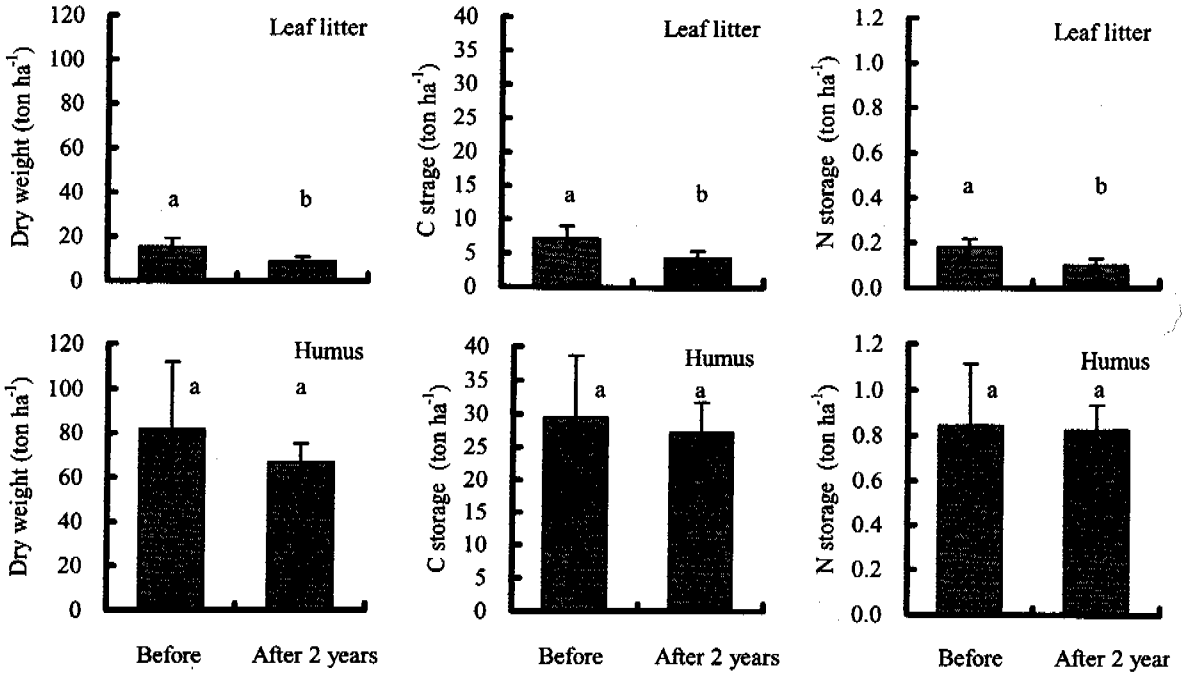

Fig. 1 Change in dry matter, carbon, and nitrogen storages in organic layer after clear-cutting in *Larix gmelinii* forest. Error bars denote standard deviation (n=8). Different letter denotes the significant difference (t-test, p <0.05).

Table 1 Change in carbon and nitrogen contents and C/N ratio in organic layer after clear-cutting

	Leaf letter		Humus	
	Before	After 2years	Before	After 2years
Carbon content (%)	47.6±1.2	48.0±2.0	37.3±7.9	41.0±7.7
Nitrogen content (%)	1.16±0.16	1.12±0.12	1.06±0.16	1.23±0.17
C/N ratio	41.1±4.7	43.3±5.0	35.0±2.6	33.2±3.2

No sigenificant difference between the before and after clear-cutting was detected (t-test, p <0.05).

The decrease of carbon storage in the stand floor was considered to be attributed to reduced inputs of litter fall and the change of the decomposition rate. According to Shibuya *et al.* (2001), the leaf mass in the stand was estimated to approximately 2 ton C ha^{-1}. It is possible to estimate the approximate amount of leaf-litter fall is also 2 ton C ha^{-1}. Assuming the annual decomposition rate balances to an amount of the litter fall in the matured stand (Shibuya *et al.*, 2001), the decomposition rate of leaf litter can be estimated as approximately 2 ton C ha^{-1}. Thus the details of the approximately 6 ton C ha^{-1} of carbon loss in the leaf litter layer shown in Fig. 1 are estimated as follows; 1) 2 ton C ha^{-1} of disappearance of leaf-litter fall and 2) 4 ton C ha^{-1} of decomposition.

The estimated 4 ton C ha^{-1} of decomposition could be 2-holds higher than the decomposition rate before the clear-cutting.

Furthermore, the clear-cutting of standing trees caused the decline of understoried vegetation, e.g. *Vaccinium vitis-idaea* (Saito *et al.*, 2001), due to the change of light condition probably. The declined vegetation supplied the litter to stand floor, which was approximately 1 ton C ha^{-1} (data not shown). Including the leaf litter from the understoried vegetation, the estimated 4 ton C $ha^{-1}$of the decomposition rate should be under estimate. The increase of decomposition rate of leaf litter following the clear-cutting may be over 2-fold.

In general, the increments of temperature and moisture conditions accelerate the decomposition of organic matter (Swift *et al.*, 1979). In this clear-cutting site, the soil temperature and moisture increased significantly compared with the stand floor (Machimura *et al.* unpublished data). Thus, the estimated increment of the leaf-litter decomposition rate may be caused by these changes of microenvironments in the soil temperature and moisture following the clear-cutting.

There are many studies about dynamics of organic matter in forest floor following clear-cutting. In those, the decomposition rate of organic matter had been generally considered to be faster in clearcuts than in forests, owing to higher temperature and moisture conditions (e.g. Swift *et al.*, 1979). While, Blair *et al.* (1988) and Prescott (1997) reported low decomposition rate in cutting site, and Wallace *et al.* (1985) reported there was no difference in the decomposition rate between the stand floor and cut floor. The previous studies demonstrate that the assumption of faster decomposition at clear-cutting site is not always valid. The results depend on regional climate (Yin *et al.*1989). There may be 'site-specific effect' (Blair *et al.*1988), but as for East-Siberian *L. gmelinii* stand, the decomposition rate in stand floor is considered to be at least increased by clear-cutting initially.

REFERENCES

Blair, J.M., Crossley Jr., D.A.(1988) : Litter decomposition, nitrogen dynamics and litter microarthropods in a southern Appalachian hardwood forest 8years following clearcutting. J. Appl. Ecol. **25**, 683-698.

Covington, W.W. (1881) : Changes in the forest floor organic matter and nutrient content following clear cutting in northern hardwoods. Ecolgy **62**, 41-48.

Federer, C.A. (1984) : Organic matter and nitrogen content of the forest floor in even-aged northern hardwoods. Can. J. For. Res. **14**, 763-767.

Kamide, K., Hatano, R., Nakahara, O., Sawamoto, T., Takahashi, K., Desyatkin, R. V. (2001) : Effect of forest fire on physico-chemical properties of taiga soil in Yakutsk, Russia. *In: Proceedings of the ninth symposium on the joint Siberian permafrost studies between Japan and Russia in 2000 (Eds Fukuda and Kobayashi)*, 104-111.

Prescott,C.E. (1997) : Effects of clearcutting and alternative silvicultural systems on rates of

decomposition and nitrogen mineralization in a coastal montane coniferous forest. For. Ecol. Manege. **95**, 253-260.

Rosencranz, A. and Scott, A. (1992) : Siberia's threatened forests. Nature **355**, 293-294.

Saito, H., Takahashi, K., Shibuya, M., Tsuno, Y., Isaev, A. P., Maximov, T. C. (2001) : Distribution of current larch seedlings affected by forest floor vegetation in a larch stand in Neleger, Yakutsk. *In: Proceedings of the ninth symposium on the joint Siberian permafrost studies between Japan and Russia in 2000 (Eds Fukuda and Kobayashi)*, 75-82.

Schulze, E. D., Schulze, W., Kelliher, F. M., Vygodskaya, N. N., Zieger, W., Kobak, K. I., Koch, H., Kusnetsova, W.A., Sogatchev, A., Issajev, A., Bauer, G., and Hollinger, D. Y. (1995) : Aboveground biomass and nitrogen nutrition in a chronosequence of pristine Dahurian *Larix* stands in eastern Siberia. Can. J. For. Res. **25**, 943-960.

Schulze, E. D., Lloyd, J., Kelliher, F. M., Wirth, C., Rebmann, C., Lühker, B., Mund, M., Knohl, A., Milyukova, I. M., Schulze, W., Zieger, W., Varlagin, A. B., Sogachev, A. F., Valentini, R., Dore, S., Grigoriev, S., Kolle, O., Panfyorov, M. I., Tchebakova, N., Vygodskaya, N. N. (1999) : Productivity of forests in the Eurosiberian boreal region and their potential to act as a acarbon sink- a synthesis. Global Change Biology: **5**, 703-722.

Shibuya, M., Tsuno, Y., Saito, H., Takahashi, K., Sawamoto, T., Hatano, R., Isaev, A. P., Maximov, T. C. (2001) : Chronosequential analysis of aboveground biomass and the carbon and nitrogen contents in natural *Larix* stands in eastern Siberia. Bull. Res. Cent. North Eurasia and North Pacific Regions, Hokkaido Univ. **1**, 57-66.

Swift, M. J., Heal, O. W., Anderson, J. M. (1979) : Decomposition in terrestrial ecosystems. Studies in ecology volume 5, Blackwell Scientific Publications.

Wallace, E.S., Freedman, B. (1985) : Forest floor dynamics in chronosequence of hardwood stands in central Nova Scotia. Can. J. For. Res. **16**, 293-302.

Yin, X., Perry, J.A., Dixon, R.K. (1989) : Influence of canopy removal on oak forest floor decomposition. Can. J. For. Res. **19**, 204-214.

Model analysis of carbon dynamics of ecosystems in eastern Siberia taking account of permafrost dynamics

K.Imanishi[1], A.Ito[2] and T.Oikawa[3]

[1]Environmental Science, University of Tsukuba, Tsukuba 305-8572, Japan

Phone: +81-298-53-6855, e-mail: planteco@kankyo.envr.tsukuba.ac.jp

[2]Frontier Research System for Global Change, Yokohama, 236-0001, Japan

Phone: +81-45-778-5599, e-mail: itoh@jamstec.go.jp

[3]Institute of Biological Science, University of Tsukuba, Tsukuba 305-8572, Japan

Phone&Fax: +81-298-53-6661, e-mail: toecolog@sakura.cc.tsukuba.ac.jp

1. Introduction

It has been suggested that the high latitudes have specially suffered from remarkable effects of the rapidly aggravating global warming (JMA, 1999). Among the high latitudes, the eastern Siberia possessing a vast forest area plays an extremely important role in the global carbon cycle (IPCC, 2001). In addition, the eastern Siberia is occupied by the permafrost extending over the widest range on the earth, which gives us cause for much concern about effects of the global warming. Therefore, we carried out an analysis of the carbon cycle model for the eastern Siberia by using the Sim-CYCLE (Ito and Oikawa, 2000). The previous report (Imanishi *et al.*, 2001) dealt with the result obtained by Sim-CYCLE which was constructed without any consideration for the permafrost dynamics.

This time, we revised its construction to apply to our target, the eastern Siberia, i.e., we newly constructed Sim-CYCLE Siberia which simulates carbon dynamics of a terrestrial ecosystem influenced by permafrost dynamics as a function of the monthly changes of soil temperature as well as of the soil water content.

2. Methods

Sim-CYCLE employed here conceptualizes the terrestrial carbon dynamics as a 5-compartment system; foliage, stem and branch, root, litter, and mineral soil (Figure 1). Sim-CYCLE Siberia offered the monthly information about the vertical distributions of soil temperature and water content along the

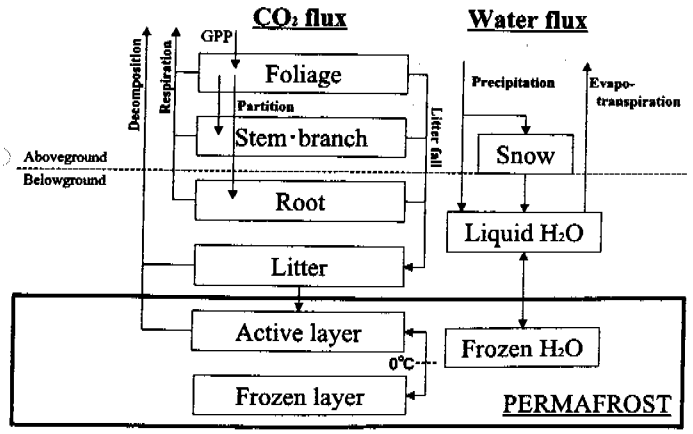

Figure 1. Structure of Sim-CYCLE Siberia.

soil depth by dividing the soil, 2 m in depth, into 20 layers every 10 cm, followed by calculating the soil temperature and the water content in each of the 20 layers.

As the soil temperature is influenced by the soil surface temperature determined by heat balance at the soil surface, such soil surface temperature that equation 1 is valid under some climate condition is obtained by repeated calculation (Kondo, 2000).

$$Rn\_s - H\_s - \lambda E\_s - G = 0 \qquad \text{equation 1}$$

where Rn is net radiation (W m^{-2}), H is sensible heat (W m^{-2}), λE is latent heat (W m^{-2}), G is soil heat flux (W m^{-2}) and subscripts _s mean soil surface.

The soil temperature was calculated by equation 2 with the soil surface temperature obtained above and the annual average atmospheric temperature as the boundary conditions. According to the equation 2, the soil temperature at step i+1 can be obtained from the known soil temperature distribution at step i (Figure 2).

$$T_{y,i+1} = rT_{y-1,i} + (1-2r)T_{y,i} + rT_{y+1,i} \quad (y=1\sim19) \qquad \text{equation 2}$$

where Ty,i is a temperature of layer y at step i and r is a parameter.

Parameter r is influenced by the specific heat that changes with the soil water content and the phase change of water. Especially, the effect is very large at about 0℃ on the permafrost (Kinoshita, 1982). Accordingly, the specific heat of the model is calculated in consideration of the soil water content and the soil temperature.

The change in soil water content originates in the migration of water from layer to layer divided into 20, which is caused by inflow of rain and thawed water followed by evapotranspiration, penetration and runoff.

The evapotranspiration was estimated by Penman-Monteith's equation with such assumption that the evaporation occurs only at the closest layers to the soil surface and lower layers are dominated by the transpiration.

Since the transpiration largely depends upon the amount of plant roots existing in each layer, this model was constructed in consideration of the root distribution in each layer. The vertical distribution of root was obtained as a function of soil depth from the equation reported by Jackson *et al.* (1996).

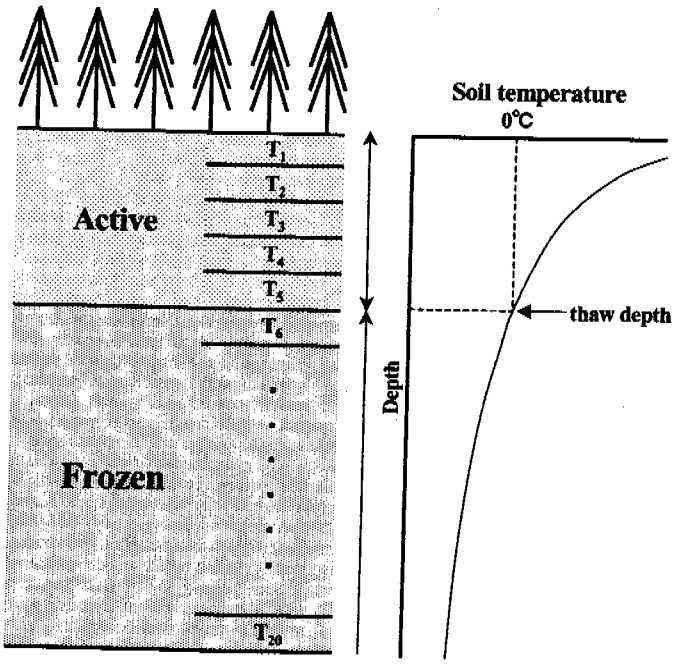

Figure 2. Calculation model for heat conduction.

3. Results and Discussions

Figure 3 shows the seasonal changes of the soil temperature profiles at plot scale obtained for Yakutsk (62 ° N, 130 ° E); the upper and lower figures illustrate the soil temperatures calculated by Sim-CYCLE Siberia and those measured by Iwahana *et al.* (2001), respectively. On the whole, both figures exhibit a similar tendency, but the calculated values were shifted to the lower temperatures when the air temperature dropped below 0 ℃, because the calculation did not take into consideration of the adiabatic effect of the snow cover on the soil surface. However, it will not affect the final result, since the calculation for the carbon cycle of this model actually becomes significant not bellow but above 0 ℃.

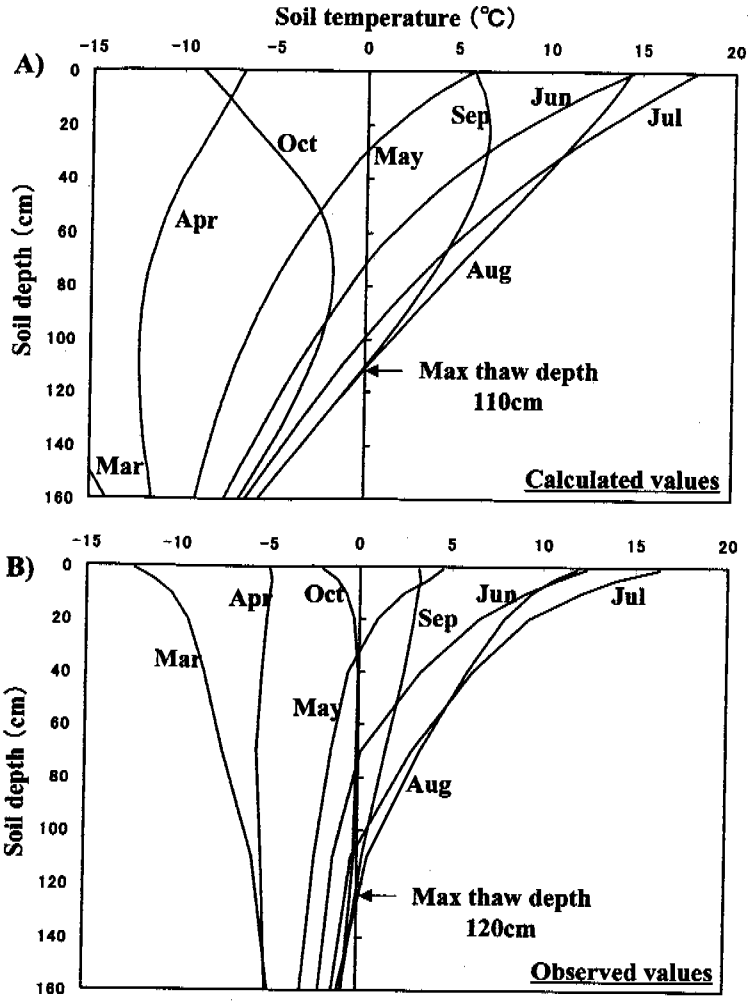

Figure 4 shows maximum thaw depth of frozen soil of all over the eastern Siberia obtained by the same

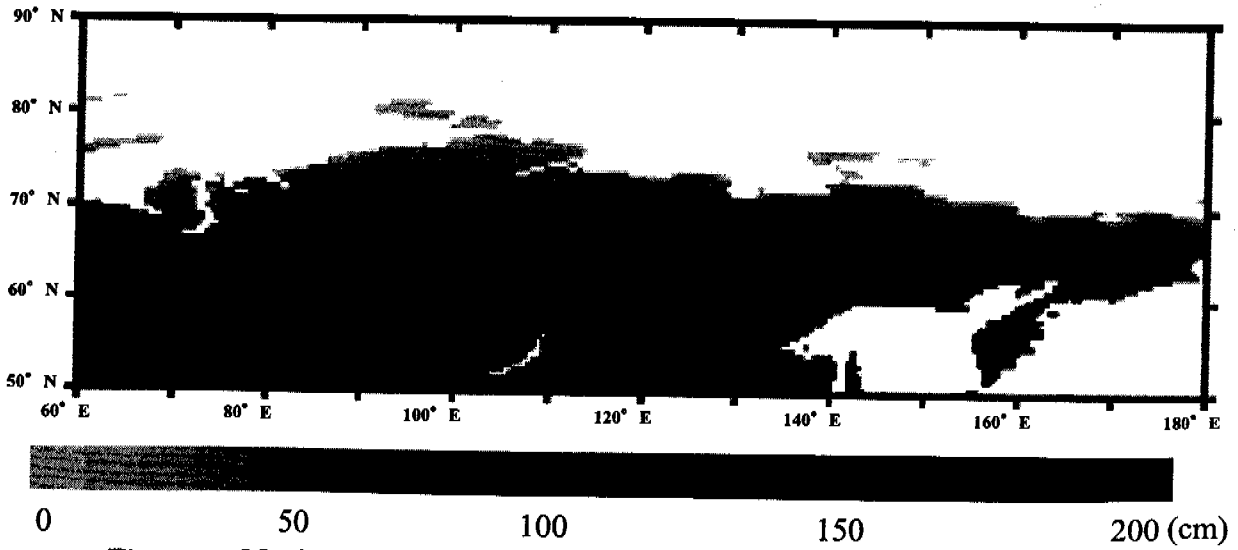

Figure 4. Maximum thaw depth map of frozen soil in the eastern Siberia estimated by Sim-CYCLE Siberia.

manner as that used for Yakutsk shown in Figure 3. This explains that the thaw depth is shallower eastward because the climate condition becomes increasingly harsh eastward.

The carbon dynamics is calculated in consideration of the above simulation of the permafrost dynamics. Table 1 summarizes the result of model simulation at steady state (NEP<0.001MgC ha^{-1} yr^{-1})., where the values reveal considerable significances, from which the most attractive points will be as follow; the total NPP values of the boreal forest and tundra, the main biome types in the eastern Siberia district, occupy nearly 80 % of the whole. The plant biomass shows high values in the forests making up such majority parts as more than 80 %. The soil organic carbon exhibits extremely higher values compared with those of the plant biomass, e.g. more than 20 times in the case of the northern taiga (deciduous) and the tundra shows about 35 time value. Furthermore, Sim-CYCLE Siberia also predicted that the total values of annual amounts of NPP, plant biomass and soil organic carbon were 5.8 PgC/year, 55 PgC and 519 PgC, respectively, i.e., 1.12 times, 1.16 times and 1.23 times the values obtained by Sim-CYCLE. There are some differences between values by Sim-CYCLE Siberia and those by Sim-CYCLE, which is due to the fact that Sim-CYCLE Siberia fractionated the soil compartment into many layers to construct a more detailed simulation of the soil temperature and soil water content.

By the addition of the thaw and freezing processes of the permafrost, Sim-CYCLE Siberia

Table 1. Comparison between values of carbon dynamics estimated by Sim-CYCLE Siberia and those by Sim-CYCLE.

	NPP(PgC yr^{-1})		Plant biomass(PgC)		Soil organic carbon(PgC)	
Biome type	Sim-CYCLE Siberia	Sim-CYCLE	Sim-CYCLE Siberia	Sim-CYCLE	Sim-CYCLE Siberia	Sim-CYCLE
mid latitude mixed woods	0.08	0.08	1.07	1.00	3.94	3.83
mid latitude broad-leaved forest	0.07	0.06	1.23	1.01	2.83	2.76
coniferous forest	0.25	0.23	4.55	4.23	15.60	14.07
southern taiga	0.54	0.51	10.17	9.43	31.04	27.06
main boreal taiga(evergreen)	0.47	0.44	8.32	7.81	24.86	22.38
main boreal taiga(deciduous)	1.32	1.19	9.92	8.01	84.82	78.23
northern taiga(evergreen)	0.33	0.30	5.46	4.86	38.83	32.25
northern taiga(deciduous)	0.90	0.80	4.93	3.95	100.57	86.75
second growth woods	0.07	0.05	0.71	0.52	3.14	2.41
second growth fields	0.16	0.13	0.35	0.27	9.57	7.91
warm or hot shrub and grassland	0.01	0.00	0.02	0.00	0.36	0.12
tibetan meadow,siberian highland	0.13	0.07	0.51	0.25	16.39	7.97
tundra	0.80	0.62	4.28	3.27	143.45	98.26
wooded tundra	0.22	0.21	2.08	1.92	24.75	22.89
cool bog and mire	0.12	0.09	0.96	0.76	7.06	5.59
cool semi-desert scrub	0.02	0.00	0.19	0.04	0.62	0.13
non-polar desert	0.00	0.00	0.00	0.00	0.03	0.01
cool croplands	0.14	0.12	0.06	0.06	4.22	3.94
warm croplands	0.15	0.13	0.07	0.07	5.79	5.54
irrigated	0.02	0.02	0.01	0.01	1.45	1.58
Total	**5.80**	**5.06**	**54.88**	**47.48**	**519.33**	**423.68**

enabled us to estimate the effect of natural and manmade disturbances on the ecosystem in connection with the permafrost.

4. Conclusions

Sim-CYCLE Siberia constructed by the present study has enabled us not only to disclose detailed dynamic states of the frozen soil centering on the permafrost but also to estimate the carbon dynamics in the ecosystems in the eastern Siberia simultaneously with achieving the simulation of the seasonal change in the frozen soil over the wide area.

The results of this carbon dynamics simulation in the eastern Siberia showed a remarkable seasonal change with peaks in June and July reflecting the effect of frozen soil. The annual amounts of NPP, the annual averages of plant biomass and soil organic carbon were estimated as 5.8 PgC/year, 54.9 PgC and 519.3 PgC respectively.

REFERENCES

Imanishi, K., Ito, A. and Oikawa, T. (2001) Model analysis of carbon dynamics of each type of vegetation in the eastern Siberia. Proceedings of the ninth symposium of the joint Siberian permafrost studies between Japan and Russia in 2000. Eds. M. Fukuda and Y. Kobayashi, 231-236.

IPCC (2001) IPCC Third Assessment Report - Climate Change 2001: The Scientific Basis. Cambridge University Press, Cambridge.

Ito A. and Oikawa T. (2000) A model analysis of the relationship between climate perturbations and carbon budget anomalies in global terrestrial ecosystems: 1970 to 1997. Climate Research 15:161-183.

Iwahana G., Machimura T., Kobayashi Y., Fukuda M. and Fedorov N. (2001) Fire effects on surface fluxes and active layer dynamics in Taiga forest over east Siberian permafrost region. Proceedings of the ninth symposium on the joint Siberian permafrost studies between Japan and Russia in 2000. Eds. M. Fukuda and Y. Kobayashi, 162-169.

Jackson, R. B., Canadell J. *et al.* (1996) A global analysis of root distributions for terrestrial biomes. Oecologia 108: 389-411.

J. M. A. (1999) Climate change monitoring report 1998. Japan Meteorological Agency, Tokyo.

Kinoshita S. (1982) Physical science of permafrost. Morikita Publishing Company Inc., Tokyo.

Kondo J (2000) Science of atmosphere adjacent to the soil surface. University of Tokyo Publishing Association, Tokyo.

Fire History of Mature Larch Forests near Yakutsk, Eastern Siberia

Takahashi, K.[1], Isaev, A.[2], Maximov, T.C.[2], Saito, H.[1]

[1]Graduate school of Agriculture, Hokkaido University. Forest Dynamics Group, CREST

[2]Institute for Biological Problems of Cryolithozone, Russian Academy of Science

1. Introduction

The distribution, species composition, structure and forest dynamics of Russian boreal forests are influenced by forest fires and different phases and stages of pyrogenic succession cover 40% to 96% of the total forested area in Siberia and the Russian Far East(FAO 2001). Estimates of annual carbon emissions to atmosphere caused by forest fires ranged from 35 to 93 million tons of carbon to 125+21 million tons(Shvidenko and Nilsson 2000, FAO 2001), of which post-fire biogenic flux comprised about 50%. Double-faced role of forest fires - distructive and dynamic - is evident in the boreal forest. Frequency of fires and their strength, as well as climate, types of fires and their distribution are influenced on regeneration. Objective of this study is to clarify the frequency of forest fires and their strength and to consider their effects on succession.

2. Study sites and methods

To investigate the fire history, sample disks which clearly showed fire scales were collected from stumps in study plots at Kenkeme(62° 12′ N, 129° 10′ E) and Neleger(62° 18′ N, 129° 30′ E) in July 2001. Study plots which were set to estimate the carbon storage of larch(*Larix gmelini*) forests were cut clearly in 1999(Kenkeme) and in 2000(Neleger). Samples are 10 disks from Neleger and 9 disks from Kenkeme. Tree rings of them were read and fire scales were decided by magnifying glass. Results of forest inventories of study plots and forest conditions of them before and after cuttings are shown in Table 1 and Photo 1, 2.

Table 1. Conditions of study plots

Plot	Location	Density (1/ha)	DBH (cm)	H (m)	BA (m^2/ha)
Neleger	62°18'N 129°30'E	2116	8.7 (0.1–42.0)	8.6 (1.3–20.5)	21.29
Kenkeme	62°12'N 129°10'E	1833	12.8 (0.9–25.5)	11.9 (2.3–21.8)	27.40

3. Results and Discussion

Samples of disks are shown in Photo 3 and 4. Information gotten from those disks are shown Table I and II. Results from this study can be summarized as follows.

1) The most advanced age of sample disks was 257 years old at Kenkeme and over 200 years old at Neleger.

2) The most fire scales observed in a disk were seven of No.3 at Kenkeme.

3) Forest fire occurred thirteen times in both study plots during about 250 years.

4) Average, the shortest and the longest intervals of fire occurrence were 13 years, 4 years and 35 years respectively at Neleger and 15 years, 3 years and 43 years at Kenkeme. Fire frequency increased since 1939 at Neleger and 1904 at Kenkeme.

5) The most sum of samples with a fire scale shown in the same year was six at Neleger and seven at Kenkeme. But common year was not observed in both study plots.

6) Minimum diameter(age) shown a fire scale was 1.0 cm(17years) at Neleger and 2.2 cm(32 years, estimated value) at Kenkeme. Bark thickness of larch increased with increasing diameter and reached 6.8 cm in maximum.

As the age of upper-story trees are over 200 years old and tree density, average diameter and height do not show an evidence of big catastrophe, it is assumed that crown fires did not occur last 150 years. There are many years when only one sample has fire scale and fire interval is about 10 years last 50 years before the last fire in both study plots. This shows that forest fires were mainly surface ones because of less litter and fallen trees during this period. Minimum diameters observed first fire scale also indicate the possibility that those surface fires killed saplings with a diameter of less than 1.0 – 2.2 cm.

REFERENCES

FAO:Global Forest Fire Assessment 1990-2000. 495pp,2001

Shvidenko,A. & Nilson,S.:Ecological Studies 138:132-150,2000

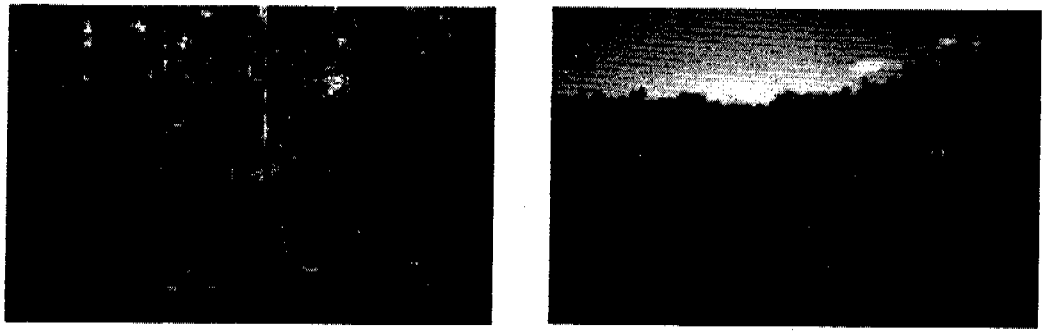

Photo 1. Neleger study plot before and after cutting

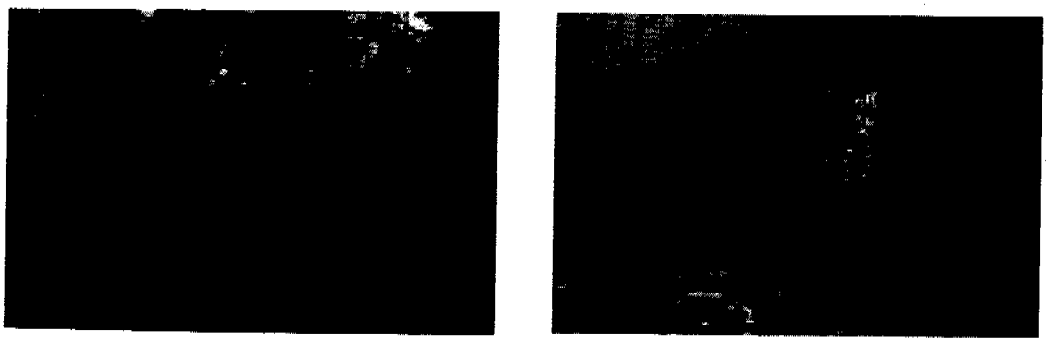

Photo 2. Kenkeme study plot before and after cutting

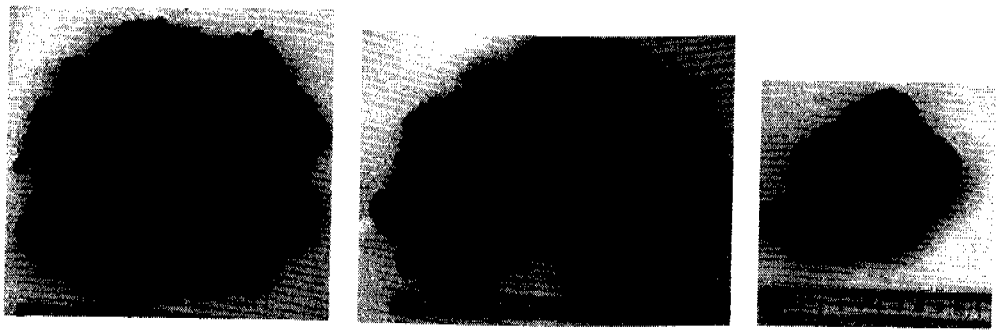

Photo 3. Disk samples of Neleger

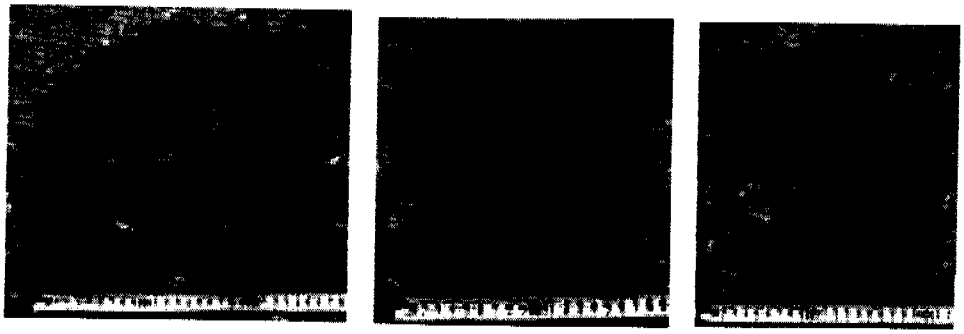

Photo 4. Disk samples of Kenkeme

Table 2. Fire occurrence and DBH damaged by fires in Neleger

Fire occurrence (A.D.)	Interval (years)	Sample No. and DBH(cm) 1	2	3	4	5	6	7	8	9	10	Sum of sample observed fire scale
1823										2.1		1
1858	35			2.0						3.5		2
1867	9									4.3		1
1891	24			6.2								1
1914	23						1.0					1
1928	14						2.0					1
1939	11		5.3	15.5	+			+	+		+	6
1944	5										+	1
1949	5		5.6		+			+	+		+	5
1954	5							+	+			2
1958	4				+							1
1972	14	7.0	7.0			4.9	5.6		+		+	6
1978	6				7.8							1
Age of sample(years)		121	132	>155	>80	112	103	−	−	>200	−	
Diameter without bark(cm)		12.5	9.3	20.5	8.3	8.7	6.8	−	−	26.2	−	
Thickness of bark(cm)		1.6	1.2	4.9	2.6	1.5	1.7	−	−	6.3	−	

Mean of diameter observed first fire scale 2.7±2.4cm

Average interval of fire 13 years

Note) +: Diameter can't be measured because of decay of a part of stump

−: Sample age can't be measured because of decay of a part of stump

Table 3. Fire occurrence and DBH damaged by fires in Kenkeme

Fire occurrence (A.D.)	Interval (years)	Sample No. and DBH(cm) 1	2	3	4	5	6	7	8	9	Sum of sample observed fire scale
1782				2.7				2.3			2
1799	17			3.4							1
1842	43			4.9							1
1848	6	2.2		5.4	3.3		3.8		5.9		5
1864	16									7.0	1
1888	24	4.9			6.8						2
1904	16									11.3	1
1911	7			9.0	8.6	6.8				13.2	4
1914	3				9.0						1
1923	9			10.0							1
1939	16									12.6	1
1943	4	12.7		11.6	12.1	10.0		22.4	18.5	12.8	7
1962	19		6.7								1
Age of sample(years)		>151	>141	257	199	>133	200	252	203	170	
Diameter without bark(cm)		16.8	7.6	21.8	14.7	18.3	23.5	29.0	22.3	15.0	
Thickness of bark(cm)		3.7	0.7	4.5	6.8	–	5.8	3.5	5.8	4.5	

Mean of diameter observed first fire scale 4.5±2.1cm
Average interval of fire 15 年
Note)−: same as Table 2.

Forest Fire and Lightning

H. Hayasaka[1,2]

[1] Graduate School of Engineering, Hokkaido University, Sapporo 060-8628, JAPAN
Phone: +81-11-706-6784, Fax: +81-11-706-67842, e-mail: hhaya@eng.hokudai.ac.jp
[2]CREST, JST (Japan Science and Technology Corporation)

1. Introduction

It may be very important for human to understand the role of forest fire on the boreal forest succession more clearly. Lightning-caused forest fire may have an important role in the boreal forest succession. The author noticed that several large lightning-caused forest fires occupy most of the annual burnt area in Alaska. In this point of view, two data sets of lightning-caused forest fire and lightning strike were used to know the relationship between lightning and lightning-caused forest fire. Simple but fundamental analyses were carried out using recent fire data for 14 years and lightning data for 11 years. Analytical results clearly showed the recent occurrence tendencies and relationship of forest fire and lightning in Alaska.

2. Forest Fires and Lightning Occurrence Trend in Alaska

2-1 Data sets

2.1.1 Data set of lightning-caused forest fire The Alaska Fire Service has data set of lightning-caused forest fires. In this paper, data from 1956 to 1999 was analyzed. Data contains fire occurrence position (latitude, longitude), burnt area and a discovery day. Small fire of burnt area less than 0.0004 km^2 is neglected. The number of the data is 7,949 cases in total. The data has 2713 cases after 1986, and they are used for the comparison with the lightning data. In the data, there are various kinds of errors. Occurrence number has some error because small fire is not included. Fire occurrence position, burning area and discovery day may have errors also because fire observation was mainly made using an airplane. We could not guess the degree of the error.
The discovery day may have an error of few days. This delay may be due to the process from the smolder to the fire. This is called "Holdover Fire".

2.1.2 Data set of lightning Lightning data is made on the basis of the measured value in nine thunderstorm observation stations in the Alaska. The data includes occurrence date and time, position (latitude and longitude), strength (positive and negative), multiple discharge information. The lightning location is being calculated using the data from multiple observation station. The detected location for the interior Alaska is comparatively accurate. The error of the position is said to be less than about a few km. The location error increases in Alaska north tundra area, and coastal area. The author tried to use data from 1986 for the comparison with the data of the forest fire

although there were much imperfect data in from 1986 to 1988. Data from 1989 to 1999 was analyzed in this paper. The average data number is about 2.7 ten thousand disregarding multiple strikes.

2-2 Occurrence Tendency of lightning-caused forest fires

The number of fires and burnt areas by lightning-caused forest fires in Alaska from 1956 to 1999 are shown in Figure 1. From Figure 1, it will be found that the average annual number of fires is about 180 with mean annual burnt areas of 2,303 km^2, and that there are short fire cycles (one or two years) in fire number. There are also long fire cycles (about 8-12 years) in burnt area of around 10,000 km^2 found in Figure 1.

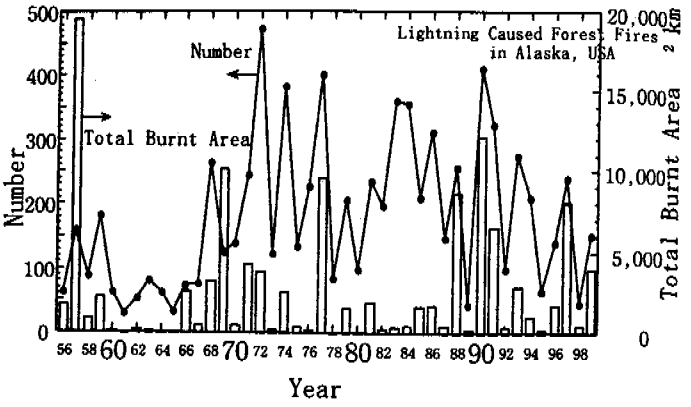

Fig. 1 Forest Fire in Alaska (1956-1999)

Figure 2 is a detail figure of Figure 1. The maximum burnt area in each year added in Figure 2 using bars. From figure 2, maximum burnt areas in 1988, 1990 and 1997 are around 2,000 km^2. Large burnt area around 2,000 km^2 is larger than total burnt area in non-fire year such as in 1986, 1987, 1992 and so on. These forest fire tendency found in Figures 1 and 2 may be explained by weather condition for lightning, dryness of the forest, and fuel accumulation in the forest.

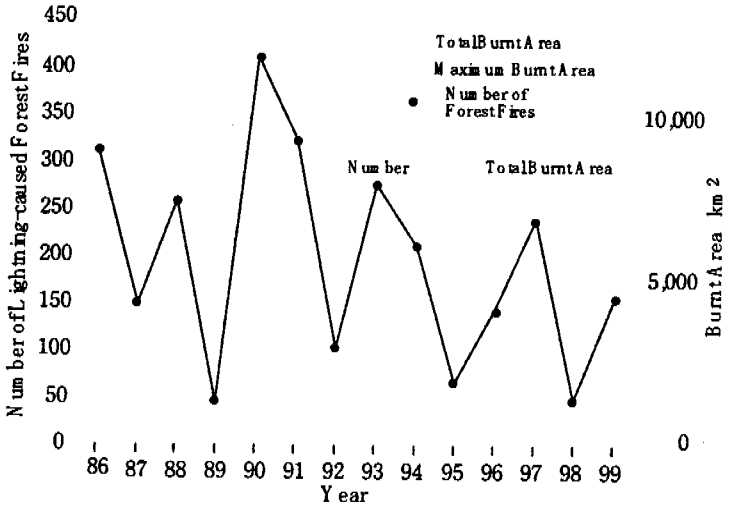

Fig. 2 Forest Fire in Alaska (1986-1999)

2-3 Occurrence Tendency of lightning and Ignition Probability

Occurrence tendency of lightning and forest fire are shown in Figure 3. The ignition probability is also shown in Figure 3. The annual ignition probabilities vary from 0.2 to 1.4 %. This general ignition probability is often used in various reports. The equation for the general ignition probability is defined in the following.

$$\alpha ap=(\text{Number of forest fires})/(\text{Number of lightning Strikes} \times 0.9) \times 100 \quad (\%) \quad (1)$$

Here, 0.9 is a ratio of negative and positive discharge.

But this general ignition probability includes lightning strikes not only to forests but also to rocks in mountains, rivers, lakes, swamps, and non-combustible substances. Here, the author would like to call this general ignition probability as apparent ignition probability.

In previous report (1), the author already indicated the ignition probabilities become higher if we consider probability for the forest area and under the scale of thundercloud. Actually, the ignition probabilities in the forest area in the vicinity of Fairbanks are from 8.2 to 18.2 %.

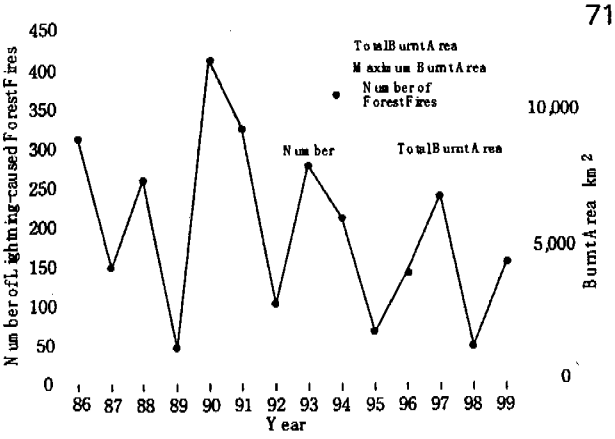

Fig. 3 Forest Fire and Lightning in Alaska

Here, the author would like to define the true ignition probability.

$$\sigma t = (\text{Number of forest fires}) / (\text{Number of lightning Strikes to forests} \times 0.9) \times 100\ (\%) \quad (2)$$

If we could extract lightning strikes to forests from whole lightning data, this equation will be more effective.

From Figure 3, average number of lightning strikes is about 2.7 ten thousand. The number of forest fires will not always follow the number of lightning strikes. For example, 3.8 ten thousand lightning strikes in 1994 could not make a lot of fire. The number of fires in 1994 was 210, average value of from 1986 to 1999.

The average apparent ignition probability is about 0.74% from Figure 3. The maximum ignition probability is 1.4% in 1990. This year, both number of forest fires and number of lightning strikes are largest from 1986. On the contrary, the apparent ignition probabilities in 1989,1992, 1995 and 1998 were less than 0.45% nevertheless the number of lightning strikes were from 1.2 to 2.7 ten thousand.

3. Climate of Interior Alaska

Average maximum temperature and average precipitation of past 30 years (1971-2000) in Fairbanks were shown in Figure 4. The x-axis in Figure 4 is day number counted from January first. Accumulated precipitation from the day number 135 is also shown in Figure 4.

From Figure 4, the average maximum temperature has a turning point at the day number 191-192. Two curves for accumulated precipitation and precipitation show that precipitation increase gradually toward August, and total precipitation exceeds 100 mm.

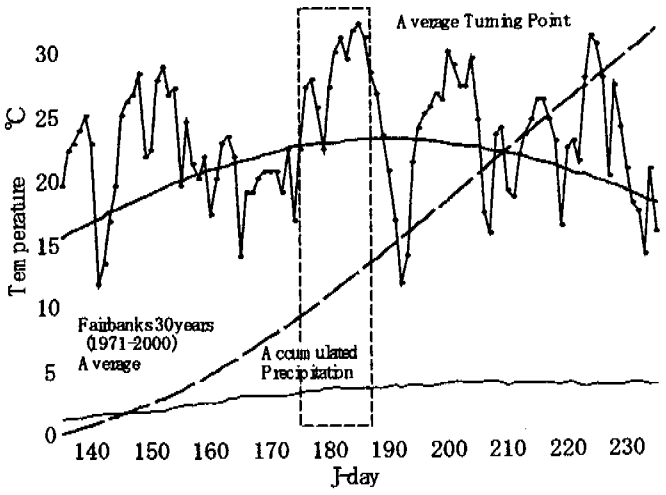

Fig. 4 Average Temperature & Rainfall in Fairbanks

4. Occurrence Tendencies of Forest fire and Lightning

Occurrence tendencies of forest fire and lightning are shown in Figure 5. Average numbers of forest fire and lightning for each day number are obtained using the above-mentioned data sets. Occurrence tendencies do not have smooth curve but clearly show how lighting and lightning-caused forest fire occur in Alaska.

Fire season starts from around day number 140 (middle of May) and ends in around day number 230 (middle of August). Severe forest fire days start from day number of 175 (end of June) and end around 187 (top of July) as shown in Figure 5. In this severe fire period, lightning occurs frequently and forest fire follows. Maximum burnt area rate reaches 217 km^2/day. After this fire season, vigorous occurrence of lightning continues about one more week. On the other hand, forest fires decrease rapidly. This may be due to precipitation. In other words, forest becomes wet.

Large top ten fires in 1986 to 1999 are also shown using figures in Figure 5. These large fires occur around the day number from 160 to180. Six large fires occurred in the severe fire period.

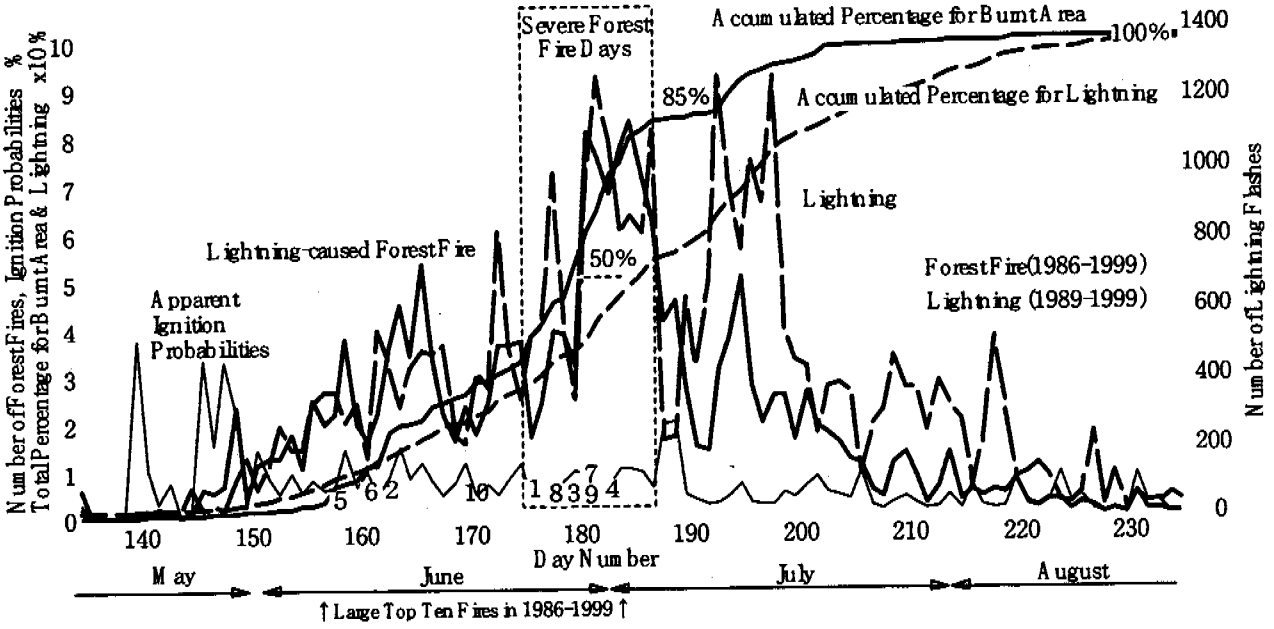

Fig. 5 Forest Fire and Lightning Tendencies in Alaska

5. Conclusions

Simple but fundamental analyses were carried out using two data sets of lightning-caused forest fire and lightning strike. Recent fire data for 14 years and lightning data for 11 years were analyzed. Analytical results clearly showed the recent occurrence tendencies of forest fire and lightning in Alaska.

The recent tendencies are in the followings:

1. Average annual burnt area from 1986 was 3,464 km^2 that is greater than 1.5 times the long-term average of 44 years from 1956.
2. Relatively small fire of burnt area under 1 km^2 occupies about 70 % of total fire occurrence.

Average burnt area per fire is 18 km^2/fire.

3. From the point of view of burnt area, it was found that only several large fires occupy most of the annual burnt area. The representative burnt area is about 250 km^2. The seven fires of this class occur and occupy half of the annual burnt area.

4. Fire season in Alaska begins in the middle of May and ends in the middle of August. Severe forest days are two weeks from the end of June.

5. Lightning occurrence has two peaks but lightning-caused forest fire occurrence shows only one peak. This difference may be due to the effect of rainfall on forest.

ACKNOWLEDGMENTS

I would like to thank M. Lynch (Alaska Fire Service) for giving me valuable data about lightning-caused forest fire.

This research is being partly sported by the Grant-in Aid for Scientific Research (A) of Japan Society for the promotion of Science.

REFERENCE

Alaska Fire Service. 1999. http://fire.ak.blm.gov/.

A grid-based model simulation of carbon dynamics and wildfire regime in East Siberian larch forest

Akihiko Ito

(Frontier Research System for Global Change, 3173-25 Showa-machi, Kanazawa-ku, Yokohama 236-0001, Japan, E-mail: itoh@jamstec.go.jp)

1. Introduction

To elucidate the functioning of boreal forests in the global carbon cycle, we should clarify the influence of wildfire on regional carbon cycle. Actually, larch forests in East Siberia are known as a fire-prone ecosystem, in which frequent fires become an essential component of the ecosystem sustainability. It has been hypothesized that fire may affect carbon dynamics by accelerating biomass turnover, degrading succession stage, and producing resistant charcoal. Moreover, global warming may bring about ramifications to the fire-carbon relationship, because fire regime is closely related to environmental conditions, such as temperature, air humidity, and soil wetness. The altered carbon cycle in the boreal forests, in turn, may modulate the atmospheric greenhouse gas level, acting as a feedback process.

The complicated interaction among the fire regime, the carbon cycle, and the global warming should be addressed with appropriate models, based on extensive observations. Gardner et al. (1996) classified fire models into three categories. (I) Empirical models, in which observed fire regime (e.g., frequency and burnt-area) is correlated with meteorological records. (II) Thermodynamics models, in which fire occurrence and expansion is described as a thermodynamic process, analogous to chemical reaction and heat conduction. (III) Cellular automaton models, which describe fire behavior as a percolation process on a horizontal grid, frequently using probabilistic approach (i.e., Monte-Carlo method). They conclude that the cellular automaton approach is most comprehensive for addressing the complicated interaction mentioned above, because it can include spatial fire pattern and carbon dynamics in an explicit manner.

This study presents an integrated model system including ecosystem dynamics, fire regime, and greenhouse-gas budget. The model system adopts the cellular automaton approach for fire behavior, which is fully coupled with carbon dynamics calculated at each grid. Then, the model is applied to simulate the long-term carbon dynamics of a larch forest in East Siberia with different fire regimes, and to estimate the variation of carbon budget in response to environmental changes.

2. Study site

The study site is a typical larch stand, located in the vicinity of Yakutsk, Russia (62°N, 130°E). In addition to dominant Dahurian larch (*Larix gmelinii*), there occur several shrub (e.g.,

Betula and Salix) and herbaceous (e.g., Carex) species. The site has sandy roam soil with a depth of permafrost, in which active layer emerges in summer (max. 1.2m). Forcing climatic variables are derived from a dataset of the U.S. National Centers for Environmental Prediction / National Center for Atmospheric Research (NCEP/NCAR). The dataset (averaged 1948-2000) indicates that annual mean air temperature of the site is –8.4°C and annual precipitation is 347 mm. The NCEP/NACR precipitation is slightly higher than other datasets (i.e., 270 mm), probably because of its large interannual variability (189 to 661 mm).

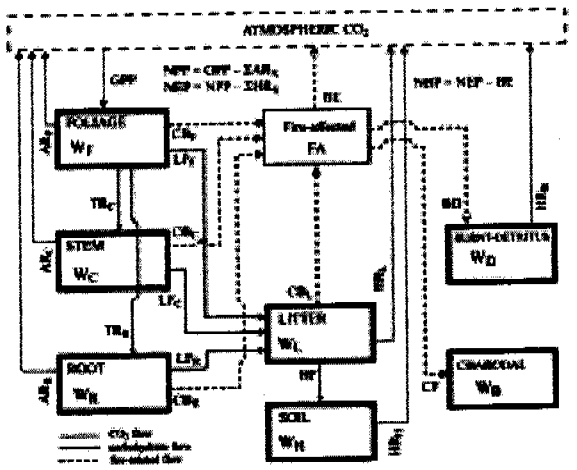

Fig. 1. Schematic diagram of the compartment model of carbon dynamics in East Siberian larch forest, including fire-related carbon flows and stocks.

3. Model simulation

The cellular automaton of wildfire has a horizontal grid-system with 200 columns and 200 rows covering the area of 100

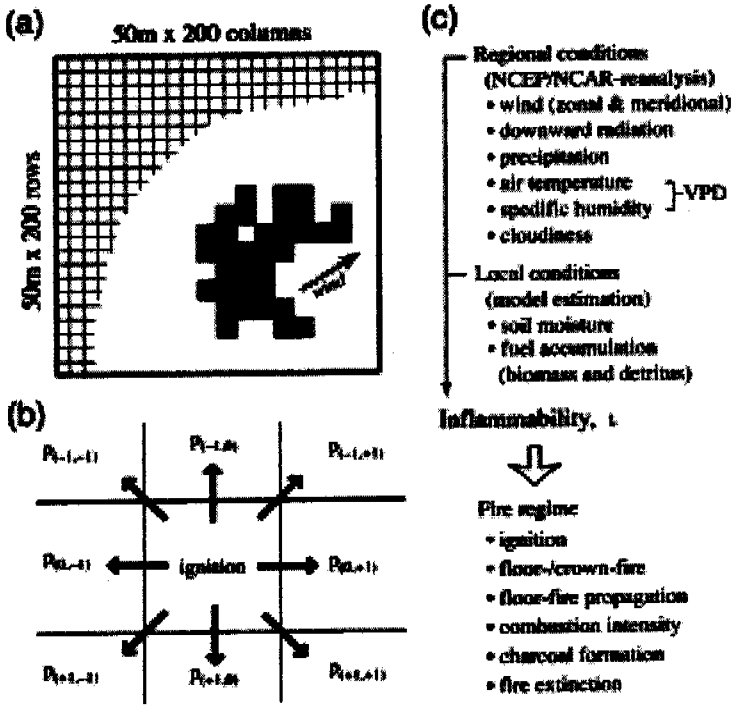

Fig. 2. Overview of the fire model. (a) Grid-based model of fire regime in the East Siberian larch forest. (b) Fire propagation simulated as a probabilistic process. (c) Environmental dependence of the fire regime, represented by a fire-affinity index (inflammability, ι).

Table 1. Ecophysiological parameters for simulations of East Siberian larch forest with Sim-CYCLE.

parameter	value	unit
Plant optics		
plant reflectivity, albedo	0.13	-
attenuation coefficient for vertical incident radiation	0.53	-
Allocation		
base allocation ratio to assimilative organ	0.05	-
allocation ratio between stem and root	0.48	-
Leaf morphology		
specific leaf area	100	$cm^2\ g^{-1}$ d.w.
Photosynthesis, single-leaf		
photosynthetic patyway	C_3	-
quantum yiedl, light-use efficiency	0.05	mol CO_2 mol^{-1} photon
maximum photosynthetic rate under optimal condition	8	μmol CO_2 $m^{-2}\ s^{-1}$
optimal temperature (ambient CO_2, 350 ppmv)	18	℃
minimum temperature	-2	℃
maximum temperature	35	℃
minimum stomatal conductance	10	mmol H_2O $m^{-2}\ s^{-1}$
parameter of maximum stomatal conductance	47000	mmol H_2O $m^{-2}\ s^{-1}$ ppmv
VPD dependence for stomatal conductance	5.5	hPa
parameter of soil water (non-stomatal) limitation	0.32	-
parameter of CO_2 dependence	35	ppmv
CO_2 compensation point	50	ppmv
Respiration		
specific growth respiration rate of foliage	0.35	g C g^{-1} C
of stem	0.08	g C g^{-1} C
of root	0.12	g C g^{-1} C
specific maintenance respiration rate of foliage	0.92	10^{-3} g C g^{-1} C day^{-1}
of stem sapwood	0.023	10^{-3} g C g^{-1} C day^{-1}
of root sapwood	0.038	10^{-3} g C g^{-1} C day^{-1}
of stem heartwood	0.0031	10^{-3} g C g^{-1} C day^{-1}
of root heartwood	0.0039	10^{-3} g C g^{-1} C day^{-1}
parameter of control temperature dependence	2	-
Litter fall		
specific mortality of foliage	0.18	10^{-3} g C g^{-1} C day^{-1}
of stem	0.0035	10^{-3} g C g^{-1} C day^{-1}
of root	0.019	10^{-3} g C g^{-1} C day^{-1}
leaf shedding rate at the end of growing period	0.3	g C g^{-1} C day^{-1}
Root morphology		
parameter of vertical distribution	0.95	-
Soil optics		
soil surface reflectivity, albedo	0.05	-
Soil decomposition		
specific decomposition rate of litter	1.34	10^{-3} g C g^{-1} C day^{-1}
of mineral soil	0.211	10^{-3} g C g^{-1} C day^{-1}
of black carbon	0.195	10^{-3} g C g^{-1} C day^{-1}
parameter of moisture requirement of litter	0.21	-
of mineral soil	0.1	-
of blackcarbon	0.1	-
parameter of air requirement of litter	0.18	-
of mineral soil	0.08	-
of black carbon	0.08	-
proportion of litter mineralization and humus formation	0.55	g C g^{-1} C

km^2 (10 km x 10 km); i.e., one grid cell represents a 50 m x 50 m patch. Simulations were performed for 600 years at daily time-step, composed of three 200-year phases: the first grow-up, the second control, and the third experiment.

For each cell, carbon dynamics is independently calculated using a process-based model, termed Sim-CYCLE (Simulation model of Carbon cycle in Land Ecosystems). The model used in this study is an expanded version of the original model (Ito & Oikawa, 2002), so that it can capture carbon flows and charcoal storage related to fire regime. For example, in addition to the original five compartments, a charcoal and detritus compartments are included, and combustion (CO_2 release) and charcoal synthesis are regarded as explicit flows (Fig.1). Decomposition of detritus is a function of soil temperature and soil moisture, similar to those of litter and humus, but with a lower susceptibility to microbial decomposition. Model parameters were calibrated (Table 1), so that the estimated growth patter would capture the observed one (Schulze et al., 1995; Sawamoto et al., 2000; Tsuno et al., 2001), on a basis of observed ecophysiological features (Koike et al., 1996; Kajimoto et al. 1999).

Fire regime in the grid-system is modeled in a stochastic manner, in which ignition, expansion, and extinction are formulated as probability of these phenomena (Fig. 2). Their environmental dependencies are represented by a single index of fire-affinity, so-called inflammability (ι), which is dependent on temperature, atmospheric humidity, soil moisture, and fuel accumulation. Using the inflammability to modulate probability, certain cells catch fire due to some random ignition processes such as lightning. This simulation assumes that litter of forest floor would catch fire at first (i.e. floor fire), and with a certain probability, tall trees would also be burnt (i.e. crown fire). Fire propagation from one cell to another cell is simulated as a percolation process, weighted by the inflammability and wind condition (velocity and direction). The percolation model of fire expansion may successfully capture the different types of fire: i.e., back fire, frank fire, and head fire. Fire extinction is also simulated using the inflammability, so that lower inflammability (e.g. rainy day) leads to higher extinction probability. Parameters for the fire regime were calibrated, so that observed seasonal change in fire events (Korovin, 1996) would be adequately simulated.

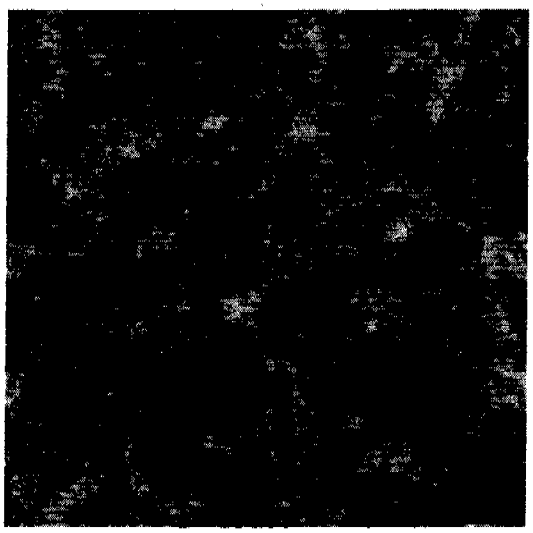

Fig. 3. Example of simulated spatial heterogeneity of biomass storage in the larch forest, induced by fire events (at the 600th year) The black area represents cells burnt recently, and light areas show cells with mature forest

4. Results and discussion

The calibrated model could represent the observed growth pattern of larch stand for about 400 years, and finally

gave a steady state of carbon dynamics. Average aboveground biomass was estimated as 50 Mg C ha^{-1}, and belowground root and soil carbon storage was estimated as 110 Mg C ha^{-1}.

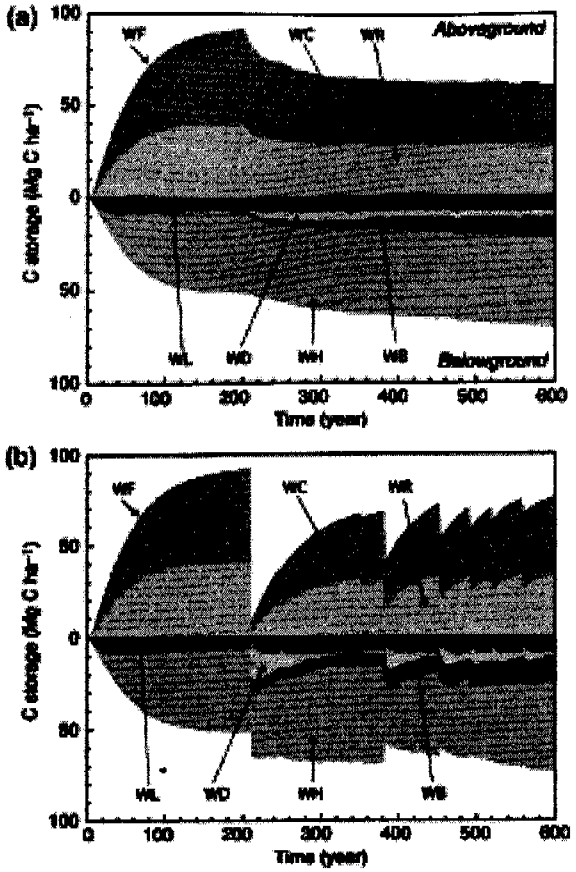

Fig. 4. Simulate temporal change in carbon storage of the larch forest for 600 years. (a) Average over the whole grid-system, and (b) example of a single cell. See Fig.1. for symbols.

As a result of fire regime, considerable spatial heterogeneity of the carbon dynamics took place over the grid-system (Fig. 3). Occurrence of fire resulted in significantly lower carbon storage of plant biomass (about –30%), whereas soil carbon storage (except for floor litter) was slightly increased because of additional detritus input due to fire (Fig. 4). In a single fire event, a substantial amount of carbon was released into the atmosphere (~30 Mg C ha^{-1}), but the ecosystem essentially acted as a net carbon sink during the following re-growth stage. The average floor-fire interval was estimated as 45~55 years, while the average crown-fire interval was over 120~150 years. Because the model assumed that a part of burnt carbon becomes resistant charcoal (cf. Fig.1), soil black carbon increased with time. However, there is little data of charcoal formation and decomposition, and therefore some estimated parameters were used to simulate the processes related to charcoal. Then, a sensitivity study for these parameters needs to be performed. Finally, fire effect on the regional carbon cycle suggested by the grid-based model study will be scaled-up to continental scale, in conjunction with a high-resolution continental terrestrial ecosystem model (e.g., Ito, 2001).

5. Concluding remarks

This study presents a process-based model of carbon dynamics for East Siberian larch forests, enabling us to estimate long-term effect of fire regime on the net carbon budget under changing environment. Since the fire regime is modeled in a process-based manner, it may be applicable to estimate responses of the boreal forest to the anticipated global change, such as atmospheric CO_2 rise, temperature warming, precipitation change, and human ignition or suppression of fire. In addition to sensitivity analysis, the forthcoming research will address the behavior of net carbon budget under changing environments.

REFERENCES

Ito, A., 2001. A broad-scale simulation of transitional change in the carbon dynamics of boreal and arctic land ecosystems along with environmental gradients. *Bulletin of the Research Center for North Eurasia and North Pacific Regions, Hokkaido University*, 1: 67-82.

Ito, A. and Oikawa, T. 2002. A simulation model of the carbon cycle in land ecosystems (Sim-CYCLE): A description based on dry-matter production theory and plot-scale validation. *Ecol.Model.* 151: 143-176.

Kajimoto, T., Matsuura, Y., Sofronov, M. A., Volokitina, A. V., Mori, S., Osawa, A. and Abaimov, A. P. 1999. Above- and belowground biomass and net primary productivity of a Larix gmelinii stand neat Tura, central Siberia. *Tree Physiol.* 19, 815-822.

Koike, T., Lei, T. T., Maximov, T. C., Tabuchi, R., Takahashi, K. and Ivanov, B. I. 1996. Comparison of the photosynthetic capacity of Siberian and Japanese birch seedlings grown in elevated CO_2 and temperature. *Tree Physiol.* 16, 381-385.

Korovin, G. N. 1996. Analysis of the distribution of forest fire in Russia. In: Fire in Ecosystems of Boreal Eurasia (Eds. J. G. Goldammer and V. V. Furyaev). Kluwer Academic Publishers, Dordrecht, 112-128.

Sawamoto, T., Hatano, R., Shibuya, M., Takahashi, K., Isaev, A. P. and Maximov, T. C. 2000. Effect of forest fire on carbon cycling in taiga soil - plant system, near yakutsk. In: Proceedings of the 8th symposium on the joint Siberian permafrost studies between Japan and Russia in 1999 (Eds. G. Inoue and A. Takenaka). Tsukuba, 230-236.

Schulze, E.-D., Schulze, W., Kelliher, F. M., Vygodskaya, N. N., Ziegler, W., Kobak, K. I., Koch, H., Arneth, A., Kusnetsova, W. A., Sogatchev, A., Issajev, A., Bauer, G. and Hollinger, D. Y. 1995. Aboveground biomass and nitrogen nutrition in a chronosequence of pristine Dahurian *Larix* stands in eastern Siberia. *Can.J.For.Res.* 25, 943-960.

Tsuno, Y., Shibuya, M., Saito, H., Takahashi, K., Sawamoto, T., Hatano, R., Isaev, A. P. and Maximov, T. C. 2001. Aboveground biomass, nitrogen and carbon contents in Larix stands in eastern Siberia. In: Proceedings of the 9th Symposium on the Joint Siberian Permafrost Studies between Japan and Russia in 2000 (Eds. M. Fukuda and Y. Kobayashi). Low Temperature Institute, Hokkaido University, Japan, Sapporo, 68-74.

Comparisons of Hydraulic Conductivity between Intact, Watered and Slightly Burnt Larch Trees in Eastern Siberia

Y. Kobayashi[(1) (2)], H. Saito[(3)], M. Fukuda[(4)], and A. N. Fedorov [(5)]

[(1)] Japan Science and Technology Corporation (JST)
[(2)] Research Center for North Eurasia and North Pacific Regions, Hokkaido University, Sapporo, 060-0809, Japan
yosikazu@pop.lowtem.hokudai.ac.jp, TEL: +81-11-706-4535, FAX: +81-11-717-3402
[(3)] Laboratory of Silviculture, Graduate School of Agriculture, Hokkaido University, Sapporo, 060-0808, Japan
[(4)] Institute of Low Temperature Science, Hokkaido University, Sapporo, 060-0818, Japan
[(5)] Permafrost Instituter, Siberian Branch, Ras, Yakutsk, 677018, Russia

1. Introduction

It has been widely recognized that interactions between ecosystems and atmosphere over Siberian taiga play significant roles in the global environment. Siberian taiga, located in permafrost region, is formed under very severe and fragile background, such as small rainfall during the growing season, relatively dry atmosphere and limited development of root system due to existences of permafrost layer. Recently, Siberian taiga faces the risk of forest fire, and it is urgent and crucial concern to evaluate the effects of forest disturbances by fires on the global environment.

A lot of observational and experimental studies are implemented to make clear the variations in H_2O, energy and CO_2 exchanges with transition of disturbed forest at the Siberian taiga ecosystem. (e.g. Arneath et al., 1996; Kelliher et al., 1997; Kelliher, et al., 1998; Ohta et al., 2001). However, little is known about some effects of fires on individual tree transpiration or photosynthesis processes which are elementary steps controlling the H_2O, energy and CO_2 exchanges over Siberian taiga ecosystem. Considering those most forest fires are classified into surface fire, and many trees survive after the surface fires, we need to make clear the effects of surface fires on transpiration or photosynthesis processes at a stand level to validate the variations in H_2O, energy and CO_2 fluxes observed at forest level.

This is a case study in order to discuss the effects of spring surface fires on hydraulic characteristics of larch tree by comparing leaf, stem and soil water potentials, soil water content and sap fluxes observed at damaged larch tree by surface fire, intact or and watered larch trees.

2. Study Site

The field observations were conducted in a natural larch (*Larix cajanderi*) forest called Neleger, which is located at about 25 km northwest of Yakutsk, Russia (62°19'N, 129°31'E). The forest canopy consists of 16~20 m high larch trees (>200yr) with stand density of 2100 trees/ha. Almost all of roots distribute in the upper active layer of 40 cm in thickness. Maximum and average diameter at breast height (DBH) are 41.8 and 8.65 cm, respectively (Yajima *et al.*, 1998). The width of stem sapwood, which supplies the leaves with water, showed roughly constant of 1.2 cm independent of stem diameter (Fig. 1). The forest floor is covered with lichen, moss and some shrubs.

Massive and frequent wildfires hit larch forests around Yakutsk region in the spring of 2002.

The north part of the experimental forest was also struck by a surface fire in mid May. The base of larch tree suffered significant damage, and scorched forest floors were observed after the surface fire. The surface fire hitting Neleger experimental forest is classified into "SC (scorched) type", *i.e.* litter not burned or partially burned (Wang, 2002). Although the surface fire was light degree, some roots near soil surface smoked until Mid July.

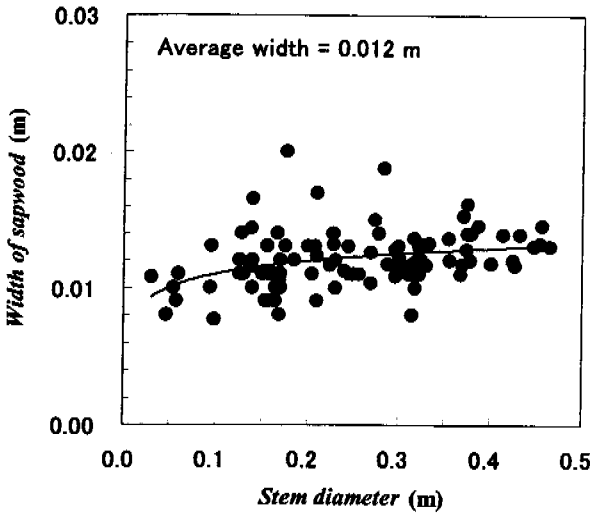

Fig. 1. Widths of sapwood against stem diameter.

We set up three different experimental plots in the larch forest; the first was a burnt plot, the second was control plot at which intact larch trees grow, and the last one was watered plot. Seven test stands of larch were selected from the three plots, and their dimensions are summarized in Table 1.

3. Method

3. 1. Field observation

Field observation was conducted from Jul. 23 to Aug. 2, 2002. Observed items were as follows; leaf water potential (Ψ_{leaf}), stem water potential at crown base (Ψ_{stem}), soil water potential (Ψ_{soil}), soil water content, sap flux (u_{sap}), net radiation (Rn) and photosynthetic photon flux density ($PPFD$). All bearing leaves of a branch at crown base are wrapped with shading vinyl bag to cancel the water potential gradient between the stem and the wrapped leaf, and the water potential of wrapped leaf is measured as Ψ_{stem} (Landsberg et al., 1976; Crombie, 1997). Soil moisture characteristic curve at the Neleger experimental forest is used to determine Ψ_{soil}. Other applied methods and measuring height/depth are shown in Table 2. We sprinkled 200 L of water on projected crown area of the test stand of watered plot at the midnights of Jul. 23 to 25.

3. 2. Data analysis

The observation data are analyzed on the basis of a concept of water flow in a

Table 1. Dimensions o the test stands

	Tree height H (m)	DBH* (cm)	Height of live crown base H_{LCB} (m)	Thickness of bark** (cm)	Width of sapwood*** (cm)	Basal area**** A (cm^2)	Sapwood area** A_{sw} (cm^2)
Control plot							
1	19.4	37.0	9.5	1.5	1.3	1074.7	130.6
2	16.2	16.1	10.5				
3	22.4	36.2	10.6				
Burnt plot							
1	17.5	33.3	8.4	0.7	1.3	870.5	120.9
2	15.6	16.7	6.7				
3	17.9	36.5	9.5				
Watered plot	19.8	31.5	11.2	1.0	1.2	778.9	110.7

* DBH: diameter at breast height (=1.2 m), ** measured at the height of 3.0 m (=measuring height of sap flux)
*** estimated from Fig. 1
**** calculated from DBH

Table 2. List of observed or caluculated items, measuring height/depth and applied methods

Item	Symbol	measuring height/depth (m)	Instrument/method
Net radiation	Rn	21.0	Net radiometer (Kipp & Zonen, model CNR1)
Photosynthetic photon flux densit	$PPFD$	〃	Photosynthetically active radiometer ()
Rain (at open space)	P	3.0	Rain gauge (R. M. Young, model 52203)
Leaf water potential (intermideate part of the	Ψ_{leaf}	14?16	Psychrometer (Decagon, model WP4)
Stem water potential	Ψ_{stem}	height of live crown base	Psychrometer and bagging method
Soil water potential	Ψ_{soil}	-0.1 and -0.3	determined by psychrometer and soil moisture characteristic curve
Soil water content	–	-0.1?-0.4	TDR sensor (Campbell, model 615 and Decagon, model ECH_2O)
Sap flux (sapwood area basis)	u_{sap}	3.0	Heat pulse sensor (Thermal logic, model "sap flow sensor")
Amount of water flow	Q	-	$Q = u_{sap} \times A_{sw}$
Sap flux (basal area basis)	q	-	$Q_{normalized} = Q / A$
Flow resistance from soil to leaf	$R_{soil\text{-}leaf}$	-	obtained from equation (1) with Q, Ψ_{soil} at the depth of 0.3 m , Ψ_{leaf}, A and H
Flow resistance from soil to stem	$R_{soil\text{-}stem}$	-	obtained from equation (1) with Q, Ψ_{soil} at the depth of 0.3 m , Ψ_{stem}, A and H

soil-plant-atmosphere continuum (SPAC). Water flux of basal area at breast height basis (q) in a SPAC is desribed by following equation:

$$q = \frac{Q}{A} = \frac{\Delta\Psi}{R \times l} \quad \cdots\cdots \quad (1)$$

where Q is the amount of water flow through SPAC, A is basal area at breast height (=1.2 m), $\Delta\Psi$ is the difference of water potential (e.g. $\Delta\Psi = \Psi_{soil} - \Psi_{leaf}$), R is unit flow resistance, l is reference length such as tree height or height of live crown base (H_{LBC}). The flow resistance, R is a variable index indicating permeability of water in a domain of a SPAC. In the present study, R is normalized by basal area at height of 1.2 m (A) and tree height (H) or height of live crown base (H_{LBC}) of each test stand.

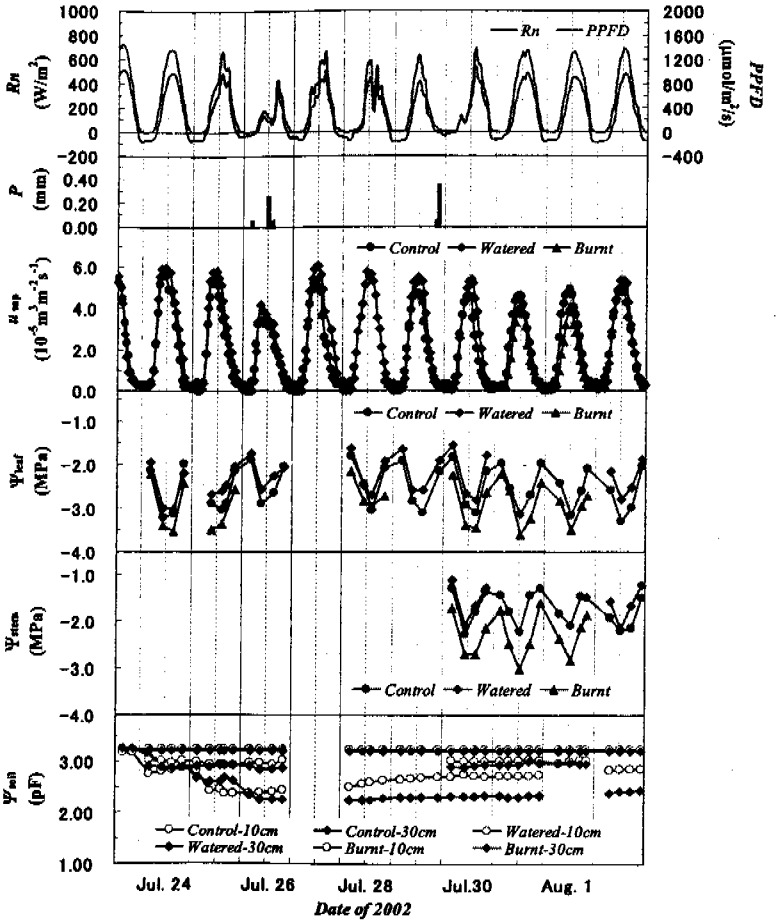

Fig. 2. Diurnal variations in the field observation items.

4. Results

The diurnal variations in observation items are shown in Fig. 2. It was generally fine weather during the observation period. A little rainfall events at an open space near the experimental forest were observed in the daytime on Jul. 26 and in the nighttime on Jul. 29, however there was no increase in soil water content in the forest. Average soil water content at the burnt plot was about

0.28 m^3/m^3, and it was higher than that at control plot of 0.15-0.20 m^3/m^3. Due to the watering effect, the average soil water content at watered plot increased from about 0.20 to 0.34 m^3/m^3. The increase in soil water content was equivalent to a decrease in pF value from pF 3.2 to pF 2.5.

Clear diurnal variations of Ψ_{leaf} were observed at the three plots, and Ψ_{leaf} at the burnt plot was always 0.2 to 0.5 MPa less than that of control plot. The daily minimum value of Ψ_{leaf} at the burnt plot reached about -3.5 MPa. As a whole, Ψ_{leaf} observed at control and watered plots in the daytime tended to decrease during the observation period, however, the tendency did not appear at the burnt plot. Decrease in Ψ_{stem} became obvious at burnt plot especially in daytime. The magnitude relation of Ψ_{stem} at the three plots was same for Ψ_{leaf}.

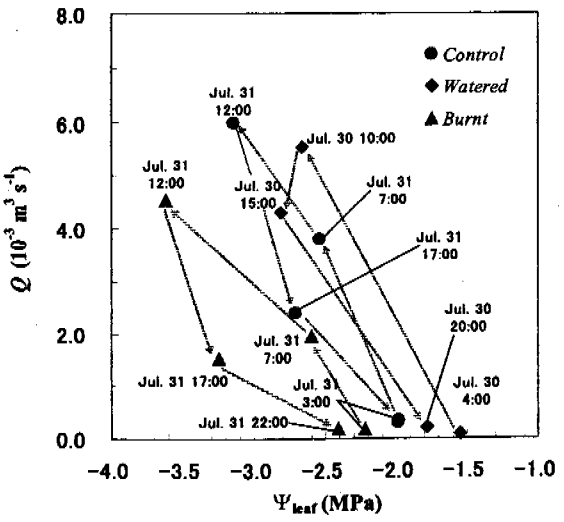

Fig. 3. Leaf water potential (Ψ_{leaf}) versus various amounts of amount of sap flow (Q) on Jul. 30 and 31, 2002.

Though the burnt plot showed relatively high soil moisture condition and lower Ψ_{leaf} which is indicating larger driving force of water flow, we also observed that u_{sap} of burnt plot was about 70-75% of that at control plot. The diurnal variations of u_{sap} at watered plot were characterized by higher daily maximum value and relatively long duration of u_{sap} peak. These characteristics of u_{sap} were actualized after Jul. 26, when the sprinkled water had infiltrated sufficiently at the soil layer in depth of 30 cm. Furthermore, cease of sap flow was recognized in late-night only at watered plot.

The relationship between Ψ_{leaf} and Q is shown in Fig. 3. Hysteresis relations are recognized at each three plots. The largest hysteresis loop is at burnt plot. This shows that there was no sufficient Q corresponding to Ψ_{leaf} at the burnt plot.

5. Discussions

The observation results suggests that the hydraulic conductivity of burnt tree is less than that of control and watered trees. Consequently, we discuss about the hydraulic conductivity of the test stands. The difference between Ψ_{soil} and Ψ_{leaf} (i.e. Ψ_{soil} - Ψ_{leaf}) at various q is shown in Fig. 4. The slope of linear regression line provides a index of total flow resistance of the test stand. Figure 4 shows the highest total flow resistance of the burnt tree and the lower flow resistance of watered tree resulting from the modification of water stress.

It can be considered that the effects of surface fire mainly cause damage to the tree stem and root system

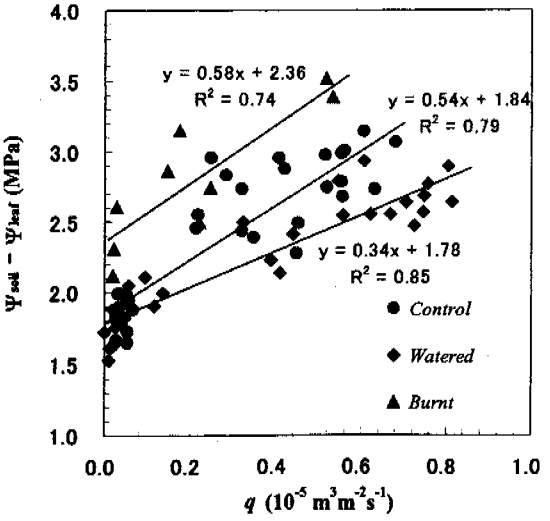

Fig. 4. Differences of water potential between soil and leaf (Ψ_{soil} - Ψ_{leaf}) plotted basal area basis sap flux (q).

near the surface. Relationships between Ψ_{soil} - Ψ_{stem} and Q of each three test stands are shown in Figure 5 to compare the hydraulic conductivity between soil to stem including root system. Normalized flow resistance, $R_{soil\text{-}leaf}$ and $R_{soil\text{-}stem}$ are listed in Table 3. It becomes appear that $R_{soil\text{-}stem}$ of burnt tree is more than 1.7 times of that estimated for control and watered trees. The result suggests the injuries of water conducting tissues of the burnt tree caused by the spring surface fire. High flow resistance of the burnt tree explains the contradictive situation of relatively high soil moisture and very low leaf water potential.

There was no obvious difference in the relationships between Ψ_{stem} - Ψ_{leaf} and q (Fig. 6). This means that there is no direct influence of the surface fire on the conducting tissues of the canopy. The results showed that the hydraulic conductivity of the burnt larch tree has been reduced due to the significant damage of water flow tissues around the base of burnt tree by surface fire.

In a theoretical sense, further decrease in Ψ_{leaf} will bring about a modification of sap flow deficit against the corresponding Ψ_{leaf}. However, as mentioned in chapter 4, the daily minimum Ψ_{leaf} of burnt tree concentrated to around -3.5 MPa. The observation result may give a suggestion about an existence of threshold of Ψ_{leaf} and transpiration.

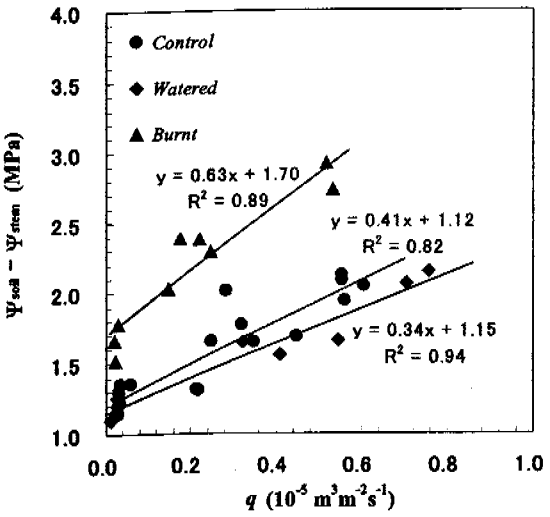

Fig. 5. Same as Fig. 4 but for differences of water potential between soil and stem (Ψ_{soil} - Ψ_{stem}).

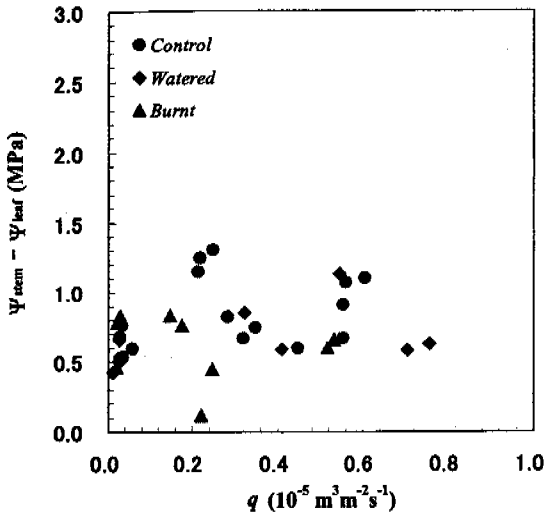

Fig. 6. Same as Fig. 4 but for differences of water potential between soil and stem (Ψ_{stem} - Ψ_{leaf}).

6. Summary

Sap flow and water potential of soil, tree stem and leaf were measured at burnt plot by surface

Table 3. List of unit flow resistance of soil-leaf ($R_{soil\text{-}leaf}$) and soil-stem ($R_{soil\text{-}stem}$)

	$R_{soil\text{-}leaf}$*		$R_{soil\text{-}stem}$**	
	(MPa·s·m^{-2})	ratio to control plot	(MPa·s·m^{-2})	ratio to control plot
Burnt	1.19×10^4	1.2	2.70×10^4	1.7
Control	1.00×10^4	1	1.55×10^4	1
Watered	0.62×10^4	0.6	1.09×10^4	0.7

*$R_{soil\text{-}leaf}$ is normalized by basal area at the breast height (1.2 m) and the tree height.

**$R_{soil\text{-}stem}$ is normalized by basal area at breast height (1.2 m) and the height of live crown base.

fire, control (intact) plot and watered plot, then flow resistance of the test stands were evaluated based on the concept of water flow in a SPAC. The burnt tree showed about 30% higher flow resistance compared to that intact tree, especially in the resistance from soil to stem including root system. It was estimated that the even a surface fire gave rise to significant inhibitions of water conducting tissues near the soil surface.

Acknowledgement

This study was supported by a research project "Permafrost Disturbance and Greenhouse Gases", CREST, JST. The authors thank Mr. R. Argunov (Permafrost Institute, Siberian Branch, RAS) for kindly support to the field observations.

REFERENCES

Arneath, A., Kelliher, F.M., Bauer, G., Hollinger, D.Y., Byers, J.N., Hunt, J.E., McSeveny, T.M., Ziegler, W., Vygodskaya, N.N., Milukova, I., Sogatchev, A., Varlargin, A., Schulze, E.-D. 1996; Environmental reguration of xylem sap flow and total conductance of *Larix gmelinii* trees in eastern Siberia. Tree Physiol. 16, 247-255.

Crombie, D.S., 1997. Water relation of jarrah (Eucalypth marginata) regeneration from seedling to the mature tree and of stump coppice. For. Ecol. Manage., 97, 293-303.

Kelliher F.M., Hollinger, D.Y., Schulze, E.-D., Vygodskaya, N.N., Byers, J.N., Hunt, J.E., McSeveny, T.M., Milukova, I., Sogachev, A., Varlargin, A., Ziegler, W., Arneath, A., Bauer, G., 1997. Evaporation from an eastern Siberian larch forest. Agric. For. Meteorol., 85, 135-147.

Kelliher F.M., Lloyd, J., Arneath, A., Byers, J.N., McSeveny, T.M., Milukova, I., Grigoriev, S., Panfyorov, M., Sogachev, A., Varlargin, A., Ziegler, W., Bauer, G., Schulze, E.-D., 1998. Evaporation from a central Siberian pine forest. Journal of Hydrology, 205, 279-296

Lansberg, J.J., Blanchard, T.W., Warrit, B., 1976. Studies on the movement of water through apple trees. J. Exp. Botany, 43, 111-119.

Ohta, T., Hiyama, T., Tanaka, H., Kuwada, T., Maximov, T.C., Ohata, T., Fukushima, Y., 2001. Seasonal variation in the energy and water exchanges above and below a larch forest in eastern Siberia. Hydrol. Process., 15, 1459-1476.

Wang, G.G., 2002. Fire severity in relation to canopy composition within burned boreal mixedwood stands.

Interannual Variation in Active Layer Thickness and Moisture Content, Neleger and Spasskaya Pad Monitoring Sites

Radomir N. Argunov and Ivan S. Vasiliev

Melnikov Permafrost Institute, Siberian Branch, Russian Academy of Sciences

Yakutsk 677010, Russia. E-mail: fedorov@mpi.ysn.ru

Tel.: +7(4112) 334-887. Fax: +7(4112) 334-476

Active layer conditions at a given locality are controlled by variation of climatic elements during the year. The rate and depth of seasonal thawing, for example, depend on the balance of soil cooling and warming, as well as on seasonal and annual variations of moisture conditions at the surface and in the soil.

From 1996 to 2001, observations of interannual variation in the thickness and moisture content of the active layer have been conducted at experimental sites located in the Spasskaya Pad and Neleger monitoring areas, the Lena-Kenkeme interfluve. This paper discusses thickness and moisture content relationships in the active layer at key sites located in different terrain types.

We will begin with a brief description of climatic conditions in the region which exert a direct influence on active-layer thickness and moisture content. During the period of observation there have been no significant differences between the winters in air temperature regime. Winters have become milder in Central Yakutia in the last ten years (Skryabin, Varlamov, Skachkov, 1998). January means do not fall below -43°C. The differences in the thermal regime of the active layer are caused by the differences in snow depth, in addition to the variation in moisture content. The snow depth varied from 30 to 50 cm during the observation period. In the anomalous years, the lowest values of snow depth for the period of instrumental observations were only 15-20 cm at the nearest weather stations in Magan and Yakutsk (Magan is 15 km south of the study area and Yakutsk is 25-30 km to the south-east). Snow is an insignificant moisture supplier for the surfaces and soils of the active layer, because there is intensive evaporation from the snow surface during the late winter and much of the snow cover vanishes under subzero temperatures. Snowmelt may have a significant influence on soil thawing only in the springs with a rapid rise of surface and air temperatures. Summer precipitation ranges from 90 to 200 mm in Central Yakutia. It is this parameter which determines the soil moisture regime and ultimately the depth of seasonal thawing. In the last six years, the summers of 1997, 1998 and 1999 were rainy, while the summers of 1996, 2000 and 2001 were dry. Moisture contents of the active layer were highly variable and exhibited different trends with time at the various depths.

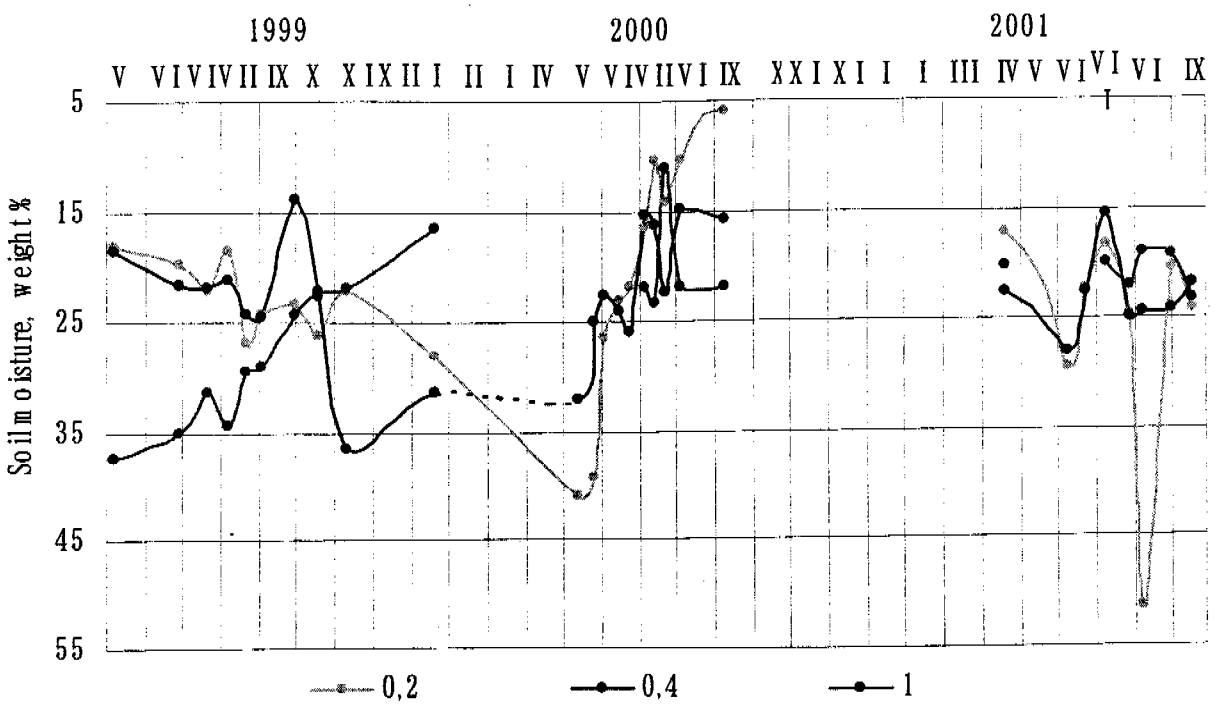

Fig. 1 Variations of the gravimetric moisture content at 0.2, 0.4 and 1.0 m depths for the observation period, 1999-2001, inter-alas terrain type.

Figure 1 shows the moisture variation in clayey loams beneath *Laricetum limnoso-vacciniosum*, inter-alas terrain type, at 0.2, 0.4 and 1 m depths for three summers and one winter (1999-2001). In order to monitor the effects of anthropogenic activities, trees were cut out in the site in November-December 2000. In the summer of 1999, moisture contents (weight basis) were in the range of 20 to 25% in the upper part of the active layer (0 to 0.4 m depth) and 30 to 35% in the lower part. In the winter 1999/2000, the moisture (ice) content of the upper frozen part of the active layer was quite high (30-40%), while that in the lower part was 15-20%. This is attributed to increased wetting of the surface and soil in 1999. Water saturation of the soil by the onset of freezing favored saturation with ice of mainly the upper part of the active layer. The higher ice content in the upper part compared to the lower part evidences the slow rate of thawing, i.e. a significant amount of moisture migrated from the lower depths toward the slowly penetrating freezing front. As a result, the ice content in the upper part of the frozen active layer was twice that in the lower part. Moisture contents throughout the active layer in the summer 2000 were nearly half those in the summer 1999 (10-25%). After the clearing, soil moisture contents ranged 20 to 30% in the summer 2001. But there was a sharp increase in moisture content at a depth of 0.2 m, which may be explained by the accumulation of rainwater on a locally settled surface due to the clearing. It is evident that soil moisture contents vary greatly with time both at particular depths and along the active layer profile. Thus it is impossible to establish a direct correlation between

thickness and moisture content of the active layer. In principle, rates and depths of thawing could be estimated for a short term with a known moisture range, but not with a maximum value for the thaw season.

As is known, pre-winter moisture content of soils plays a significant role in thaw depth (Maksimova and Minailov, 1973). It determines ice saturation of the active layer upon freezing, and consequently, thawing in the following summer. Values of pre-winter moisture content depend on the frequency and duration of rain events in August and September.

Figure 2 shows the pre-winter moisture contents for Septembers of the rainy (1997), moderately rainy (1998) and dry (2001) summers at the key sites in five terrain types.

1. *Laricetum vacciniosum* on clayey loams, inter-alas terrain type.

There are differences in moisture content variability between depth levels. Moisture contents vary from 10 to 40% in the upper part of the active layer (0-0.4 m), from 13 to 25% in the middle part (0.5-0.9 m), and from 13 to 40% or greater in the lower part. Over the six years of observation, the depth of thaw was greatest in 1997 (1.25 m), when early-summer precipitation (late May-early June) gave an impetus to rapid thawing and August rains caused the increased pre-winter moisture contents in the lower part of the active layer, up to 48%. The depth of thaw was shallowest in 2001 (1.05 m). Rains in May-June of that year were frequent but light and had little effect on the thawing rate. The second half of the summer was dry. The dry soils had greater thermal resistance, and the depth of thaw was reduced.

2. *Mixtoherboso-graminosum* dry meadow, alas terrain type.

Interannual changes of the soil moisture content exhibited a layered pattern. In the dry meadow on the alas, the soil moisture content to a depth of 0.3 m varied from 10 to 60% depending on surface moisture conditions. Moisture content in the depth interval 0.5-1.4 m showed little variation, being in the range of 12 to 20%. Below 1.5 m, it varied from 8 to 23%. In 1997, despite of the rainy summer, the lower part of the active layer (at 1.8 m) had least moisture because it had been desiccated earlier and did not moisten during that summer. Conversely, the lower part of the active layer thicker than 1.5 m had no time to dry up in the dry summer following several rainy summers. This explains a relatively high moisture content (23%) during the dry summer of 2001. Thus when the active layer is thicker than 1.5 m, its lower part can be notably moistened only after several consecutive rainy summers and desiccate after prolonged droughts. So the greatest depths of thaw (1.82 and 1.85m) occurred in the summers of 1999 and 2000. In the rainy years 1997 and 1998 the dense grass growth prevented deeper thawing, and the depths close to the average values were observed (1.78 and 1.75 m). The year 2001 had the shallowest thaw depth, because of the desiccation of the upper 0.6 m of sandy loam (moisture content 5-10%) from July through September.

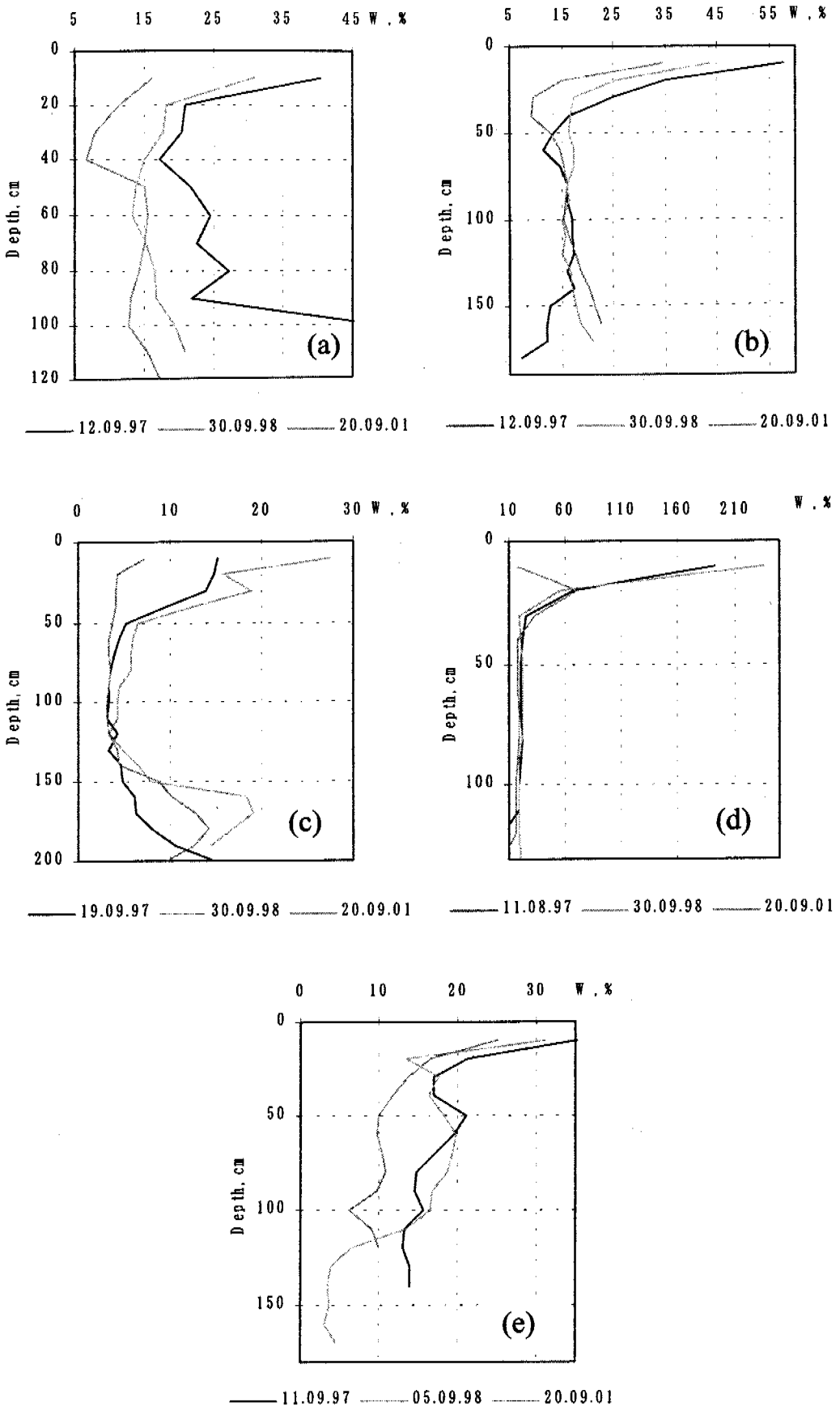

Fig. 2 Pre-winter moisture contents for various terrain types. (a) inter-alas, (b) alas, (c) sand ridge, (d) inter-ridge depression and (e) slope.

3. *Pinetum limnoso-arctostaphylosum*, sand-ridge terrain type.

Year-to-year variation in the moisture content of the upper 0.4 m of sands was 4 to more than 20%. The smallest range of variation (2 to 6%) was observed in the depth interval 0.5-1.4 m. In the lower part of the active layer (below 1.6 m) the moisture content was up to 10-18%. At the end of the dry summer of 2001, only the base of the active layer (2 m depth) had a similar value. The depths of thaw were greatest in 1997 and 1999 (2 m), close to the averages in 1998, 2000 and 2001 (1.9 and 1.92 m), and shallowest in 1996 (1.86 m). Thus the active layer thickness in sandy deposits increases notably in rainy years and decreases in drier years. Percolation of rainwater in the rainy years causes increased heat input into the ground. But ice saturation at the base of the frozen active layer (gravimetric moisture content 13-14%) after the rainy summer 1997 prevented deeper thawing during the summer 1998.

4. *Carex-calamagrostis* wet meadow (tussock) on peaty-loamy deposits, inter-ridge depression terrain type.

The active layer here is oversaturated in rainy years. In the years with lowest precipitation, groundwater disappears in August. After the three rainy years the low-lying surfaces in the summers of 1999 and 2000 were covered with water. So pre-winter moisture data were obtained only for 1997, 1998 and 2001. Moisture content in the peat layer (to 0.3 m depth) varied from 20 to 236%. From 0.4 m to the base of the active layer, the clayey loams had moisture contents in the range of 16 to 24%. The depths of seasonal thaw were greatest in 1999 and 2001 (1.45 and 1.5 m). The surface was covered with water throughout the summer of 1999. Temporary water accumulated the solar heat and favored deep thawing. In the very dry summers the surface and ground water disappear by the end of thaw. The greatest thickness of the active layer measured in 2001 (1.5 m) is evidence of the most favorable moisture conditions for soil thawing.

5. Thin-trunk *Laricetum limnoso-arctostaphyloso-vacciniosum*, the east-facing slope of medium angle.

Three levels are observed in the moisture content distribution within the active layer. Moisture contents vary from 13 to 35% in the upper 0.2 m of the soil, from 6 to 20% in the depth interval 0.4-1.0 m, and from 3 to 14% at the depths below 1.1 m. Seasonal thawing was deepest in 1997 and 1999, 1.7 and 1.8 m respectively. Moisture contents during these years were highest in the top 1 m of the active layer. The shallowest depth of thaw (1.3 and 1.22m) were characteristic of the last two dry years. The active layer thickness in 2001 was affected by the severe winter thermal regime in the soil, along with the dry summer. Winter orographic inversion added to the cooling of the soils in ravines and other topographic lows in the low-snow winter 2000/2001. As the observation point is located on the mid-slope, groundwater that appears during the period of rains is not retained. But its warming effect during thaw in the rainy seasons is significant.

From our observations the following conclusions can be drawn.

- In clayey loams and sandy loams, moisture contents in the lower part of the active layer thicker than 1.5 m can change significantly only after several consecutive wet or dry years. In single rainy or dry summers, moisture contents may remain constant in the lower part of the active layer with a thickness of more than 1.5 m.
- In sands, active layer thickness increases in rainy years and decreases in dry years. In rainy years, percolation of water has a warming effect and contributes to deeper thawing. But ice saturation of the sandy active layer upon freezing after rainy summers can retard thawing in the following summer due to additional heat losses to melt the ice.
- The combination of a dry summer and a preceding snowless winter has a negative effect on active layer thickness in topographic lows. Winter orographic inversion adds to the cooling of soils in ravines and slopes during low-snow winter.
- Comparison of data on active layer thickness and soil moisture content has shown that, in general, the dry summers had the shallowest depths of seasonal thaw, while the rainy summers had the greatest depths. However this relationship holds true for dry and mesic locations. In low-lying locations, changes of moisture conditions in the surface cover and in the soil, as well as differences in the grass density have different effects on seasonal thaw depth.

REFERENCES

Maksimova L.N., Minailov G.P. (1973). Relationship between long-term variability of seasonal thaw and pre-winter moisture content. In *Merzlotnye Issledovania*, Issue XIII. Moscow University Press, Moscow, pp.110-115.

Skryabin P.N., Varlamov S.P., Skachkov Y.B. (1998). *Interannual Variability of the Ground Thermal Regime in the Yakutsk Area*. Novosibirsk. 143 pp.

Interannual Variation of Upper Permafrost Temperatures in Taiga Landscapes near Yakutsk

P.Konstantinov[1], M.Fukuda[2]

[1] Permafrost Institute, Siberian Branch, RAS, Yakutsk, 677010, Russia. E-mail: konstantinov@mpi.ysn.ru
[2] Institute of Low Temperature Science, Hokkaido University, Sapporo, 060-0819, Japan.
E-mail: mfukuda@pop.lowtem.hokudai.ac.jp

1. Introduction

In relation to possible climate warming, the recent interest in studying temporal variations of upper permafrost temperature has aroused in northern regions. The poorly studied question on this problem is variability of permafrost temperature under natural conditions, outside the development zones. But a great variance of undisturbed landscapes causes the extensive research on this theme.

2. Study site and Field Research Procedure

Interannual variability of upper permafrost temperature is being studied in the area situated 25 km north-west of Yakutsk in the Lena-Kenkeme interfluve, Central Yakutia (East Siberia, Russia). The study area is a bedded aggradation plain with elevations 200-220 m a.s.l. The bedrock predominantly consists of sandstone, aleurolite and argillite. The Quaternary deposits are 5-10 m in thickness. Sands and sandy loams with low ice content dominate in the southern part of the area, whereas ice-rich clayey loams and sandy loams with numerous polygonal ice wedges occur in the northern portion. Thermokarst landforms, such as alas depressions and pingos, are widespread in the northern part. The vegetation is middle taiga dominated by larch forest. The greater part of the primary forest was cut and now is being recolonized by secondary birch forest. The study area is underlain by continuous permafrost 400-500 m in thickness. Typical permafrost temperatures at 15-20 m depths are -2.0...-3.5°C.

The thermal regime of the upper permafrost layers is studied at experimental sites where boreholes were made to depths of 3.2 to 20 m for regular temperature measurements (Fukuda, Fedorov and Rusakov, 1998; Konstantinov, Rusakov, Fukuda, 2001). Measurements of permafrost temperature have been made beginning from October 1996. Mean annual air

temperatures and perennially frozen grounds are determined for a conventional annual period – from 1 October of a current calendar year to 30 September of a following calendar year.

3. Results and Discussion

Fig.1 shows variations of the mean annual air temperature at the Yakutsk weather station for the last 30 years. As seen from the plot, the observation period covering 1996 to 2001 is relatively 'warm' in the 30-year record. The amplitude of interannual variation of mean annual air temperature was generally small during the period 1996-2001 (1.8°C). This value cannot be referred to great interannual temperature difference which may get significantly high values in the Yakutsk town region.

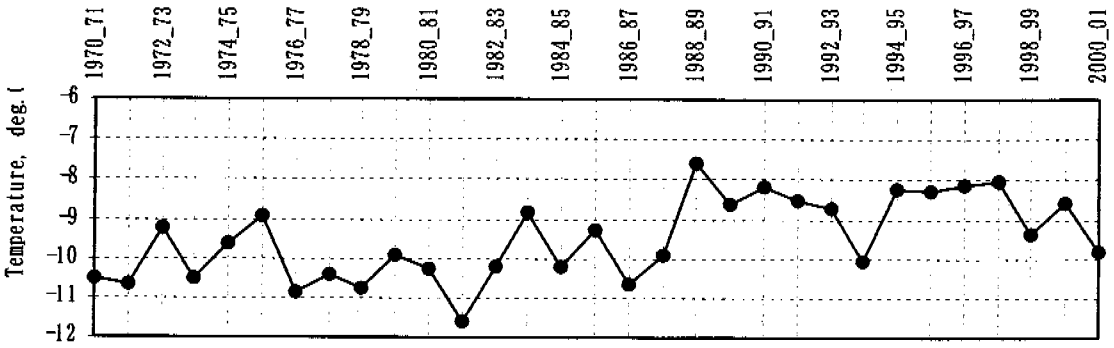

Fig. 1. Mean annual temperature of air (1970-2001). Yakutsk station. Note: the annual period starts on 1 October of the current calendar year and ends on 30 September of the next calendar year

Fig.2 contains plots of pre-winter moisture content of the active layer at larch forest site for the period 1996 to 2001. The moisture content of the active layer significantly increased from 1997 to 1999, when a 6-8-fold increase in gravimetric moisture content occurred at some depths. This was caused by an increase in the summer precipitation during 1997 to 1999. The succeeding summers (2000-2001) were dry, so pre-winter moisture contents of the active layer sharply decreased and approached the values observed in the summer 1996. As is known, an increase in moisture content of the active layer slows down soil freezing rates. As a result, freeze-up of the active layer occurs on later dates, thus reducing time for ground cooling and preventing very low temperatures in the upper permafrost layers. Therefore the

soil moisture conditions in 1997-1999 were most favorable for warming of the active layer and the permafrost.

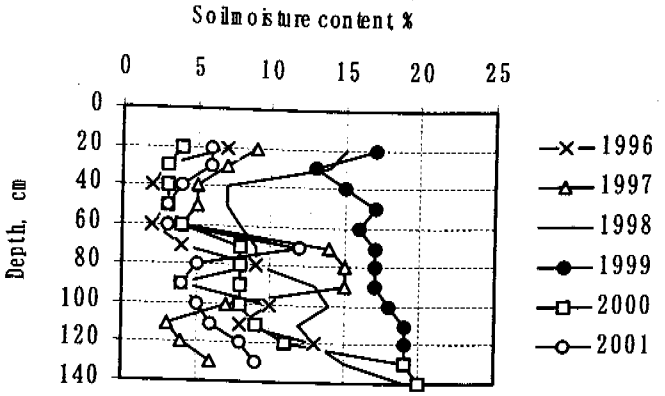

Fig. 2. Interannual variation in pre-winter moisture content of the active layer. Larch forest.

The accumulation dynamics of the snow cover at borehole site 1 for the observation period is shown in Fig.1.3. As seen from the plots, the snow depth experienced considerable variability during the period of observations. In the winter 1996-1997 the snow depth was close to the long-term norm, while in the winter 2000-2001 it was below the norm. The winters 1997-1998, 1998-1999 and 1999-2000 were characterized by deep snow cover with the higher rates of snow accumulation in early winter. As is known, the early establishment of

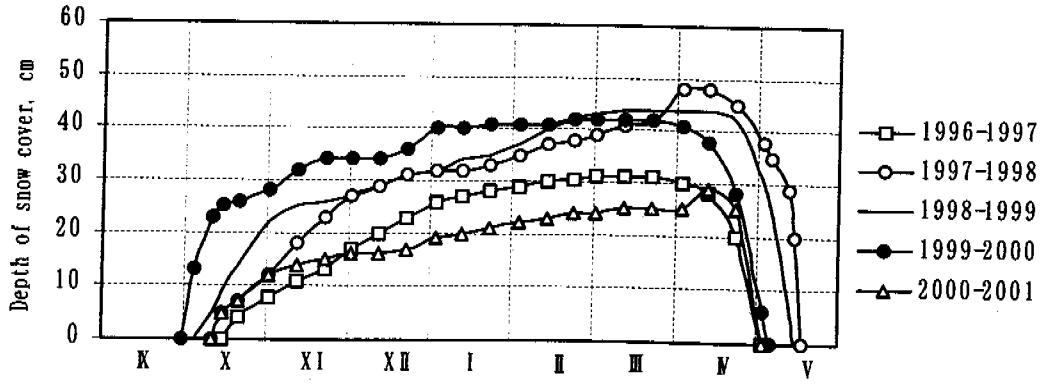

Fig. 3. Snow cover accumulation in the winters 1996-1997, 1997-1998, 1998-1999, 1999-2000 and 2000-2001. Larch forest.

a thick snow cover strongly reduces heat losses from the ground. This is especially true for the winter 1999-2000. Over the observation period, the timing and accumulation dynamics of the snow cover varied over a wide range and thus contributed to large interannual variations of the upper permafrost temperature.

Figures 4-6 contain the plots showing the interannual variations of the upper permafrost temperatures at depths of 3.2, 5.0 and 7.0 m for experimental sites in larch and birch forests, and of the mean annual permafrost temperatures at a depth 3.0-3.2 m over five full years, from October 1996 through September 2001. Comparison with the plot of the mean annual air temperature variations shows that the interannual variation of the permafrost temperature during the observation period does not coincide with the interannual variation of the air temperature (see Fig.1). But there is a direct relationship between the thermal regime of the permafrost and the interannual variations of the snow depth and pre-winter soil moisture content (see Fig. 2-3). In the annual periods with excess moisture in soils and increased snow cover depth (October 1997-September 2000) a 1.6-2.5-fold decrease in the

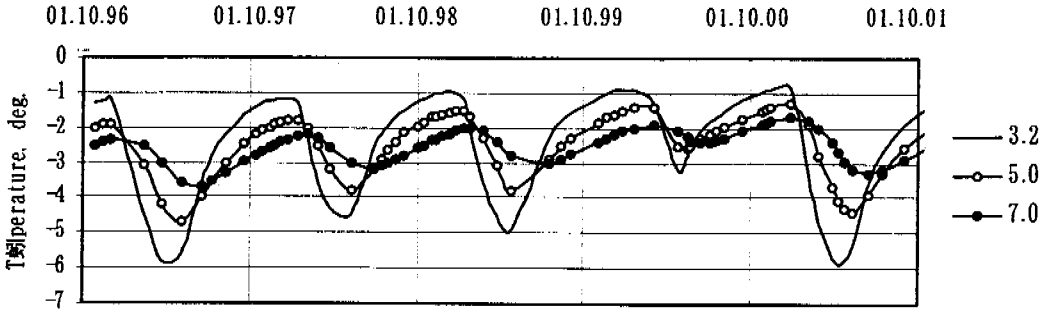

Fig. 4. Interannual variation of permafrost temperature. October 1996 - September 2001. Larch forest.

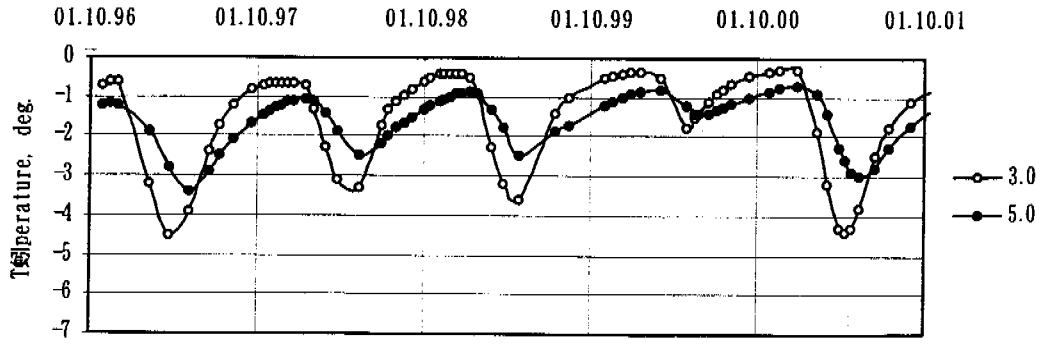

Fig. 5. Interannual variation of permafrost temperature. October 1996 - September 2001. Birch forest.

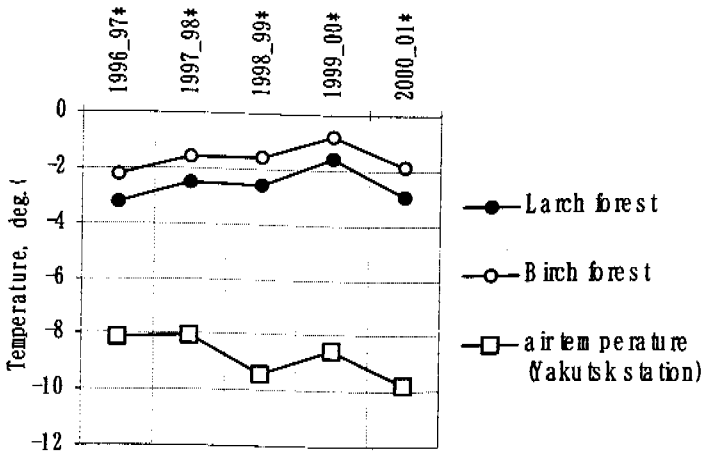

Fig. 6. Interannual variation in the mean annual permafrost surface temperature in taiga Landscapes (Spasskaya station) and air temperature (Yakutsk station)

amplitude of annual temperature fluctuations of the upper permafrost and a 1.1-1.6-fold increase in mean annual temperatures occurred compared to colder annual periods (October 1996-September 1997, October 2000-September 2001). Anomalously high temperatures of the permafrost occurred in the year October 1999 – September 2000 when the pre-winter moisture content and the snow depth (especially in early winter) were the greatest in the observation period. This may be explained by the reason that the winter heat loss of grounds decrease with increasing snow cover depth and heat-isolating property of a snow cover increases with increasing pre-winter soil moisture content.

4. Conclusion

Thus, the upper layers of the permafrost in the taiga landscapes near Yakutsk are subject to short-term interannual temperature variations of large amplitude that may be caused by changes in the amount and regime of precipitation in the absence of noticeable year-by-year variations in the air thermal regime.

REFERENCES

Konstantinov P., Rusakov V. and Fukuda M. (2001): Thermal Regime of the Upper Permafrost Layers in Taiga Landscapes,Yakutsk Area, 1996-2000. *Proceedings of the Ninth Symposium on the Joint Siberian Permafrost Studies between Japan and Russia in 2000*, Sapporo, Japan, 23-24 January, pp. 204-209.

The Effect of Recent Climatic Change on the Surface of Permafrost Landscapes in Central Yakutia

Alexander Fedorov, Pavel Konstantinov

Permafrost Institute SB RAS, Yakutsk, Russia, 677010
Phone +7-4112-33-43-18, Fax +7-4112-33-44-76, e-mail: fedorov@mpi.ysn.ru

Annotation

Authors conduct observations of the surface dynamics at the Yukechi site near Yakutsk (Siberia) since 1992. The data on surface subsidence of non-forest inter-alas landscapes are considered in this paper. The surface subsidence was up to 7-8 cm on well-drained flat inter-alas areas and reached 14-15 cm at thermokarst depression in 1993-2001. The surface subsidence trend corresponds to recent climate change. Surface subsidence on flat inter-alas landscapes is, perhaps, a good indicator of climate change and permafrost degradation.

1. INTRODUCTION

Systematic observations of the ground thermal dynamics, depth of seasonal thawing and surface subsidence of non-forest land have been carried out at the Yukechi location since 1992. Yukechi is situated 50 km south-east of Yakutsk on the right bank of the Lena River (Fig.1). It is a typical landscape of Central Yakutia with thick ice-reach Quaternary deposits (ice complex) and widely distributed alasses (Fig.2). The surface slightly dips to the northwest and its altitudes are 200-220 m a.s.l. The Yukechi site belongs to the south-western marginal part of the Abalakh plain with prevailing alas relief.

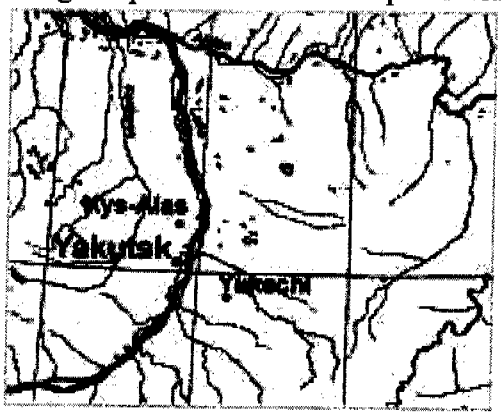

Fig.1. Location map of experimental site

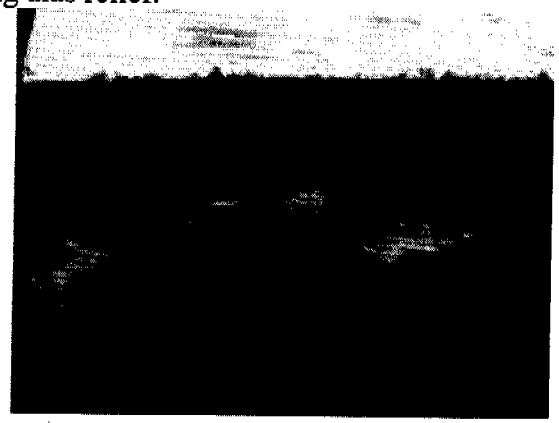

Fig.2. Typical landscapes near Yukechi

The upper horizons of the Quaternary sediments are predominated by sandy and clayey silts/loams, sometimes with inter-layers of fine-drained silty sand (Fig.3). These soils have unique saline and mineralogical-petrographic compositions in alas basins due to specific features of sedimentation during the thermokarst process. Wedge ice is commonlyspread in the areas between alasses and occurs at a depth of 2-2.5 m (Fig.4). The upper parts of ice veins are 1-1.5 m deep and 2.5-3 m wide. Cross sizes of ground blocks

between ice veins do not exceed 5-6 m as a rule. The depth of seasonal thawing varies between 1.2 and 2.5 m depending on landscape conditions.

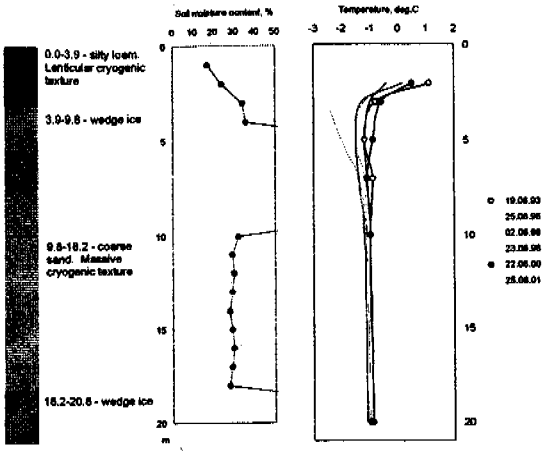

Fig. 3. Cryolithological profile at borehole 10, Yukechi

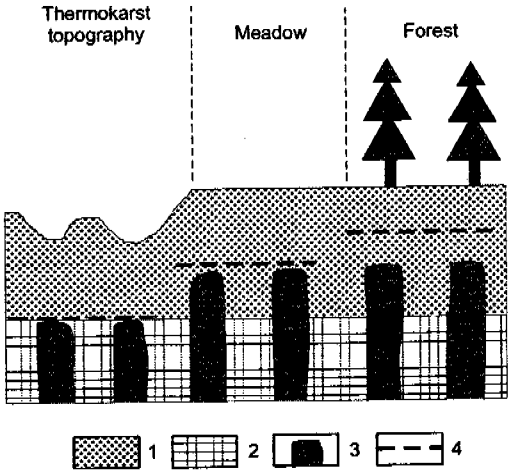

1-ice poor ground; 2-ice-saturared ground; 3-wedge ice; 4-top of permafrost.

Fig.4. Schematic profile of upper part of ice-complex

The observation task is to obtain the information on permafrost degradation under recent climatic change in Central Yakutia. The surface dynamics in well-drained inter-alas areas is connected with climate changes.

2. DATA SOURCES AND METHODS

To study the dynamics of thaw subsidence, twelve observation sites were established at the Yukechi site for the purpose of surveying the dynamics of the inter-alas surfaces (Fig.5). Within these sites, there are 125 marker points for determining relative elevations, including three benchmarks at depths down to 4 m. Of these, leveling has been carried out at 33 points since 1992 and on the rest of the points since 1993-94.

Before this report our scientific task was to study the surface subsidence on thermokarst form of relief (Fedorov et al., 1998; Fedorov, Fukuda, 2001). Now we have new data on surface subsidence on well-drained inter-alas landscapes with stable condition. The markers were set on each observation sites.

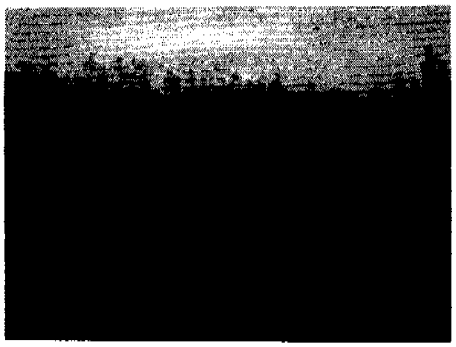

Fig.5. Study of cryolithological condition, Yukechi

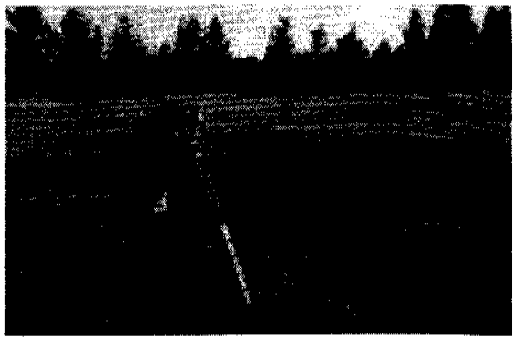

Fig.6. Surface survey, Yukechi

Surveys were made every year in August-September, i.e. at the end of the ground thawing season (Fig.6). Measurements were made using the NS4 level with the mean-square error within 3 mm. This report presents the data for the 1992-2001 period.

3. RESULTS

Our observation at Yukechi shows that the surface dynamics on thermokarst depressions has the tendency for subsidence during the period of 1992-2001. In the central parts of wet thaw depressions with a relative depth of 2-2.5 m the rate of the subsidence was 5-10 cm/year with the tendency for lakes formation. In the inter-depression flat sites, where thermokarst began, the surface subsidence rate was 2.6-5.4 cm/year (Fedorov, Fukuda, 2001). We note also that at some points of well-drained flat inter-alas surfaces the rate of subsidence was 0.5-0.8 cm/years.

By now we have analyzed in detail the surface dynamics on well-drained flat inter-alas sites. The tendency on various sites is the same because we take topography data of site 2 for demonstration (Fig.7). Analysis of the data shows that each point develops differently. On well-drained flat inter-alas areas (markers A, B and C) the stable surface conditions remained until 1995. A small surface subsidence was marked in 1996-1997. The condition of 1998-1999 was stable. In 2000-2001 the surface subsidence increased.

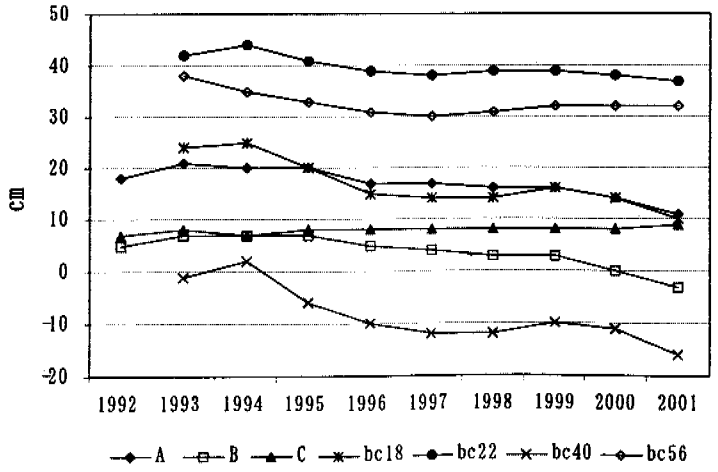

Fig.7. Surface subsidence on the site 2, Yukechi
A, B, C – markers on flat inter-alas;
bc18, bc22, bc56 – markers near small thermokarst depression.

On well-drained inter-alas sites near thermokarst depression the surface subsidence was marked in 1995-1996. The stable condition was typical for 1997-1999. The 2000-2001 period was featured by directional subsidences, a like the well-drained flat inter-alas areas.

We note the surface dynamic events from stable condition to subsidence on well-drained inter-alas areas with ice-rich deposits during short period. However, the surface subsidence made up to 7-8 cm on well-drained flat inter-alas sites and up to 14-15 cm near thermokarst depression occurred in 1993-2001. This fact shows that surface subsidence trends are connected with to climate change.

Three sites were developed for surface dynamics observation on small thermokarst drains in 1995. The sites were placed at three surface levels between 1.5-2 m. Wedge ice occurs at a depth of 2-2.5 m. Where thermokarst is active when the seasonal thawing reaches the upper parts of the wedge ice. On the sites near flat inter-alas areas the thickness of the layer between seasonal thawing layer and ground ice is 5-20 cm. This thickness is very small to resist climate change. The probability of surface subsidence after ground ice thawing is very high on non-forest inter-alas landscapes in Central Yakutia.

As Yakutsk Weather Station data for 1992-2000 indicate, the recent climatic situations have considerable departures from usual ones.

Mean annual air temperature. According to records of the Yakutsk weather station, during the period of 1931-2000 the mean annual air temperature was –10.0°C. During the period of observations at Yukechi (1992-2000) the mean was –8.8°C (13% departure). That is, the period of our observations was concurrent with a significant increase in air temperature (Figure 8). This increase is a regional phenomenon that is a feature of most territory of Central Yakutia (Fedorov, Svinoboev, 2000; Skachkov, 2000).

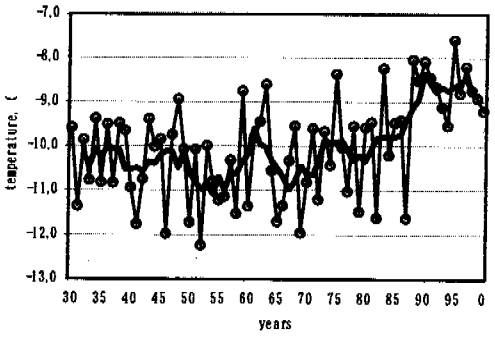

Fig.8. Variability of mean annual air temperature in Yakutsk

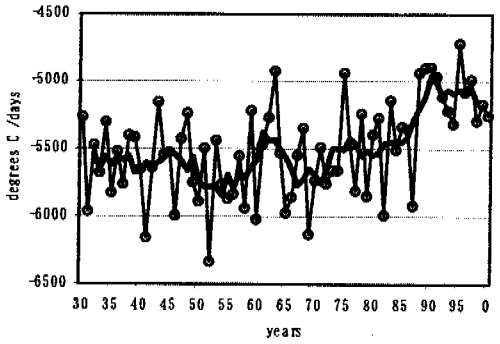

Fig.9. Variability of air freezing index in Yakutsk

Air freezing index. Earlier M.K.Gavrilova, V.T.Balobaev, A.V.Pavlov, et al. recorded a significant increase in recent winter temperature. During the period of 1992-2000 the mean freezing index was -5129°C while long-term mean was -5500°C (7% departure). This shows that observations period were conducted under abnormally warm winters (Figure 9).

Air thawing index. Summer temperatures are not so abnormal compared to the winter ones (Figure 10). However, the period of 1992-2000 is characterized by an increase in summer temperatures. The mean thawing index was 1978°C, long-term mean being 1899°C (4% departure).

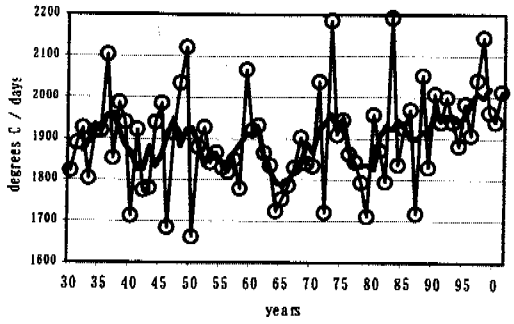

Fig.10. Variability of air thawing index in Yakutsk

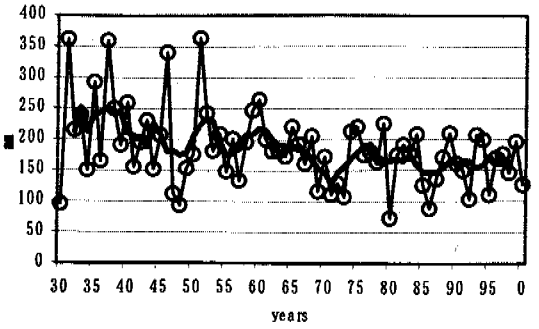

Fig. 11. Variability of summer precipitation in Yakutsk

The annual precipitation was by 27 mm lower than the long-term mean (15% departure). It essentially influences on geocryological and ecological condition of Central Yakutia landscapes (Figure 11).

Soil temperature at a depth of 3.2 m. However regular observations of soil temperature in Central Yakutia are conducted since 1931, a lot of causes do not let us to construct proved retrospective schemes of soil temperature development. These causes are relocations of the stations and related changes in lithological conditions, as well as strong influence of the anthropogenic factor on soil temperature regime.

In order to remove the heterogeneity of data series caused by relocations of the stations, as well as by the anthropogenic effects, the observed temperatures were converted to relative values. Normalized anomalies were calculated for each year as follows:

$$A = (i - i_{av}) / \delta$$

where i is the value for a given year; i_{av} is the long-term mean of a continuous series; δ is the root-mean-square deviation of a series.

Correlation coefficients for measured temperatures between the stations (Yakutsk, Pokrovsk and Churapcha) are not very high, but quite strong with the generalized values: 0.8-0.87 for temperature at a depth of 1.6 m and 0.79-0.81 at a depth of 3.2 m.

We constructed a generalized scheme of variations in soil temperature in Central Yakutia at a 3.2 m depth (Figure 12) according to recent monitoring data obtained at different sites (Rusakov, Skryabin, Varlamov, Skachkov and Konstantinov, Permafrost Institute). In the context of this scheme, the observation period is characterized by values above or near zero exceeding long-term characteristics.

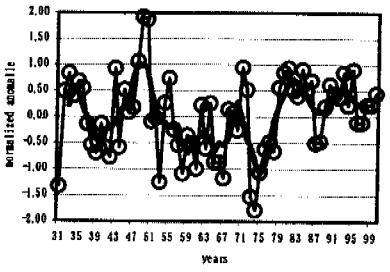

Fig.12. A generalized scheme of variation in soil temperature Central Yakutia

4. CONCLUSIONS

The thawing of upper ground ice was observed during the last 10 years on non-forest inter-alas landscapes in Central Yakutia. Surface subsidence on these areas reached 7-8 cm

and near small thermokarst depression was up to 14-15 cm in 1993-2001. This fact says about surface subsidence dependence on climate change.

Many climatic parameters were observed to change during this period. The small layer between seasonal thawing layer and ground ice on the non-forest inter-alas areas cannot protect the permafrost landscapes from degradation. The upper parts of ground ice (wedge ice) thaws and causes the surface subsidence.

At present the non-forest permafrost landscapes of Central Yakutia, separately on inter-alas surfaces, have critical condition that is related to recent climate change. Surface subsidence on flat inter-alas landscapes is, perhaps, a good indicator of climate change and permafrost degradation.

REFERENCES

Fedorov, A.N., Svinoboev, A.N. (2000). Variations in air temperature of vegetation cover in the Republic of Sakha (Yakutia). In: Climate and Permafrost: Complex Research in Yakutia. Pp. 68-75.

Skachkov, Yu.B. (2001). Present-day climate change in Central Yakutia. In: Climate and Permafrost: Complex Research in Yakutia. Pp. 55-63.

Fedorov A., Fukuda M. (2001). Some Observation Results of Surface Dynamics in Permafrost Landscapes, Yakutsk Area. *Proceedings of the Ninth Symposium on the Joint Siberian Permafrost Studies between Japan and Russia in 2000. Sapporo, Japan, 23-24 January 2001*, pp.199-203.

A.N.Fedorov, P.Ya.Konstantinov, I.S.Vassiliev, N.P.Bosikov, Ya.I.Torgovkin, V.V.Samsonova (1998). Observations of permafrost-landscape dynamics related to anthropogenic disturbances, Yukechi study site, Central Yakutia // *PERMAFROST. Seventh International Conference. June 23-27,1998. Proceedings. Yellowknife, Canada*, p. 259-263.

Pedogenic Processes in Alas Soils in Central Yakutia, Russia

Hatano, R.[1,2], Nakahara, O.[1], Desyatkin, R.V.[3], Okoneshnikova, M.V.[3] and Kamide, K.[1],

[1] Graduate School of Agriculture, Hokkaido University, Sapporo, 060-8589, Japan
Phone: +81-11-706-3857, Fax: +81-11-706-4960, e-mail: hatano@chem.agr.hokudai.ac.jp
[2]Field Science Center for Northern Biosphere, Hokkaido University, Sapporo, 060-8589, Japan
[3]Institute of Biological Problems of Cryolithozone, Russian Academy of Science, Yakutsk, Russia

Abstract

The soils of four Alases, which is round shaped grassland with small pond in the center, were chemically characterized with comparing the Taiga forest soils surrounding the Alases, in central Yakutia, northeast Siberia. Alases have been formed with drying of pond which had been made by subsidence with permafrost thawing after strong forest fires in about 5000 to 18000 years. Alas soils had higher pH, EC and Na saturation than forest soils. Older Alas soils had higher pH and higher Na saturation, and most B horizons were characterized as Natric horizons. These facts clearly indicate that long term alkalization is the predominant pedogenetic process associated with Alas formation. Crystallinity of Fe oxide, which was estimated as (Fed-Feo)/Fed where Fed is the dithinite-citrate extractable Fe content and Feo is the oxalate extractable Fe content, was lower in Alas soils than forest soils. Furthermore, older Alas showed much lower crystallinity of Fe oxide. These indicate that reduction and oxidation may periodically occur in Alas soils associated with thawing and freezing of permafrost.

Key Words: Alas, permafrost, Siberia, ferrihydrite, alkalization,

1. Introduction

Alases in east Siberia are thermokarsts, which have been formed by subsidence due to thawing a upper part of permafrost after strong forest fires in several hundred to a few ten thousands years ago (Fitzpatrick 1983). Even in central Yakutia only, there are more than 16,000 Alases in number, 4,500km^2 in area (Desyatkin 1990). Different sized Alases have different ages and larger Alas should be much older (Desyatkin 1990). Subsidence makes water pond in initial stage of Alas formation, then pond gradually dries up due to small amount of precipitation in east Siberia which is for example about 250 mm in central Yakutia. However, all soils in east Siberia are frozen from soil surface in winter, and the frozen soils thawed out from the soil surface in summer. Therefore free water accumulates in topsoil at early stage of thawing. During long term Alas drying, salts gradually accumulates to the center of Alas, because salts can not leach out due to presence of permafrost and occurrence of lateral water flow to the center of Alas (Desyatkin 1993). Therefore, Alas soils can be characterized by two main chemical reactions of reduction-oxidation and salinization-alkalinization. Objective of this study is to evaluate change in the soil characteristics after forest fire by comparing the soil properties of different aged Alases and adjacent forests.

2. Material and Methods

Table 1 shows outline of sampling sites. Soil survey was conducted at 4 Alases with different sizes and forests adjacent to the Alases other than the biggest one. Size of Alas ranged from about 100 m to 14 km. Age of Alas estimated from the size was 1000BP for Dyode Kelleriki (D), 5000BP for Neleger (N), 8000-9000BP for Ulakhan Sykkhan (U) and 16000-18000BP for Tungle (T) (Kaplina, 1981; Desyatkin, 1990). As all Alases had a pond in the center, survey in Alas was conducted at two points apart from the pond at a 1/4 distance between pond (Alas 1) and forest and at a half distance between pond and forest (Alas 2). Soil samples were taken from the genetic horizon after soil profile description. Each sample was air-dried and sieved through a 2 mm mesh for chemical analysis in the laboratory.

Soil pH was measured in supernatant suspension of 1:2.5 soil:deionized water mixture. EC was modified by multiplying 5 to the value measured in the supernatant suspension of 1:5 soil:deionized water mixture. Base cations and CEC in mineral horizons were measured by Schöllen-Berger method. By using the data, Ca and Na saturation and Base saturation (BS) were obtained. Carbonate carbon content was determined by measuring the amount of CO_2 produced with adding 2M-HCl to the soil sample in erlenmeyer flask. Total carbon and nitrogen were measured on dry combustion using a Vario-EL (ELEMENTAR) equipped with a thermal conductivity detector. Natric horizon was identified by using criteria of EC<4 dS m^{-1}, ESP>15 % and pH>8.5, and also Salic property was identified by using criteria of EC>4 dS m^{-1}, ESP<15 % and pH<8.5 (FAO, 1988). Calcareous property was also identified by using a criterion of carbonate C content >2 %.

According to Blume and Schewertman (1969), crystallinity of soil Fe was obtained for mineral horizons. Dithionite-citrate extractable Fe (Fed) and acid Oxalate extractable Fe (Feo) was determined by selectively extraction method. Crystallinity was calculated as (Fed-Feo)/Fed. Dithinite-citrate solution extracts both crystalline Fe oxide and non crystalline Fe oxide, but acid Oxalate solution extracts only non-crystalline Fe oxide as ferrihydrite (Parfitt and Childs, 1988). Therefore, higher value of (Fed-Feo)/Fed indicates more weathered soil.

Table 1 Characteristics of Alas investigated

Name of Alas	Diameter of Alas	Depth of cave	Estimated age
Dyode Kelleriki (D)	100-175 m	11m	1000
Neleger (N)	500-1000 m	4m	5000
Ulakhan Sykkhan (U)	725-1545m	14m	8000-9000
Tungle (T)	6800-12800m	25m	16000-18000

*estimation from morphological features of Alas

3. Results

All soils had permafrost within a depth of 2 m, therefore they are classified as Gelisols (Soil Survey Staff, 1999). Texture was SiCL to LiC, which Alas soils had finer texture. Table 2 shows all analytical data of soils investigated. Alas soils had no organic (O) horizons. However, older U and T Alas showed lake deposition (LD)

Table 2 Results of chemical analysis

Site	Horizon	Depth cm	pH water	EC dS/m	TN %	TC %	CEC cmol/kg	Ca sat. %	Na sat. %	BS %	Fed %	Feo %	(Fed-Feo) /Fed	diagnostic properties
D-Forest	E	0 - 8/13	5.9	0.20	0.03	0.68	21.3	7.0	0.6	14.8	0.71	0.18	0.75	-
	B1	8/13 - 41	7.1	0.18	0.02	0.40	20.3	12.3	1.2	23.6	0.85	0.19	0.78	-
	B2ca	41 - 67	8.9	0.58	0.02	0.90	14.3	84.0	4.2	98.7	0.51	0.10	0.81	-
	BC	67 - 105+	8.8	0.42	0.00	0.36	10.9	18.5	4.2	33.1	0.49	0.10	0.80	-
D-Alas1	Acag	0 - 6	9.2	4.19	0.24	3.95	15.0	18.0	4.0	33.1	0.75	0.70	0.07	-
	B1cag	6 - 22	9.3	1.93	0.04	0.86	13.2	27.6	11.7	71.5	0.74	0.58	0.23	-
	B21cag	22 - 58	9.3	1.18	0.03	1.57	8.5	115.1	11.7	165.3	0.48	0.30	0.38	-
	B22cag	58 - 85	9.1	0.78	0.03	1.12	12.8	93.9	4.8	124.9	0.50	0.31	0.39	-
D-Alas2	Aca	0 - 9/20	8.6	3.01	0.19	2.88	24.8	38.7	4.5	92.2	0.50	0.30	0.39	-
	B1ca	9/20 - 40	8.8	1.34	0.13	1.78	24.2	43.1	5.2	70.5	0.57	0.39	0.33	-
	B2ca	40 - 80	8.7	1.08	0.04	1.07	20.0	56.1	3.7	81.8	0.67	0.30	0.55	-
N-Forest	E	0 - 4/9	6.9	0.36	0.07	1.87	24.1	13.2	1.3	36.9	0.64	0.16	0.75	-
	E/B11ca	4/9 - 13	8.0	1.02	0.07	1.73	34.8	40.5	0.8	57.1	0.74	0.14	0.81	-
	E/B12ca	13 - 23	8.6	0.76	0.07	1.68	38.5	48.1	0.9	63.4	0.65	0.13	0.80	-
	B2ca	23 - 56+	8.9	0.72	0.06	1.39	38.0	32.3	1.3	51.4	0.77	0.13	0.83	-
N-Alas1	A	0 - 13/27	7.1	3.63	1.06	13.74	36.0	25.0	1.5	51.4	0.60	0.39	0.35	-
	AB	13/27 - 20/35	8.8	2.11	0.13	1.98	36.3	33.0	5.1	71.5	0.43	0.25	0.42	-
	B1g	20/35 - 50	8.8	3.59	0.05	0.74	34.6	33.3	8.9	76.4	0.54	0.18	0.67	-
	B2cag	50 - 138+	8.4	4.16	0.04	1.12	19.2	79.3	9.8	129.7	0.69	0.17	0.75	Salic
N-Alas2	A	0 - 3/13	7.2	0.71	0.49	5.99	34.6	23.0	0.7	53.5	0.55	0.36	0.34	-
	B1ca	3/13 - 20	9.5	1.22	0.06	1.62	17.9	71.7	9.1	133.1	0.48	0.21	0.56	-
	B21ca	20 - 48	9.5	2.21	0.04	1.22	24.9	50.5	11.0	92.1	0.58	0.15	0.74	-
	B22ca	48 - 80	9.2	2.64	0.04	1.08	23.9	56.9	10.4	95.7	0.56	0.11	0.80	-
	B23ca	80 - 110	8.7	3.81	0.05	1.15	24.3	65.3	9.0	108.0	0.76	0.18	0.76	-
	B3ca	110 - 130+	8.7	2.68	0.07	1.19	24.9	62.1	5.9	91.7	0.45	0.17	0.61	-
U-Forest	E	0 - 4	5.33	0.12	0.04	0.82	12.0	6.2	0.4	10.1	0.28	0.12	0.56	-
	B1	4 - 24	5.62	0.14	0.02	0.35	11.5	10.5	0.4	16.8	0.36	0.20	0.45	-
	B21ca	24 - 34	6.09	0.08	0.02	0.23	9.0	9.2	0.6	15.2	0.49	0.11	0.78	-
	B22	34 - 64	6.18	0.07	0.01	0.20	6.8	10.2	0.6	17.1	0.29	0.06	0.81	-
	BC	64 - 100+	6.36	0.06	0.01	0.16	4.4	9.8	0.8	19.4	0.15	0.04	0.74	-
U-Alas1	AG	0 - 22	9.03	5.43	1.18	18.73	39.0	25.0	25.0	140.5	0.58	0.58	0.00	Calcareous
	LD1	22 - 40	9.26	7.45	0.91	17.07	38.0	24.8	25.1	138.8	0.52	0.49	0.05	Calcareous
	LD2	40 - 69	9.38	3.23	0.37	7.45	24.3	26.3	16.5	121.4	0.47	0.42	0.11	Natric
	B1ca	69 - 87/92	9.42	3.01	0.17	2.55	12.4	46.9	20.7	156.8	0.40	0.39	0.03	Natric
	LD3g	87/92 - 92-105	9.38	3.37	0.03	0.76	7.3	92.1	30.5	221.5	0.29	0.26	0.12	Natric
	B2ca	92-105 - 113	9.3	3.61	0.02	0.60	6.1	95.7	35.0	232.3	0.23	0.22	0.02	Natric
	LD4	113 - 120+	9.14	4.14	0.08	1.55	11.2	62.7	23.4	180.5	0.45	0.33	0.26	-
U-Alas2	LDg	0 - 19	8.86	0.92	0.46	5.14	25.0	52.5	2.6	99.3	0.18	0.14	0.20	-
	Bca/LD	Cryoturbation	9.56	1.08	0.11	2.28	11.7	83.0	7.1	147.9	0.16	0.11	0.30	-
	Bca/E		9.5	0.59	0.02	0.41	5.3	177.9	9.9	220.9	0.10	0.09	0.15	-
	Bca/LD2		8.73	0.40	0.16	2.58	24.0	9.1	0.9	14.2	0.16	0.11	0.30	-
	Bca/BC		9.06	0.38	0.01	0.21	5.0	41.6	2.6	63.9	0.14	0.09	0.31	-
	BC	104 - 152+	8.88	0.48	0.02	0.28	8.8	22.4	2.7	50.2	0.34	0.12	0.65	-
T-Alas1	Aca	0 - 15	9.21	2.02	0.32	3.93	20.9	40.5	8.8	123.1	0.57	0.48	0.16	-
	LD1ca	15 - 24	9.36	2.48	0.45	4.92	29.4	26.7	10.8	101.2	0.68	0.54	0.21	-
	Gca	24 - 58	9.73	3.34	0.16	3.01	19.2	34.4	20.7	119.2	0.54	0.54	0.00	natric
	B1gca	58 - 74	9.66	3.00	0.10	1.78	14.5	51.6	24.3	117.7	0.42	0.39	0.07	natric
	B2gca	74 - 100	9.51	3.58	0.06	1.30	12.0	73.7	27.5	145.0	0.38	0.38	0.00	natric
	LD2ca	100 - 105	8.95	4.44	0.11	1.49	10.2	76.6	36.3	172.0	0.42	0.35	0.17	-
	B3gca	105 - 130+	8.82	3.99	0.08	1.33	15.2	73.1	21.8	143.5	0.59	0.45	0.23	natric
T-Alas2	E	0 - 15/23	9.11	0.90	0.11	1.72	13.1	55.9	1.7	123.6	0.32	0.24	0.25	-
	B1ca	15/23 - 47	9.94	2.14	0.04	1.28	11.0	62.9	27.9	146.6	0.44	0.43	0.03	natric
	LD1	47 - 52	9.86	3.09	0.06	1.34	16.7	53.6	22.8	129.1	0.59	0.25	0.57	natric
	B2ca	52 - 61	9.64	1.95	0.03	1.00	11.5	77.6	21.5	147.8	0.35	0.29	0.17	natric
	LD2	61 - 67	9.15	4.39	0.18	2.57	23.9	40.6	15.9	108.1	0.49	0.40	0.19	-
	B3ca	67 - 103	8.82	3.46	0.05	1.36	12.6	83.6	16.2	138.8	0.35	0.30	0.14	natric
	LD3	103 - 110+	8.56	3.28	0.03	0.95	15.6	73.8	8.2	112.0	0.49	0.21	0.58	-

LD means lake deposition.

horizons, indicating that soil erosion occurred during the Alas formation process. The pH values of O horizons in forest soils were less than 6, which were low compared to those of mineral horizons. The B horizons showed high pH values more than 7 and the pH values of deeper C horizons were close to 9. Alas soils had much higher pH values than forest soils. All the B and C horizons showed high pH more than 8.5 as a criteria of the Natric horizon (FAO, 1988). These tendencies were clearly shown in histogram of pH values (Fig. 1).

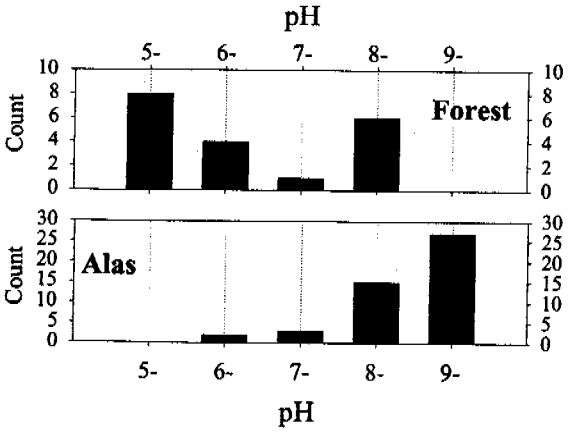

Figure1. Histogram of pH values of forest soils and Alas soils

EC values of O horizons in forest soils were higher than in mineral horizons. Although mineral B and C horizons in LN-forest showed relatively high EC values more than 0.7 dS m^{-1}, other forests showed low EC value less than 0.5 dS m^{-1} (Table 2). Alas soils showed much higher EC values than forest soils, but the values showed wide range from 0.38 to 7.45 dS m^{-1}. EC values decreased with increasing depth in D and U Alas. Soil closer pond in U Alas showed higher EC. These tendencies were also clearly shown in histogram of EC values (Fig. 2).

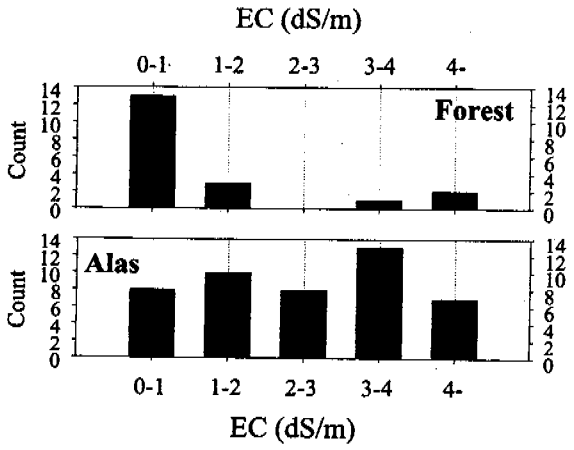

Figure2. Histogram of EC values of forest soils and Alas soils

The BS values in forest soils were almost below 50 % other than Bca horizons (Table 2). The Ca saturation was also high in Bca horizons. However Na saturation was low below 5 %. On the other hand, Alas soils showed considerably high BS values often more than 100 % from shallower horizons. Both Ca and Na saturation were also high in the horizons with high BS saturation. Especially almost all horizons in the soil closer pond of U and both soils of T Alas showed Na saturation more than 15 %, which is a criteria of Natric horizon (FAO, 1988). There was a only one horizon with Salic properties in N Alas. Natric B horizon was observed in old U and T Alas.

The values of (Fed-Feo)/Fed as crystallinity of Fe oxide were high in forest soils but low in Alas soils. Forest soils showed vertically constant crystallinity value, while Alas soils showed relatively lower crystallinity value in upper layer and older Alas soils had lower values (Table 2). This tendency was clearly shown in histogram of crystallinity (Fig. 3).

4. Discussion

Alas soils had higher values of pH, EC and Na saturation than forest soils and older Alas soils had Natric horizons (Table 2). This clearly shows occurrence of long-term alkalization mentioned by Desyatkin (1993). The long-term alkalization in Alas occurs with the redistribution of carbonate, which accumulated in the subsoil above the permafrost in forested soil, associated with lateral and upward water flow during the drying of Alas-pond. Present results supported it well. On the other hand, the Alas soils had lower values of (Fed-Feo)/Fed than forest soils and the values decreased with increase of size and age of Alas. Generally, the value of (Fed-Feo)/Fed increases in weathered and old soils (Blume and Schewertman, 1969). However, it has been pointed out that Feo increases in paddy field (Wang et al. 1993), in wet land (Johnstone et al. 1995), in the B horizons of Podzols (Lundstrom et al., 2000) and in young tephra (Dahlgren, 1997; Adjadeh and Inoue, 1999;), that indicated accumulation of non-crystalline oxyhydroide as ferrihydrite (Parfitt and Childs, 1988). Johnston et al. (1995) showed that Feo contents in soils strongly depended on parent materials, but depth of the peak of Feo decreased in mineral horizon with increasing wetness of soil. Tolchev et al. (2002) showed that Fe crystallization from ferrihydrite proceeds under the complete oxidation condition performed by addition of H_2O_2, and through the wide range of soil pH from 2.5 to 13 and temperature from 20 to 85 °C. This suggests that Fe crystallization in Alas soil would be possible to occur, although Fe crystallization decreases with decreasing temperature. However, the present result of (Fed-Feo)/Fed in Alas soil showed that non-crystalline Fe formation exceeded Fe crystallization in upper horizons under oxidation condition (Table 2). This suggests that Fe reduction also occurred with permafrost thawing in summer season as well as Fe oxidation. Subsided thermokarst-topography of Alas makes more water accumulate from surrounding forest soils, which can promote the Fe reduction. This is supported by occurrence of CH_4 emission from the Alas soils in summer season (Morishita et al., 2001).

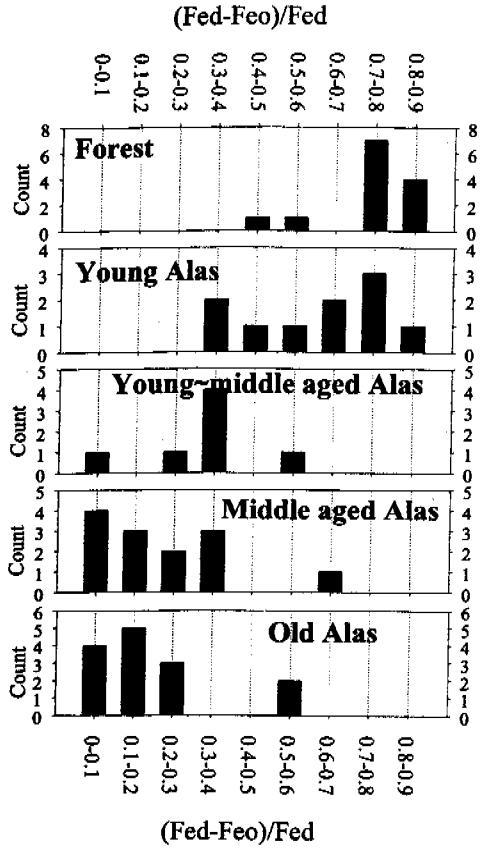

Figure 3. Histogram of (Fed-Feo)/Fed of forest soils and Alas soils

Acknowledgement

The authors wish to thank Prof. M. Fukuda of Hokkaido University, the leader of Crest program of Japan Science and Technology Corporation (JST), for his supporting this study and valuable comments. The authors thank Prof. K. Takahashi, Dr. M. Shibuya, Dr. H. Saito, Dr. K. Kushida, Dr. Y. Kobayashi and Dr. G. Iwahana of Hokkaido University, Dr. T. C. Maximov, Dr. A.P. Isaev of Institute of Biological Problems of Cryolithone, Russian Academy of Sciences. This study was supported by the CREST program of Japan Science Technology Corporation (JST).

REFERENCES

Adjadeh TA and Inoue K 1999: Mineralogical properties of Andisols of the Kitakami mountain range, northeastern Japan, *Soil Sci. Plant Nutr.*, 45, 101-114

Blakemore, L.C., Searle, P.L. and Daly B.K. 1981: Soil Bureau Laboratory Methods: A. Methods for Chemical Analysis of Soils, NZ *Soil Bureau Sci.*, Report 10A.

Blume, H. P., and Schwertmann, U. 1969: Genetic evaluation of the profile distribution of aluminium, iron and manganese oxides; *Soil Science Society of American Proc.* 33 p438-444

Dahlgren, R.A., Dragoo, J.P., and Ugolini, F.C. 1997: Weathering of Mt. St. Helens tephra under a cryic-udic climatic regime, *Soil Sci. Soc. Am. J.*, 61, 1519-1525

Desyatkin R. V. 1993: Syngenetic soil salinization during thermokarst alas formation. *Eurasian Soil Sci.* 25, 38-46

Desyatkin. R. V. 1990: Soil formation in Alases. ; *Pochvovedeniye.* 12: 5-15

FAO. 1988. Revised legend of the FAO-UNESCO Soil Map of the World. p.119. FAO, Roma

Fitzpatrick, E. A. 1983: Thermokarst, in Soils, p222-223, Longman, New York

Holmgren, G.G.S. 1967: A rapid citrate dithionite extractable ion procedure, *Soil Sci. Soc. Amer. Proc.*, 31, 210-211

Ivanov M.S. 1984: Cryogenic structure of quaternary deposits of the Lena-Aldan depression. *Nauka, Novosibirsk,* p126 (in Russian)

Johnston, C.A., Pinay, G., Arens, C., and Naiman, R.J. 1995: Influence of soil properties on the biogeochemistry of a beaver meadow hydrosequence, *Soil Sci. Soc. Am. J.*, 59, 1789-1799

Kaplina T.N. and Lozhkin A.V. 1978:The age of Alas deposits of the Primorie lowland of Yakutia: radiocarbon grounds. In Izv AS USSR, 2, 69-76 (in Russian)

Lundstrom, U.S., van Breemen, N., Bain, D.C., van Hees, P.A.W., Giesler, R., Gustafsson, J.P., Ilvesniemi, H., Karltun, E., Melkerud, P.A., Olsson, M., Riise, G., Wahlberg, O., Bergelin, A., Bishop, K., Finlay, R., Jongmans, A.G., Magnusson, T., Mannerkoski, H., Nordgren, A., Nyberg, L., Starr, M., and Strand, L.T. 2000: Advances in understanding the podzolization process resulting from a multidisciplinary study of three coniferous forest soils in the Nordic Countries, Geoderma, 94, 335-353

Morishita, T., Hatano, R., Sawamoto, T., Nakahara, O., Takahasi, K., Isaev, A.P., Desyatkin, R.V., and Maxiov, T.C. 2001: Methane fluxes in forest, glassland and wetland soils, near Yakutsk, Russia. *Proceedings of the*

ninth symposium on the joint Siberian permafrost studies between Japan and Russia in 2000, 150-155.

Parfitt, R. L. and Childs, C. W. 1988: Estimation of forms of Fe and Al. A review, and analysis of contrasting soils by dissolution and Moessbauer spectroscopy. *Aust. J. Soil Res.*, 26, 121-144

Shi, T., Reeves, R.H., Gilichinsky, D.A., and Friedmann, E.I. 1997 Characterization of viable bacteria from Siberian permafrost by 16S rDNA sequencing. *Microbial Ecol.*, 33, 169-179

Tolchev, A.V., Kleschov, D.G., Bagautdinova, R.R., Pervushin, V.Y. 2002: Temperature and pH effect on composition of a precipitate formed in $FeSO_4$-H_2O-H^+/OH^--H_2O_2 system, *Materials Chemistry and Physics*, 74, 336-339

Soil Survey Staff 1999: Keys to Soil Taxnomy, 8th edition, p 600, Pocahontas Press, Inc, Blacksburg, Virginia, USA

Wang, H.D., White, G.N., Turner, F.T. and Dixon, J.B. 1993: Ferrihydrite, Lepidocrocite, and Goethite in Coatings from East Texas Vertic Soils, *Soil Sci. Soc. Am. J.*, 57, 1381-1386

Changes in fossil pollen assemblages from alasses, central Yakutia, eastern Siberia

F. Katamura[1] , J. Mori[1] , M. Fukuda[1], R.V. Desyatkin[2]

[1]Institute of Low Temperature Science, Hokkaido University, N19 W18, Sapporo 060-0819, JAPAN
E-mail: katamura@pop.lowtem.hokudai.ac.jp
[2]Institute of Biological Problems of Cryolithozone, Russian Academy of Science, Yakutsk, RUSSIA

1. Introduction

A large number of thermokarst depression, i.e. alas, are existed in central Yakutia, eastern Siberia. Alas was formed by thermal disturbance of ice complexes in ground, for example, rising air temperature or destruction of vegetation. Once alas is formed, reforestation is difficult because of salt accumulation. It is said that alasses in central Yakutia were developed during Holocene climatic optimum (French, 1996). However, the chronology of alas formation and local vegetation change around alas are not well known. The reconstruction of alas formation history and past environmental changes around alas might be important for understanding climatic trends in future. Pollen analysis is useful for reconstruction past vegetation changes.

The objectives of this study are, 1) reconstruction of vegetation history around alasses by means of pollen analysis, 2) collecting modern pollen assemblage from surface sediment and comparing it with vegetation around the sampling in order to assist interpretation of fossil pollen record.

2. Study sites

The study sites are two thermokarst lakes, Ulakhan Sykkhan alas and Uinakh alas, and terrace of right bank of the Lena River, central Yakutia (Fig.1).

Ulakhan Sykkhan Alas

The Ulakhan Sykkhan alas (62° 09′ 57.0″ N, 130° 31′ 54.3″ E) is located approximately 45km northeast of Yakutsk. The area of the alas is 0.64km^2, which has pond at center of it. There are no surface inflow and outflow streams. Vegetation around alas is *Larix gmelinii* forest, however *Betula platyphylla* is dominant on the border between alas and forest. Several detailed studies have been performed on vegetation of Ulakhan Sykkhan alas (Uemura, 1998; Desyatkin, 2000).

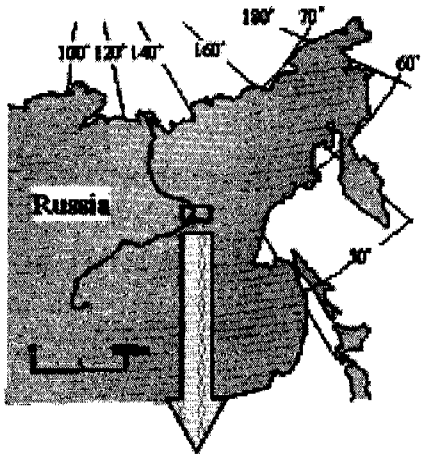

Uinakh Alas

The Uinakh Alas (62° 09′ 22.8″ N, 130° 38′ 34.5″ E) is located approximately 50km northeast of Yakutsk, and 5km northeast of Ulakhan Sykkahan alas. The alas has 500m in width and 300m in length, which has shallow pond at center of it. The vegetation is similar to that of Ulakhan Sykkahan alas. It is dominated with *Larix gmelinii* and *Betula platyphylla*.

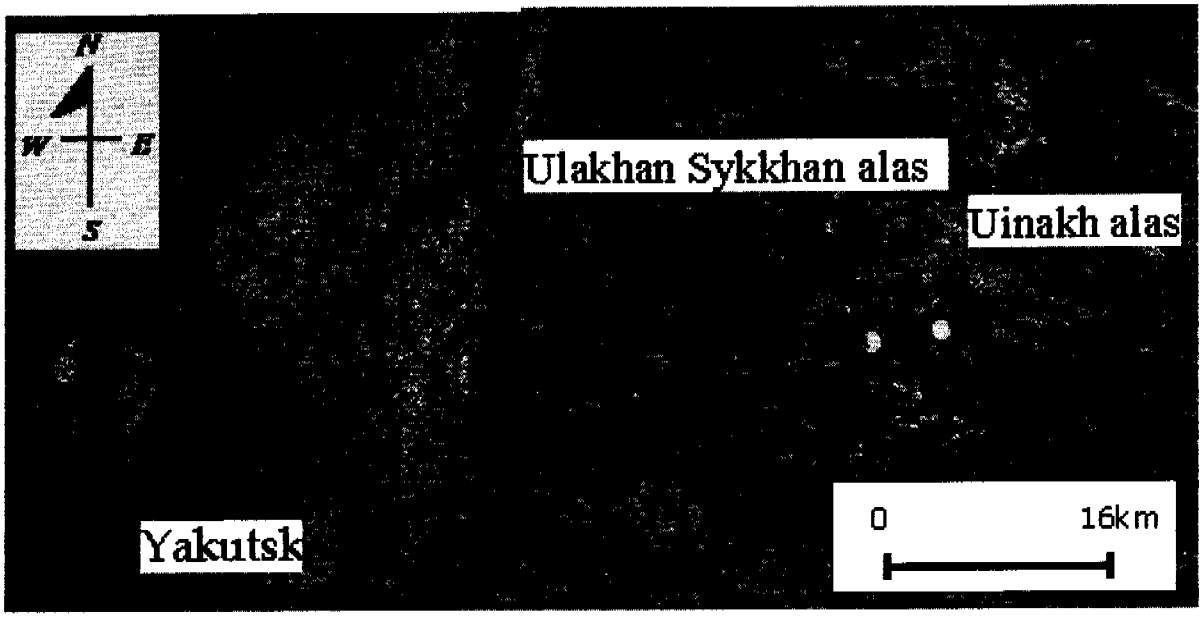

Fig. 1. Map showing the location of the studied sites.

3. Method

Surface samples were obtained from 11 sites along a north-south transect crossing the Ulakhan Sykkhan alas (Fig. 2), including two sites from larch forest (sites 1 and 11). A 128cm and 96cm long sediments samples were collected by shovel from Ulakhan Sykkhan alas and Uinakh alas, respectively. Samples from sediments were cut by shovel, and the deeper frost sediment was obtained with boring machine.

Each sample, which was divided into $1cm^3$ cube, was processed for pollen analysis according to standard methods (Birks and Birks, 1980). The sediments were subsampled at every 2 or 4cm intervals. At least 200 pollen grains were counted for each sample at 400× magnification, except for low concentrated sample. Relative frequency was calculated based on the arboreal pollen number.

4. Results

Surface sample from Ulakhan Sykkhan alas

Pollen assemblages from surface samples are shown in Fig. 3. *Pinus* is the most abundant taxon ranging from 42.0 to 83.2% except for site 11. However, pine trees are rare around the alas at present. Today *Piuns silvestris* community is distributed on sandy soil along the Lena River. This indicates that *Pinus* pollen was transported by the wind from long distance. On the other hand, *Larix* pollen comparatively low in spite of high vegetation cover around alas. *Betula* is sometimes over represented such as site 11. Grass, sedge and herbaceous taxa such as Poaceae, Cyperaceae and *Artemisia* were do not appear in the forest. Trace amount of these taxa indicates that source plants grow nearby. *Pediastrum*, algae, was found from only pond area.

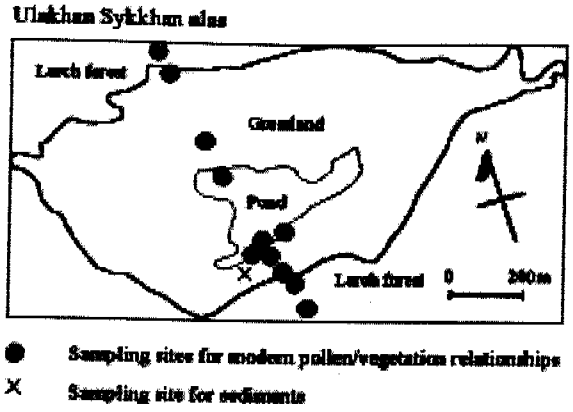

Fig. 2. Sampling sites for surface and sediments samples at Ulakhan Sykkhan alas.

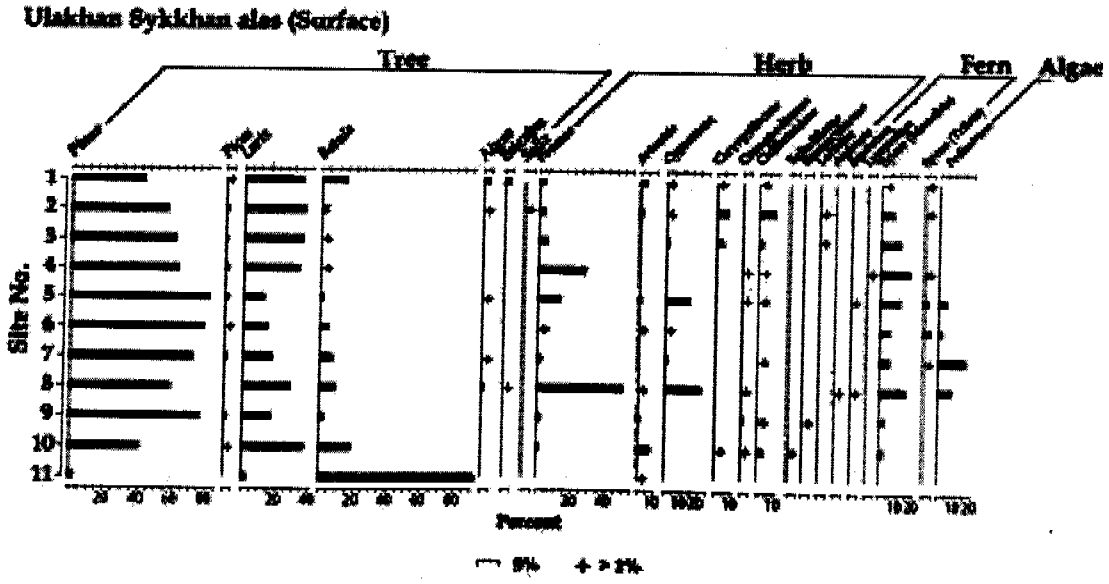

Fig. 3. Surface pollen diagram from Ulakhan Sykkhan alas. Relative frequency was calculated based on the total arboreal pollen number.

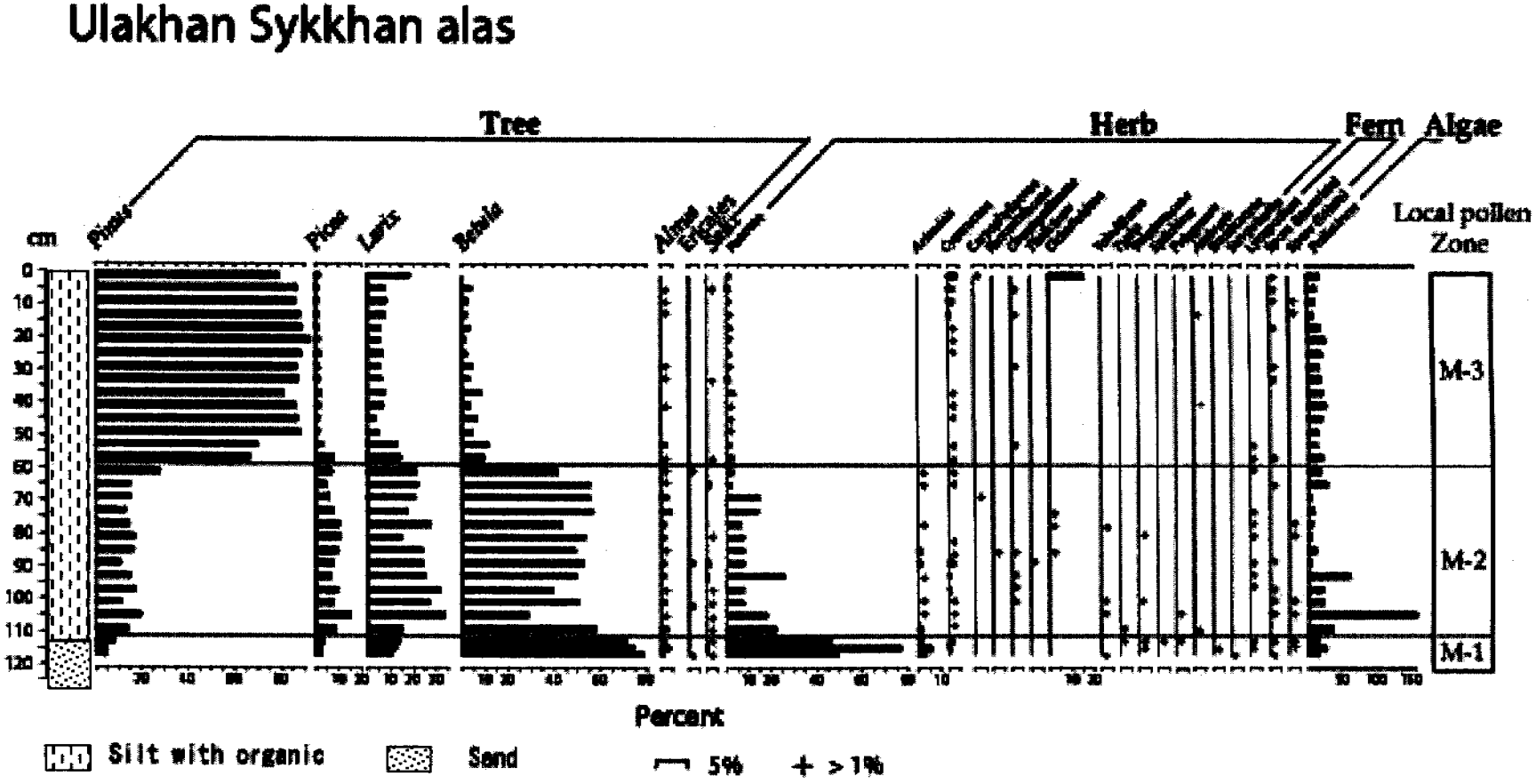

Fig. 4. Pollen diagram from Ulakhan Sykkhan alas. Relative frequency was calculated based on the total arboreal pollen number.

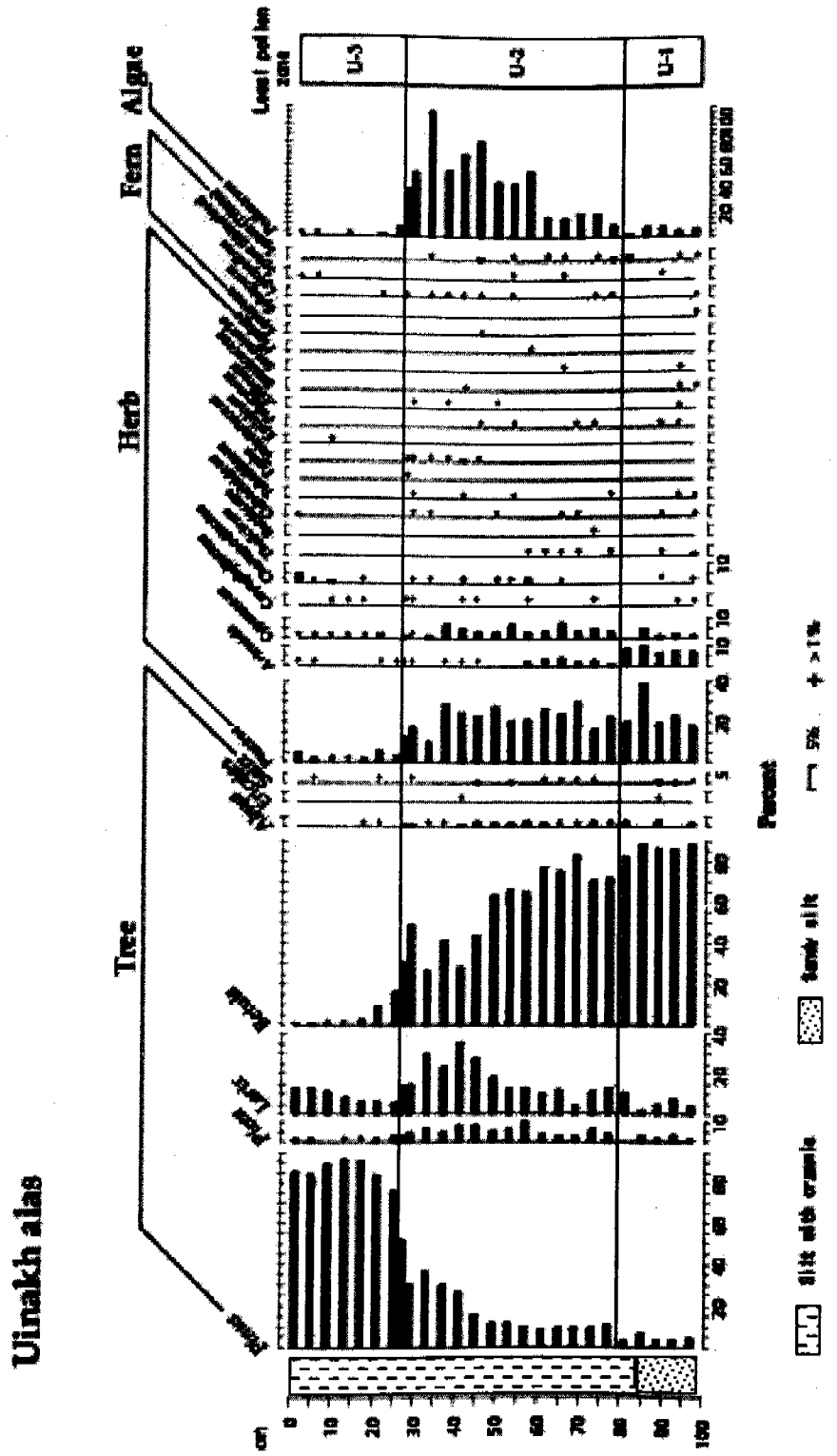

Fig. 5. Pollen diagram from Uinakh alas. Relative frequency was calculated based on the total arboreal pollen number.

Ulakhan Sykkhan alas

Three local pollen zones, M-1 (111-118cm), M-2 (59-111cm) and M-3 (0-59cm) in ascending order were discriminated (Fig. 4.). Pollen concentration is extremely low in the bottom of sandy sediment (118-128cm). Zone M-1 is characterized by high percentages of *Betula* (72.2-79.4%), with Poaceae (46.5-77.8%) and *Artemisia* (1.58-2.80%) Pollen. It is suggested that sand accumulation period was early stage of alas. Landscape around the alas was probably birch-larch forest. Zone M-2 is characterized by increasing of *Pinus* (10.4-28.1%), *Picea* (4.35-15.0%), *Larix* (15.3-34.4%) and dominant *Pediastrum*. Birch-larch forest was replaced by larch-birch forest. Zone M-3 is characterized by a sharp increase of *Pinus* (67.0-93.0%), and a decline of *Picea* (0.4-2.6%), *Betula* (0.6-11.6%) and *Larix* (3.8-18.4%). Pine trees were expanded on sandy soils along the Lena River, which suggest present vegetation was formed during in Zone M-3 period.

Uinakh alas

Three local pollen zones U-1 (79-98cm), U-2 (26-79cm) and U-3 (0-26cm) in ascending order were discriminated (Fig. 5.). Zone, U-1, is dominated by *Betula* (81.1-87.8%) with Poaceae (17.3-38.8%) and *Artemisia* (6.4-10.2%). Zone U-2 is characterized by increasing *Pinus* (7.4-51.8%), *Picea* (2.6-9.7%), *Larix* (4.4-36.0%) and dominant *Pediastrum* (11.7-119.0%). *Betula* gradually decreased (28.1-71.2) except for a few samples. The uppermost zone U-3 is characterized by high percentages of *Pinus* pollen.

Changes in pollen assemblages from Uinakh Alas are similar to that of Ulakhan Sykkhan alas, which suggest that these vegetation changes represent regional change.

5. Discussion

Local pollen zones U-1, U-2 and U-3 are well correlated to M-1, M-2 and M-3 respectively by similarity of each pollen assemblage. So we established regional pollen zone Y-1, Y-2, and Y-3 (Table 1). Vegetation during Zone Y-1 period was birch-larch forest with grass and wormwood on sandy sediment. Although we did not measure any radiocarbon dates yet,

Table 1. Vegetation history around two alasses in central Yakutia.

Local pollen zones		Regional pollen zones	Vegetation history
Ulakhan Sykkhan	Uinakh		
M-3	U-3	Y-3	Modern vegetation
M-2	U-2	Y-2	Larch-birch forest
M-1	U-1	Y-1	Birch-larch forest with grass and wormwood

two radiocarbon ages, 8,590±80 BP and 8,670±90 BP, were measured on 60-65cm in depth from another site of the Uinakh alas (Fukuda et al., 1995). *Larix* pollen is relatively low even in surface sample from larch forest (e.g. Andreev et.al., 2001). Our surface data from larch forest shows the same trend. According to Velichko (1997), after 6000 yr BP pine trees were dominated on sandy soil in central Yakutia.

6. Conclusion

•Pollen analyses were carried out to surface and sediments samples obtained from two alasses, central Yakutia, eastern Siberia.

•Surface samples show that; (1) percentage of *Larix* is relatively low even in samples from larch forest, (2) herb taxa indicate local presence of the source plants, and (3) *Betula* pollen is sometimes over-represented.

• The pollen zones of obtained from two alasses show distinct three vegetation types. Zone Y-1 is characterized by dominance of *Betula* with Poaceae and *Artemisia*. Zone Y-2 is characterized by increasing of *Picea* and *Larix*. Zone Y-3 is marked by increase *Pinus*, which is interpreted as establishment modern vegetation.

REFERENCES

Andreev, A.A., Klimanov, V.A. and Sulerzhitsky, L.D. (2001) Vegetation and climate history of the Yana River Lowland, Russia, During the last 6400yr. Qurternary Science Reviews, Vol.20, 259-266

Birks, H.J.B. and Birks, H.H. (1980) Quaternary palaeoecology. Edward Arnord, London.

Desyatkin, R.V., Nikolaeva, M.C., Desyatkin, A.R., Stepanova, M.A., Ishii, Y. and Yabuki, H. (2000) Geobotanical map of "Ulakhan Sykkhan" alas. Activity report of GAME-Siberia 2000

French, H.M. (1996) The Periglacial Environment. 2nd edition, London press

Fukuda, M., Sento N., Kunitky, V.V. and Nakamura, T (1995) Radio carbon dating results of organic materials obtained from eastern Siberian Permafrost. Proceeding of the forth symposium on the joint Siberian permafrost studies between Japan and Russia in 1995

Uemura, S., Kanda, F., Tsujii, T. and Isaev, A.P. (1998) concentric pattern and asymmetry in the vegetation of alas, Eastern Siberia. Janpan phytogeography and Taxon, Vol.46, 71-76

Velichko, A.A., Andreev, A.A. and klimanov, V.A. (1997) Climate and vegetation dynamics in the tundra and forest zone during the Late Glacial and Holocene. Quaternary Internationl. Vol. 41/42, 71-96

Aerosol Chemical Composition over West Siberia based on the Results of Airborne Sounding in 1997-2001.

B.D. Belan, O.A. Krasnov, D.V. Simonenkov and G.N. Tolmachev

Institute of Atmospheric Optics SB RAS; 1, Akademicheskii Avenue, 634055, Tomsk, Russia.
Phone: +7-3822-259894; Fax: +7-3822-259086; E-mail: bbd@iao.ru

1. Introduction

Data on chemical composition of atmospheric aerosol is very important for the understanding a wide range of problems in atmospheric physics and optics. Chemical composition of aerosol particles determines their refraction index and, consequently, regularities of dissipation and absorption of solar radiation in the atmosphere. Aerosol particles can contain heavy metals with carcinogenic properties. Therefore some investigations are of an ecological importance. Also a dissolution of sulfate aerosol particles in cloud drops results in formation of acid rainfalls. Thus, the study of chemical composition of aerosol is an important part of atmospheric studies.

Institute for Atmospheric Optics has been carrying out regular (1 flight per month) airborne sounding over southern regions of West Siberia since July 1997. Some results of analysis of more than 400 aerosol samples made over this region during last almost five-year studies onboard airborne laboratory are presented in this paper.

2. Sites and Methods

Airborne surveys have been performed onboard "Antonov-30" aircraft laboratory in the 500 to 7000 m atmospheric layer mainly over forest zone on the right bank of southern part of Novosibirsk impoundment (so called "Ob' Sea") near boundary of Novosibirsk and Altai regions, and, on several occasions, over forest marshland of Tomsk region (near Plotnikovo village) not far from Novosibirsk region boundary. In our studies we try to perform flights under clear sky weather conditions. Aerosols are sampled onto Petryanov filters (AFA-type) during 10-15 min time period at each level. The volume of air pumped through each filter is from 1 to 4 m^3. Then aerosol samples are analyzed in the Analytic Chemistry Laboratory of Environmental Monitoring at the Tomsk State University. Physico-chemical techniques of quantitative analysis of the chemical composition of aerosol matter are given in table 1.

Table 1: Detectability threshold and accuracy of techniques used in analysis of atmospheric aerosol samples collected on Petryanov'filters.

Chemical component	Technique	Threshold, μg/filter	Accuracy %
Br^-, NO_3^-, SO_4^{2-}	Ion chromatography	0.6	8
Cl^-	Ion chromatography	0.1	12
F^-, NH_4^+, NO_3^-	Ionometry	0.2	10
Na^+, K^+	Flame photometry	0.2	10
Ag, Ba, Cu, Mg, Mn, Pb, Sn, V	Atomic-emission spectroscopy	0.01	20
Al, B, Co, Cr, Mo, Ni, Si, Ti, Zn	Atomic-emission spectroscopy	0.02	20
Ca, Fe, Ga, W	Atomic-emission spectroscopy	0.1	20
Cd	Atomic-emission spectroscopy	0.2	20

3. Results and Conclusions

Analysis of samples enabled us to reconstruct smoothed histograms of ion and element differential distributions of aerosol matter (fig.1). The number of samples in which concentration of element or ion was higher than a detection limit is given in brackets. Ranges of frequency distributions are in accord with X-scales points (>1.25E-05…2.5E-05; >2.5E…0.00005 – the next; etc.).

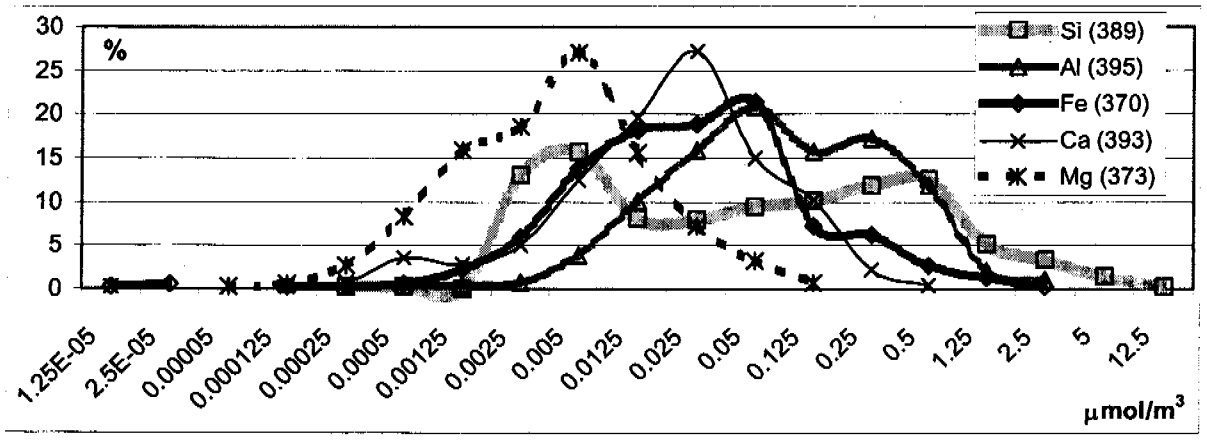

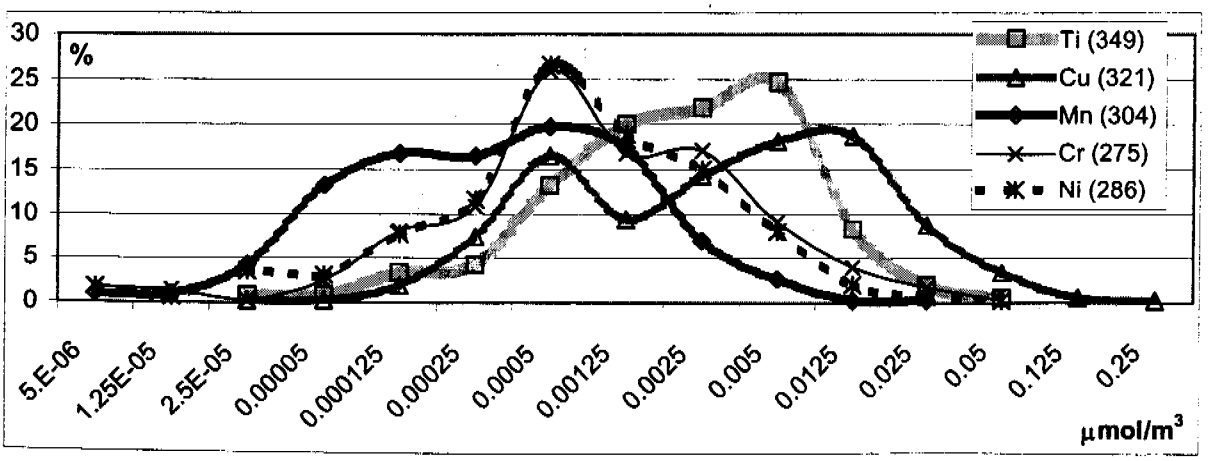

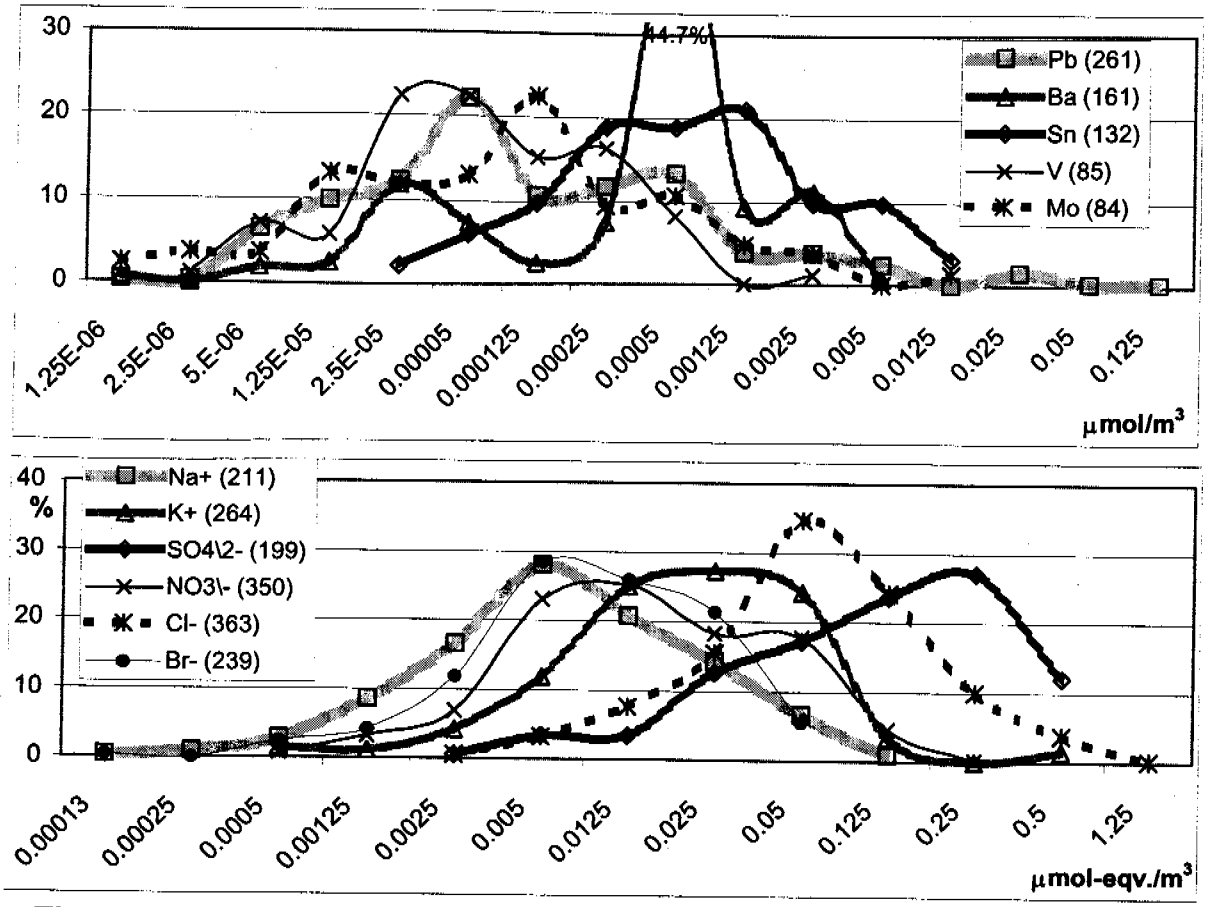

Figure 1: Differential distributions of ion and element concentrations in the atmospheric aerosol over West Siberia.

Average ion and element concentrations for the chemical matrix of aerosol inclusive Si, Al, Fe, Mg, Ca, Ti, Cu, Mn, Cr, Ag, Pb, Ni, Ba, Sn, V, Mo, Co, B, K^+, Na^+, Cl^-, SO_4^{2-}, NO_3^-, Br^-, F^-, NH_4^+ (fig.2) were computed taking into account a differential distribution in order to except abnormally high values (tabl. 2).

Table 2: Database structure of the aerosol chemical composition and results of statistical processing at significance level P = 0.1%* (values of concentration are given in µg/m^3)

	N	$N_{>\text{threshold}}$	Max. val.	N*	Max. val.*	Means*	STD*
Cu	370	321	30.864	299	2.124	0.5069	0.5410
Ag	332	35	0.100	26	0.003	0.0014	0.0004
Ti	400	349	3.505	328	0.769	0.2026	0.1858
Sn	400	132	2.038	115	0.477	0.1335	0.1228
Ca	400	393	27.985	319	3.333	1.0208	0.7645
V	400	85	0.193	84	0.037	0.0088	0.0096
Al	400	395	94.637	349	16.400	4.0863	4.0382
Fe	400	370	161.856	306	7.035	1.9126	1.6960
Si	400	389	658.242	311	16.000	3.1177	4.1971
Pb	400	261	27.054	225	0.199	0.0419	0.0516
Cr	400	275	3.230	246	0.332	0.0837	0.0819

Mg	400	373	5.892	332	0.612	0.1625	0.1471
Mn	400	304	2.323	275	0.149	0.0367	0.0372
Ni	400	286	3.665	261	0.320	0.0804	0.0794
Ba	400	161	1.271	156	0.460	0.1199	0.1143
Mo	352	84	2.333	73	0.067	0.0150	0.0171
B	183	31	2.680	30	0.474	0.1745	0.1508
Co	104	8	0.003	8	0.003	0.0023	0.0006
Na^+	402	211	5.750	192	1.003	0.2763	0.2420
K^+	402	264	31.700	250	4.240	1.3575	0.9771
SO_4^{2-}	402	199	52.740	194	36.585	10.9093	8.6683
NO_3^-	402	350	16.402	326	6.389	1.6761	1.5470
Cl^-	402	363	64.032	335	12.627	3.8568	2.9379
Br^-	334	239	8.901	234	4.562	1.3580	1.0724
NH_4^+	48	22	2.577	22	2.577	0.7106	0.8697
F^-	96	56	1.314	56	1.314	0.3614	0.3494

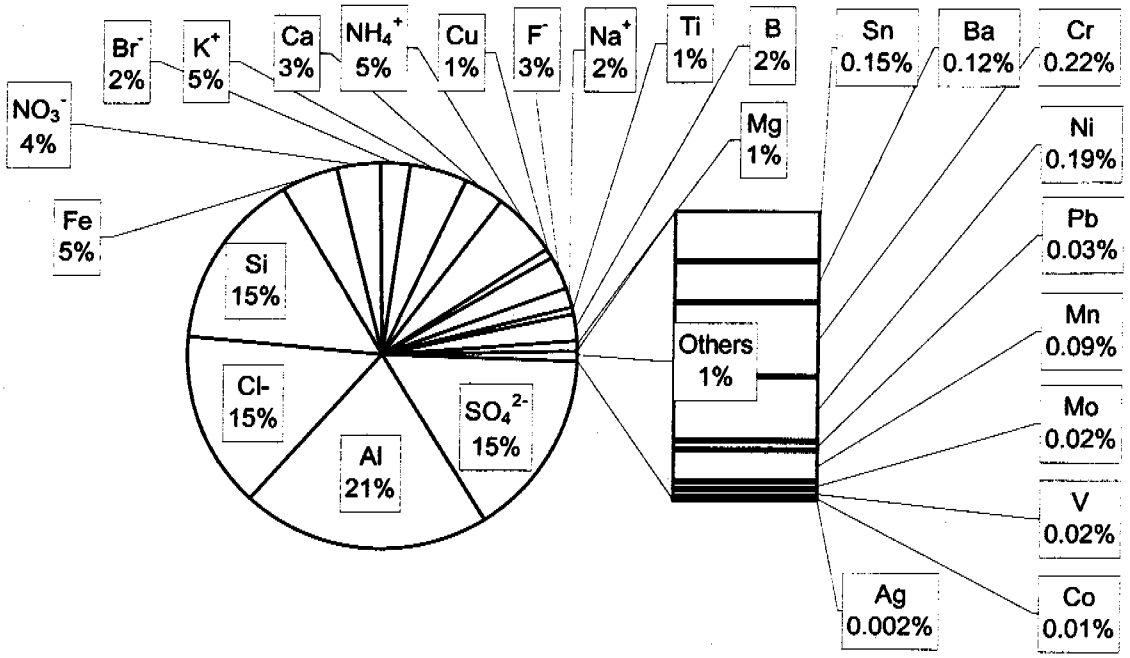

Figure 2: Relative chemical composition (mol.%) of aerosol matter in the atmospheric layer from 500 to 7000 m over West Siberia based on the results of airborne sounding (1997-2001)

Data obtained during this study showed that at all altitudes there is a seasonal behavior of the concentrations of some elements and ions. Amplitude of the seasonal behavior is higher in the boundary layer. Concentration peaks at higher altitudes in the vertical distribution were observed during springtime that, most likely, can be a result of trans-boundary transport (fig.3).

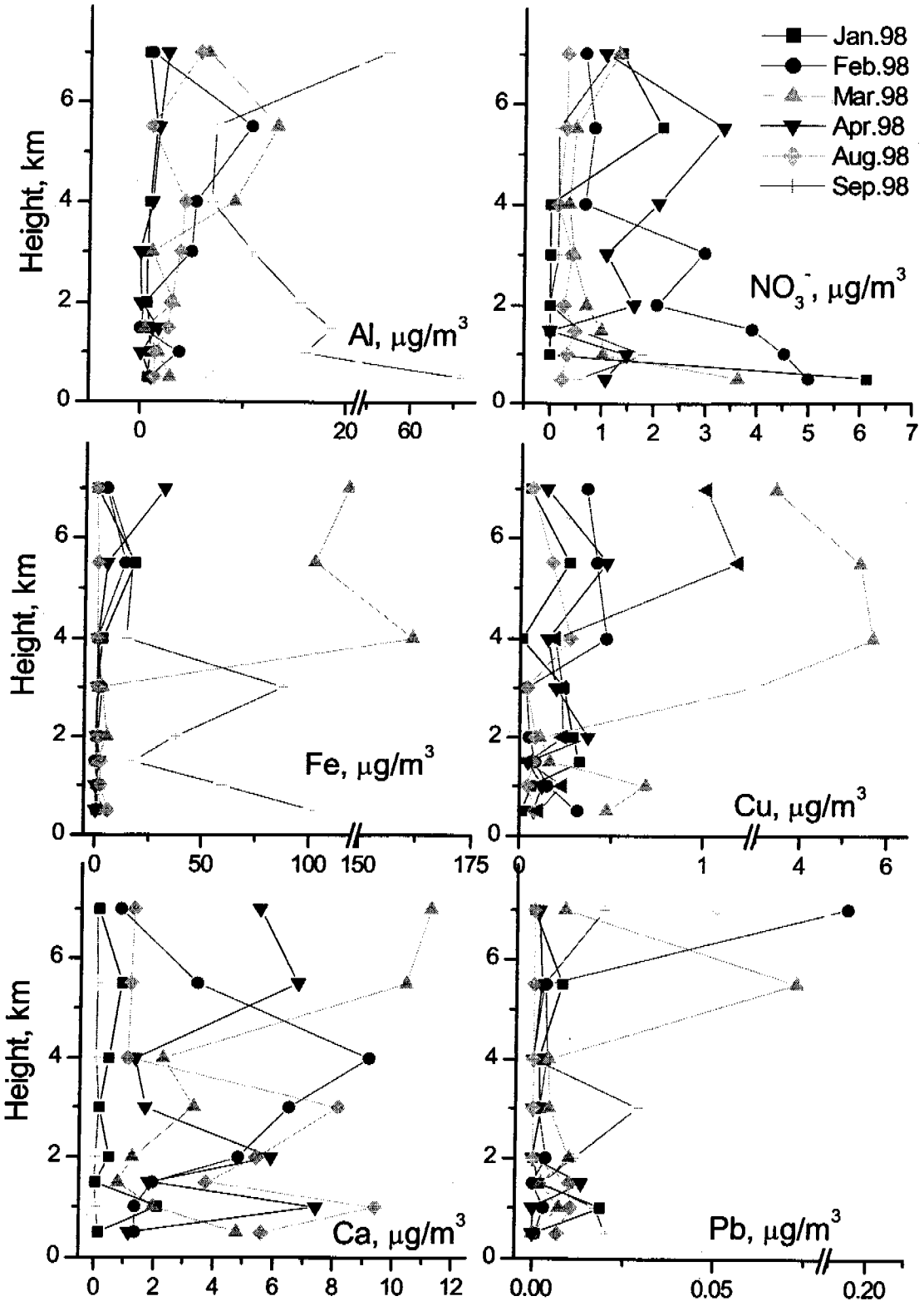

Figure 3: Representative vertical distributions of a number of aerosol chemical components for different months of year.

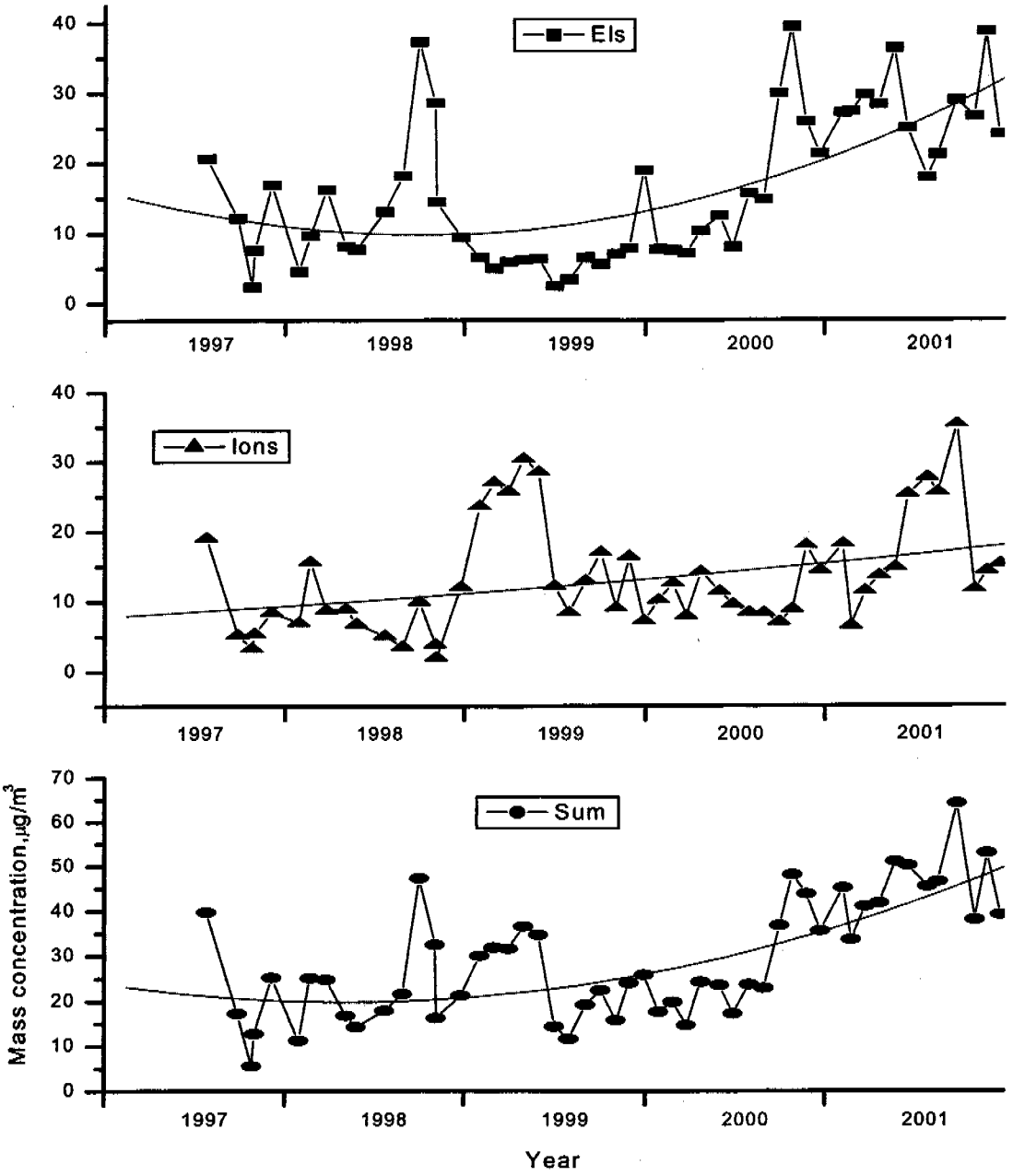

Figure 4: Long-term behavior of total ion (Ions) and element (Els) concentrations, and their total sum (Sum) in aerosol matter; solid line - 4 order polynomial fittings.

Many-year behavior of total mass concentration of definable ions and elements, especially that of elemental part of aerosols, is in a good agreement with many-year behavior of the number concentration of atmospheric aerosol over West Siberia [1].

REFERENCE

Arshinov M.Yu., Belan B.D., Kovalevskii V.K., et al. (2000) : Many-year variability of tropospheric aerosol above West Siberia. *Atmos. Oceanic Opt.* Vol.13, No.6-7, pp.580-583.

Application of remote sensing data to revising the boundary between Subtaiga and South Taiga vegetation zones in West Siberia.

A. M. Peregon, S. V. Vasiliev

Institute of Soil Science and Agrochemistry SB RAS, Novosibirsk, Russia, 630099, e-mail: peregon@issa.nsc.ru

1. Introduction

The boundaries of nature zones in West Siberian plain are placed almost in parallel and strictly from a west to the east. In this connection their width keeps equal enough. From a north to the south the zones changes as follows: tundra, forest-tundra, forest, forest-steppe and steppe with well expressed subzones.

In the early attempts to divide the West Siberia plain into geographic areas dependent on climatic features, many researchers did not mark out intermediate areas between zones as they can not be characterized by the special flora. Within the limits of forest area, P. N. Krylov (1913) marked out a swamp-coniferous zone in a north and swamp-birch zone in the south. The zoning concept as applied to West Siberian Taiga was first promoted by B. N. Gorodkov (1916). Since then four subzones are usually distinguished in Taiga zone: North, Middle, South Taiga and Subtaiga. This concept is used in research and in practice till now. Boundary of the South Taiga subzone established by B. N. Gorodkov were repeatedly updated, although the position of southern boundary (at Turinsk-Tara latitude) has undergone no essential changes in subsequent scientific studies. The northern boundary was updated considerably.

In spite of the fact that indicators, which divide the zones and subzones, are described in considerable detail, we still have a problem of their accurate differentiation and there is vagueness in assigning geographical membership of specific territory. Moreover, abundance of wetlands exerts such a profound influence on all nature components, so that zonal features in distribution of vegetation cover become obscure. The aim of this work is to clarify location of a boundary between South Taiga – Subtaiga subzones and propose a system of indicators that determines membership in certain subzone.

2. Materials and Methods

The central part of Ob-Irtysh interfluve represent the large and compound peat-swamp system (Great Vasyugan Bog). This unique bog-system is considered to be largest in a world. Originality and scientific value of Great Vasyugan Bog consists not only of its large sizes, but also in diverse landscape structure. It is situated at the boundary of two botanic-geographical zones: South Taiga and Subtaiga.

Our study sites were located at south edge of Great Vasyugan bog within the limits of Ob – Irtysh watershed. (Fig. 1).

The absolute elevation of territory varies from 120 up to 130 m. The rivers valleys run deep to 5-8 m, that account for development of numerous streams (10-15 km long) and

supports a good drainage of the band with the width 3-5 km abutting to the river. The forest is common on streamside borders, while swamped landscapes occupy the watershed area. The climate of the region is sharply continental. Annual atmospheric precipitation exceeds 400 mm. (The natural conditions..., 1963).

We made geobotanical observation of forest-mire boundaries using the common geobotanical methods and satellite image (coloured non-transformed image, Resurs MSU, 42 m/pixel).

During observation the basic types of soil, vegetation communities and landscapes within the area of satellite image have been investigated. On study area it is possible to meet different vegetation types: dark coniferous and small-leaved forests, meadows, various bog types etc.

The spatial data interpretation for determination of boundaries between the various vegetation types has been conducted using LANDSAT-7 satellite image with MapInfo 6.0 software for Windows 98.

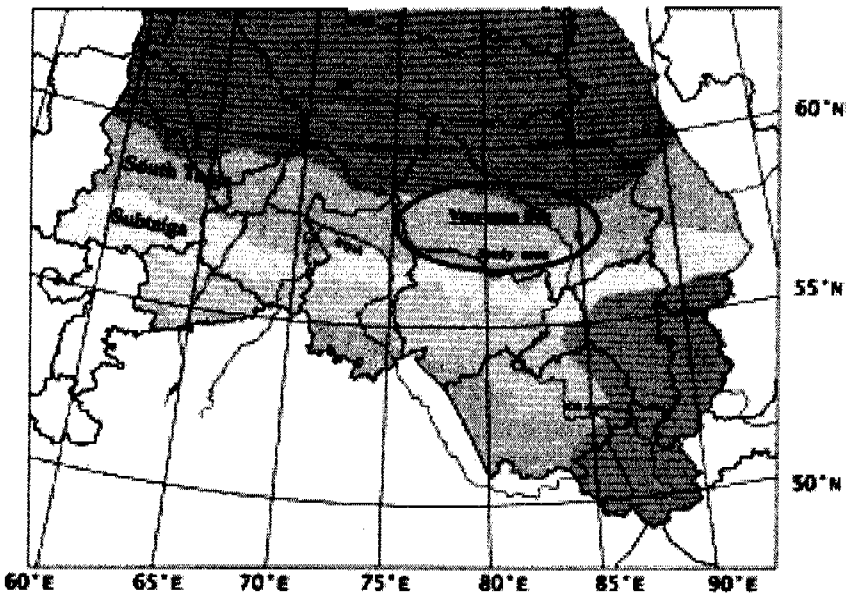

Fig.1. Study area (South edge of Great Vasyugan Bog)

3. Results and Discussion

The vegetation cover of study area is composed by native small-leaved (birch and aspen) forests with advanced herbaceous-motley grass cover and typical shrub layer. At the second growth of forest and undergrowth the birch and aspen dominate (spruce, pine and cedar are observed less frequently).

The sites of spruce forests with a touch of birch, cedar and asp are found only in the river valleys (flood-plains) and on the territory north of Tara river, near wide swamp areas. The second growth and undergrowth of these forests is composed by abies, spruce and element of cedar, asp and birch.

Characteristic for study area is significant extent of swamps. Initial stage of paludification is indicated by birch small reed (Calamagrostis) forests with high grasses, with transition in extensive depressions to wet birch-sedge-reed communities and sedge forest communities.

The vegetation cover in typical Subtaiga and South Taiga forests is presented (Table 1) with examples of geobotanical descriptions. These descriptions show that the difference of vegetation cover in forests of these subzones is observed in tree-level structure. The basic tree species in both subzones is birch and aspen but in tree species structure of South Taiga forests spruce, cedar and abies (frequently) are present. In the understory vegetation cover no considerable difference is observed. It is composed by combination of species typical for

vegetation cover under forest canopy of small-leaved and coniferous forest types. Thus a diversity of vegetation species for small-leaved forests is increased.

Table 1. Vegetation cover descriptions in typical forests of Subtaiga and South Taiga zones

Growth		Subtaiga		South Taiga	
		Total cross-section areas of tree stem (m^2/ha)			
1	Asp (A)	1	1	5	2
1	Birch (B)	1	2	7	7
1	Spruce (S)	0.03			12
1	Cedar (C)			1	3
1	Abies (AB)			0.21	
2	Asp	12	8		
2	Birch	6	4		
2	Spruce		0.11		1
2	Cedar				0.02
2	Abies				1
Undergrowth		S,C,A,B	A,B	S,A,B,AB	S,AB,C,A
	Species group	Projective cover			
Filipendula ulmaria (L.) Maxim.	Typical species of small-leaved forest	10		10	
Rosa acicularis Lindl.		10	0.1	10	0.1
Equisetum pratense Ehrh.		0.1	2	3	15
Carex macroura Meinsh.		0.1	30	15	0.1
Stellaria bungeana Fenzl.		0.1	0.1	1	0.1
Rubus saxatilis L.		10		1	3
Aegopodium podagraria L.		20	30		0.1
Ribes hispidulum (Jancz.) Pojark.		0.1	5	10	2
Ribes nigrum L.		0.1	1		2
Orobus vernus		0.1	0.1	0.1	5
Lonicera xylosteum L.		3	1	0.1	0.1
Angelica sylvestris L.		0.1		0.1	0.1
Polemonium caeruleum L.		2		0.1	
Solidago virgaurea L.			0.1	0.1	0.1
Cacalia hastata L.		1		10	
Calamagrostis arundinacea (L.) Roth				15	
Lactuca sibirica (L.) Maxim.				1	
Dryopteris carthusiana (Vill.) H. P. Fuchs				1	
Allium victorialis L.			5		10
Vaccinium vitis-idaea L.	Typical species of coniferous forest				0.1
Carex globularis L.					30
Hylocomium splendens					1
Pleurozium schreberi (Brid.) Mitt.					1
Calamagrostis obtusata Trin.		3	10		3
Sorbus sibirica Hedl.		15	3	4	0.1
Equisetum sylvaticum L.		3	3	0.1	20
Trientalis europaea L.		1	0.1	0.1	0.1
Oxalis acetosella L.		0.1		0.1	5
Majanthemum bifolium (L.) F.W.Schmidt		2		0.1	0.1
Pyrola minor		0.1			
Calamagrostis langsdorffii (Link.) Trin.	May be found in all places		0.1	3	
Spiraea salicifolia L.		0.1	0.1		0.1
Other species		19	11	15	2

Soil cover is complex. At drained territories it is formed by the gray forest soils in combination with sod-podzolic soils. For non-drained watersheds widespread occurrence of

meadow-swamp and peat-swamp soils is typical. Gray forest soils are dominant all over study area.

In order to evaluate position of detailed vegetation communities in subzones system it is necessary to apply the criteria, which exist for South Taiga and Subtaiga (Zanin, 1972; Ufimzeva, 1972; Lyubimova, 1972; Ilyina, Lapshina, Lavrenko, 1985).

Very important factor of zoning is climate, but a primary indicator for zoning at region is vegetation cover type.

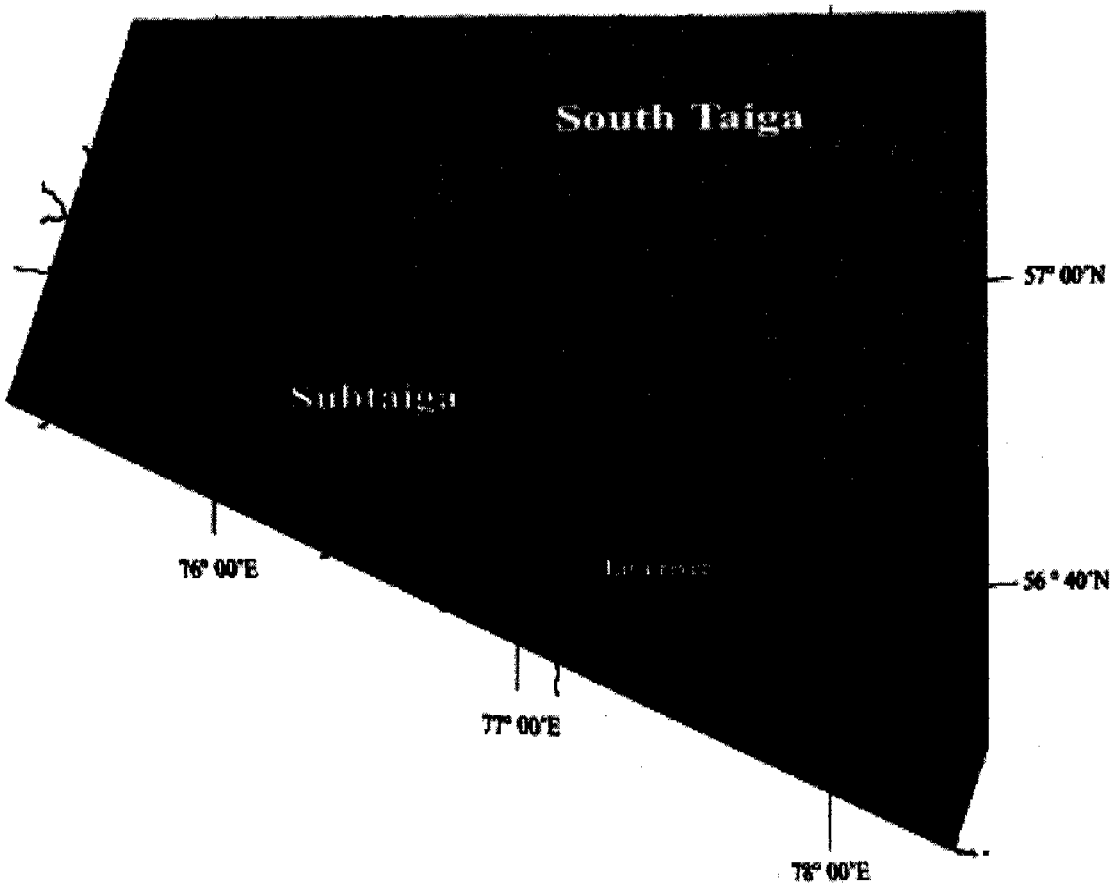

Fig. 2. South edge of Great Vasyugan Bog (Tara river region)

A South Taiga subzone is typically covered by spruce and cedar with a touch of birch and asp, major soil types are sod-podzolic, gley derno-podzolic and sod-gley heavy clay soils. The characteristic feature of South Taiga subzone is presence of abies in dark coniferous forests. Its quantity is not too big, but in botanic-geographical respect it is typical for this subzone. In the lower level there are Sorbus sibirica, Rosa azicularis and rich understory which includes dark coniferous species. In herbaceous cover a rich forest motley grass is observed. At present, a considerable area (about 72 % of woodland) is covered by birchen and asp-birchen forests. They grow at semi-hydromorphic and hydromorphic soils with various degree of gleyzation. Some part of these forests evolved from dark coniferous forests and its grass layer similar to that of dark coniferous.

South Taiga transition to Subtaiga is gradual. Alongside the transition the coniferous species disappear, except for the pine, which is confined mainly to sandy soils. The basic zonal formation is deciduous (birchen and aspen) forests at the gley gray forest and meadow soils with thick grass layer which consists mostly of gramineous plants. The swampy abies-greens with a touch of cedar and abies appear in the northern edge of subzone along the boundary of mossy swamps. In addition to typical mossy swamps a considerable fraction is occupied by various sedge-grassy swamps, which is overgrown frequently with a birch. In the east the reed-plot is widespread. On pristine floodplain terraces the forest-steppe vegetation advances far northward and appear in South Taiga. The northern border of subzone coincides with southern border of dark coniferous forests.

In described communities the spruce and abies are characteristic of South Taiga subzone and are found in floodplane vicinity. The prevalent soil type is gray forest soil. Being based on this facts we refer this territory to Subtaiga zone.

For validation of conclusions made, the boundary between subzones was defined more exactly by applying the remote sensing data (satellite image of medium resolution, LANDSAT-7).

The reconstructed boundary (Fig. 2, 3) demonstrates the areas of primary expansion of vegetation communities both Southern Taiga and Subtaiga types. These communities differ considerably in color and pattern on satellite image. Thus vegetation communities of Subtaiga types occur in the form of «islands» to the north of primary boundary of their extent.

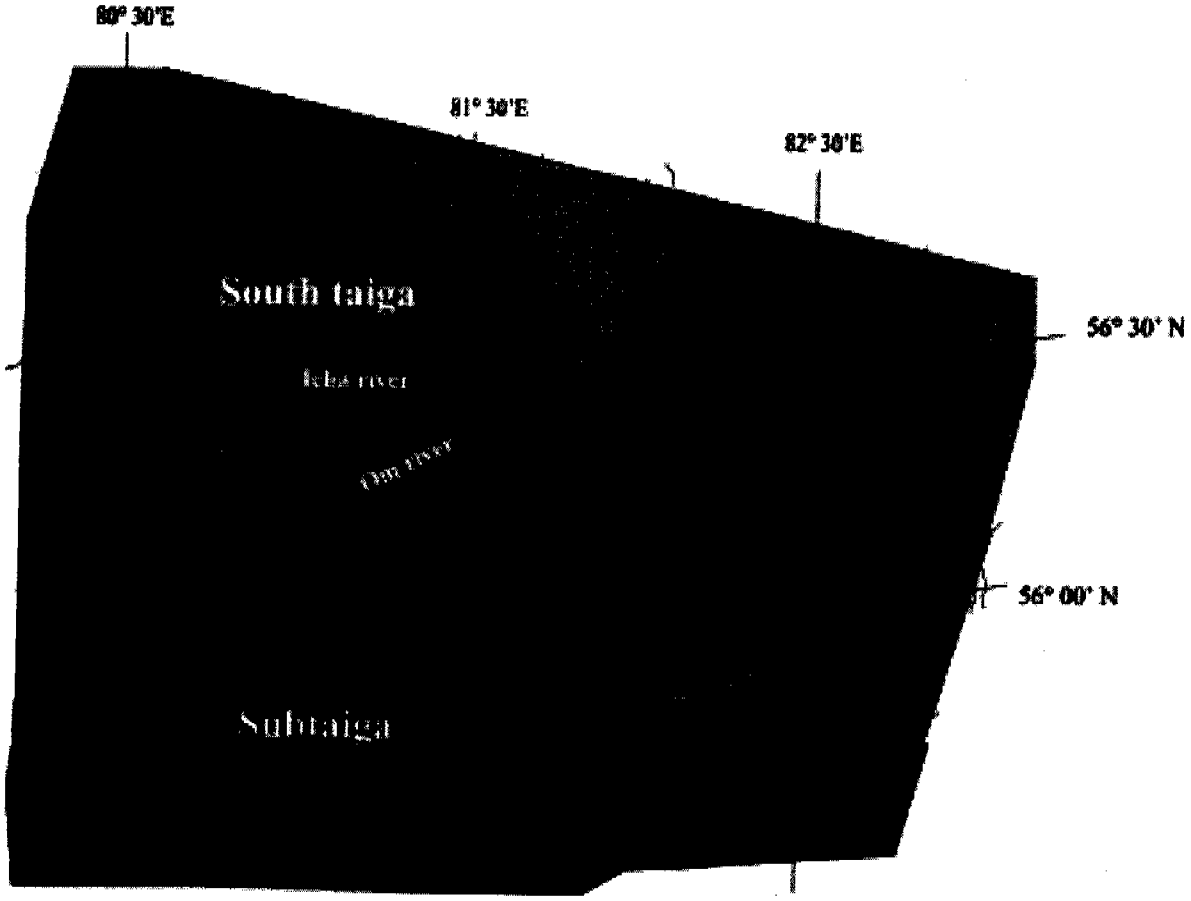

Fig. 3. South edge of Great Vasyugan Bog (Om-Baksa rivers region)

4. Conclusions

Most if not all researchers draw a boundary between South Taiga subzone and Subtaiga on 56° 00' - 56° 30' N. On the basis of this study one should conclude that in Tara (Malaya Icha) rivers area the South Taiga-Subtaiga boundary extends up to around 57° 00', that is to the north of currently assumed. To a South Taiga subzone it is possible to attribute only upper minor river areas of Novosibirsk region's north part (Bolshaya and Malaya Icha, Om, Tartas rivers) where in vegetation cover a prevalence of dark coniferous forests are to be observed on sod-podzolic and gley sod-podzolic soils.

Within the limits of south-eastern part of Great Vasyugan Bog (fig. 3) at Om-Baksa rivers area the boundary between subzones takes up position to the south (it is on 56° 00' - 56° 30' N). These results agree closely with opinion of most researchers.

It is necessary to note that the Subtaiga southern boundary at Ob-Irtysh watershed within the bounds of Baraba-plane is clearly defined. In the north, the Subtaiga boundary is not strongly pronounced, and transition from Subtaiga to South Taiga vegetation occurs gradually.

Thus Ob-Irtysh basin represent itself the perfect field for demonstration of zonal phenomenon. Zonal division is obscured by strong presence of wetlands and therefore the zonal classification on wetland covered watershed is difficult. The vegetation in general is constructed by many alternate vegetation association groups.

The representation accuracy of transition regions on the maps of vegetation cover structure is significant for objective description of geographical regularity that permits to clarify the zonal and subzonal position of large territories during geobotanical and soil zoning.

Acknowledgements

This study received partial financial support from INTAS, project «Climate in Relation to Carbon Accumulation: spatial and temporal analyses of West Siberian peat ecosystems (CIRCA)» No. 99-01718.

REFERENCES

Gorodkov B. N. Experence of dividing West-Siberian plain into botanico-georaphical regions.- Year-book of Tobol. Province museum, 1916, vol. 27, p. 1-56.(In Russian)

Ilyina I. S., Lapshina E. I., Lavrenko N. N. Vegetation cover of West Siberian plain – Novosibirsk: Nauka, 1985. (In Russian)

Krylov P. N. Vegetation in Baraba steppe and in places adjacent to it. Prior report about botanic research in Siberia and Turkestan at 1912 year.1913, p.72. (In Russian)

Lyubimova E. L. The vegetation of Ob-Irtysh interfluve.//The natural conditions of Ob - Irtysh interfluve development.- Moscow, 1972.- p. 302-322. (In Russian)

Sotchava V. B., Isachenko T. I., Lukitcheva A. N. The common features of geographic distribution of forest vegetation in West Siberian plain.- Proceedings of All-Union geographic association, 1953, N 2, p. 126-139. (In Russian)

Sotchava V. B. The geographical aspects of Siberian Taiga.- Novosibirsk, Nauka, 1980, 256 p. (In Russian)

The natural conditions and resources USSR. West Siberia.- The publishing house of AS USSR,- Moscow, 1963.- 481 pp. (In Russian)

The natural conditions of central part of West Siberian plain.- Moscow, the publishing house of MGU, 1977.- 216 pp. (In Russian)

Ufimzeva K. A. The soils of Ob - Irtysh interfluve.//The natural conditions of Ob - Irtysh interfluve development.- Moscow, 1972.- p.255-302. (In Russian)

Zanin G. V. The nature division of Ob-Irtysh interfluve.//The natural conditions of Ob - Irtysh interfluve development.- Moscow, 1972.- p. 347-380. (In Russian)

Modeling of spectral characteristics of post-fire forest floors in east Siberian taiga for satellite data interpretation

K. Kushida[1]*, A. P. Isaev[2], G. Takao[3], M. Fukuda[1], T. C. Maximov[2]

[1] Institute of Low Temperature Science, Hokkaido University, Sapporo, 060-0819 Japan
[2] Institute of Biological Problems of Cryolithozne, Russian Academy of Science, Yakutsk, 677891, Republic of Sakha, Russia
[3] Hokkaido Research Center, Forestry and Forest Products Research Institute, Sapporo, 062-8516 Japan
* Fax: +81-11-706-7142, e-mail: kkushida@lowtem.hokudai.ac.jp

1. Introduction

Forest fire plays an important role in dynamics of boreal forest ecosystems. A Recent increase of Siberian forest fire induces permafrost degradation and forest destruction where forest recovery is prevented by salt accumulation or by changes of the ground thermal regime. Positive feedback effects of boreal forest destruction on global warming have been pointed out especially in east Siberian taiga, and further investigations on the relationship between boreal forest and global climate are requested. The forest state and its carbon budget are influenced by both numbers of years after forest fire and the severity of the fire as well as other factors such as tree species and forest situation. Remote sensing technique is necessary as a tool for monitoring the forest status and the according carbon budget. Since number of plant species in east Siberian taiga is less than that of temperate or tropical forests, we focused on modeling of east Siberian taiga forest spectral reflectance based on component spectral characteristics. There are many radiative transfer models of vegetation canopies (Asrar, 1989; Myneni *et al.*, 1989), however, little field measurements of spectrum of boreal forest elements except for studies by Daughtry (1989) and Mesarch *et al.* (1999) in North America or BOREAS Project (Williams, 1991; Sellars *et al.*, 1997; Gower, 1997) in Canada. If number of forest spectral components are enough small that we can easily decompose the whole spectrum into the components, accumulation of the componential spectral characteristics and interpretation of the whole spectral reflectance from this are useful. Boreal forest ecosystems have smaller numbers of the components than other forests such as temperate or tropical forests.

In our former studies in 1999 and 2000, spectral characteristics of forest floors of *Larix cajanderi* (Dahurian larch, larch), *Pinus sylvestris* (Scotch pine, pine), and *Betula platyphylla* (Paper birch, Birch) communities and grassland in east Siberian taiga zone were measured, and a radiative transfer model of the forest and a forest floor model as a submodel of the forest model were discussed for satellite data interpretation (Kushida et al., 2000; Kushida et al., 2001). In the summer in 2001, we set three plots for evaluation of the models. One is matured larch forest, another is birch forest that passed 19 years after fire, and the other is grassland that passed 6 years after fire. In these plots, distributions of spectral reflectances in the forest floors were measured,

forest floor plant species and tree crowns were mapped by sketching and interpretation of photos taken in the forest floors, and height and diameter at breast height of all the trees were measured. IKONOS satellite imagery that has 1m resolution was taken over the plots. The radiative transfer model will be evaluated with the IKONOS imagery and estimation of the forest characteristics from remotely sensed data will be tested in the next step. In this paper, we discuss forest floor spectral characteristics of the three plots.

2. Methods

2-1 Site specification

Our study site named Neleger (N62° 20', E129° 30') were located in east Siberian boreal forest near Yakutsk city, continuously underlain by permafrost. In 2001, we set plots in (1) matured larch forest (Neleger F site), (2) birch forest that passed 19 years after fire, and (3) grassland that passed 6 years after fire. The sizes of the plots were 30m X 30m (larch) and 20m X 20m (birch and grassland). The larch plot was larger than the other two since the trees are higher and larger area should be taken account when side-looking satellites take images. Spectral reflectances of the plots were measured from 20th July to 5th August, 2001. The summer in 2001 was drier year than usual years as reported in some literatures in this "proceedings of the tenth symposium on the joint Siberian permafrost studies between Japan and Russia in 2001". The forest floor plant species and tree crowns were mapped by sketching and interpretation of photos taken in the forest floors, and height and diameter at breast height of all the trees were measured. 1m X 1m sized 900 and 400 photographs were taken for mapping of the forest floor plant species in the larch and grassland plots, respectively. The data was integrated as Geographical Information System (GIS). IKONOS imagery was taken over the plots on 11 July, 2001 from 45 degrees zenith angle.

2-2 Spectral measurement

A spectroradiometer (GER 2600, Geophysical & Environmental Research Corp., New York, USA) was used for the forest floor measurements. Spectral radiance in 350-2500 nm can be measured with this instrument. Bandwidth of the instrument was 1.5 nm in 400-1050nm, and 6.5nm in 1050-2500nm. We set the spectroradiometer at 1m height just above the soil surface and measured a part of an objective forest floor and a white panel in a 10cm radius circle alternatively.

Table 1. Site description and number of data

Site	Number of observations	Number of data	Number of data after quality control
Larch (F site, Neleger)	828	94	82
Birch (19 yr., Neleger)	728	47	36
Grassland (6 yr., Neleger)	247	36	30

A reflectance factor to the nadir direction was calculated by dividing radiance of the forest floor by radiance of the white panel that was corrected with a standard. We measured one same area in a 10cm radius circle more than four times till differences of the reflectance data due to fluctuations of the solar incidence were little, and chose five pairs that have close reflectance values to add up and eliminate noises. For noise reduction, five adjacent spectral data are also averaged. In the following analysis, the number of samples for average is set to five. The data that have more than 5 % coefficient of variation in visible to near infrared or more than 10 % in middle infrared is removed for quality control. The number of samples in each plot before and after the quality control is shown in Table 1. Solar incidences on the forest floors were mixtures of specular and diffused radiation that were changing temporally. In the following analysis, we did not account for the difference of the solar illumination; however, we analyzed the spectrum including these effects.

2-3 Forest floor model

Reflectance of a forest floor is assumed as a liner combination of component spectral reflectances in each wavelength. This assumption is based on the fact that the trees are taller than the height of the forest floor vegetation and that the patch size of components of forest floor is smaller than that of sensor resolution. The rough observation of the forest floor fulfilled these assumptions. Principal component analysis of the spectral data was used for obtaining the equation of the liner combination model and inspecting the assumption of the linearity.

3. Results and Discussions

Spectral reflectance characteristics of forest floors in the three plots are shown in Figure 1. The plot in matured larch forest (Neleger F site) is mainly composed of fallen leaves and *Vaccinium vitis-idaea*, and the plot in birch forest that passed 19 years after fire is mainly composed of fallen leaves and non-vegetated area, though many other species took place. *Vaccinium vitis-idaea* has higher reflectances than non-vegetated area, and that was the main reason why reflectances of the birch plot lower than the larch plot in 700-1000 nm. The plot in the grassland that passed 6 years after fire has higher reflectance in 700-1000 nm than the other two plots and the shape of the spectral curve was different from the other two in the spectral region. These were due to high vegetation cover. 1000-2500 nm of the grassland plot had large variation because it was rainy when the measurement was carried out, and the data in the region was excluded from the analyses. Higher average reflectance in the plot in matured larch forest (Neleger F site) in 2001 than 2000 (Kushida et al., 2001) in 1000-2500 nm was caused by dryer condition in 2001 than in 2000.

1% of the total variations of the data are assumed to have not enough information and the threshold of accumulated contributing ratio was set to 99%. As a result of principal component

analysis for each forest floor, five to six components were enough to explain more than 99% of the total variation from the average values of the spectral reflectance data. This means the spectrum for each forest floor can be expressed as a combination of six to seven components in spite that the original spectrums have more than one hundred spectral bands. The component spectrums of the forest floors are shown in Figure 2, and the scatter diagrams of the second and the third components are shown in Figure 3. The first components tend to contain largeness of the spectrally integrated reflectances. By reading the shape of the component spectrums, the first and second components in each plot showed richness of the green vegetation, and the third and higher components in each plot showed detailed compositions of plant species and other factors such as wetness that were original to the plots. The third component of the larch plot may contain wetness since the spectral curve of the component had a peak in 1300-1500 nm that contains a water absorption band. Detailed analyses of interpretation of the components by comparing each of the spectral reflectances and component scores with the plant species composition where the reflectance was measured by using plant species distribution map is the next step.

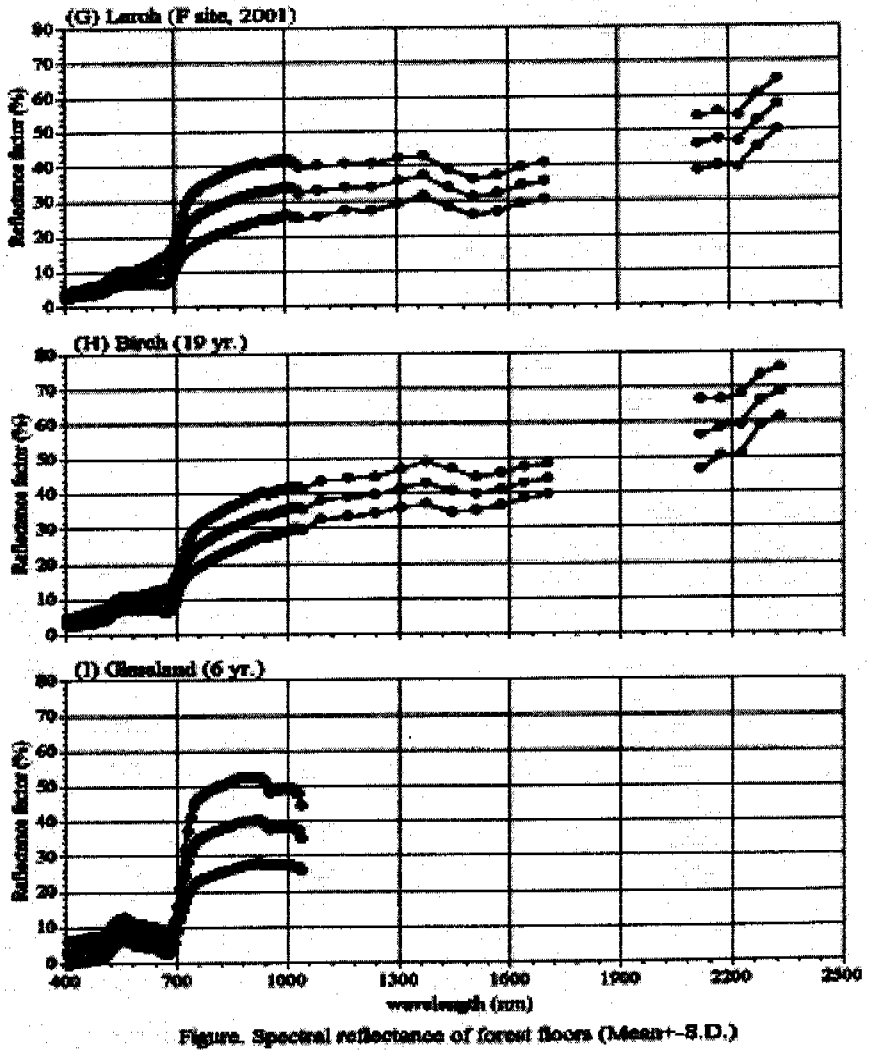

Figure. Spectral reflectance of forest floors (Mean+-S.D.)

Figure 1. Spectral reflectance of forest floors (Mean±S.D.)

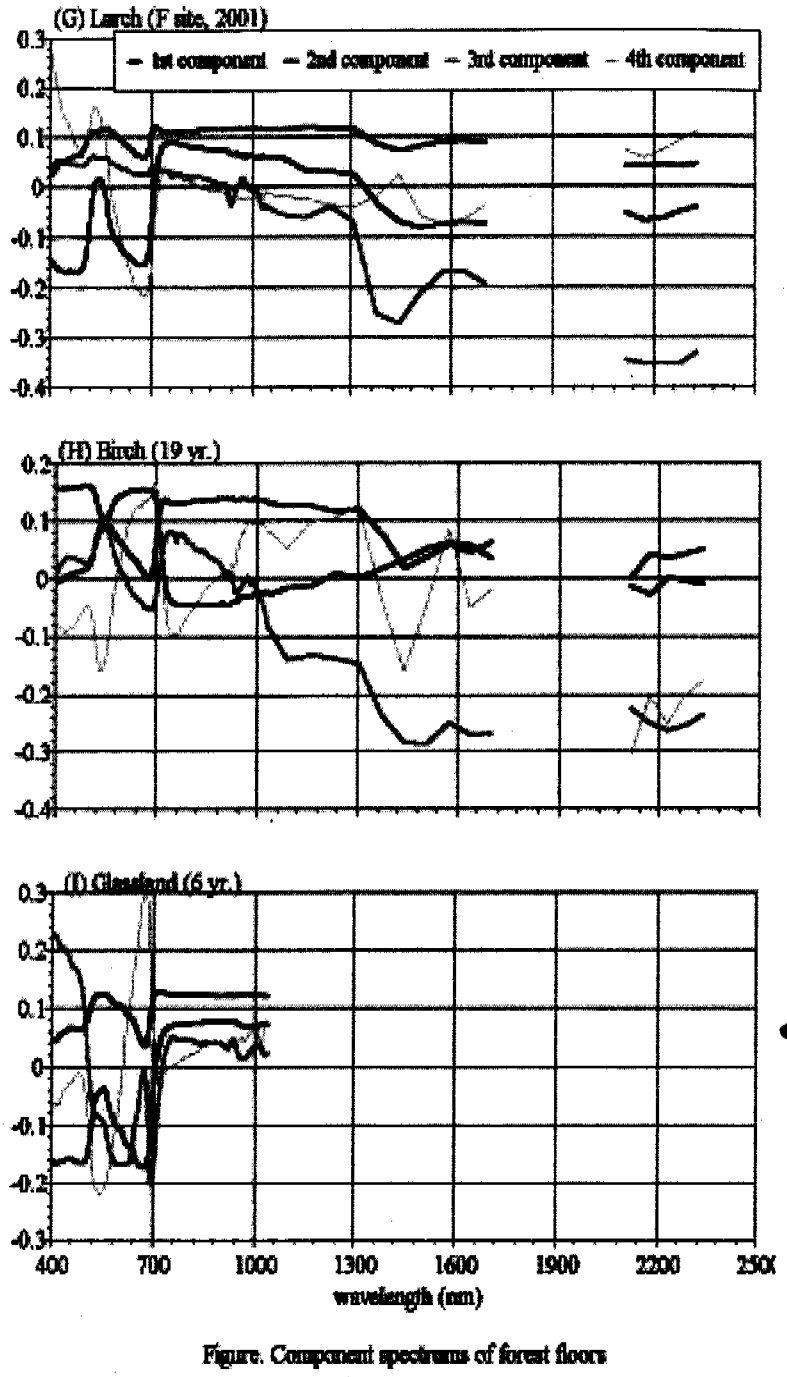

Figure. Component spectrums of forest floors

Figure 2. Component spectrums of forest floors

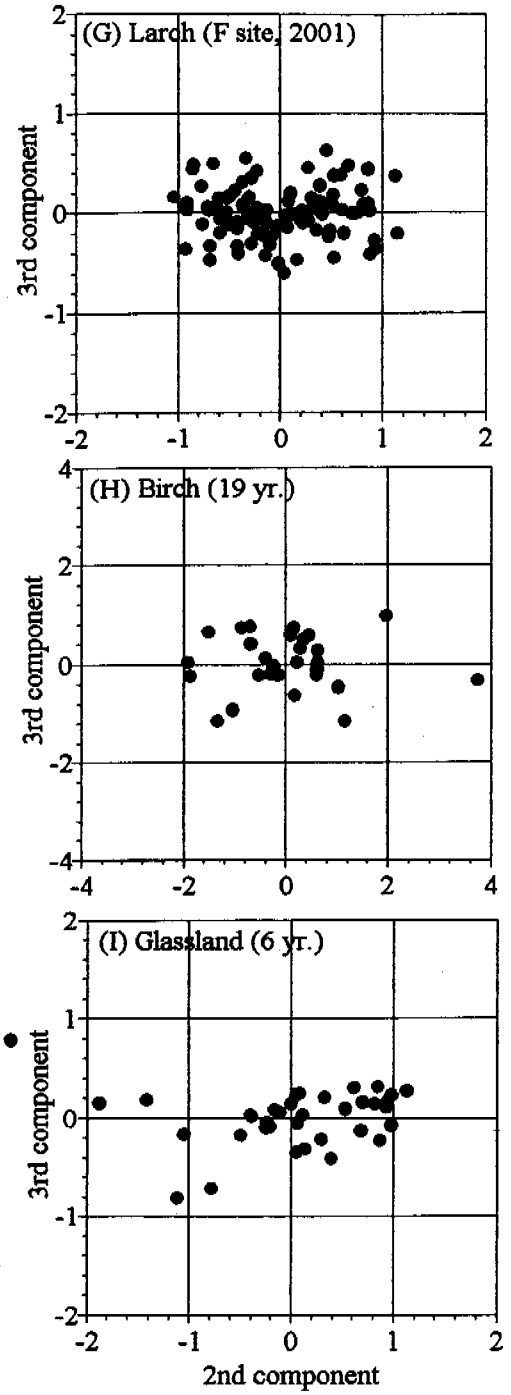

Figure 3. Scatter diagrams of principal components

4. Conclusions

Each of the spectrums of forest floors in east Siberia: (1) matured larch forest (Neleger F site), (2) 19 years birch forest, and (3) 6 years grassland after fire were expressed as a liner combination of 4 or 5 component spectrums. The liner combination model can be used for: 1. Constraints of inversion models of forest radiative transfer, and 2. Decomposition of forest floor spectrum obtained from the an inversion model into forest floor elements such as vegetated part, burned scar,

fallen leaves and estimation of the area ratio of the elements. By combining these know ledges with distributions of forest floor plant species and tree crowns, and height and diameter at breast height of all the trees that were measured simultaneously with the forest floor spectrums in the study plots. The radiative transfer model will be evaluated with the IKONOS imagery taken simultaneously with the measurements and estimation of the forest characteristics from remotely sensed data will be tested in the next step.

Acknowledgements

The authors wish to thank B. C. Maximov and C. T. Maximov for all the support in field works in the east Siberian boreal forest. This study was supported by CREST program of Japan Science and Technology Corporation (JST).

REFERENCES

Asrar, G. (1989) : Theory and applications of optical remote sensing. Wiley-Interscience.

Daughtry, C. S. T., L. L. Biehl and K. J. Ranson (1989) : A new technique to measure the spectral properties of conifer needles. *Remote Sens. Environ.*, **27**, pp. 1981-1991.

Kushida, K., G. Takao, M. Fukuda, T. C. Maximov, A. V. Kononov (2001): Modeling of forest floor spectral reflectance characteristics in east Siberian taiga for satellite data interpretation. Proceedings of the ninth symposium on the joint Siberian permafrost studies between Japan and Russia in 2000, pp. 254-259

Kushida, K., G. Takao, M. Fukuda, T. C. Maximov, A. V. Kononov (2000): Componential spectral characteristics of larch and pine communities in eastern Siberia. Proceedings of the eighth symposium on the joint Siberian permafrost studies between Japan and Russia in 1999, pp. 90-97

Mesearch, M. A. et al. (1999) : A revised measurement methodology for conifer needles spectral optical properties: evaluating the influence of gaps between elements", Remote Sens. Environ., **68**, 177-192.

Myneni, R. B. *et al.* (1989) : A review of the theory of photon transport in leaf canopies. *Agric. and Fore. Meteorol.*, **45**, 1-153.

Sellers, P. J., F.G. Hall, R.D. Kelly, A. Black, D. Baldocchi, J. Berry, M. Ryan, K.J. Ranson, P.M. Crill, D.P. Lettenmaier, H. Margolis, J. Cihlar, J. Newcomer, D. Fitzjarrald, P.G. Jarvis, S.T. Gower, D. Halliwell, D. Williams, B. Goodison, D.E. Wickland, and F.E. Guer (1997) : BOREAS in 1997: Experiment overview, scientific results, and future directions. J. Geophys. Res. BOREAS Special Issue **102 (D24)**, pp. 28731-28769.

Williams, D. L., (1991) : A comparison of spectral reflectance properties at the needle, branch and canopy level for selected conifer species", Remote Sens. Environ. **35**, pp. 1979-1993.